

APPLICATION OF DIGITAL IMAGE PROCESSING TECHNIQUES
TO THE PHOTOMETRIC TESTING OF VEHICLE HEADLAMPS

by

Stephen John Cartwright

A Thesis
Submitted for the
Degree of
Doctor of Philosophy

to

The University of Aston in Birmingham

September 1986

SUMMARY

THE UNIVERSITY OF ASTON IN BIRMINGHAM

APPLICATION OF DIGITAL IMAGE PROCESSING TECHNIQUES TO THE PHOTOMETRIC TESTING OF VEHICLE HEADLAMPS

by

Stephen John Cartwright

PhD Thesis 1986

The aim of this Interdisciplinary Higher Degrees project was the development of a high-speed method of photometrically testing vehicle headlamps, based on the use of image processing techniques, for Lucas Electrical Limited.

Photometric testing involves measuring the illuminance produced by a lamp at certain points in its beam distribution. Headlamp performance is best represented by an iso-lux diagram, showing illuminance contours, produced from a two-dimensional array of data. Conventionally, the tens of thousands of measurements required are made using a single stationary photodetector and a two-dimensional mechanical scanning system which enables a lamp's horizontal and vertical orientation relative to the photodetector to be changed. Even using motorised scanning and computerised data-logging, the data acquisition time for a typical iso-lux test is about twenty minutes.

A detailed study was made of the concept of using a video camera and a digital image processing system to scan and measure a lamp's beam without the need for the time-consuming mechanical movement. Although the concept was shown to be theoretically feasible, and a prototype system designed, it could not be implemented because of the technical limitations of commercially-available equipment.

An alternative high-speed approach was developed, however, and a second prototype system designed. The proposed arrangement again uses an image processing system, but in conjunction with a one-dimensional array of photodetectors and a one-dimensional mechanical scanning system in place of a video camera. This system can be implemented using commercially-available equipment and, although not entirely eliminating the need for mechanical movement, greatly reduces the amount required, resulting in a predicted data acquisition time of about twenty seconds for a typical iso-lux test.

As a consequence of the work undertaken, the company initiated an £80,000 programme to implement the system proposed by the author.

Key Words: Headlamp, Photometry, Digital Image Processing,
Test Equipment, Video Camera

ACKNOWLEDGEMENTS

I would like to thank my Main Supervisor, Dr John Archer-Hall (Department of Vision Sciences), for his help and enthusiasm during the project. Thanks are also due to my Associate Supervisor, Dr Peter Best (Department of Computer Science), and my IHD Tutor, Dr Alastair Cochran, for their advice and suggestions. The work of Mr Derek Hickson, formerly of the IHD Department, in helping to arrange the project is also gratefully acknowledged.

I am indebted to Mr Brian Kingett (Training Manager), Mr Fred Laishley (Q&R Services Manager), and Mr Charles Spencer (Chief Engineer, Lighting Division), without whose co-operation the project could not have taken place.

I would like to express my appreciation to my Industrial Supervisor, Mr Geoff Draper (Deputy Chief Engineer, Lighting Division), whose commitment to the development of the Company's photometric test facilities was the driving force behind the initiation of the project, its continued Company support throughout various organisational changes and the implementation of the system recommended by the author. The help of my colleagues on the Optical Design Section, whose vehicle lamp development work provides the reason for the project's existence, and of the staff of the Prototype Department, who produced various mechanical components, is also gratefully acknowledged.

It is a pleasure to acknowledge the advice and assistance of Mr Bob Wanek, Mr Maurice Jones, Mr Roger Bourdon and Mr John Allen of

Gems of Cambridge Limited, and Mr Tom Hogan, of Pathway Systems, who were always willing to share their knowledge and experience even though there was no certainty of their receiving an order.

I am particularly grateful to Mrs Pamela Barrett (Planning Manager), for arranging to have the manuscript typed, and to Miss Maria Anderton, her secretary, for the considerable time and effort spent on this task.

LIST OF CONTENTS

| Chapter | | Page |
|---------|---|------|
| | SUMMARY | i |
| | ACKNOWLEDGEMENTS | ii |
| | LIST OF CONTENTS | iv |
| | LIST OF FIGURES | xv |
| | LIST OF TABLES | xix |
| | GLOSSARY OF ABBREVIATIONS | xx |
| | GLOSSARY OF MAIN SYMBOLS AND SUBSCRIPTS | xxi |
| 1 | INTRODUCTION | 1 |
| | 1.1 The Company | 1 |
| | 1.2 The Project Origin | 2 |
| | 1.3 The Structure of the Thesis | 4 |
| 2 | VEHICLE LIGHTING | 6 |
| | 2.1 Introduction | 6 |

| | | |
|-------|---|----|
| 2.2 | Headlamp Systems | 11 |
| 2.3 | Headlamp Intensity Distributions | 13 |
| 2.4 | Legal Requirements | 19 |
| 2.5 | Lamp Design and Manufacture | 22 |
| 2.6 | Photometric Testing - An Overview | 24 |
| 2.6.1 | Road Testing | 24 |
| 2.6.2 | Darkroom Testing | 25 |
| 2.6.3 | Production Line Testing | 26 |
| 3 | QUANTITATIVE TEST METHODS AND EQUIPMENT | 28 |
| 3.1 | Basic Principles | 28 |
| 3.2 | Types of Test | 39 |
| 3.2.1 | Point to Point | 39 |
| 3.2.2 | Iso-Lux Tests | 43 |
| 3.2.3 | Cross-Section Tests | 44 |
| 3.3 | Practical Test Equipment | 46 |
| 3.3.1 | Types of Goniophotometer | 46 |
| 3.3.2 | Reduced-Length Photometers | 50 |
| 3.3.3 | Automatic Photometers | 52 |
| 4. | PHOTODETECTOR SYSTEMS FOR HEADLAMP PHOTOMETRY | 55 |
| 4.1 | General Considerations | 55 |
| 4.2 | Silicon Photodiode Detector Systems | 62 |

| | | |
|-------|--|----|
| 5. | OVERVIEW OF THE PROJECT | 68 |
| 5.1 | Work Carried Out | 68 |
| 5.1.1 | Completion and Commissioning of the E&D Department Automatic Photometer | 68 |
| 5.1.2 | Study of the Subject Areas Relevant to Video Photometry | 70 |
| 5.1.3 | Development of the Video Photometry Concept | 71 |
| 5.1.4 | Design of a Prototype Video Photometer and the Detailed Evaluation of Commercially Available Equipment | 76 |
| 5.1.5 | Design of a High-Speed Photometer | 77 |
| 5.1.6 | Planning and Partial Implementation of a Photometric Data Processing Scheme | 78 |
| 5.1.7 | Miscellaneous Work | 80 |
| 5.2 | Thesis Structure | 81 |
| 6 | THE E&D DEPARTMENT AUTOMATIC PHOTOMETER | 85 |
| 6.1 | Hardware | 85 |
| 6.2 | Software | 88 |
| 7. | MEASUREMENT SURFACE IMAGING WITH A VIDEO CAMERA - FUNDAMENTALS | 92 |
| 7.1 | Introduction | 92 |

| | | |
|-------|---|-----|
| 7.2 | Basic Imaging Methods | 93 |
| 7.3 | Possible Viewing Arrangements | 96 |
| 7.4 | Screen Pixels | 99 |
| 7.5 | Photometric Analysis of the Proposed Imaging Method | 102 |
| 7.5.1 | Far Screen Pixel and Near Screen Pixel Illuminance Relationship | 104 |
| 7.5.2 | Near Screen Pixel Illuminance and Luminance Relationship | 106 |
| 7.5.3 | Near Screen Pixel Luminance and Sensor Pixel Illuminance Relationship | 107 |
| 7.5.4 | Sensor Pixel Illuminance and Video Output Signal Relationship | 110 |
| 7.5.5 | Far Screen Pixel Illuminance and Video Output Signal Relationship | 111 |
| 7.6 | Advantages of a Solid-State Camera | 112 |
| 7.7 | Comparison of Conventional and Video Photometry Approaches to Illuminance Measurement | 115 |
| 8 | THE USE OF AN IMAGE PROCESSING SYSTEM FOR VIDEO PHOTOMETRY - FUNDAMENTALS | 117 |
| 8.1 | Introduction | 117 |
| 8.2 | Screen Illuminance Array Acquisition | 118 |
| 8.2.1 | Digitization and Storage of the V_{SEP} values | 119 |
| 8.2.2 | Calculation of the E_{FSCP} ' values from the V_{SEP} 'values | 120 |

| | | |
|-------|--|-----|
| 8.2.3 | SIA Generation from the E_{FSCP} ' values | 121 |
| 8.3 | Screen Illuminance Array Storage | 121 |
| 8.4 | Screen Illuminance Array Display | 122 |
| 8.5 | Screen Illuminance Array Processing | 122 |
| 8.6 | Screen Illuminance Array File Storage | 123 |
| 9. | POTENTIAL APPLICATION AREAS FOR A VIDEO OR HIGH-SPEED PHOTOMETRY SYSTEM | 124 |
| 9.1 | The Conventional Tests | 124 |
| 9.1.1 | Point to Point Tests | 124 |
| 9.1.2 | Cross-Section Tests | 125 |
| 9.1.3 | Iso-Lux Tests | 125 |
| 9.2 | Interactive Design Processing | 126 |
| 9.3 | New Methods of Presenting Performance Data | 128 |
| 9.4 | Reflector Testing | 130 |
| 9.5 | Automatic Aiming | 131 |
| 9.6 | Generation of Data for Development of 'Performance Prediction' Software | 132 |
| 9.7 | Generation of Data for 'Chess' | 133 |
| 10 | MEASUREMENT SURFACE IMAGING WITH A VIDEO CAMERA - FURTHER DETAILS | 134 |
| 10.1 | Introduction | 134 |
| 10.2 | Far Screen Pixel and Near Screen Pixel Illuminance Relationship | 135 |

| | | |
|--------|---|-----|
| 10.3 | Near Screen Pixel Illuminance and Luminance Relationship | 137 |
| 10.4 | Near Screen Pixel Luminance and Sensor Pixel Illuminance Relationship | 138 |
| 10.4.1 | Camera Lens Aberrations | 138 |
| 10.4.2 | Off-Axis Image Illuminance Reduction | 139 |
| 10.4.3 | Camera Flare | 140 |
| 10.5 | Sensor Pixel Illuminance and Video Output Signal Relationship | 141 |
| 10.5.1 | Spectral Response Characteristics | 142 |
| 10.5.2 | Sensitivity | 143 |
| 10.5.3 | Clocking characteristics and Video Signal Generation | 144 |
| 10.5.4 | Dark Signal Characteristics | 145 |
| 10.5.5 | Responsivity Variations | 146 |
| 10.5.6 | Noise Characteristics | 148 |
| 10.5.7 | Blooming Characteristics | 148 |
| 10.5.8 | Sensor Pixel Geometry | 149 |
| 10.5.9 | Blemishes | 150 |
| 10.6 | Far Screen Pixel Illuminance and Video Output Signal Relationship | 150 |
| 10.7 | The Fairchild CCD3000 Camera | 152 |
| 10.7.1 | Spectral Response Characteristics | 152 |
| 10.7.2 | Sensitivity | 153 |
| 10.7.3 | Clocking Characteristics and Video Signal Generation | 153 |
| 10.7.4 | Dark Signal Characteristics | 154 |
| 10.7.5 | Responsivity Variations | 155 |
| 10.7.6 | Noise Characteristics | 155 |

| | | |
|----------|---|-----|
| 10.7.7 | Blooming Characteristics | 156 |
| 10.7.8 | Sensor Pixel Geometry | 156 |
| 10.7.9 | Blemishes | 157 |
| 11 | THE USE OF AN IMAGE PROCESSING SYSTEM FOR VIDEO PHOTOMETRY - FURTHER DETAILS | 158 |
| 11.1 | Introduction | 158 |
| 11.2 | Digitization and Storage of the V_{SEP} Values | 158 |
| 11.2.1 | Single Range Digitization Methods | 163 |
| 11.2.1.1 | Method (a) | 164 |
| 11.2.1.2 | Method (b) | 164 |
| 11.2.1.3 | Evaluation | 165 |
| 11.2.2 | Multiple Range Digitization Methods | 167 |
| 11.2.2.1 | Method (a) | 168 |
| 11.2.2.2 | Method (b) | 170 |
| 11.2.2.3 | Evaluation | 172 |
| 11.2.3 | Conclusions | 174 |
| 11.3 | Calculation of the E_{FSCP} ' Values from the V_{SEP} ' Values | 174 |
| 11.3.1 | Calculation of VX_{SEP} ' from V_{SEP} ' | 176 |
| 11.3.2 | Calculation of E_{FSCP} ' from VX_{SEP} ' | 177 |
| 11.4 | SIA Generation from the E_{FSCP} ' Values | 179 |
| 11.4.1 | Method (a) | 180 |
| 11.4.2 | Method (b) | 180 |
| 11.4.3 | Method (c) | 182 |
| 11.5 | Ambient Light Correction | 183 |

| | | |
|------|--|-----|
| 11.6 | Main Video Photometry System Design | 184 |
| | Considerations | |
| | 11.6.1 The Method of Digitizing the Camera's Video Signal | 184 |
| | 11.6.2 SIA Size | 184 |
| | 11.6.3 Frame-Store Utilization | 185 |
| | 11.6.4 The Method of Representing the SIA Element Values | 186 |
| | 11.6.5 Software | 186 |
| 12 | REDUCED-LENGTH PHOTOMETER ANALYSIS METHOD | 189 |
| | 12.1 Introduction | 189 |
| | 12.2 The Reduced-Length Photometer Model | 190 |
| | 12.3 The Analysis Procedure | 198 |
| 13 | FOUR METRE REDUCED-LENGTH PHOTOMETER PERFORMANCE | 213 |
| | 13.1 Introduction | 213 |
| | 13.2 Performance Study | 215 |
| | 13.3 Conclusions | 221 |
| 14 | AN INTEGRATED PHOTOMETRIC DATA PROCESSING SCHEME | 224 |
| | 14.1 Description | 224 |
| | 14.1.1 Computer-Based Photometers | 226 |

| | | |
|--------|--|-----|
| 14.1.2 | Photometric Data Files | 229 |
| 14.1.3 | Photometric Data File | 229 |
| | Processing Software | |
| 14.2 | Implementation | 230 |
| | | |
| 15 | THE PROPOSED VIDEO PHOTOMETRY SYSTEM | 234 |
| 15.1 | Introduction | 234 |
| 15.2 | Overall Description | 235 |
| 15.3 | The Front-End | 241 |
| 15.4 | System Construction | 245 |
| 15.5 | The Image Processing System | 248 |
| 15.5.1 | Introduction | 248 |
| 15.5.2 | Evaluation of Commercially Available | 252 |
| | Image Processing Systems | |
| 15.5.3 | Conclusions | 257 |
| 15.6 | The Camera | 258 |
| 15.6.1 | Introduction | 258 |
| 15.6.2 | General Electric TN2506 | 264 |
| 15.6.3 | Reticon MC9256 | 266 |
| 15.6.4 | I2S IS200 | 268 |
| 15.6.5 | Conclusions | 271 |
| 15.7 | Conclusions | 272 |
| | | |
| 16 | AN ALTERNATIVE APPROACH TO HIGH-SPEED PHOTOMETRY | 273 |
| 16.1 | Overall Description | 273 |

| | | |
|------|--|-----|
| 16.2 | Comparison with the Video Photometry Approach | 276 |
| 16.3 | The Measurement Surface | 279 |
| 16.4 | SIA Acquisition Procedure | 281 |
| | | |
| 17 | THE PROPOSED HIGH-SPEED PHOTOMETRY SYSTEM | 285 |
| | | |
| 17.1 | Introduction | 285 |
| 17.2 | System Description | 286 |
| 17.3 | The Gems and the Micro-Computer | 289 |
| 17.4 | The Photodiode Sub-System | 290 |
| 17.5 | The Analogue Input Sub-System | 291 |
| 17.6 | The Rotary Table Sub-System | 293 |
| 17.7 | The System Software | 294 |
| 17.8 | Ancillary Hardware | 295 |
| 17.9 | Implementation | 295 |
| | | |
| 18 | DISCUSSION | 299 |
| | | |
| 18.1 | Introduction | 299 |
| 18.2 | Video Rate Analogue to Digital Conversion | 301 |
| 18.3 | Camera Evaluation and Performance | 303 |
| | 18.3.1 Evaluation | 303 |
| | 18.3.2 Performance | 304 |
| 18.4 | Other Potential Problem Areas | 308 |
| 18.5 | Recommended Approach to Further Video Photometry Work | 309 |
| 18.6 | Epilogue | 310 |

| | |
|--|-----|
| LIST OF CONTENTS OF APPENDICES | 311 |
| LIST OF FIGURES IN APPENDICES | 314 |
| LIST OF TABLES IN APPENDICES | 315 |
| APPENDIX A THE CONCEPT OF HEADLAMP INTENSITY | 317 |
| APPENDIX B REDUCED-LENGTH PHOTOMETERS | 320 |
| APPENDIX C AMBIENT LIGHT IN A VIDEO PHOTOMETRY SYSTEM | 324 |
| APPENDIX D REDUCED-LENGTH PHOTOMETER ANALYSIS PROGRAM | 327 |
| APPENDIX E FOUR METRE REDUCED-LENGTH PHOTOMETER PERFORMANCE: BLUR PATCH DATA TABLES | 347 |
| APPENDIX F IMAGE PROCESSING EQUIPMENT CONSIDERED | 367 |
| APPENDIX G THE AUTOMATIC PHOTOMETER/GROUP COMPUTER FILE TRANSFER SYSTEM | 369 |
| APPENDIX H PHOTOMETRIC DATA FILES AND THEIR PROCESSING | 376 |
| LIST OF REFERENCES | 418 |
| BIBLIOGRAPHY OF USEFUL READING | 439 |

LIST OF FIGURES

| Fig. | | Page |
|------|--|------|
| 2.1 | Perspective View of a Road Scene from the Position of a Vehicle's Headlamp | 14 |
| 2.2 | A Typical Main Beam Intensity Distribution | 16 |
| 2.3 | Typical Dipped Beam Intensity Distributions | |
| | a) 'E' Beam (Left Hand Rule of Road) | 18 |
| | b) 'SAE' Beam (Right Hand Rule of Road) | 20 |
| 3.1 | Principle of Goniophotometer Operation | 30 |
| 3.2 | Principle of Operation of Type A and B Goniometers | |
| | a) Type A | 31 |
| | b) Type B | 31 |
| 3.3 | Co-ordinate Systems for Type A and B Goniometers | |
| | a) Type A | 35 |
| | b) Type B | 36 |
| 3.4 | Plane and Spherical Measurement Surfaces | 38 |

| | | |
|-----|--|-----|
| 3.5 | ECE Regulation Dipped Beam Test Points and Zones (Left Hand Rule of Road) | 41 |
| 3.6 | An Example Iso-Lux Diagram | 45 |
| 4.1 | Photodiode Transimpedance Amplifier | 63 |
| 5.1 | Work Carried Out During Period of Project | 69 |
| 5.2 | Basic Video Photometry Concept | 72 |
| 6.1 | E&D Department Automatic Photometer - Functional Block Diagram | 86 |
| 7.1 | Video Photometry System Using a Transmissive Screen | 94 |
| 7.2 | Possible Viewing Arrangements for a Video Photometry System Using a Reflective Screen | |
| | a) Viewing Arrangement (a) | 97 |
| | b) Viewing Arrangement (b) | 97 |
| | c) Viewing Arrangement (c) | 98 |
| | d) Viewing Arrangement (d) | 98 |
| 7.3 | Screen Pixel Imaging in a Video Photometry System | 101 |
| 7.4 | Camera Imaging System Parameters | 101 |

| | | |
|------|--|-----|
| 11.1 | Video Signal Digitization - Multiple Range Method (a) | |
| | a) Frame 1 | 169 |
| | b) Frame 2 | 169 |
| 11.2 | Video Signal Digitization - Multiple Range Method (b) | |
| | a) Frame 1 | 171 |
| | b) Frame 2 | 171 |
| 11.3 | SIA Generating Methods - Effective Measurement Points and Flux Collection Areas | |
| | a) Method (a) | 181 |
| | b) Method (b) | 181 |
| | c) Method (c) | 181 |
| 12.1 | Reduced-Length Photometer Model | |
| | a) Overall Configuration | 191 |
| | b) A Pencil of Rays | 195 |
| | c) A Single Ray in the Pencil | 196 |
| | d) Limiting Off-Axis Angle | 197 |
| | e) Limiting Effective Lamp Size | 199 |
| | ($ POIWFS \leq LNSSZE/2$) | |
| | f) Limiting Effective Lamp Size | 200 |
| | ($ POIWFS > LNSSZE/2$) | |
| | g) Off-Axis Angle of Ray | 207 |
| | ($RSPR > 0$) | |

| | | |
|------|--|-----|
| h) | Off-Axis Angle of Ray (RSPR < 0) | 208 |
| 13.1 | Focal Planes for a Single-Element Reduced Length Photometer Imaging a Flat Far Screen | 220 |
| 14.1 | Photometric Data Processing Scheme | 227 |
| 15.1 | Proposed Video Photometry System | |
| a) | SIA Processing Operations | 238 |
| b) | Measurement Surface for Extended Field of View | 242 |
| c) | Outline Layout of Front-End | 244 |
| d) | Screen and Supports | 247 |
| 16.1 | Basic Concept of the 'High-Speed Photometer' | 274 |
| 16.2 | Measurement Surface for the 'High-Speed Photometer' | 280 |
| 16.3 | Near Screen Pixel Array for the 'High-Speed Photometer' | 280 |
| 17.1 | The 'High-Speed Photometer' - Functional Block Diagram | 288 |

LIST OF TABLES

| Table | | Page |
|-------|---|------|
| 3.1 | Example of ECE Regulation Photometric Requirements | 42 |
| 4.1 | Lamp Illuminance Range Information | 60 |
| 11.1 | Possible Frame-Store Data Coding Formats for SIA Elements | 187 |
| 12.1 | Relationship Between Physical and Effective Lamp Sizes for Reduced-Length Photometer Analysis | 194 |
| 12.2 | Example of Data Produced by 'RLP' Program | 209 |
| 13.1 | Effective Lamp Size Information for Reduced-Length Photometer Study | 214 |

GLOSSARY OF ABBREVIATIONS

| | |
|-------|---|
| ADC | Analogue to Digital Converter |
| BSI | British Standards Institution |
| CCD | Charge-Coupled Device |
| CHESS | Comprehensive Headlamp Environment Systems Simulation Model |
| CID | Charge Injection Device |
| DMA | Direct Memory Access |
| DSSNU | Dark Signal Shading Non-Uniformity |
| DVM | Digital Volt Meter |
| ECE | Economic Commission for Europe |
| E&D | Engineering and Design |
| FET | Field Effect Transistor |
| IEEE | Institute of Electrical and Electronic Engineers |
| IPS | Image Processing System |
| MOS | Metal Oxide Silicon |
| PDF | Photometric Data File |
| PRSNU | Photoresponse Shading Non-Uniformity |
| Q&R | Quality and Reliability |
| RB | Replaceable Bulb |
| RLP | Reduced-Length Photometer |
| SAE | Society of Automotive Engineers |
| SB | Sealed Beam |
| SIA | Screen Illuminance Array |

GLOSSARY OF MAIN SYMBOLS AND SUBSCRIPTS

Symbols

| | |
|-----------|--|
| d | distance (m) |
| f | lens focal length (m) |
| f/ | camera lens aperture |
| i | current (A) |
| k | constant |
| m | magnification |
| n | number of analogue to digital converter bits |
| r | resistance (Ω) |
| s | photodetector diameter (m) |
| t | time (s) |
| u | lens object distance (m) |
| v | lens image distance (m) |
| x | distance (m) |
| y | distance (m) |
| α | angle |
| β | angle |
| γ | angle |
| δ | angle |
| λ | wavelength (m) |
| ρ | reflection factor |
| θ | angle |
| A | area (m ²) |
| C | constant |
| D | camera lens diameter (m) |
| E | illuminance (Lx) |

| | |
|--------------|---|
| F | luminous flux (Lm) |
| I | luminous intensity (Cd) |
| K | constant |
| L | luminance (Cdm^{-2}) |
| Q | analogue to digital converter bit size |
| R | responsivity (VLx^{-1} or ALx^{-1}) |
| T | lens transmission factor |
| V | voltage (V) |
| VD | sensor voltage component produced by dark current (V) |
| VN | sensor voltage component produced by noise (V) |
| VX | sensor voltage component produced by exposure (V) |
| $V(\lambda)$ | photopic response |
| X | exposure (Lxs) |

Subscripts

| | |
|------|-------------------------------|
| i | integration |
| ADC | analogue to digital converter |
| c | camera |
| FSC | far screen |
| FSCP | far screen pixel |
| NSC | near screen |
| NSCP | near screen pixel |
| OS | offset |
| OUT | output |
| P | point P |
| PD | photodiode |
| PP | peak to peak |

R reduced-length photometer
S point S
SEP sensor pixel
V voltage

The following are used in conjunction with the above subscripts:

AV average eg R_{SEPAV} : average R_{SEP} value
FS full scale eg V_{ADCFS} : full scale V_{ADC} value
MAX maximum eg $E_{FSCPMAX}$: maximum E_{FSCP} value
MIN minimum eg $E_{FSCPMIN}$: minimum E_{FSCP} value
SAT saturation eg V_{SEPSAT} : V_{SEP} value at saturation
SMS spherical measurement surface eg $E_{FSCPSMS}$: E_{FSCP} value for a spherical measurement surface

A primed symbol (eg V_{SEP}') indicates a digital representation of that quantity.

1. INTRODUCTION

1.1 The Company

Lucas Industries consists of seven principal operating Companies in the United Kingdom, which design and manufacture a wide range of engineering products for the automotive, aerospace and engineering industries. Their activities are supported by a Group Research and Computing Centre at Shirley, Solihull and are complemented by a worldwide network of distributors and service outlets. Lucas manufacturing interests also extend to many overseas countries through a chain of subsidiary and associate Companies. In 1984, the Group employed over 65,000 people worldwide and the total value of sales exceeded 1,300 million pounds. Further information about the Group can be found in reference (1).

Lucas Electrical Limited is one of the seven principal operating Companies and produces a wide range of electrical equipment for cars, commercial vehicles and tractors, including ignition, fuel injection, starting, generating and lighting systems.

The Lighting Division of Lucas Electrical manufactures a wide range of vehicle lighting equipment, including headlamps, tail-lamp clusters and auxiliary lamps for the world markets; the majority of these lamps are custom designed and manufactured for specific vehicle models. The Division's headquarters and main manufacturing base is a 22 acre site at Cannock, Staffs. There are also two smaller manufacturing units at Hall Green, Birmingham and Telford,

Shropshire. A total of about 2,000 people are employed at these sites and over 7 million lamps are manufactured every year, the major customers being British Leyland and Ford. In addition, the Division has close links with the following vehicle lighting equipment manufacturers, which are partly owned by the Company: Metalurgica Rossi in Brazil, Carello in Italy and Hella Manufacturing in Australia.

The author was employed in the Engineering and Design (E&D) department, which is responsible for all aspects of lamp design and the development of new vehicle lighting concepts, and reported to Mr G R Draper, who was Lighting Project Engineer, and later, Deputy Chief Engineer.

1.2 The Project Origin

Photometric testing, which essentially involves measuring the illuminance values produced by a lamp at various points in its beam, has played a part in headlamp design and manufacture for many decades. It has become increasingly important over recent years, however, as a result of:

- a) the design of more complex lamps, which require more optical development than traditional round lamps
- b) the need to investigate the effects that new materials and manufacturing processes have on photometric performance

- c) increased customer interest in photometric performance
- d) more stringent quality control, to improve product consistency
- e) the development of new concepts in headlamp systems design.

The conventional method of carrying out quantitative photometric tests is time consuming; using the traditional manual equipment, a simple test takes several minutes and a comprehensive evaluation, requiring thousands of illuminance measurements, can take several hours. Consequently, various automatic test systems have been developed over the years in order to reduce the time taken for these tests. These systems have mainly been developed by Lucas Electrical's Instrumentation department, situated at the Company's headquarters in Hockley, Birmingham, which designs special purpose test equipment for all the product Divisions. The author was employed in the Instrumentation department between January 1978 and October 1981, and immediately prior to undertaking the IHD project, was involved in the design of the E&D department 'Automatic Photometer', which is currently the Division's most sophisticated test system; it enables a comprehensive performance test to be carried out in several tens of minutes, as opposed to several hours using the manual equipment.

During the period when the 'Automatic Photometer' was being designed, Mr Draper had asked Mr Laishley, the manager of the Instrumentation department, if the idea of using a video camera for high-speed photometric testing could be investigated as the possible basis for the next generation of test equipment; it was hoped that this technique would provide a means of reducing the time taken to

carry out a comprehensive test to a few seconds.

Around the same time, the author had applied and been accepted for a place on the University of Aston Interdisciplinary Higher Degrees Scheme, which awards higher degrees for research projects undertaken in industry or other outside organisations. The scheme also includes coursework in subjects such as management, problem solving and communication in order to assist the student's general career development. Information about the scheme can be found in reference (2).

The author considered that the investigation of the use of a video camera for high-speed photometry would be suitable as the basis of an IHD project and that it would be beneficial to both the Company and the author if undertaken in this way. The Company agreed, the project was accepted by the IHD scheme and the author joined the Lighting Division and moved to the Cannock site.

1.3 The Structure of the Thesis

Chapters 2 - 4 provide the relevant background knowledge relating to headlamp testing. Chapter 2 describes the subject of vehicle lighting and gives an overview of the various types of photometric testing undertaken. The test methods and equipment used for making quantitative measurements of a lamp's performance are described in Chapter 3, with Chapter 4 providing more information on the use of photodetectors for illuminance measurement.

Chapter 5 provides an overview of the work carried out for the project and describes the structure of the remainder of the thesis.

It is assumed in this thesis that the reader has a reasonably comprehensive knowledge of the subjects of optics, photometry, electronic instrumentation, computing, digital image processing and video camera operation; see Bibliography. Some of the Chapters require a detailed knowledge of various specialised topics within the above areas; details are given in Chapter 5.

2. VEHICLE LIGHTING

2.1 Introduction

This description of the subject of vehicle lighting considers only headlamps; signal lamps, such as direction indicators and stop lamps, are not discussed since the project was not concerned with the testing of this type of lamp.

A vehicle's headlamp system is used in conditions of poor visibility to illuminate the road scene ahead (i.e. the road, other vehicles, pedestrians etc.) in order that it may be seen clearly by the vehicle's driver. The system also signals the presence of the vehicle to other road users.

The design of effective headlamp systems is a complex task, for the following reasons:

- a) Road scene illumination is only one of a large number of factors which influence the process of visual perception i.e. 'seeing', when undertaking the complex task of driving.
- b) The presence of a vehicle's headlamps in the field of view of the driver of another vehicle can cause him to experience the phenomenon known as glare. This occurs when an object which has a much higher luminance than the background level to which the eye is adapted appears in the field of view.

Glare may be merely uncomfortable (discomfort glare) or actually reduce visual efficiency (disability glare); see reference (3), for example. The most fundamental problem in headlamp design is that of effectively illuminating the road scene ahead for the driver of the vehicle whilst at the same time minimising glare for the drivers of other vehicles.

- c) Road layouts vary considerably. Furthermore, the position of a moving vehicle relative to a given road layout and to any other vehicles present is constantly changing.
- d) The presence and effectiveness of streetlighting influences the type of vehicle lighting required.
- e) Vehicle headlamps must not only meet various lighting performance requirements as specified by the customer (i.e. the vehicle manufacturer), and by the law (see section 2.4), but also the customer's requirements for:

- i) Styling - The Size, Shape and Appearance of the Lamp

Recent advances in headlamp manufacturing technology have enabled lamps to be made in a wide variety of shapes and sizes. Vehicle stylists have taken full advantage of these advances and virtually all new vehicles now have lamps which are unique to that particular model.

Unfortunately, styling requirements often conflict with lighting performance requirements.

ii) Environmental Performance

Headlamps must be able to withstand the wide variety of temperatures, atmospheric conditions, vibrations and contaminants that they are subjected to when fitted to a vehicle.

iii) Cost

Sacrifices in performance often have to be made in order to keep costs down to realistic levels.

- f) The effectiveness of a vehicle's headlamp system depends not only on the characteristics of the lamps, but also on their aim, i.e. the way in which their intensity distributions are positioned in relation to the road; all vehicles have a means of mechanically adjusting the aim of the lamps. Thus, the headlamp designer does not have full control over the 'on-the-road' performance of his system as fitted to any individual vehicle.

Consequently, it is not surprising that many approaches to headlamp system design have been adopted or proposed at different times and in different countries. In fact headlamp development has owed more to technical ingenuity than a carefully reasoned approach based on visual performance requirements. Information on some of the types of headlamp system which have been used in the past can be found in reference (4); this thesis considers only systems which are in current use.

Current headlamp systems provide two types of beam: the main beam, sometimes referred to as the driving beam, and the dipped beam, sometimes called the passing or meeting beam. The main beam is for use when there are no other vehicles present in the immediate vicinity and the problem of glare does not arise. The purpose of this type of beam is to provide the best possible illumination of the road scene ahead. The dipped beam is for use when other vehicles are present and restricts the illumination of the road scene ahead in order to reduce the glare experienced by other drivers to an acceptable level. It is, of course, the vehicle driver's responsibility to choose the most appropriate beam for any given driving situation.

Various types of headlamp system are used to provide these two types of beam. A motorcycle has a single lamp which provides both beams. Most other vehicles have two lamps, both of which are used to provide a contribution to both main and dipped beams. A higher level of performance can be obtained by a four-lamp system or by the addition of auxiliary lamps. These various types of system are described in more detail in section 2.2.

The basic principle of operation of each lamp in a system is the same. Luminous flux, emitted by a filament, is collected and redistributed by a reflector; a lens, consisting of many separate zones, each having different refractive characteristics, is used to provide the final shaping of the beam. A lamp can produce both types of beam by using a light source having two separate filaments, only one of which is energised at any time. The intensity of a lamp's beam varies with direction and produces a characteristic 'beam pattern' when used to illuminate a given surface; routine headlamp testing is

carried out by assessing, either qualitatively or quantitatively, the beam pattern produced on a plane test screen placed vertically in front of the lamp. This enables an experienced vehicle lighting engineer to estimate the 'on-the-road' beam pattern that the lamp will produce.

The lamp designer's basic aim is to produce a bulb, reflector and lens combination which provides an intensity distribution (and hence 'on-the-road' beam pattern) which satisfies the appropriate dipped or main beam visual performance requirements outlined above and meets the appropriate legal requirements, which are considered in section 2.4. Information about practical lamp design approaches can be found in reference (5).

Owing to the many problems facing the lamp designer, many different types of dipped and main beam intensity distributions have been produced or proposed over the years and much research has been carried out to determine their relative performance. The types of intensity distribution which are of importance today are considered in section 2.3.

2.2 Headlamp Systems

There are three basic types of headlamp system in use today:

a) The One Lamp System

The main area of application for this type of system is motorcycles. A single lamp produces both types of beam by means of a double-filament source.

b) The Two Lamp System

This type of system is found on the majority of modern vehicles and consists of two lamps each having a double-filament source. Each lamp provides a contribution to both the dipped and main beams of the vehicle.

c) The Four Lamp System

The lamps are mounted in pairs. The inner, or 'number one' units are of a single filament type and provide the main beam. The outer, or 'number two' lamps of each pair provide the dipped beams; in some instances, these units also incorporate a second filament, powered at the same time as the 'number one' units, to supplement the main beam.

A recent development is the twin-pocket lamp, which combines two reflector pockets, each with its own source, in a single unit. A pair of these lamps effectively produces a four lamp system.

The performance of a standard headlamp system can be improved by the addition of auxiliary lamps, of which there are two basic types: driving lamps and fog lamps. Driving lamps are intended to be used in conjunction with the main beam and essentially have the same type of beam pattern. Fog lamps are designed to be used instead of the dipped beam in foggy conditions and have a very wide beam with a sharp horizontal cut-off. For photometric testing purposes, auxiliary lamps can be regarded as a type of headlamp, although the test details are different.

Headlamps and auxiliary lamps can be one of two basic types: sealed beam (SB) or replaceable bulb (RB). In a sealed beam unit, the lens, reflector and filament/terminal assembly are fused into an indivisible, sealed unit which has to be replaced complete. Except for the filament/terminal assembly, SB units are generally of an all-glass construction. They are generally made as standard units and fitted to a variety of vehicles. An RB type lamp is assembled from separate components and is generally of a more complex construction than an SB unit. The major components of a typical modern RB lamp are the body (with brackets for mounting to the vehicle), the reflector (with an adjuster system for aiming the lamp when fitted to a vehicle), the lens and the bulb.

The SB and RB types of lamp both have their advantages and disadvantages (see reference (6) for example), but the greater scope for styling, aerodynamic efficiency and beam control offered by the RB type have made the SB type virtually obsolete in Europe; nearly all European cars now have custom-designed RB lamps which are used exclusively on that model. The Americans have traditionally used only

the SB type but are now starting to use the RB type also.

Many new materials and manufacturing methods have recently been developed for the RB type lamp. The most significant advance is probably the use of plastic materials for reflectors and bodies; see reference (7). Complex reflector forms, which could not be pressed in metal, can be produced by plastic moulding and provide a wide variety of styling and performance possibilities. Two important applications have been the twin-pocket lamp, described above, and the homofocal reflector; the latter consists of several segments of different focal length with a common focal point and provides the advantages of short and long focal length reflectors in one unit. Reference (8) gives more details about homofocal reflectors.

2.3 Headlamp Intensity Distributions

This section considers the types of main and dipped beam intensity distributions which are currently in use.

Although a vehicle's main and dipped beams normally consist of the light emitted by two or more lamps, beam intensity distributions are usually considered in terms of the output of one lamp for simplicity. Fig. 2.1 shows the perspective view of a road scene from the position of a vehicle's headlamp; a lamp's intensity distribution will be considered in relation to this view. (The co-ordinate systems used to represent directions from a lamp will be considered in Chapter 3.)

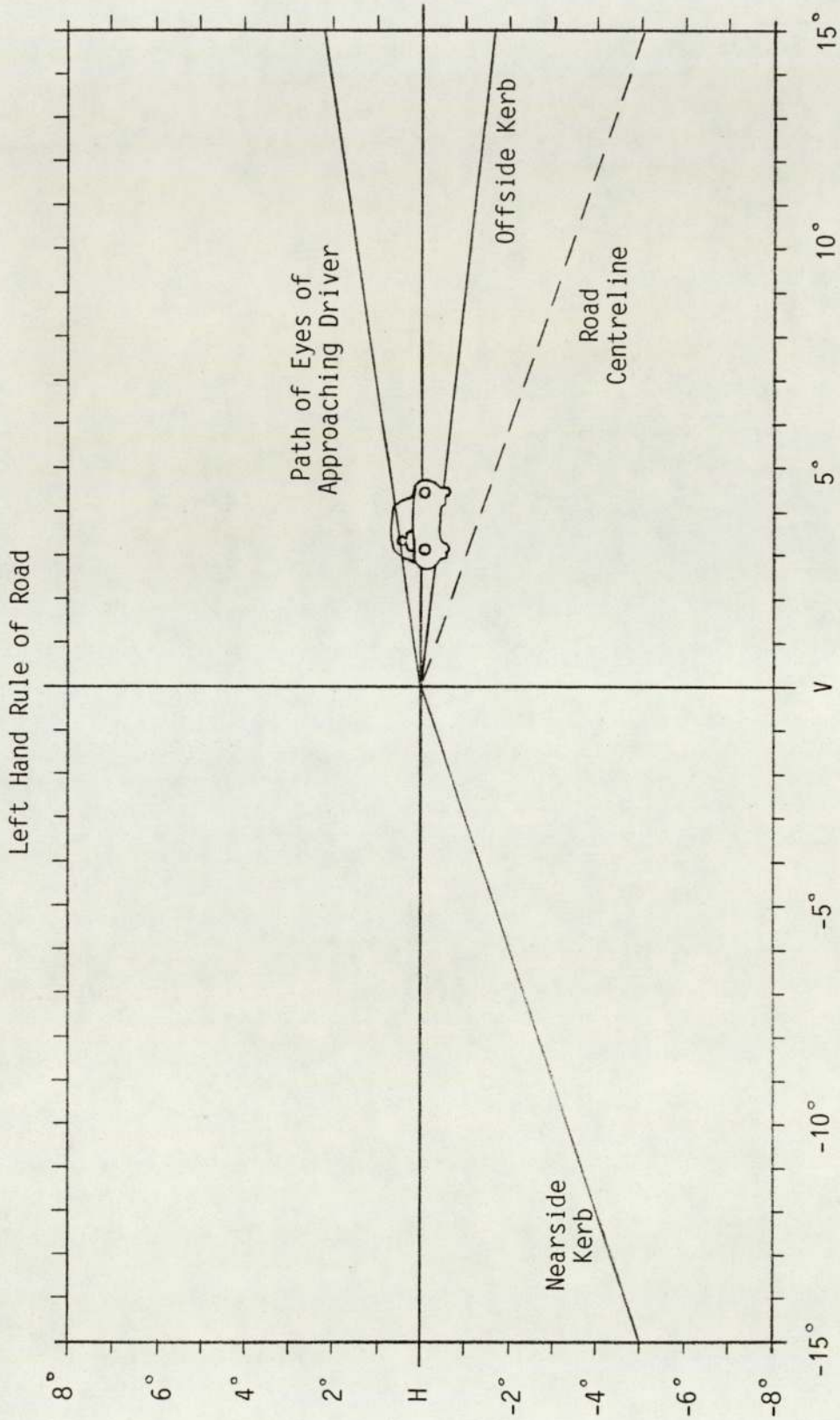


Fig. 2.1 Perspective View of a Road Scene from the Position of a Vehicle's Headlamp

a) Main Beam

Although there have been many types of dipped beam, most lamps are designed to have the same basic type of intensity distribution for their main beam output. Fig. 2.2 shows a typical lamp's main beam intensity distribution, aimed correctly in relation to the road scene. The central high intensity part of the beam illuminates the road far into the distance, with the parts of the road closer to the vehicle lit by the lower intensity parts of the beam. (The beam is intended to be used only when oncoming vehicles (see Fig. 2.1) are not present.) The distribution is essentially symmetrical and hence the same for both left and right hand rules of the road.

b) Dipped Beam

The difficulty in defining an intensity distribution which effectively illuminates the road scene ahead without dazzling an oncoming driver can be appreciated from Fig. 2.1. It is this difficulty which has given rise to the many different types of dipped beam intensity distribution which have been used or proposed over the years. Two basic types of intensity distribution, both asymmetrical, are of importance today: the European 'E' beam and the American 'SAE' beam.

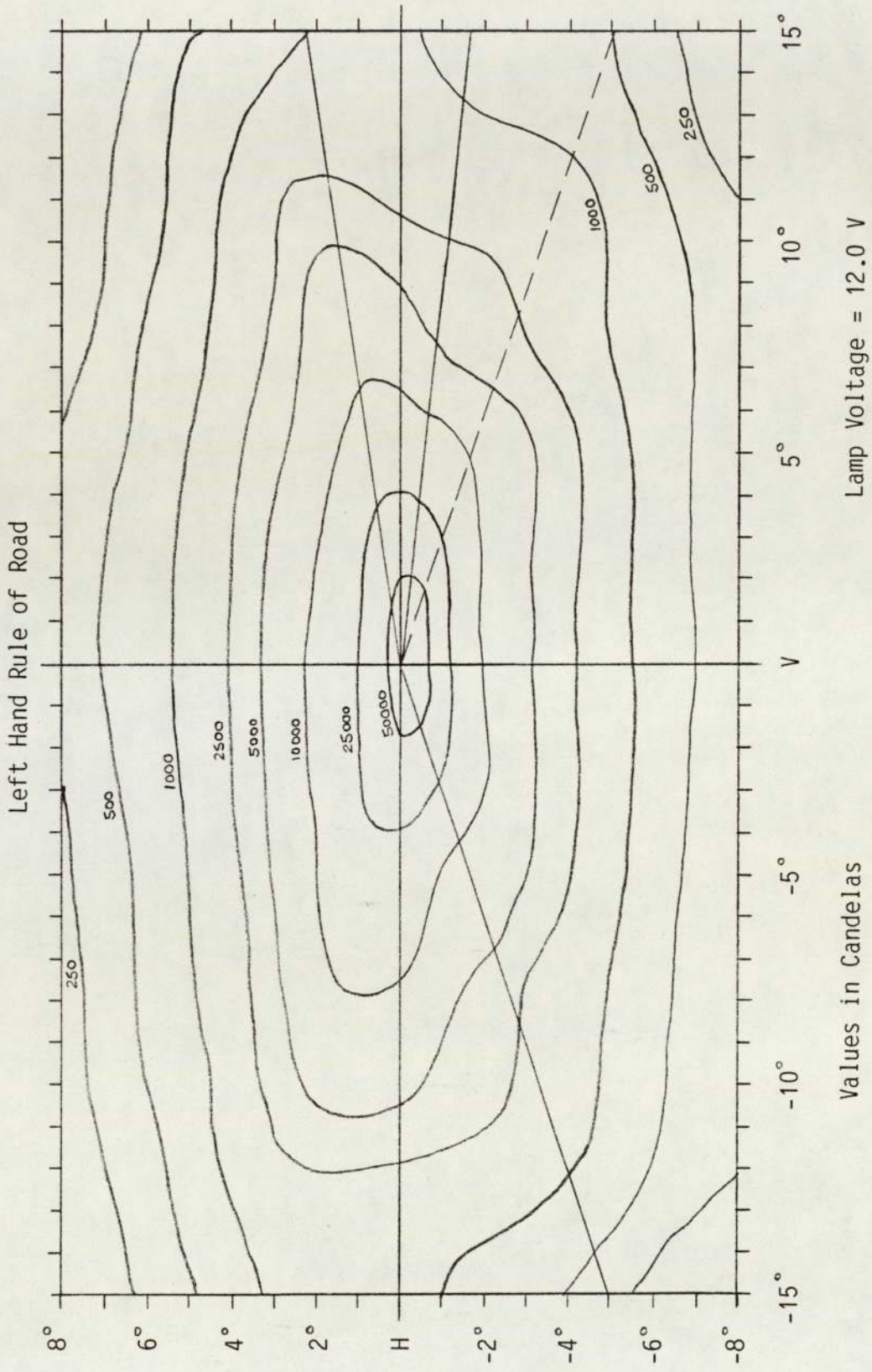


Fig. 2.2 A Typical Main Beam Intensity Distribution

i) The 'E' Beam

The 'E' beam, first introduced in about 1955, is used throughout Europe and exists in both left and right hand rule of road versions. Its specification is defined by the Economic Commission for Europe (ECE), which is part of the United Nations organisation. The 'E' beam is now used on virtually all new vehicles sold in Britain, having replaced the older 'Anglo-American' type of beam, the latter essentially being a left hand rule of road version of the 'SAE' beam (see below).

The intensity distribution of a typical lamp designed to produce a left hand rule of road 'E' beam, aimed correctly in relation to the road scene, is shown in Fig. 2.3a. It is characterized by the well-defined cut-off between the high and low intensity parts of the beam. This cut-off is horizontal on the offside of the road, to avoid dazzling the oncoming driver, and slopes at fifteen degrees above the horizontal on the nearside, to provide better illumination of the areas in the vicinity of the nearside kerb than would be provided by a totally horizontal cut-off. The sharp cut-off characteristics are produced by partially shielding the bulb filament.

ii) The 'SAE' Beam

The 'SAE' beam, which is used in America, Canada and various other countries, is named after the Society of

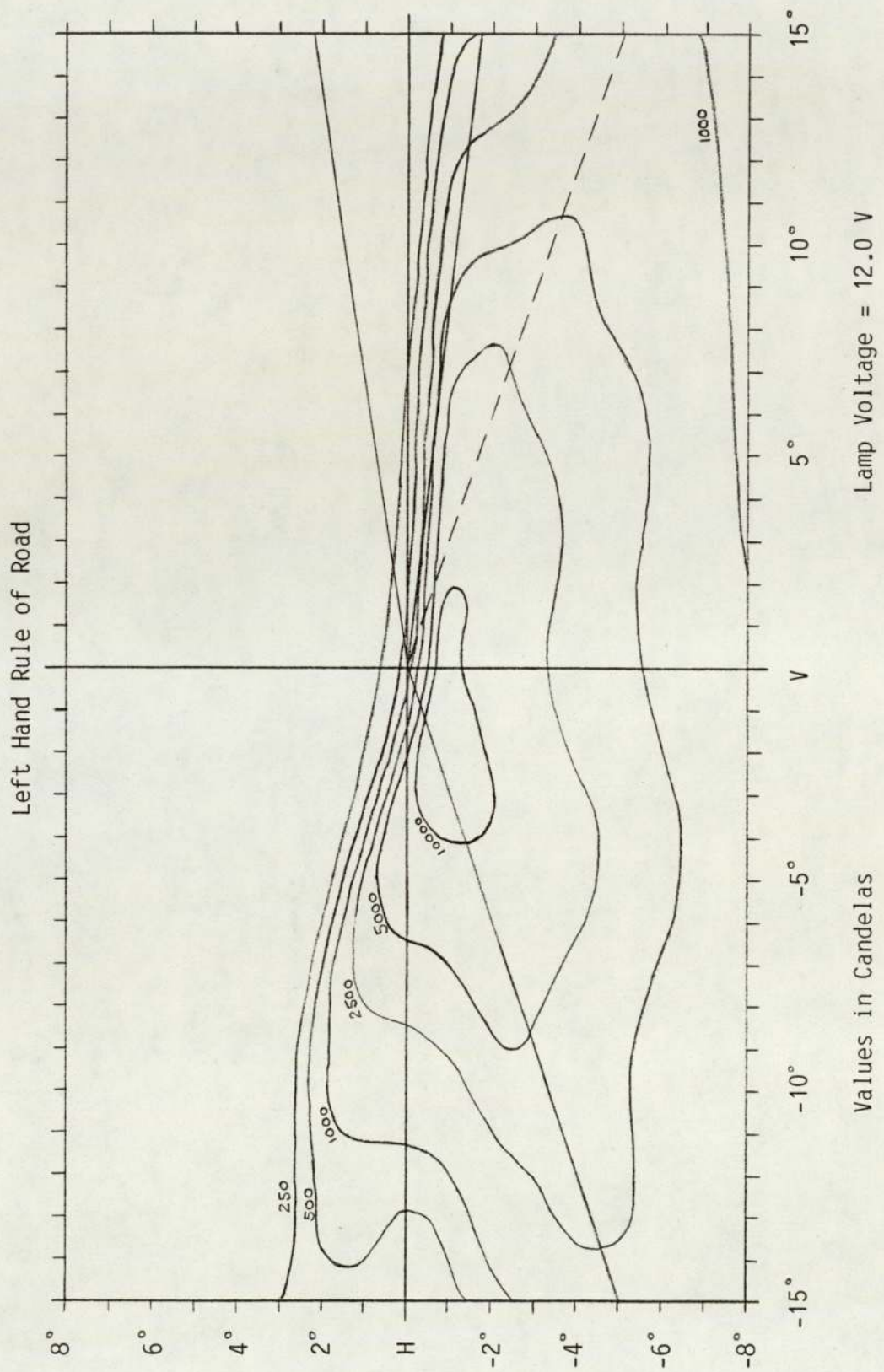


Fig. 2.3a Typical Dipped Beam Intensity Distributions - 'E' Beam (Left Hand Rule of Road)

Automotive Engineers, the American organisation which defined the required intensity distribution. Being an American standard, it is written for right hand rule of road. However, left hand rule of road versions of the beam are in use in various parts of the world, including Japan. The intensity distribution of a typical lamp designed to produce an 'SAE' beam, aimed correctly in relation to the road scene, is shown in Fig 2.3b. Compared to the 'E' beam, the intensity changes are of a more gradual nature, and the intensity values in the directions corresponding to the oncoming driver's path are higher. (It should be noted however, that the lamp supply voltages are different; the European regulations require the lamps to be tested at 12.0 V, whereas the American regulations specify 12.8 V.)

A great deal of research has been carried out into the relative merits of these two types of dipped beam but there has been little agreement amongst the various researchers, mainly because of the complex psycho-physical factors involved; see reference (7), for example.

2.4 Legal Requirements

Most countries have defined certain legal requirements for vehicle lighting. These requirements vary from country to country but are concerned with such aspects as the number and type of lamps required, their construction, mounting positions and photometric

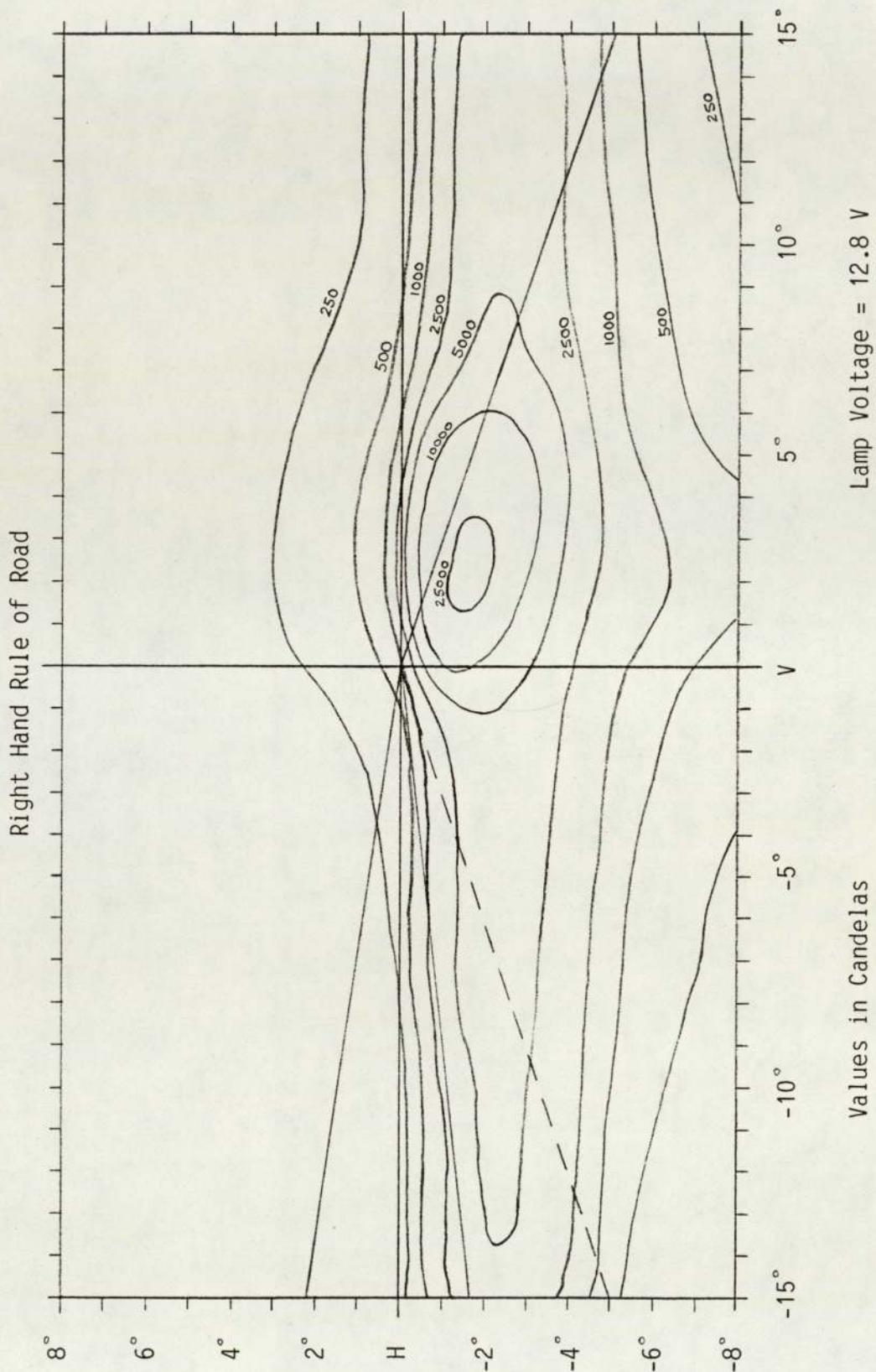


Fig. 2.3b Typical Dipped Beam Intensity Distributions - 'SAE' Beam (Right Hand Rule of Road)

performance.

The British legal requirements are based on regulations defined by the British Standards Institution (BSI) and the Economic Commission for Europe (ECE). The aspects of the regulations which are of relevance to the project are the ECE photometric specifications for main and 'E' beam performance, which are contained in reference (9). (The BSI regulations relate to lamps producing the 'Anglo-American' type of dipped beam and are of little relevance today.) These specifications effectively define certain beam intensity distribution characteristics which must be satisfied by a lamp. The specifications do not state how the quantitative data they contain is derived, but they clearly take into account not only visual performance requirements but also the performance levels which can be obtained in practice from a bulb, reflector and lens arrangement, since different minimum lamp performance levels are quoted for the various types of bulb permitted. For example, the performance required to meet the specification is lower for a lamp designed to use a gas-filled bulb than for a lamp which uses a halogen bulb. This would obviously not be the case if the specifications were based purely on visual performance considerations.

The American legal requirements are based on regulations defined by the Society of Automotive Engineers (SAE) and are mainly written for various types of sealed beam lamps. Again, the regulations do not state how the quantitative data they contain is derived.

Both the ECE and SAE regulations specify the minimum required

photometric performance levels by effectively defining minimum and/or maximum intensities for a number of critical directions in the beam and as such still allow the designer a reasonable amount of freedom to adopt a beam distribution which meets the customer's requirements.

Prototype samples of a new lamp have to be submitted to an approved test house, which is the BSI for the United Kingdom, and if they meet the requirements of the relevant regulation are granted 'type approval' allowing lamps of that type to be fitted to a vehicle.

The regulations also require that each lamp produced to a given 'type approved' design meets a certain minimum photometric standard. In the case of the ECE regulations an allowance is made for the effects of normal component and assembly variations by means of a 'production conformity' version of the specification which is less stringent than the 'type approval' version which the prototype must meet. For the SAE specifications, there is only one minimum photometric standard which should be met by both prototype and production lamps. The checking of production lamps is carried out in practice by testing batch samples; even the relatively simple photometric test required to determine whether or not a lamp meets the appropriate specification is too time-consuming to enable each individual lamp produced to be checked.

2.5 Lamp Design and Manufacture

This section gives a brief overview of the events leading to the volume manufacture of a new lamp, with the emphasis on the steps

concerning photometric performance.

- a) Most lamps are custom designed for a specific vehicle model. The starting point for the design is based on the customer's requirements for photometric performance, styling, environmental performance and cost. Many compromises are necessary and the experience of the designers plays an important role in making sure that the requirements are broadly compatible. The basic design parameters of the system, such as the number of lamps to be used and the reflector material (i.e. metal or plastic) are normally decided at this stage.
- b) The detailed mechanical and optical design of the lamp is undertaken. Again this work relies heavily on the experience of the designers; although certain photometric characteristics of a new design can be calculated or predicted by experimental work, there is no way at present of fully determining the performance in advance.
- c) The manufacturing tools are designed and made. (All major lamp components, except lenses and bulbs, are made by Lucas. Lenses are designed in-house and made by specialist glass manufacturers. Headlamp bulbs are of several standard types and are made by general lighting equipment manufacturers such as Philips and Thorn.)
- d) Prototype samples of the lamp are produced.
- e) The photometric and environmental performance of the prototypes

is assessed.

- f) If the lamp does not meet the legal or customer's requirements then design modifications must be made. Major changes necessitate re-tooling which is very expensive and time consuming.
- g) 'Type approval' is obtained, as described in section 2.4.
- h) Volume manufacture commences. Batch samples are regularly checked for conformity to the relevant specifications by the Quality and Reliability (Q&R) department, enabling production problems to be detected and corrected.

2.6 Photometric Testing - An Overview

Three methods of photometric testing are carried out by the Company: road testing, darkroom testing and production line testing. Each of these is now considered.

2.6.1 Road Testing

Road testing enables the beam distribution characteristics of a lamp or lamp system to be assessed in relation to the various visual performance requirements. It is carried out by fitting the lamps to a test vehicle and evaluating their performance at night-time under various static and dynamic conditions on both public roads and a private test track. These tests are frequently undertaken by the E&D

department and the results heavily influence lamp design philosophy.

Only qualitative assessments are normally made; it is difficult to make meaningful comparisons between quantitative measurements made on different occasions because of the variations which occur in atmospheric conditions, ambient illumination, lamp supply voltage and lamp aim.

Most of the tests undertaken involve comparing a lamp or lamp system with a suitable reference. This is achieved by fitting several systems to a single test vehicle; a switching system allows the driver to change quickly from one system to another.

Road tests play an important role in lamp development. They are, however, time consuming, inconvenient and do not generate reliable quantitative data. Consequently, they are supplemented by darkroom tests.

2.6.2 Darkroom Testing

The objective of darkroom testing is to determine, normally in quantitative terms, the beam distribution characteristics of an individual lamp for interpretation and evaluation by lighting engineers.

There are two main darkrooms on the Cannock site; one is used by the E&D department for development work and the other by the Q&R department for testing production samples.

The main purposes of the tests carried out by the E&D department are:

- a) The assessment of prototype samples of new or modified designs. Particularly important is the testing to the type approval specifications before submission to the British Standards Institution.
- b) The investigation of the effects of changes in lamp design parameters, such as bulb position, or manufacturing methods, such as reflector aluminising.
- c) The assessment of competitors' products.

Darkroom tests involve shining the lamp at a vertical test screen, normally white, placed at a suitable distance in front of the lamp. (The subject of lamp to screen distance is considered in section 3.3.1.) A beam pattern is produced on the screen, from which a lighting engineer can estimate the lamp's on-the-road beam distribution characteristics. The most important darkroom tests, however, are those which involve quantitative measurements; these are the only tests which will be considered in the remainder of the thesis.

2.6.3 Production Line Testing

The objective of production line testing is to detect any major component or assembly faults in a production lamp by means of a quick and simple qualitative check of the lamp's beam or beams. An item of test equipment known as a 'beam checker' is used; this is a compact

self-contained unit which back-projects a lamp's beam onto a small screen by means of a simple optical system. The beam can be viewed on the screen under normal factory lighting conditions.

3. QUANTITATIVE TEST METHODS AND EQUIPMENT

3.1 Basic Principles

These tests involve acquiring and presenting quantitative photometric data for a single lamp. The data consists of either the lamp's intensity values in various directions or the illuminance values it produces at various points on a given surface relative to the lamp. In both cases, the actual measurements carried out are of illuminance at points on a given surface, which will be referred to here as the measurement surface; the equivalent intensity values can be calculated from the illuminance measurements by means of the inverse-square and cosine laws of illumination. (See Appendix A.) The basic task to be performed by a headlamp photometry system, therefore, is the measurement of point illuminance values.

For a plane surface, the illuminance at a point, E , is defined as the luminous flux, dF , incident on a small element of the surface surrounding the point, divided by the area of the element, referred to here as the flux collection area, dA .

Thus
$$E = \frac{dF}{dA}$$

It is important to note, therefore, that when the term 'illuminance at a point' or 'point illuminance' is used it refers to a point on a given plane and that if the orientation of that plane is changed then, in general, the illuminance at that point will also change. (It is possible to define non-directional measures of

illuminance (10) but these are not used in the field of headlamp photometry.)

The apparatus traditionally used in the vehicle lighting industry for measuring the light distribution characteristics of a lamp is a goniophotometer, which essentially consists of a goniometer and a stationary photodetector, as shown in Fig. 3.1.

The term photodetector is used here to mean a device for measuring point illuminance values; photodetectors are considered in detail in Chapter 4.

A goniometer is a mechanical device for mounting a lamp and turning it through horizontal and vertical angles to enable any direction in the lamp's beam to be aligned with the photodetector. There are two possible types of goniometer construction, the difference being in the way the horizontal and vertical axes of rotation interact. The goniometers are referred to by the SAE as type A and type B (11) and are shown in Fig. 3.2. With the type A goniometer, the position of the axis of rotation for the vertical setting is fixed i.e. it is not affected by the horizontal setting; the position of the axis of rotation for the horizontal setting, however, changes as the vertical setting is adjusted. The opposite situation applies to the type B goniometer.

The goniometer and photodetector should be positioned such that:

- a) the axis of the photodetector passes through the point of intersection of the goniometer's axes of rotation

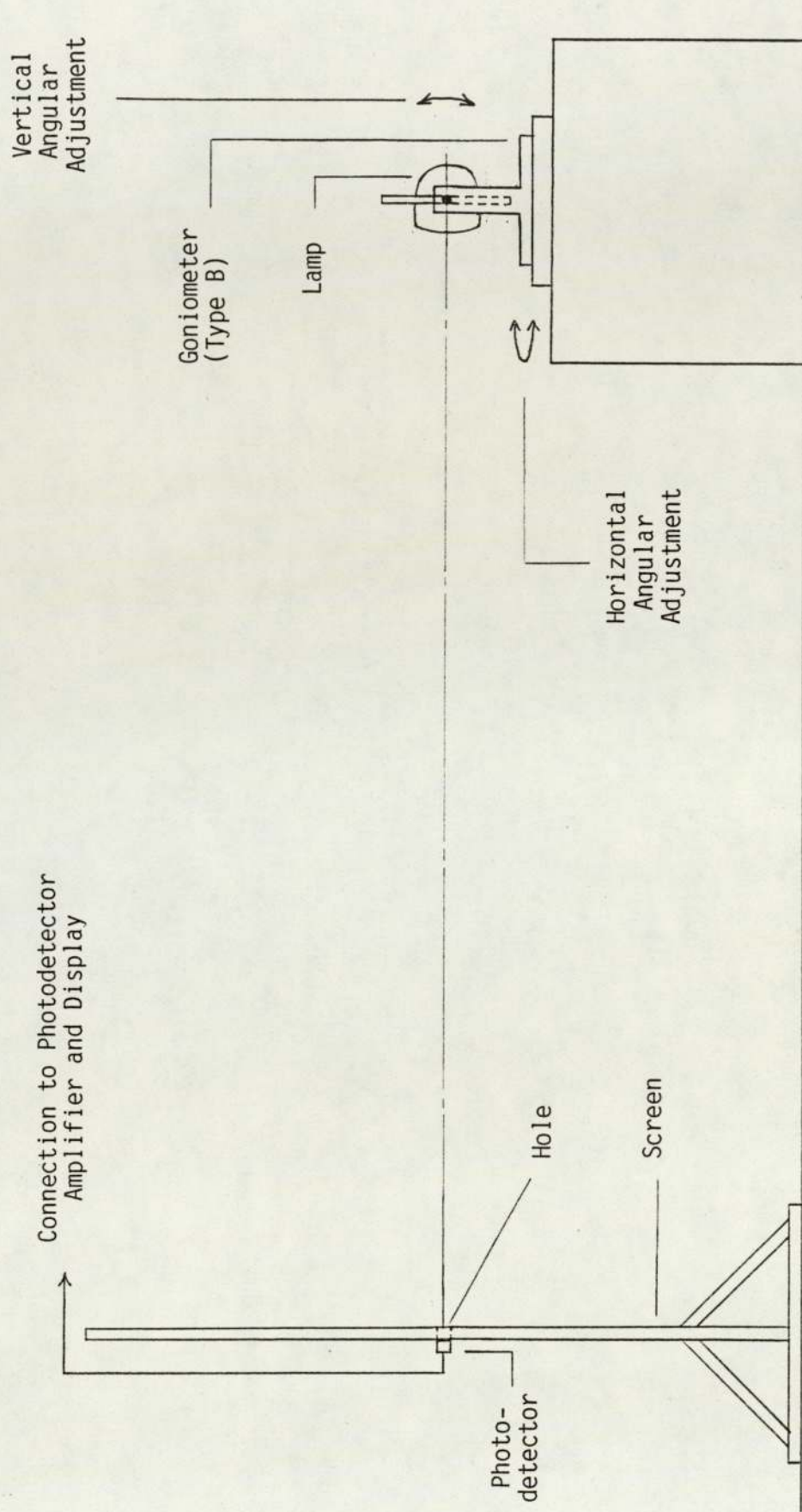
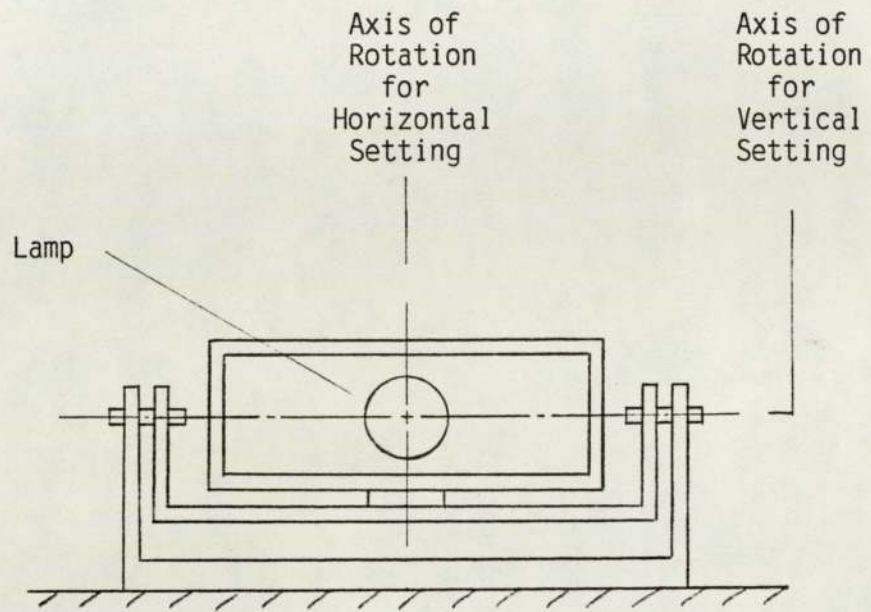
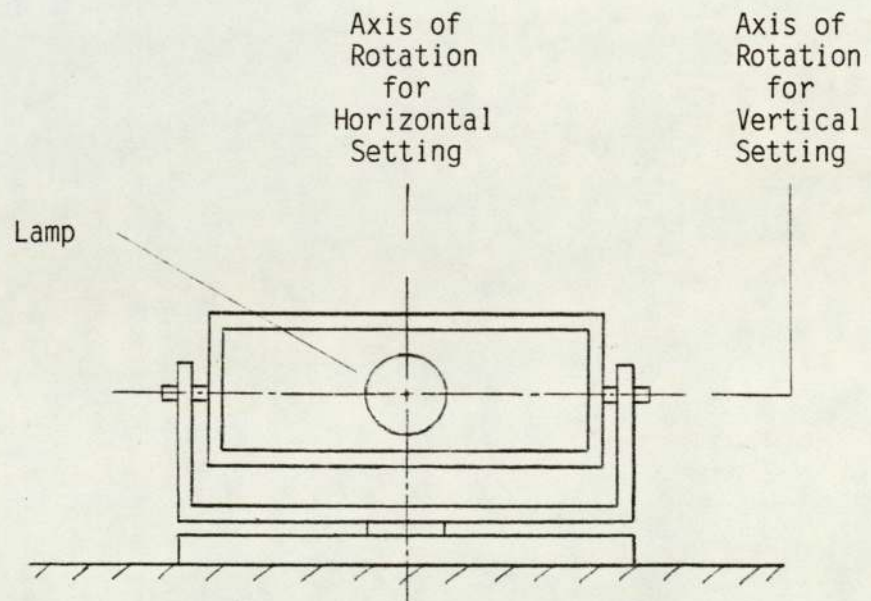


Fig. 3.1 Principle of Goniophotometer Operation



a) Type A Goniometer



b) Type B Goniometer

Fig. 3.2 Principle of Operation of Type A and B Goniometers

- b) the goniometer's fixed axis of rotation is perpendicular to the axis of the photodetector.

The subject of photodetector to lamp distance is considered later.

The overall test procedure for measuring a lamp with a goniophotometer varies with the type of lamp and the number and types of beams it produces. The procedure for measuring a single-pocket lamp producing an 'E' type dipped beam and a main beam is given below as an example.

- a) The goniometer is adjusted such that the non-fixed axis of rotation is perpendicular to the axis of the photodetector.
- b) The lamp is mounted on the goniometer and a specified voltage applied to the dipped beam filament of the bulb. (A pre-calibrated bulb is normally used, the voltage being set to give a specified flux output; bulbs are calibrated using an integrating sphere (12).)
- c) The lamp is aimed, which, for this type of lamp involves positioning the horizontal and sloping cut-off areas of the beam relative to certain reference points and lines on the test screen in such a way that certain criteria are met. (Other types of lamp use different aiming procedures. For example, American lamps are aimed mechanically; the procedure involves positioning the lamp so that its physical orientation relative

to the photodetector and test screen satisfies certain criteria and is carried out without reference to the actual beam produced.)

- d) The required dipped beam point illuminance measurements are made, the number and the positions of the points to be measured depending on the type of test being carried out; see section 3.2.

- e) A specified voltage is applied to the main beam and a second set of measurements made; the aim of the lamp is not changed since one of the important requirements for any lamp producing both dipped and main beams is that the positional relationship between the two satisfies certain criteria.

By making measurements with a goniophotometer, the photodetector is always at the same distance from the lamp and always perpendicular to the flux being measured. Consequently, this is equivalent to taking readings on a spherical surface centred on the lamp, with a radius equal to the perpendicular distance between the lamp and the photodetector. (This spherical surface does not, of course, physically exist in the test set-up.) For a given point on the spherical surface, the plane of measurement in the definition of illuminance given above is that plane which passes through the point and whose normal at the point passes through the centre of the goniometer. The BSI and SAE regulations are based on the use of a spherical test surface.

Points on the spherical measurement surface, or the equivalent

directions from the centre of the lamp, are most conveniently described by the use of a spherical co-ordinate system, which requires the definition of a polar axis and a zero meridian (13). For each of the two goniometer types there are polar axis and zero meridian positions which result in the numerical values of the spherical co-ordinates of a given point on the surface being equivalent to the angular adjustments of the goniometer required to bring the flux reaching that point onto the photodetector; see Fig. 3.3. The positions of the polar axes and zero meridians are different for each type of goniometer; thus the numerical co-ordinate values of a given point on the spherical measurement surface, and hence the goniometer adjustments required to measure the illuminance at this point, are different for each type of goniometer. For angles of less than 5° the differences are small and the two goniometer types can be considered equivalent. For larger angles, however, these differences must be taken into account otherwise large errors will be produced; conversion formulae are given in reference (11). The SAE regulations are based on the use of a type A goniometer.

The ECE regulations define minimum and/or maximum illuminance values for a series of points and zones, specified by a rectangular cartesian co-ordinate system, on a plane vertical test screen mounted at 25 m from the lamp. Although it would be possible to make ECE test point measurements by keeping the lamp stationary and moving the photodetector to each point of interest, this would not be very convenient in practice. Consequently, a conventional goniophotometer system is used by both the Company and BSI to carry out testing to ECE regulations, the direction of each test point on the plane test screen being calculated in terms of the goniometer movement required and

The lamp is mounted on a type A goniometer whose axes of rotation are initially positioned as shown. Horizontal and vertical adjustments of α° and β° respectively, as shown, enable the illuminance at point S to be measured by the photodetector.

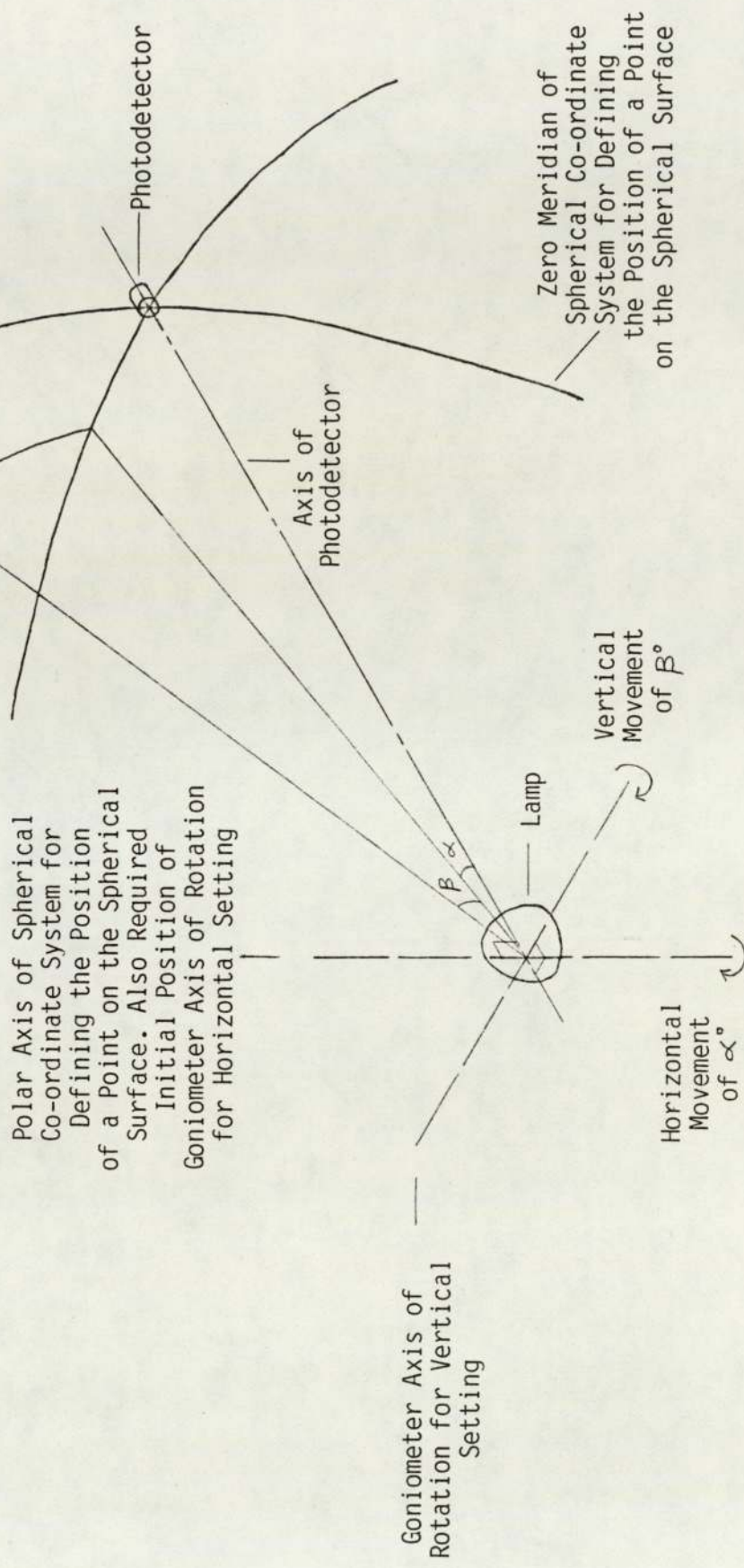


Fig. 3.3a Co-ordinate System for Type A Goniometer

The lamp is mounted on a type B goniometer whose axes of rotation are initially positioned as shown. Horizontal and vertical adjustments of γ° and δ° respectively, as shown, enable the illuminance at point T to be measured by the photodetector.

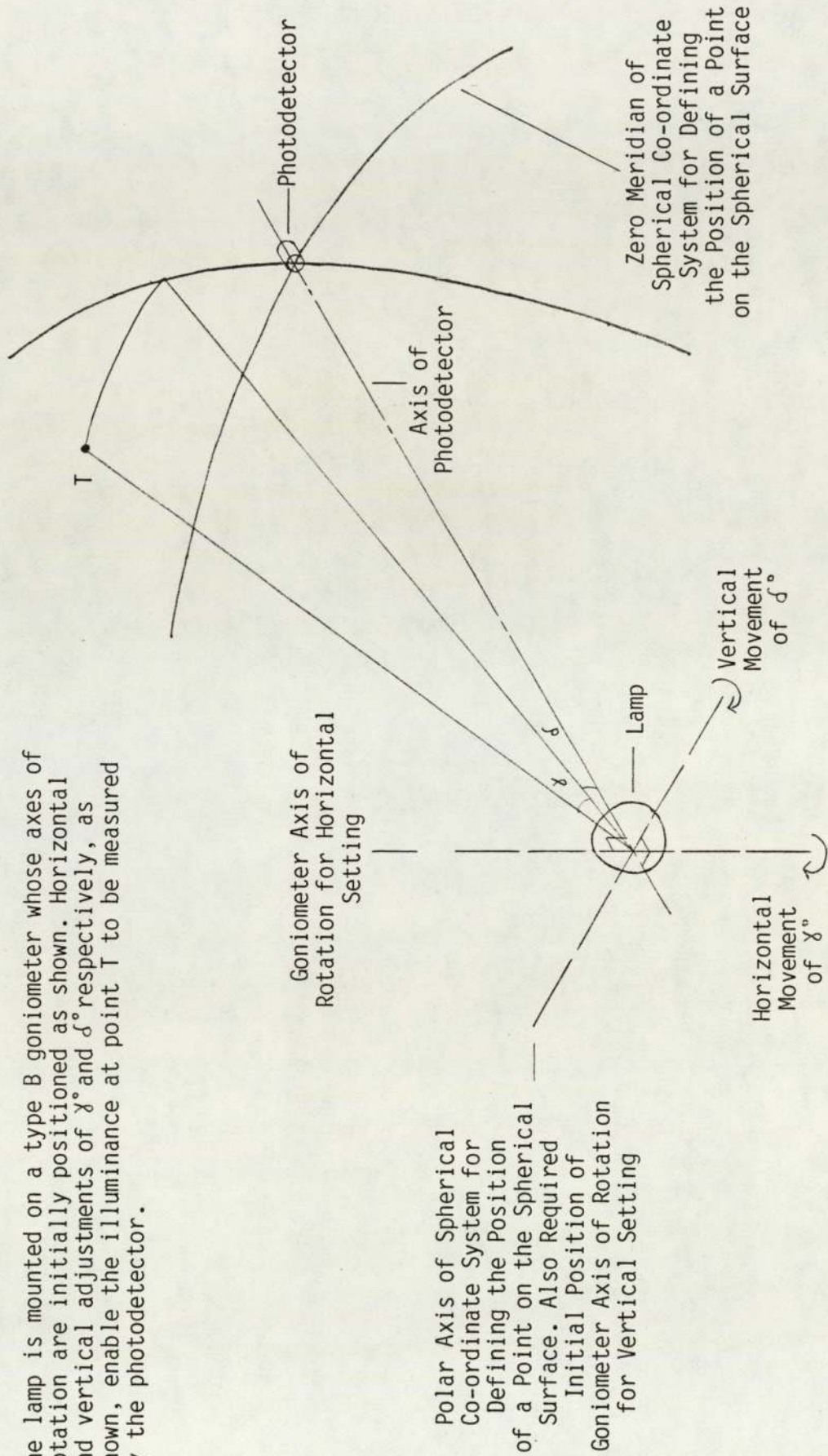


Fig. 3.3b Co-ordinate System for Type B Goniometer

illuminance measurements made in the normal way.

The geometric and photometric relationships between plane and spherical measurement surfaces are now considered.

Fig. 3.4 shows a lamp which has an intensity I in the direction defined by angles α and β , where α and β are measured for a type A goniometer; see Fig. 3.3a. Fig. 3.4 also shows plane and spherical measurement surfaces, both of which lie at a distance d from the lamp.

The point of intersection of the direction being considered with the spherical measurement surface, S , is conveniently defined by angles α and β . For the plane measurement surface, the point of intersection, P , is conveniently defined by the rectangular cartesian co-ordinates x and y .

x and y are related to α and β by the equations:

$$x = d \cdot \tan \alpha \quad (3.1)$$

$$y = d \cdot \tan \beta \cdot \sec \alpha \quad (3.2)$$

Point S lies at a distance d from the lamp. The illuminance at point S , E_S is given by the equation:

$$E_S = \frac{I}{d^2} \quad (3.3)$$

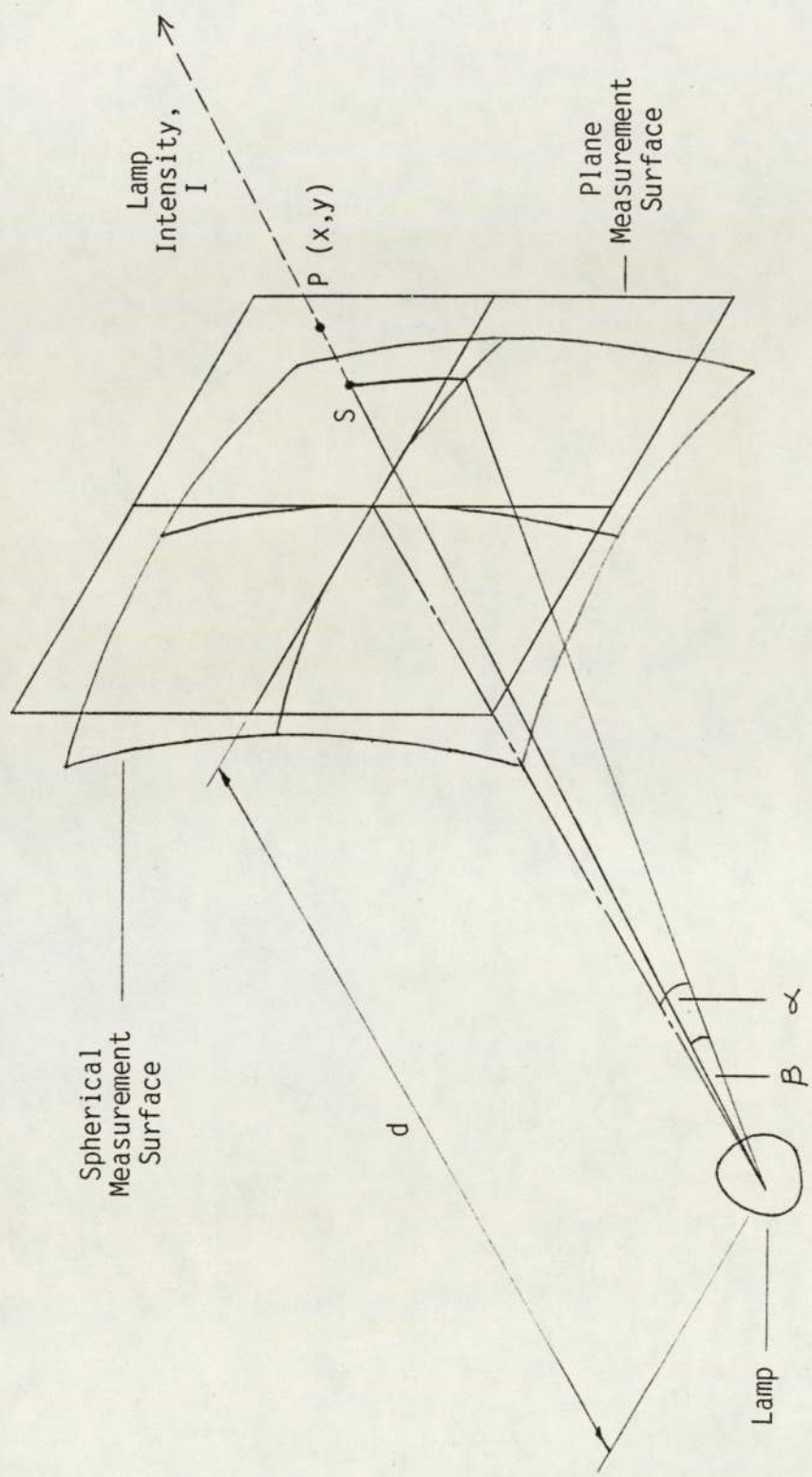


Fig. 3.4 Plane and Spherical Measurement Surfaces

Point P lies at a distance (d. sec α . sec β) from the lamp.
The illuminance at point P, E_p , is given by the equation:

$$E_p = \frac{I \cdot \cos^3 \alpha \cdot \cos^3 \beta}{d^2} \quad (3.4)$$

Therefore

$$E_p = E_s \cdot \cos^3 \alpha \cdot \cos^3 \beta \quad (3.5)$$

3.2 Types of Test

Three basic types of test are carried out using goniophotometer systems: point to point, iso-lux and cross-section.

3.2.1 Point to Point Tests

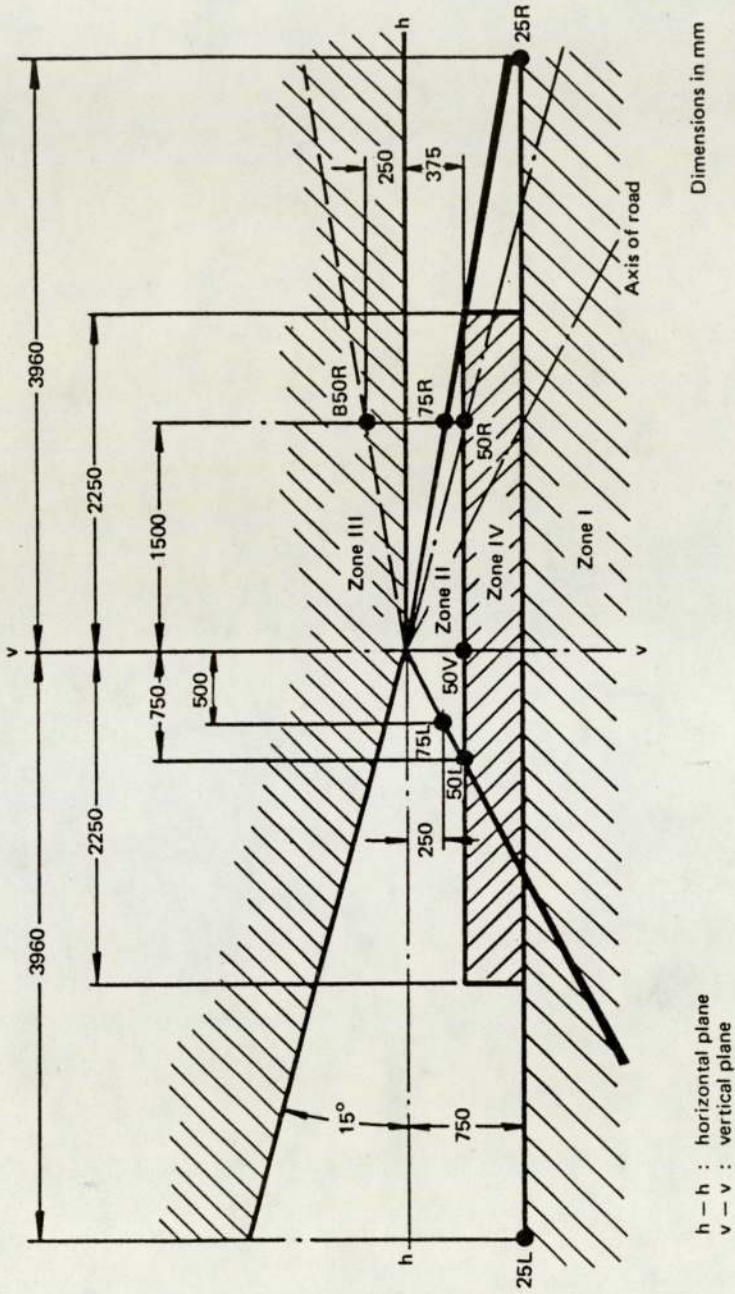
Point to point tests are carried out by taking illuminance readings at a small number of points (generally between ten and thirty) on the measurement surface. It is this type of test which is used to determine whether or not a lamp meets the appropriate legal requirement. For development work, additional points to those given in the regulations are often measured to provide more details of the lamp's characteristics.

There are various SAE regulations for the types of lamps permitted in America. The required lamp performance levels are specified as minimum and maximum intensities in various directions, defined by spherical co-ordinates. The rationale behind the choice of test directions and intensity levels for the various types of beam is

not given in the regulations.

The derivation of the test points at which measurements are required for the ECE regulations is easy to understand in principle, although they do not give full details. The test screen is considered as a perspective view of the road ahead as 'seen' by the headlamp. By defining the dimensions of a 'standard' road, and the position of the lamp and test screen relative to this road, points on the test screen which correspond to points on the road can be found by projecting lines from the lamp to the screen and the road. Similarly points on the screen which correspond to the directions in which it is important to minimise glare can also be found. The ECE regulation dipped beam test points and zones, for left hand rule of road, are shown in Fig. 3.5; the points are assigned names which reflect their corresponding three-dimensional positions but details of the 'standard' road and the assumed lamp position are not given in the regulations. The minimum and maximum illuminance values specified for the dipped beam test points and zones in the 'type approval' version of ECE regulation 20 are given in Table 3.1; this regulation applies to lamps using the H4 type of bulb.

A point to point test takes several minutes; when there are a large number of points to be measured, it is significantly quicker to use an automatic, rather than a manual, goniophotometer; see section 3.3.1.



The ECE Regulations specify test points and zones on a plane test screen mounted at 25 m from the lamp. This diagram shows the dipped beam points and zones for left hand rule of road.

Fig. 3.5 ECE Regulation Dipped Beam Test Points and Zones (Left Hand Rule of Road)

| TEST POINT | ILLUMINANCE AT 25 m (LUX) | |
|------------|------------------------------------|---------|
| | MAXIMUM | MINIMUM |
| B50R | 0.4 | - |
| 75L | - | 12 |
| 75R | 12 | - |
| 50R | 15 | - |
| 50L | - | 12 |
| 50V | - | 6 |
| 25R | - | 2 |
| 25L | - | 2 |
| Zone III | 0.7 | - |
| Zone IV | - | 3 |
| Zone I | 2 x Measured Illuminance at 50L | - |

Notes:

- i) The above values are from Regulation 20, which specifies a minimum main and dipped beam performance level for headlamps which use the H4 type halogen bulb.
- ii) The values given are the dipped beam 'type approval' requirements for left hand rule of road lamps; the 'production conformity' requirements are less stringent. (See section 2.4.)

Table 3.1 Example of ECE Regulation Photometric Requirements

3.2.2 Iso-Lux Tests

These tests involve taking readings at a large number of points and plotting a diagram showing illuminance contours (to give an iso-lux diagram) or intensity contours (to give an iso-candela diagram). These tests are more complex and time consuming than point to point tests but provide a much more comprehensive picture of a lamp's characteristics. They are at present carried out only by the E&D department for development work.

There are two basic methods of producing an iso-lux or iso-candela diagram. The first, used with manual goniophotometers, involves choosing a required illuminance or intensity contour value, using the goniophotometer to 'follow' this value around the beam and directly plotting the positions at which it occurs on the diagram. The procedure is repeated for all values of interest. Producing an iso-lux diagram in this way can take several hours, and there is always the danger of missing multiple contours of a given value. The second method involves taking illuminance readings at an array of predetermined points and then mathematically deriving and plotting the required contours from this data. The E&D department Automatic Photometer uses this method, and reduces the time taken to produce an iso-lux diagram to tens of minutes.

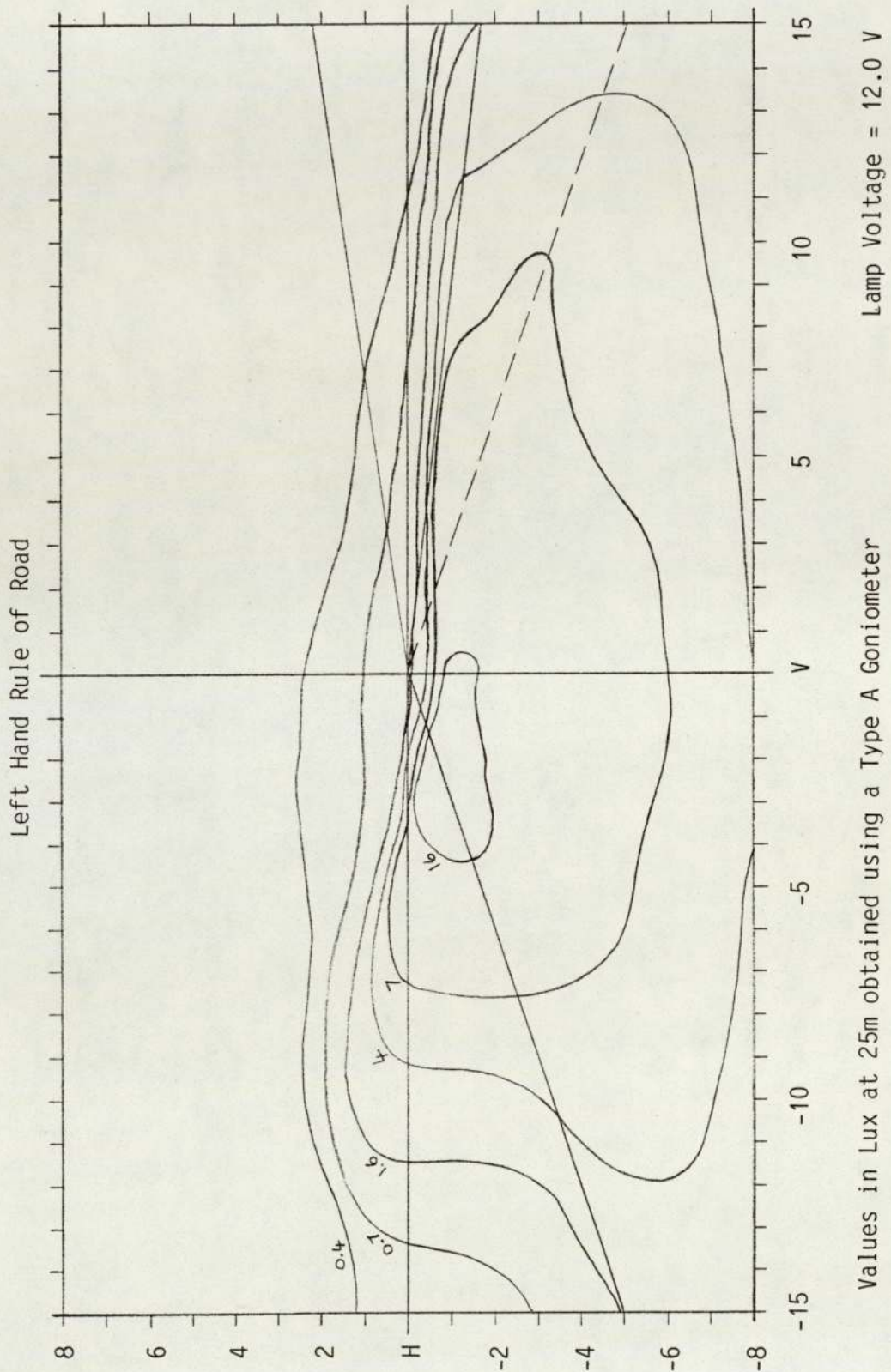
Having acquired illuminance data from a spherical surface, it must now be represented on a two-dimensional diagram. This is the same problem faced by the map-maker and it cannot be achieved without some type of distortion. Consequently, cartographers have developed a variety of different map projections, each with its advantages and

disadvantages; see reference (14), for example. In the vehicle lighting industry, however, the approach used is to plot a diagram in which the two angular variables of position are drawn as a simple rectangular grid. For small angles, the diagram can also be considered as a view of the test screen and a perspective view of the road ahead. Consequently, diagonal lines representing the road and the path of the oncoming driver, as used on the ECE test screen, are often shown on the diagram as well. It should be noted that the positions of these lines are only approximate, although the errors are not significant for small angles.

Iso-lux diagrams are typically plotted over an angular range of $\pm 15^\circ$ horizontally and $\pm 8^\circ$ vertically (represented by $\pm 15^\circ$ H, $\pm 8^\circ$ V). When a lamp's wide angle characteristics are of interest, the range is typically extended to $\pm 30^\circ$ H, $\pm 8^\circ$ V. An example of an iso-lux diagram is shown in Fig. 3.6.

3.2.3 Cross-Section Tests

These tests are carried out by making illuminance measurements at a series of points along a given line on the measurement surface and presenting the results as a table of values or as a graph of illuminance or intensity as a function of position. The data is acquired by taking readings for various angular positions on one axis of the goniometer whilst the other is kept in a fixed position. This type of test, which can be carried out in a few minutes, is not as important as the other two but is useful for showing certain beam characteristics. Like iso-lux tests, they are presently used only for



Values in Lux at 25m obtained using a Type A Goniometer

Fig. 3.6 An Example Iso-Lux Diagram

development work.

3.3 Practical Test Equipment

3.3.1 Types of Goniophotometer

Many different goniophotometer systems of varying complexity have been developed over the years. There are six main areas in which they differ:

a) Usage - Headlamp or Signal Lamp

Signal lamp testing is carried out in the same basic way as headlamp testing, but:

- i) is restricted to point to point testing
- ii) involves measuring points over a larger angular field
- iii) requires a photodetector capable of accurately measuring coloured light at low illuminance levels.

Consequently, the detailed design of headlamp and signal lamp goniophotometer systems varies.

b) Manual or Automatic

With a manual goniophotometer, the operation of the goniometer and the recording of the photodetector reading are carried out

by hand. This type of system can be used to carry out all three types of test; iso-lux tests, however, are very tedious and time-consuming. With an automatic goniophotometer (normally known as simply an automatic photometer), the goniometer is motorised and has a control system which enables it to step through a series of pre-determined points; furthermore, the illuminance reading at each point is automatically recorded. The first systems of this type were designed only for point to point testing but the latest equipment can perform all three types of test. The various automatic photometers are described in more detail in section 3.3.3.

c) Full or Reduced-Length

A distance of greater than about 15 metres is required between the lamp and the test screen for the beam pattern and the illuminance measurements to be meaningful (see Appendix A); the ECE and SAE regulations specify 25 metres and 60 feet respectively. The type of goniophotometer required therefore occupies a considerable amount of space. A method of reducing the space required has been in use for many years, however, and is described in section 3.3.2.

d) Goniometer Type

As described previously, there are two basic types of goniometer construction, both types being in use within the Company. All of the Company's goniophotometer systems built

within the last few years use a type A goniometer, as recommended by the SAE regulations.

e) Photodetector Type

Several different types of photodetector have been used in the Company's goniophotometers over the years. At the start of the project, all of the existing systems used vacuum tube or selenium barrier cell photodetectors; details of these types of device can be found in reference (15). For the E&D department Automatic Photodetector, however, the author chose the more modern and more suitable silicon photodiode type of device. In addition, several of the older photodetectors were replaced by silicon devices during the course of the project.

Photodetectors are considered in more detail in Chapter 4.

f) Flux Collection Area

The size and shape of the flux collection area (normally equal to the light sensitive area of the photodetector) affects the value of the illuminance reading produced for a point in the beam when it lies in an area of non-uniform illuminance, which is, of course, nearly always the case with the type of beams measured in headlamp photometry. The variations are potentially the highest with the 'E' type dipped beam because of the high illuminance gradients in the cut-off regions.

It is surprising, therefore, that there is no agreed standard within the industry for the size of the area to be used.

Traditionally, the SAE regulations have not provided any guidelines regarding the size of the area to be used, although this situation changed with the 1984 edition, reference (11). This publication states that 'the actual effective area of the sensor used for making the photometric measurements should fit within a circle whose diameter is approximately 0.009 times the distance from the measured light source to the sensor'; no lower limit or reasoning behind the choice of upper limit is given in the regulation although it is stated that 'some differences in measurements due to large differences in sensor sizes may be experienced, particularly in areas of high luminous intensity gradients'. The ECE regulations state that the illuminance values 'shall be measured by means of a photo-receptor, the effective area of which shall be contained within a square of 65 mm side'; this is for a lamp to screen distance of 25 m. Again no lower limit or reasoning is given in the regulations.

The flux collection areas of the Company's goniophotometers vary with the type of photodetector used; in all cases, however, the sizes are below the maximum limits given above. As mentioned previously, the flux collection area normally corresponds to the light sensitive area of the photodetector used. Sometimes, however, when the light sensitive area of the photodetector is not of a suitable size, then a simple lens system is used to collect light falling on an aperture of the required flux collection area and re-distribute it onto the light sensitive area of the photodetector.

3.3.2 Reduced-Length Photometers

If a large convex lens is placed in front of a headlamp, then the beam pattern which would be produced on a test screen at infinity will now be produced at a reduced size on a test screen in the focal plane of the lens. For any other required lamp to screen distance, for example 25 m, there is a corresponding new screen position between the lens and its focal plane. For conciseness, a screen placed at the required imaging distance will subsequently be referred to as the 'far screen', and the screen used in conjunction with the lens as the 'near screen'.

The various distances involved are related by the equation:

$$\frac{1}{v} = \frac{1}{f} + \frac{1}{(d-x)} \quad (3.6)$$

where

d = Distance of lamp to far screen

x = Distance of lamp to lens

f = Focal length of lens

v = Distance of lens to near screen

If m is the magnification i.e. (size of near screen image)/(size of far screen image), then

$$m = \frac{v}{(d-x)} \quad (3.7)$$

Appendix B gives the derivation of these equations.

The lens characteristics determine how closely the image produced on the near screen relates to that which would be obtained on the far screen. Since the illuminance measurements are all made on-axis, however, they are not affected by the quality of the image on the remainder of the screen. The on-axis near and far screen illuminance values are related by the equation:

$$E_{NSC} = k \cdot E_{FSC} \quad (3.8)$$

where

E_{FSC} = Illuminance on a circular photodetector of diameter s mounted on the axis of the system at the far screen

E_{NSC} = Illuminance on a circular photodetector of diameter $(m.s)$ mounted on the axis of the system at the near screen

k = A constant.

The value of k can be determined for a practical reduced-length photometer by calibrating with a lamp of known intensity; the photodetector system is normally designed to display the equivalent far screen illuminance value.

Most of the Company's present goniophotometers use either 2 m

or 4 m focal length plano-convex lenses, the resulting systems being known as 2 m or 4 m reduced-length photometers.

3.3.3 Automatic Photometers

The main developments in photometric test equipment have been in the area of automation to overcome the limitations of the conventional manual goniophotometer. Three different types of 'Automatic Photometer' have been produced within the Company to date and are described below.

- a) The first system was commissioned in about 1972 for the point to point testing of signal lamps. It essentially consists of:
 - i) a motorised goniometer with a paper-tape operated control system and position display system
 - ii) a photodetector with DVM display and teletype hard copy system, synchronized with (i).

This system makes measurements at a pre-determined series of points, coded on paper-tape, and provides a print-out of the result. Two systems of this type were produced, one for development work and one for production sample testing. They were originally used at the Hall Green, Birmingham site but are now at Cannock. They are still in limited use but their obsolete hardware makes them difficult to maintain.

- b) The second system, commissioned in 1978, was designed for the

point to point testing of headlamps by the Q&R department at Cannock. It essentially consisted of:

- i) a motorised goniometer with control and position display system
- ii) a photodetector and DVM display
- iii) an eight bit microcomputer system (computer, teletype and floppy disc system) interfaced to the above.

This system was similar to the signal lamp point to point system but stored the test point sequences on floppy disc. The results could be stored on disc in addition to being printed out.

The system was upgraded to the same specification as the E&D Automatic Photometer (see below) in 1985.

- c) The third system, commissioned in 1982, was designed for the testing of headlamps by the E&D department at Cannock. It was based around similar hardware to the Q&R system, but was designed to extend significantly the automatic photometer concept. It provides comprehensive data acquisition, processing and storage facilities for point to point, iso-lux and cross-section tests by means of a suite of software running under a general purpose operating system on the rig's microcomputer. The basic concepts behind the software were developed by the author in conjunction with ERA Technology of

Leatherhead, Surrey, who were commissioned to write it. This photometer system is relevant to this project because:

- i) the design, construction and commissioning of the rig took longer than planned and occupied most of the author's time during the first six months of this project; see section 5.1

- ii) the rig's design concepts, and the experience gained from implementing them, have influenced the approach to the design of the proposed video and high-speed photometers.

Consequently, this equipment is described in more detail in Chapter 6.

4. PHOTODETECTOR SYSTEMS FOR HEADLAMP PHOTOMETRY

4.1 General Considerations

In a headlamp photometer, the required point illuminance values are obtained by means of a photodetector system, which normally consists of the photodetector itself and associated electronic circuitry; the photodetector converts the luminous flux falling on it into an electrical voltage or current, which is then measured and indicated to the user by the appropriate circuitry.

The ideal photodetector has a constant and accurately known responsivity for all measurement conditions of interest, where responsivity is defined by the equation:

$$\text{Responsivity} = \frac{\text{output voltage (or current)}}{\text{illuminance}} \quad (4.1)$$

Such a photodetector would enable an unknown value of illuminance to be determined by measuring the voltage or current produced and applying the equation:

$$\text{Illuminance} = \frac{\text{output voltage (or current)}}{\text{responsivity}} \quad (4.2)$$

A practical photodetector, however, does not have a constant and accurately known responsivity. In addition, the circuitry used to measure and indicate the photodetector output voltage or current can introduce further inaccuracies. In general, however, it is the photodetector itself which is the critical element and determines the

overall performance of the system. The main problem areas which can be encountered with a practical photodetector are as follows:

- a) Its light sensitive area may not equal the required flux collection area.
- b) It may have a spectral response which differs from the required $V(\lambda)$ (i.e. photopic) response, as defined by the International Commission of Illumination in 1924; see references (16, 17).
- c) Its sensitivity may be of an unsuitable value i.e. the photodetector may:
 - i) Produce an insufficiently large voltage or current output for the minimum illuminance value to be measured

and/or
 - ii) Saturate at some illuminance value below the maximum to be measured.
- d) It may have a non-linear illuminance/output signal relationship.
- e) It may produce an output when not illuminated i.e. a dark signal.
- f) It may produce noise, in addition to the required signal.
- g) Its speed of response to changes in illuminance may be too slow.

- h) The variation of output signal as a function of the angle of incident flux may not match the true variation in illuminance as described by the cosine law.
- i) Its characteristics may vary with temperature.
- j) It may exhibit:
 - i) Memory effects i.e. previous levels of illuminance influence the output signal

and/or
 - ii) Ageing effects i.e. its characteristics gradually change with time.
- k) It may have characteristics which differ slightly from the 'typical' characteristics quoted by the manufacturer.

Consequently, any practical photodetector system has to be carefully calibrated, which involves illuminating the photodetector system with various known values of illuminance; this procedure is performed by means of a standard lamp whose intensity is known. However, the characteristics of incandescent lamps are such that a lamp's intensity can vary when set up on different occasions and during the time taken to carry out the calibration procedure. Consequently, the basic accuracy with which the intensity of the calibrating source is known is much lower than, say, a standard voltage source for calibrating voltmeters.

Furthermore, the calibration procedure itself can easily introduce further inaccuracies; for example, it may be difficult to align exactly the lamp's reference direction with the photodetector.

As a result of the relatively low accuracy of the standard lamps, the problems involved in using these to calibrate a photodetector system and the fact that photodetector systems do not have constant responsivities for all measurement conditions of interest, it is not possible to measure illuminance with the same level of accuracy that most other physical quantities can be measured. Furthermore, it is often difficult to estimate the level of accuracy of any given system. In general it is not realistic to expect the results obtained from two different calibrated photodetector systems to agree to better than about 3% over the range of illuminance values which is found in headlamp photometry; lower accuracies sometimes have to be tolerated.

Each of the eleven photodetector problem areas given above are now considered in more detail in the context of headlamp photometry.

- a) As mentioned in section 3.3.1, if the photodetector is not of a suitable size, then a simple lens system can be used to collect light falling on an aperture of the required flux collection area and re-distribute it onto the photodetector's light sensitive area.
- b) At first sight, it might appear that any departure of a photodetector's spectral response from the required $V(\lambda)$ response would automatically introduce errors into the

measurement process. This is not necessarily so, however. Provided the spectral composition of the light to be measured is the same as that of the lamp used to calibrate the system, then no errors will be produced. If the spectral composition of light to be measured is different, however, then errors will be introduced; these errors are normally largest when dealing with light of a single colour rather than broad-band light.

In headlamp photometry, the spectral composition of the light varies to a certain extent owing to the different types of bulbs and the different test voltages used. The various types of reflecting and refracting elements used in headlamps also modify the spectral composition of the light from a bulb in slightly different ways. In all cases, however, the light to be measured has a generally similar and continuous spectral composition, covering the whole of the visible region.

It is not vital for headlamp photometry, therefore, that the spectral response of the photodetector system is exactly equivalent to $V(\lambda)$. The basic aim is to have a system with a relatively good match; it is reasonable to assume that such a system, when calibrated with a suitable source, will not produce appreciable errors as a result of its non-ideal spectral response when measuring the type of light produced by headlamps.

- c) The range of illuminance values to be measured by a headlamp photometer varies with the type of lamp and type of test; details are given in Table 4.1 for measurements made at 25 m.

| LAMP TYPE | HIGHEST ILLUMINANCE VALUE LIKELY TO BE ENCOUNTERED | ILLUMINANCE MEASUREMENT RANGE WHICH ENABLES, FOR THE MAJORITY OF LAMPS: | |
|------------------------|---|--|--|
| | | THE ECE/SAE TEST POINT VALUES TO BE MEASURED | A USEFUL ISO-LUX DIAGRAM TO BE PRODUCED |
| HEADLAMP - DIPPED BEAM | 100 | 0.1 - 50 | 0.4 - 50 (1) |
| HEADLAMP - MAIN BEAM | 250 | 4 - 150 | 1 - 150 |
| AUXILIARY DRIVING LAMP | 250 | 4 - 150 | 1 - 150 |
| SPOT LAMP | 1000 | 4 - 400 | 10 - 400 (2) |
| FOG LAMP | 50 | 0.1 - 20 | 0.1 - 20 (2) |

Notes:

- (1) The lowest illuminance contour value normally shown at present on a Lucas dipped beam iso-lux diagram is 0.4 lux; an additional contour of a lower value (0.2 lux, say) would be useful in many cases, however.
- (2) Fog and spot lamp tests are not carried out as frequently as headlamp tests.

Table 4.1 Lamp Illuminance Range Information (lux at 25m)

If a reduced-length photometer is being used, then the actual illuminance values to be measured by the photodetector system are correspondingly higher. (See Chapter 7.)

The sensitivity of the device used must be such that the minimum and maximum values of interest can be measured satisfactorily.

- d) The illuminance/output signal relationship of the photodetector should be linear over the range of illuminance values of interest in order that the signal can be interpreted in a straightforward manner.
- e) Ideally, the photodetector will not produce a dark signal; if it does, however, then its associated circuitry should provide a means of eliminating it from the final output signal.
- f) The noise level should be insignificant in relation to the required signal for all illuminance values of interest.
- g) Photodetector response time is not a critical factor for manual goniophotometer systems, but is important in automatic systems, where readings are taken in quick succession.
- h) With a conventional headlamp goniophotometer system, the photodetector is always perpendicular to the direction of the flux and so the characteristics of the photodetector for non-perpendicular illumination are not normally of importance.

- i) The temperature characteristics of the photodetector should be such that the changes in the temperature of the equipment that will be encountered in the darkrooms will not introduce any significant measurement errors.

- j)
 - i) Memory effects are very undesirable since successive measurements often have large illuminance differences.

 - ii) Ageing effects are again undesirable but need not be a serious drawback providing regular calibration is carried out.

- k) Since any individual headlamp photodetector system has to be carefully calibrated with a standard lamp, then any small differences in the characteristics of the device used from the 'typical' characteristics are usually of little significance.

The next section describes silicon photodiode detector systems, which are currently the most suitable type for headlamp photometry.

4.2 Silicon Photodiode Detector Systems

A silicon photodiode essentially consists of either a PN or PIN type semiconductor junction (18), and can be operated in various modes (19,20). The most suitable mode of operation for headlamp photometry is the zero bias mode, using an operational amplifier as a transimpedance amplifier (21); see Fig. 4.1. In this mode, the photodiode generates a current proportional to illuminance:

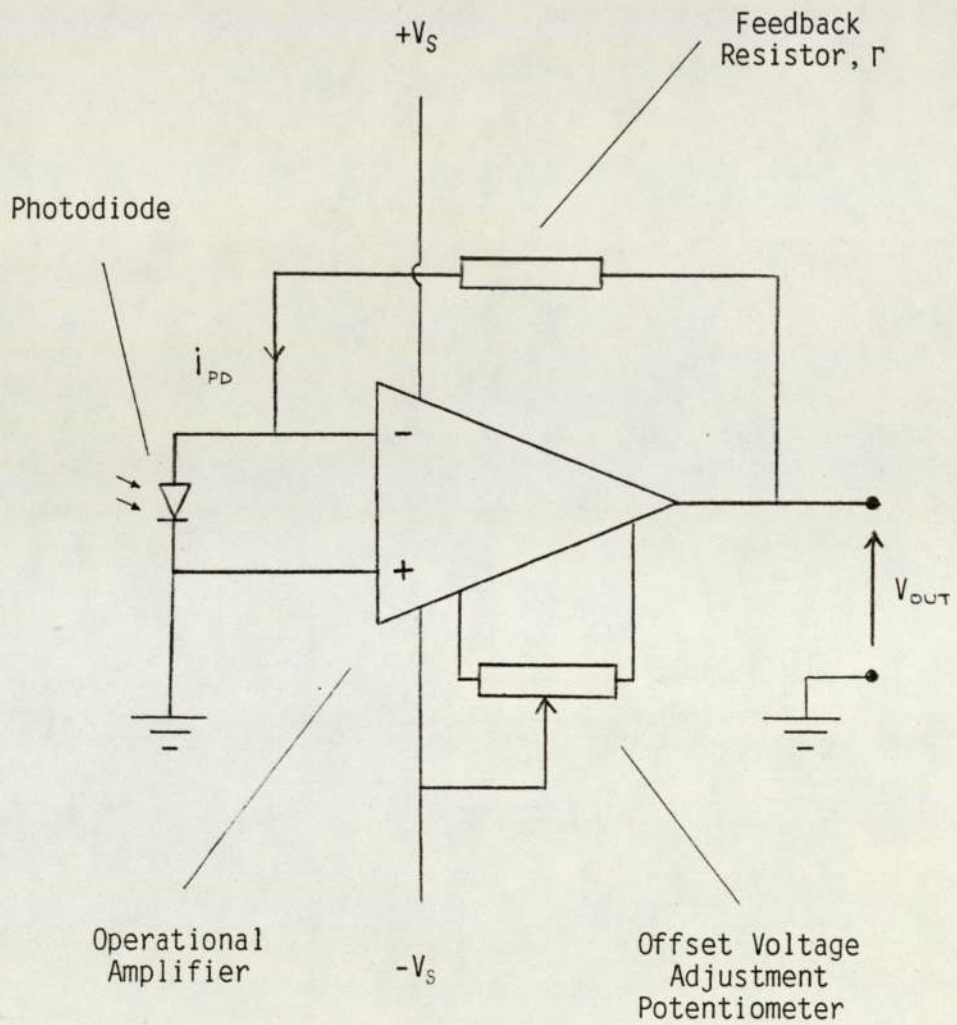


Fig. 4.1 Photodiode Transimpedance Amplifier

$$i_{PD} = R_{PD} \cdot E_{PD} \quad (4.3)$$

where

E_{PD} = Photodiode illuminance (Lx)

R_{PD} = The photodiode's photometric responsivity, for light of a given spectral composition (ALx^{-1})

i_{PD} = Current generated by the photodiode (A).

The operational amplifier converts this current into an output voltage, V_{OUT} :

$$V_{OUT} = i_{PD} \cdot r + V_{OS} \quad (4.4)$$

where

r = Feedback resistance

V_{OS} = Offset voltage.

This equation is only valid if the current flowing into the operational amplifier's inverting input is negligible compared to the generated photocurrent; this condition can readily be met by using an operational amplifier with a FET input stage. The offset voltage can be set to zero by means of a trimmer resistor; see Fig. 4.1.

The performance of a silicon photodiode is now discussed in relation to the problem areas given in the last section.

- a) Many different silicon photodiodes, having a wide range of light sensitive areas, are available. If necessary, however, the flux collection area can be changed as described in the last section.
- b) Silicon photodiodes are available with built-in colour filters to modify the inherent spectral response of the silicon, which extends from approximately 400 nm to 1100 nm (22), to achieve a $V(\lambda)$ response. The quality of match varies with cost. Devices manufactured by Lichtmesstechnik (LMT) of Berlin have a very high level of matching (23), but cost several hundred pounds. The United Detector Technology (UDT) PIN 10-AP (24), offers a reasonably close match and costs approximately £150; this device was used in the E&D Automatic Photometer and has subsequently been used in other rigs. Detectors with an approximate $V(\lambda)$ response are available from various sources for a few pounds.
- c) i) Silicon photodiodes generally have sufficient sensitivity to enable the minimum illuminance value of interest to be accurately measured.
- ii) Photodiode saturation is not usually a problem, but can easily be overcome by means of a neutral density filter.
- d) Silicon photodiodes have the required linear illuminance/output signal relationship. UDT quote a typical linearly deviation of only 0.5% for their photodiodes (25).

- e) A silicon photodiode produces no dark current when operated in the zero bias mode (26).
- f) Photodiodes generate a very low level of noise and can typically be used to measure illuminance values over a dynamic range of $10^6:1$ (27). In general, therefore, photodiode noise is not a critical factor when designing photodetector systems for headlamp photometry.
- g) A major advantage of silicon photodiodes over the older types of device is their response speed. A photodiode can respond in a few microseconds, or less; a selenium barrier cell can take several seconds.
- h) The performance of a photodiode for non-perpendicular angles of incident illumination is not normally relevant. (See earlier.)
- i) The two parameters of a silicon photodiode that can vary significantly with temperature are the dark current and the responsivity (26). Since no dark current is produced when operated in the zero bias mode, then the first of these factors does not apply. UDT quote a typical responsivity variation of $0.2\% / ^\circ\text{C}$ for a planar diffused diode operated in the zero bias mode (26); this does not cause significant errors providing the ambient temperature is kept reasonably constant. LMT produce detectors with built-in thermostatic stabilisation to eliminate changes in characteristics caused by temperature variations.

- j) Silicon photodiodes do not exhibit any significant memory or ageing effects, unlike selenium devices.

- k) Slight deviations of the characteristics of the device used from the 'typical' characteristics are not significant. (See earlier.)

Using high quality components, the transimpedance amplifier circuit given here provides high linearity, low noise, low offset voltage, high response speed, low changes in characteristics with temperature and high long-term stability.



5. OVERVIEW OF THE PROJECT

Section 5.1 describes the work carried out during the period of the project. The structure of the thesis, and the way this relates to the work carried out, is described in section 5.2.

5.1 Work Carried Out

The work carried out can be divided into seven main categories, as shown in Fig. 5.1; it can be seen that some of the tasks were carried out concurrently. The main tasks undertaken in each of the seven categories are described in sections 5.1.1 to 5.1.7; the remainder of the thesis is mainly concerned with categories 3 - 6.

5.1.1 Completion and Commissioning of the E&D Department Automatic Photometer

Prior to the IHD project, the author (then employed in the Instrumentation department) had been engaged on the design of the E&D department Automatic Photometer. At the time of the IHD project initiation, it was planned that the construction and commissioning of this equipment would be completed by October 1981. However, owing to redundancies in the Instrumentation department, which severely reduced the support services available, and delays in the delivery of the software, this work was not completed until March 1982, and occupied a large proportion of the author's time between October 1981 and March 1982.

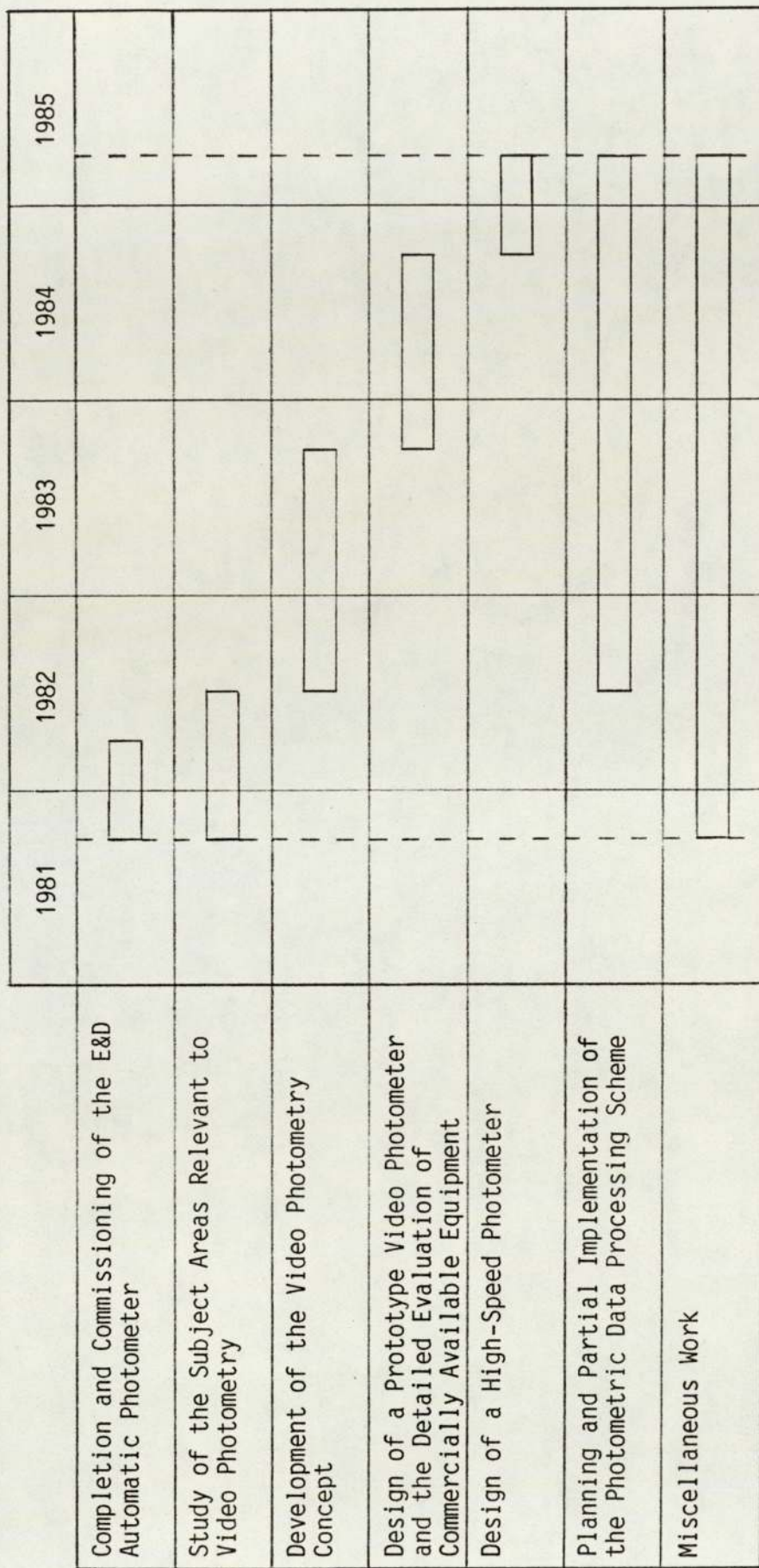


Fig. 5.1 Work Carried Out During Period of Project

5.1.2 Study of the Subject Areas Relevant to Video Photometry

Firstly, a study was made of the subjects of photometry, optics and digital image processing and a literature search undertaken to find any material of a more specialised nature which would be relevant to the project. Useful material relating to the following areas was found and studied:

- a) The operational principles and characteristics of vacuum tube and solid-state cameras and sensors.
- b) The use of video cameras as measurement instruments, particularly in the field of remote sensing by spacecraft; this is an area in which it is very important to have accurate quantitative data, and a considerable effort is often made to correct the effects of non-ideal camera characteristics.

No material directly relating to the use of video cameras for headlamp photometry was found.

In addition, contact was made (in late 1981) with various manufacturers of solid-state cameras and image processing systems to gain a broad appreciation of the characteristics and capabilities of commercially available equipment. In particular, discussions were held with Fairchild, the leading manufacturers of charge-coupled device (CCD) solid-state cameras, who, at this time, employed a specialist CCD Product Marketing Engineer in the United Kingdom to provide applications advice to potential users. This engineer provided details of their current cameras and informed the author that

a new camera, with 'anti-blooming' characteristics (see section 5.1.3), would be available in the near future.

5.1.3 Development of the Video Photometry Concept

A basic configuration for measuring the photometric performance of a headlamp with a video camera and an image processing system was devised by the author; it is shown in Fig. 5.2 and its proposed operation is as follows:

A beam pattern is produced on a plane test screen, placed at a convenient distance in front of the lamp, by means of a conventional reduced-length photometer (RLP). A solid-state video camera is placed adjacent to the lamp so that an image of the beam pattern on the screen is formed on the camera's sensor, which is scanned electronically within the camera to produce an analogue electrical signal. The video signal from the camera is fed to the image processing system, which, at the operator's command, digitizes one frame and stores it in the frame-store as a two-dimensional array of numerical data.

It was shown that, providing the RLP, screen, camera and image processing system had certain 'ideal' characteristics, the acquired data would enable the calculation of a second array of numerical data, accurately representing the illuminance values which would be produced at a specified two-dimensional array of points on the far screen; this second array of data will be referred to as a screen illuminance array (SIA). The SIA would be the basic unit of data in the system and could be used to produce an iso-lux diagram of the lamp's beam pattern

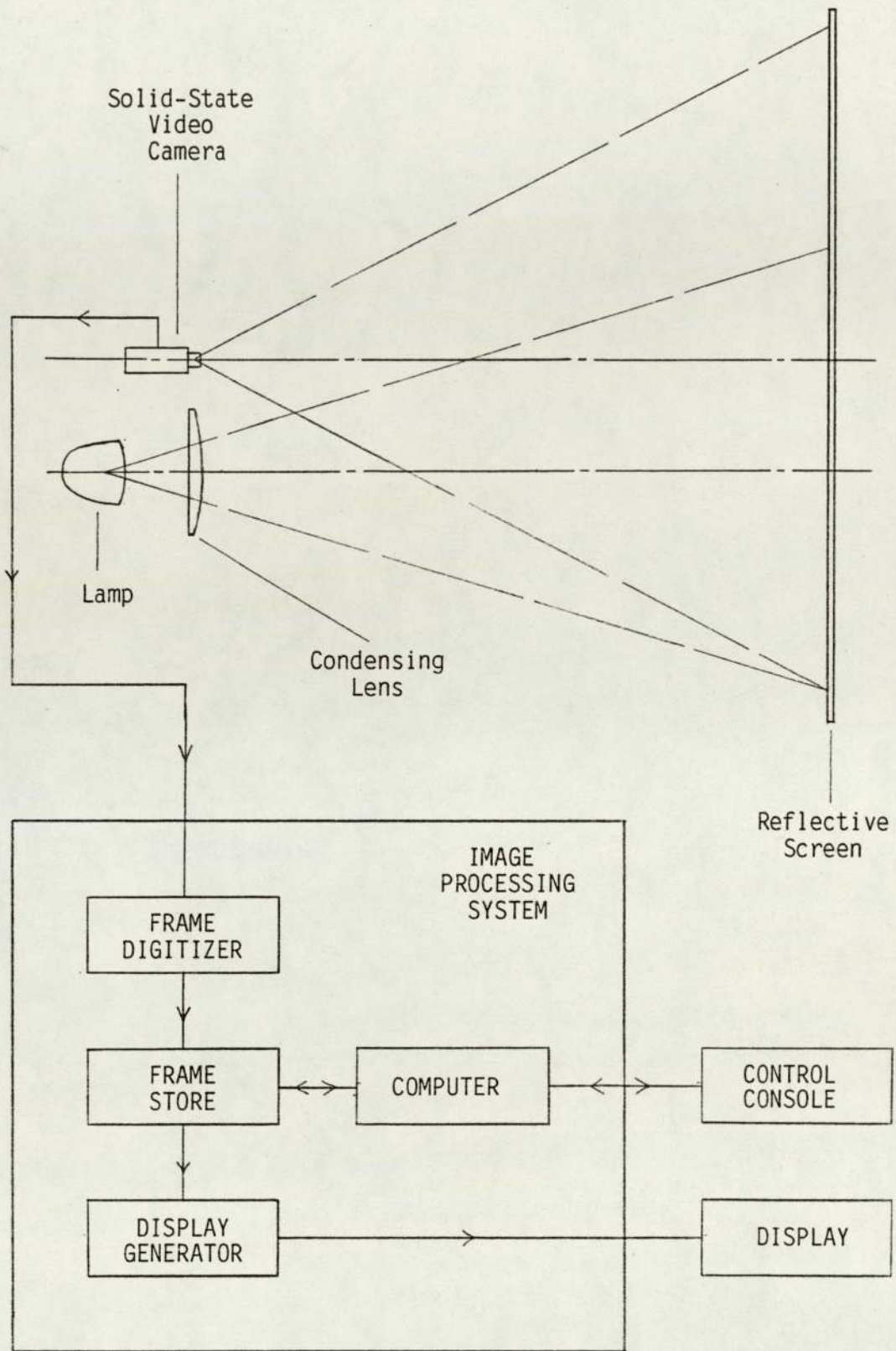


Fig. 5.2 Basic Video Photometry Concept

on the monitor. An SIA could also be processed by various operations, the nature of which would depend on the applications to be catered for.

The main advantage that this type of system would have over the conventional goniophotometer is an increased speed of data acquisition; the need for mechanical scanning would be eliminated and a frame of data from the camera could be acquired in a fraction of a second. The potential application areas for such a system were studied.

It was shown that, in practice, the RLP, screen and camera would have various non-ideal characteristics and that these could essentially be divided into two groups:

- a) Those whose effects could be corrected in a reasonably straightforward manner by processing the digitized video signal. This group includes the characteristics of the screen and some of those of the camera.
- b) Those whose effects could not be corrected in a reasonably straightforward manner, and which, in a successful practical video photometry system, must be sufficiently low that they could be ignored. This group includes the characteristics of the RLP and those of the camera not included in group (a).

A more sophisticated SIA acquisition procedure which could be used to correct the effects in group (a) was devised.

As explained in section 4.3.2, the off-axis imaging performance

of an RLP does not affect the illuminance measurements produced by a conventional goniophotometer. With the video photometry approach, however, the whole of the screen is used for making measurements and consequently the off-axis RLP performance will influence the accuracy of the data obtained.

Since no work had previously been carried out to assess off-axis RLP performance, the subject was studied by the author as part of this project. It was decided to carry out a theoretical investigation, for the following reasons:

- a) There was no suitable lens available within the department at the time for experimental work, and it takes approximately 8 months for a lens to be delivered after an order has been placed.
- b) It was considered that it would be useful to be able to study the effects of changing the various lens parameters, such as surface curvature and focal length; this cannot be carried out experimentally without purchasing many lenses, which, at a cost of approximately £1000 each, is not feasible.

The following work was carried out:

- a) A method of analysing the performance of an RLP, based on ray tracing calculations, was devised; a Fortran program was written to enable the ray tracing calculations to be carried out by computer.

- b) A criterion of RLP acceptability was proposed.
- c) Various configurations were analysed.

It was estimated from the above work that a suitably configured 4 m system, which was the most convenient length for a prototype system to be implemented in the E&D darkroom, would provide a satisfactory imaging performance providing the horizontal field of view was limited to approximately $\pm 13^\circ$ off-axis.

In addition to the problems of non-ideal RLP, screen and camera characteristics, it was found that currently available image processing systems are not ideally suited to the proposed type of video photometry system because:

- a) They are primarily designed for use with vacuum tube type cameras.
- b) They carry out the digitization process with a lower resolution than is required to provide accurate quantitative data over the range of illuminance values encountered in headlamp photometry.

Various methods by which these problems could be overcome were proposed by the author. Only one of them was considered feasible, however, since the others would:

- a) Require complex image processing system modifications.
- b) Result in a data acquisition time of about ten seconds or

longer; this level of performance can be obtained using the 'high-speed photometry' approach, which has fewer potential problem areas.

The recommended method does have one drawback, however; it requires a camera with 'anti-blooming' characteristics i.e. a camera with the property that part of its sensor can be illuminated at a level beyond that required to saturate the output video signal without affecting the correct operation of the remaining part of the sensor. Such cameras were not commercially available at the time, although the author had been informed by Fairchild that they were planning to introduce one at the beginning of 1983.

5.1.4 Design of a Prototype Video Photometer and the Detailed Evaluation of Commercially Available Equipment

Having analysed the proposed concept in detail, it was considered that there would be many problems to be overcome if the theoretical advantages of speed and flexibility were to be realised whilst at the same time maintaining the levels of accuracy available using the conventional approach. Nevertheless, it was decided to continue the work and attempt to implement a prototype system for the E&D department.

The following work was carried out; tasks (b), (c) and (d) were essentially carried out concurrently.

- a) A basic system design was produced and the requirements for the camera and the image processing system formulated.

- b) The darkroom was prepared for the equipment and the necessary ancillary equipment designed and made.

- c) Commerically available image processing systems were evaluated in detail. The 'Gems System 33', made by Gems of Cambridge Ltd, was chosen as the most suitable basis for a video photometry system. It was agreed that the design scheme based on the use of an anti-blooming camera should be used.

- d) It had been hoped that the Fairchild anti-blooming camera would now be available. This was not the case, however. Furthermore, their CCD Product Marketing Engineer had now left the company and had not been replaced and there was no other person on their UK staff who had sufficient technical knowledge to provide the level of support required. Consequently, three cameras from other manufacturers were evaluated for use with the proposed system. None of these was considered suitable; it was also found that the level of technical support available in the UK from these manufacturers was insufficient for the proposed application.

In view of the many problems experienced in trying to find a suitable camera, it was concluded that it was not feasible to implement a video photometry system at the present time.

5.1.5 Design of a High-Speed Photometer

An alternative approach to high-speed photometry was proposed by the author. It is again based on the use of an image processing

system, but, in place of a video camera, uses a one-dimensional array of discrete photodiodes mounted in a vertical line on the centre of the test screen. The lamp is mounted on a rotary table which scans the beam over the array of photodiodes. In this way, an SIA could be acquired in approximately ten seconds, which is still sufficiently fast to enable a system of this type to be used for the potential video photometry applications. Furthermore, the method does not suffer from many of the potential sources of error inherent in the video photometry approach.

It was apparent from the image processing system evaluation work undertaken that it would be possible to implement this type of system, which will be referred to as a high-speed photometer, using currently available equipment. Consequently, an overall system design was produced, based on the work carried out previously for the proposed video photometry system.

5.1.6 Planning and Partial Implementation of a Photometric Data Processing Scheme

It is clear that computers will play an increasingly active role within the E&D department for the acquisition and processing of photometric data. In addition to future computer-based photometers, which will be used to acquire and present photometric data, it is also planned to use computerised systems for predicting the photometric performance that will be produced by a given headlamp design and for analysing the relationship between a lamp system's photometric performance and a driver's visual performance.

In order to gain the maximum benefit from such facilities it will be necessary for them to be implemented in such a way that they will form an integrated system, so that data can easily be transferred between them.

The author decided to plan a suitable photometric data processing system, since no previous work had been carried out in this area; each project had previously been treated as self-contained.

The key elements of the proposed scheme are:

- a) The use of the Lucas Industries IBM mainframe computer, situated at the Shirley site but linked to Cannock via telephone lines, as a common processing element for the required software.
- b) The use of a standard file structure for storing photometric data, and transferring it between the various software packages to be introduced.
- c) The linking of all computer-based photometers to the IBM mainframe.
- d) The use of a general purpose suite of software for carrying out commonly required operations, such as iso-lux diagram plotting, on the IBM mainframe; this would avoid the re-implementation of these facilities when a new computer-based photometer is introduced.

The proposed scheme was adopted in principle by the department, although its full implementation was clearly outside the scope of this project. Nevertheless, certain parts of the work necessary for its implementation were carried out by the author. These were:

- a) The implementation of a file transfer facility between the Automatic Photometer and the IBM mainframe.
- b) The definition of a file structure for storing photometric data and the writing of an example program to show how the data can be accessed.

5.1.7 Miscellaneous Work

During the period of the project, the author was called upon to carry out several other tasks relating to the company's test equipment and computing facilities. These are listed below:

- a) The maintenance of the E&D Automatic Photometer and the upgrading of the control console from a teletype to a VDU and printer.
- b) The selection of new equipment for the E&D 25 m photometer.
- c) The selection of a new E&D department graphics terminal for accessing the Lucas Group mainframe computer.
- d) Assisting in the commissioning of a Ford software package for evaluating headlamp performance, on the Lucas Group mainframe

computer.

- e) Assisting in the design of a beam test rig for production line testing of lamps being sold to American customers.

- f) Assisting in the upgrading of the Q&R department Automatic Photometer to the same specification as the E&D rig, and the upgrading of the Q&R department Automatic Signal Lamp Photometer.

5.2 Thesis Structure

This section describes the structure of the thesis and the way it relates to the work carried out. The specialised areas of background knowledge required are also stated, further details being given in the appropriate Chapters.

Chapter 6 provides an outline description of the E&D department Automatic Photometer. A knowledge of microcomputers is assumed.

Chapter 7 describes the fundamental concepts of imaging an headlamp photometer's measurement surface with a video camera; an equation relating the far screen illuminance which would be produced by a lamp and the camera's video output signal is derived. It is shown that the basic video photometry concept is theoretically feasible.

The basic role of an image processing system in a video photometer is covered in Chapter 8. In particular, the method by

which an SIA would be acquired is discussed. A knowledge of digital electronic systems, image processing system architecture and analogue to digital conversion is assumed.

The potential application areas for a headlamp photometry system capable of acquiring, processing and displaying SIA's in a few tens of seconds or less are described in Chapter 9.

Chapter 10 describes measurement surface imaging with a camera in more detail. The various non-ideal characteristics which the reduced-length photometer, screen and camera might exhibit in a practical video photometer, their effects on the far screen illuminance/video output signal relationship and whether or not these effects can be corrected in a reasonably straightforward manner, are discussed. A detailed knowledge of solid-state camera characteristics is assumed.

The role of the image processing system in the video photometer is considered in more detail in Chapter 11. In particular, a more sophisticated SIA acquisition procedure, which can be used to correct some of the effects of non-ideal system characteristics, is described.

Chapter 12 describes the reduced-length photometer analysis method, including the use of the computer program. (Full details of the program are given in Appendix D.) The method is used in Chapter 13 to assess the performance of various four-metre configurations; the numerical performance data referred to in this Chapter is to be found in Appendix E.

The Photometric Data Processing Scheme is described in Chapter 14. Further information relating to this scheme is given in Appendices G and H; see later.

Chapter 15 describes the proposed prototype video photometry system and the camera and image processing system evaluation work undertaken.

A description of the alternative approach to high-speed photometry, based on the use of a one-dimensional array of discrete photodiodes, a rotary table and an image processing system, is given in Chapter 16. The system it is proposed to implement is described in more detail in Chapter 17.

Chapter 18 discusses the possible technological developments which will influence the future feasibility of video photometry and gives the recommended approach to further work in this area.

Appendix A explains how the concept of light source intensity, which is normally defined for a point source, can be applied to a headlamp.

The reduced-length photometer formulae given in section 3.3.2 are derived in Appendix B.

Appendix C describes how the effects of ambient light falling on the measurement surface can be corrected, if necessary, in a video photometry system.

A detailed description and listing of the computer program written for the reduced-length photometer analysis method is given in Appendix D. A detailed knowledge of ray tracing and Fortran is assumed.

Appendix E contains the numerical performance data for the reduced-length photometer configurations referred to in Chapter 13.

A list of the image processing equipment which was evaluated for use with the proposed prototype video photometry system is given in Appendix F.

The Automatic Photometer/Group Computer file transfer system is described in Appendix G; a knowledge of data communications is assumed.

Appendix H describes the Photometric Data File structure and gives an example program to show how the data can be accessed; a detailed knowledge of Fortran is assumed.

6. THE E&D DEPARTMENT AUTOMATIC PHOTOMETER

This Chapter gives further information about the E&D department Automatic Photometer, which was briefly described in section 3.3.3. It is assumed that the reader has a knowledge of microcomputer hardware and software; see bibliography.

6.1 Hardware

Fig. 6.1 shows a functional block diagram of the rig, which uses a 4 m reduced-length photometer system.

The microcomputer hardware essentially consists of an Intel 8080 based central processing unit, 32K random access memory, parallel and serial I/O ports, a floppy disk controller, a bootstrap module and an analogue input module, made up from 'Multibus' boards (28). It is interfaced to a VDU, a printer, twin 8" floppy disk drives, a plotter, the goniometer control and display units, the photodetector system and the headlamp power supply system.

The goniometer is of type A (see section 3.1) and is driven by a stepper motor on each axis. These motors are powered by two drive units, the input signals for which are derived from the control unit; this unit enables the movement of the goniometer to be controlled manually, for aiming the lamp, or by the computer, for carrying out the point illuminance measurements. The stepper motors are fitted with optical encoders which feed signals to the display unit to show

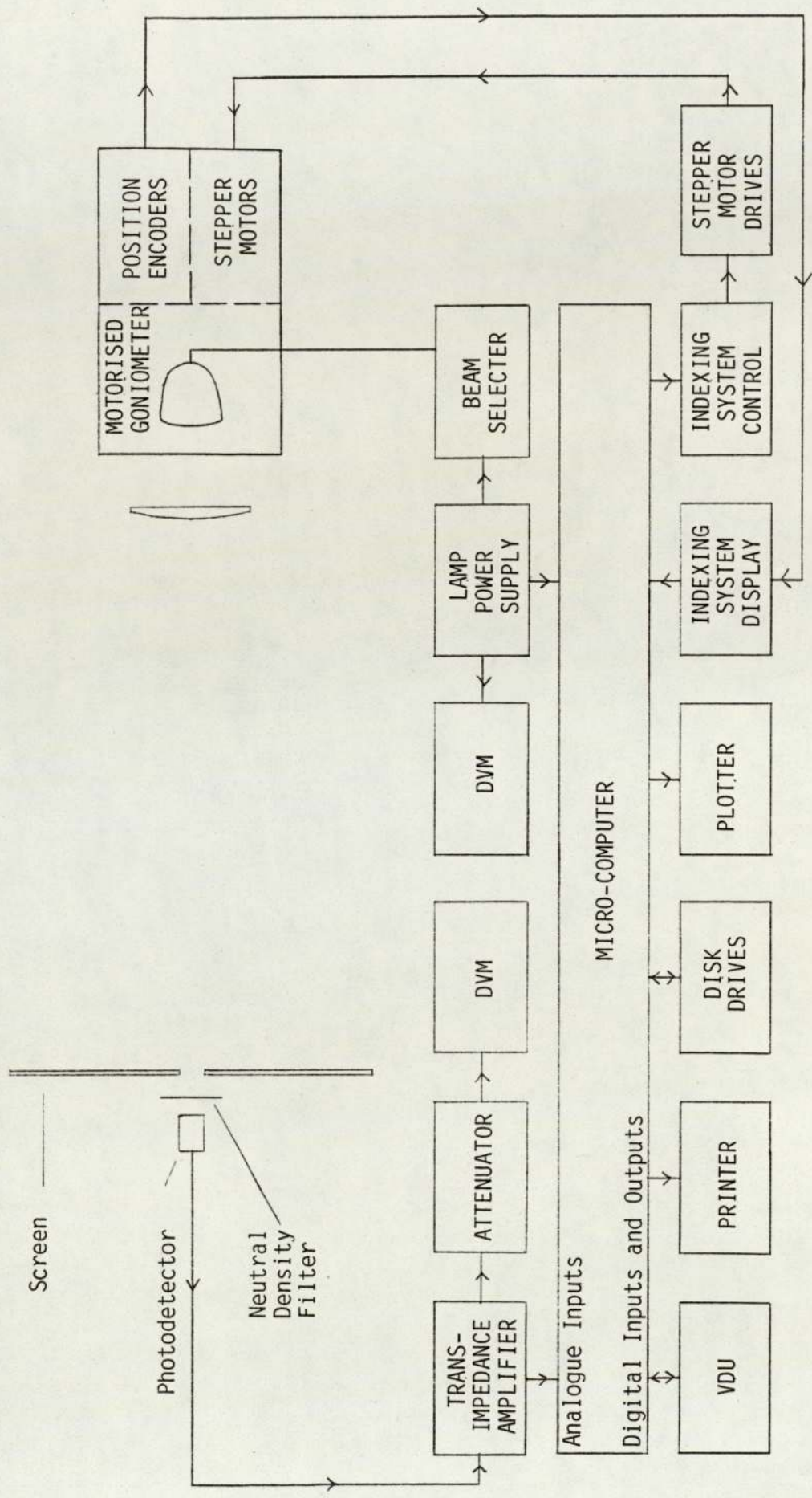


Fig. 6.1 E&D Department Automatic Photometer - Functional Block Diagram

the angular position of the goniometer relative to user-defined reference points. The display unit is interfaced to the computer to enable it to check that the goniometer has responded correctly to a command to move to a specified position.

The photodetector system consists of a photodetector, a neutral density filter, a transimpedance amplifier, an attenuator unit and a DVM. The photodetector is a silicon PIN photodiode with built-in photopic filter and is mounted in a small box which positions it a few centimetres behind a hole in the screen and minimises the amount of ambient light falling on it; the box also contains a neutral density filter, without which the maximum photodetector illuminance permissible for a linear illuminance/photocurrent relationship would be exceeded. The photocurrent generated by the photodetector is fed into a transimpedance amplifier designed to produce an output of 0 to 10 V for a photodetector illuminance range corresponding to 0 to 400 lux at 25 m. The amplifier's output is fed to one channel of the computer's analogue input module. A software-programmable instrumentation amplifier in this module applies a gain of 1, 2 or 4 and carries out 12 bit analogue to digital conversion; the use of the instrumentation amplifier gives effective full scale illuminance values of 400 lux, used for spot lamp measurements, 200 lux, used for headlamp main beam measurements, and 100 lux, used for dipped beam and fog lamp measurements. The maximum quantisation error values for the spot lamp, headlamp main beam, headlamp dipped beam and fog lamp ranges are 0.048, 0.024, 0.012 and 0.012 lux respectively. The transimpedance amplifier's output is also fed to a DVM via an attenuator unit, which allows either the illuminance at 25 m (in lux) or the lamp's intensity (in candelas) to be displayed; the attenuator setting does not affect

the computer input.

The headlamp power supply system essentially consists of a 0 to 30 volts, 10 amps power supply, a DVM and a switch for powering either the dipped or main beam filaments of a lamp. The headlamp voltage is sensed at the bulb and fed back to the power supply and DVM to eliminate errors caused by cable voltage drops. The system is interfaced to the computer's analogue input module to enable a run-time check that the correct voltage has been set to be made.

6.2 Software

The software consists of the CP/M operating system (29) and 13 custom programs (30, 31), written in PL/M (32) by ERA Technology of Leatherhead, Surrey. The programs PPRUN, PPSPEC, PPPRINT and PPTAB are used for point to point tests, ILRUN, ILSPEC and ILPLOT for iso-lux tests and XSRUN, XSSPEC and XSPLIT for cross-section tests. The remaining 3 programs, CTEST, LIST and FILEP, are used for all three types of test. The way in which the software is used is essentially the same for each type of test; point to point testing is considered first.

A set of test point readings is obtained by setting up the lamp on the goniometer, manually aiming it and running the PPRUN program. This program obtains the list of points at which readings are to be taken, and the other data required to carry out the test, from a previously created 'point to point test' (PPT) file and from the operator. The program directs the goniometer to each of the required points and reads in the illuminance values. (For lamps which produce

two beams, either one or both can be tested.) After all of the readings have been acquired, the results are output to the VDU (and printer if required) and also stored in a 'point to point result' (PPR) file; the contents of this file can subsequently be output to the VDU (and printer) by the PPPRINT program. The results of several different lamp tests, stored in separate PPR files, can be combined in a single listing by the PPTAB program.

A PPT file is produced in 2 stages, as follows. Firstly, the PPSPEC program is used to create a 'point to point specification' (PPS) file detailing the number (either 1 or 2) and the types (dipped, main, fog or spot) of beams to be tested and the test points to be used for each beam. (The beam type is required in order that the gain of the instrumentation amplifier in the analogue input module can be set by PPRUN when the test is carried out.) Secondly, the PPT file is created by means of the CTEST program; this file contains a copy of the required PPS file and, optionally, lamp type and sample, bulb type and sample and test voltage information. If the lamp, bulb and voltage information is omitted from the PPT file when it is created, then it is entered when PPRUN is executed. In addition to the pre-defined parameters described above, PPRUN, PPSPEC and CTEST all enable the operator to enter general comments which are stored in the associated PPR, PPS and PPT files for future reference.

The above file creation procedures provide a high degree of operational flexibility. Once created, a PPS file can be used to create several different PPT files, each tailored to a particular use. For example, a general purpose PPT file can be created, requiring the operator to enter all of the lamp, bulb and voltage

information (and the PPR file name) when the file is used by PPRUN. For use when many samples of a given lamp using a standard calibrated bulb and a given test voltage are to be tested, a more specific PPT file can be created, requiring only the lamp sample number (and the PPR file name) to be entered at run-time.

For iso-lux tests, an 'iso-lux specification' (ILS) file, created by ILSPEC, contains information detailing the number and types of beams to be tested, the angular limits and increments of the area of the beam to be scanned and a set of default contour values. An 'iso-lux test' (ILT) file, created by CTEST, contains a copy of the required ILS file, and, optionally, lamp, bulb and voltage information. ILRUN is used to carry out an iso-lux test and produces an 'iso-lux result' (ILR) file containing the acquired data; the information required to carry out the test is obtained from an ILT file and from the operator. ILRUN also produces, if required, an iso-lux plot, using the default contour values, in one of 9 standard formats. ILPLOT is used to produce an iso-lux plot from data stored in an existing ILR file, again in one of 9 standard formats, and enables different contour values to the default ones to be chosen if desired.

For cross-section tests, a 'cross-section specification' (XSS) file, created by XSSPEC, contains information detailing the cross-section scan required. A 'cross-section test' (XST) file, created by CTEST, contains a copy of the required XSS file and, optionally, lamp, bulb and voltage information. XSRUN is used to carry out the test and produces a 'cross-section result' (XSR) file containing the acquired data; the information required to carry out

the test is obtained from an XST file and from the operator. XSRUN also produces, if required, a cross-section plot. XSPLIT is used to produce a plot from data stored in an existing XSR file.

The LIST program is used to list all of the parameters contained in a specified PPS, PPT, ILS, ILT, XSS or XST file. FILEP lists the names and the contents of the comment fields of all the specification, test and result files on a specified disk.

7. MEASUREMENT SURFACE IMAGING WITH A VIDEO CAMERA - FUNDAMENTALS

7.1 Introduction

This Chapter considers the fundamental aspects of measurement surface imaging with a video camera.

The reasons for proposing the use of a solid-state camera (rather than the conventional vacuum tube type) and a plane, reflective test screen (rather than a spherical and/or transmissive screen) for a video camera based photometry system are given in section 7.2, and four possible viewing arrangements are described in section 7.3.

The concept of screen pixels and the geometric aspects of the system are considered in section 7.4.

An equation describing the relationship between the far screen illuminance which would be produced by a lamp and the camera's video output signal is derived in section 7.5 and shows that the basic video photometry concept is theoretically feasible.

Section 7.6 considers in detail the advantage of the solid-state type of camera for the proposed application and a comparison of the conventional and video photometry approaches to test screen illuminance measurement is given in section 7.7.

7.2 Basic Imaging Methods

The video photometry system proposed in section 5.1 uses a solid-state camera to image a plane reflective screen. In principle, however, a video photometry system could use one or more of the following alternative elements:

a) A Vacuum Tube Video Camera

The solid-state type of camera has several important advantages over the vacuum tube type for the proposed application; these are considered in section 7.6, after the proposed imaging method has been described in more detail. As a consequence of these advantages, only the solid-state type of camera is considered in detail in this thesis.

b) A Transmissive Screen

A transmissive screen, viewed by a camera as shown in Fig. 7.1, could be used in place of a reflective one. There are 3 main drawbacks, however:

- i) As will be described in section 7.5.2, the screen is required to act as a uniform diffuser and it was considered that this characteristic would be easier to achieve over the large area required with a reflective screen.

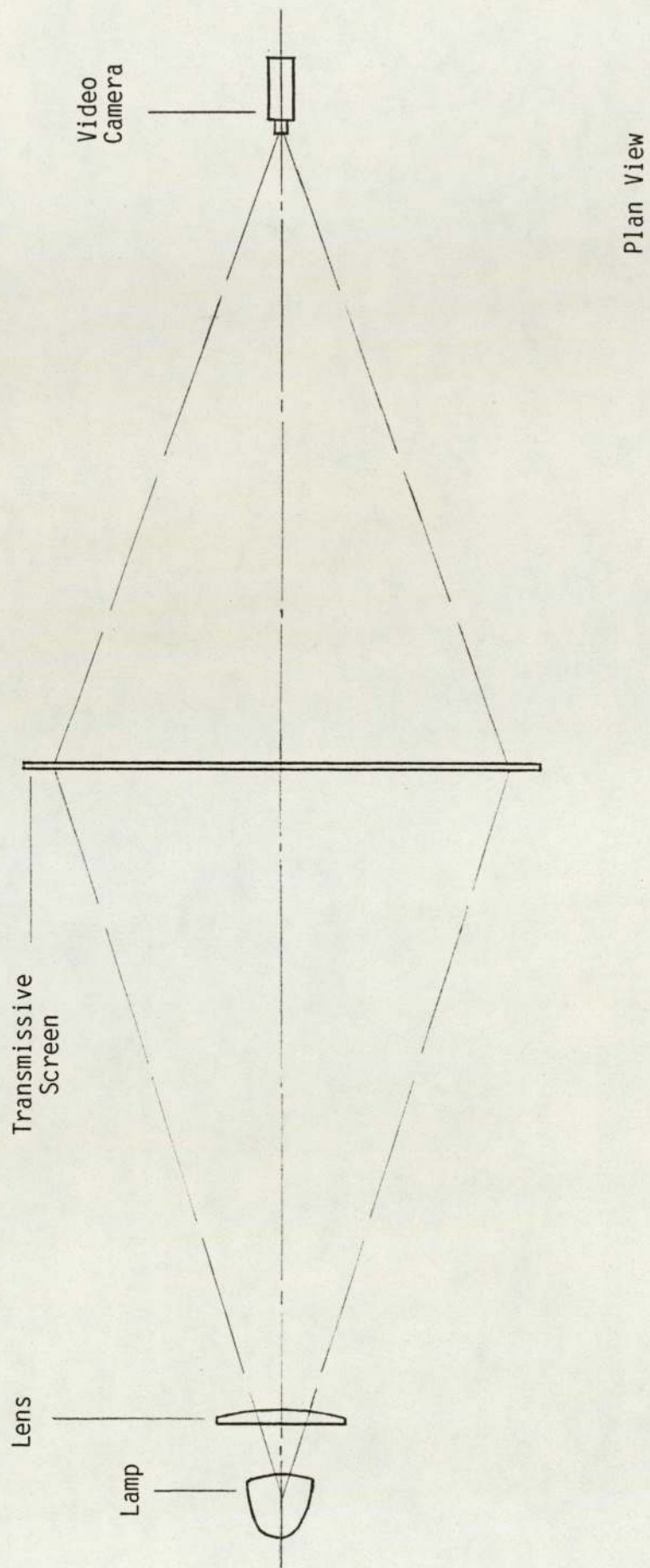


Fig. 7.1 Video Photometry System Using a Transmissive Screen

ii) A transmissive system would produce higher losses, which would probably give rise to camera sensitivity problems; see later.

iii) It would require a larger area for its construction.

Consequently, only the reflective system will be considered in detail in this thesis; most of the material, however, is equally applicable to the transmissive type.

c) A Spherical Measurement Surface

A spherical measurement surface, as effectively used in a conventional goniophotometer, could be used instead of a plane one. There are 2 main drawbacks, however:

i) Since a camera sensor is flat, it cannot image a spherical surface without distortion. Consequently, geometric transformation processing of the output image would be necessary, which would add complexity to the system and slow down its operation.

ii) The construction of a large spherical test screen would not be a simple task.

A spherical measurement surface is therefore not very suitable for a video photometry system and only a plane test screen will be considered here, despite the fact that a system with the latter type of surface will not produce results of a type

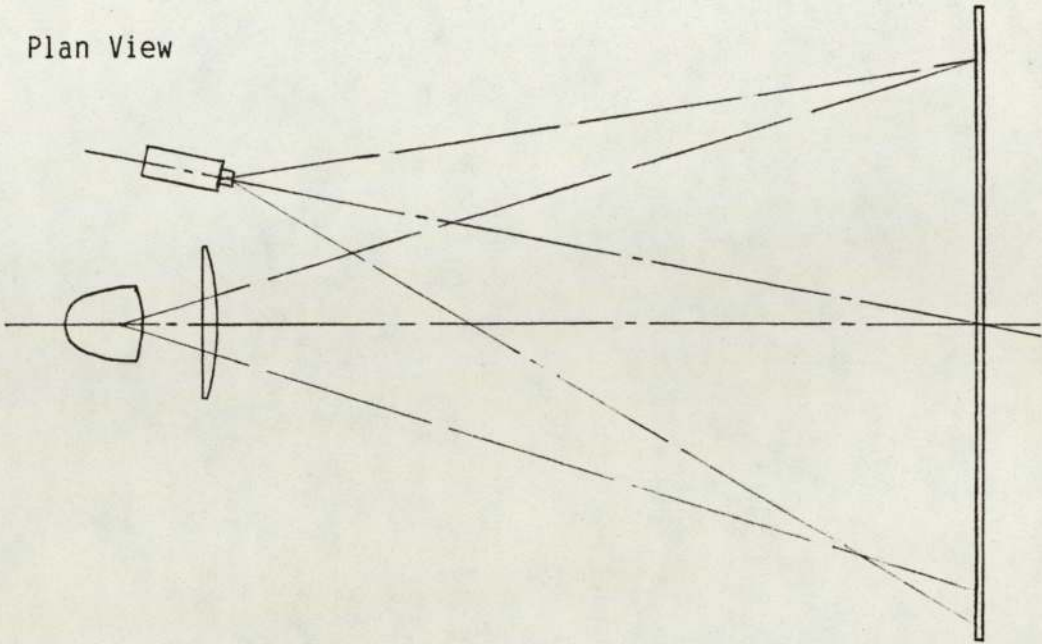
directly compatible with conventional goniophotometer systems.

7.3 Possible Viewing Arrangements

Four possible viewing arrangements are shown in Fig. 7.2 and are described below.

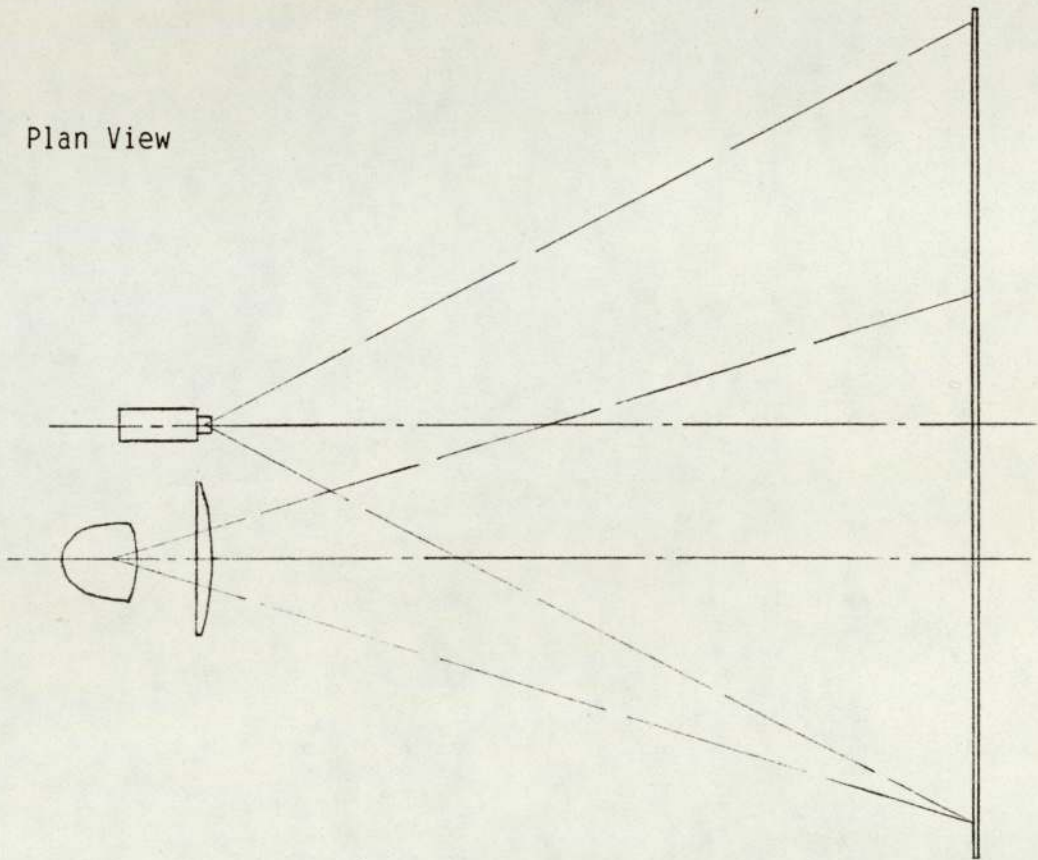
- a) With the arrangement of Fig. 7.2a, the camera axis is not perpendicular to the screen and hence the image of the screen will be distorted. This arrangement is not very suitable, therefore; in the next 3 arrangements, the camera views the screen without distortion.
- b) In Fig. 7.2b, the screen is viewed without distortion but not symmetrically; as shown, the camera views more of the left hand part of the screen than the right. Consequently, it does not make optimum use of the camera's sensor.
- c) In Fig. 7.2c, the beam-splitter enables the camera to view the screen symmetrically and hence make optimum use of the sensor. This additional component adds complexity, however, and reduces the amount of light reaching the camera, which could cause sensitivity problems; see later. Furthermore, the beam splitter could affect the spectral composition of the light reaching the camera.
- d) This arrangement, shown in Fig. 7.2d, is an extension of arrangement (b) with each half of the screen viewed separately

Plan View



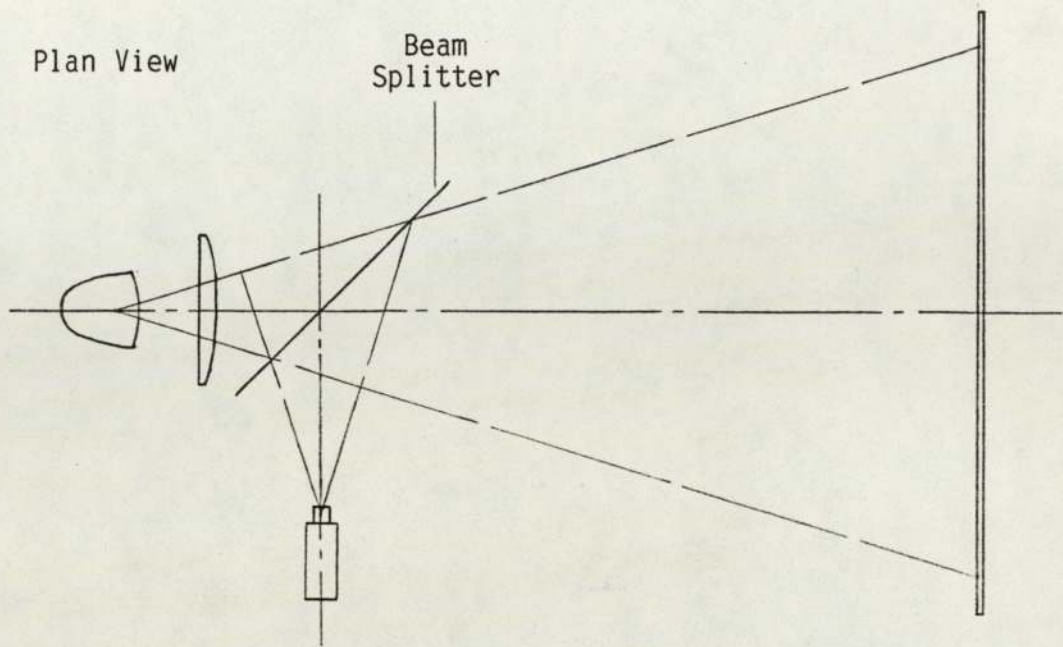
a) Viewing Arrangement (a)

Plan View

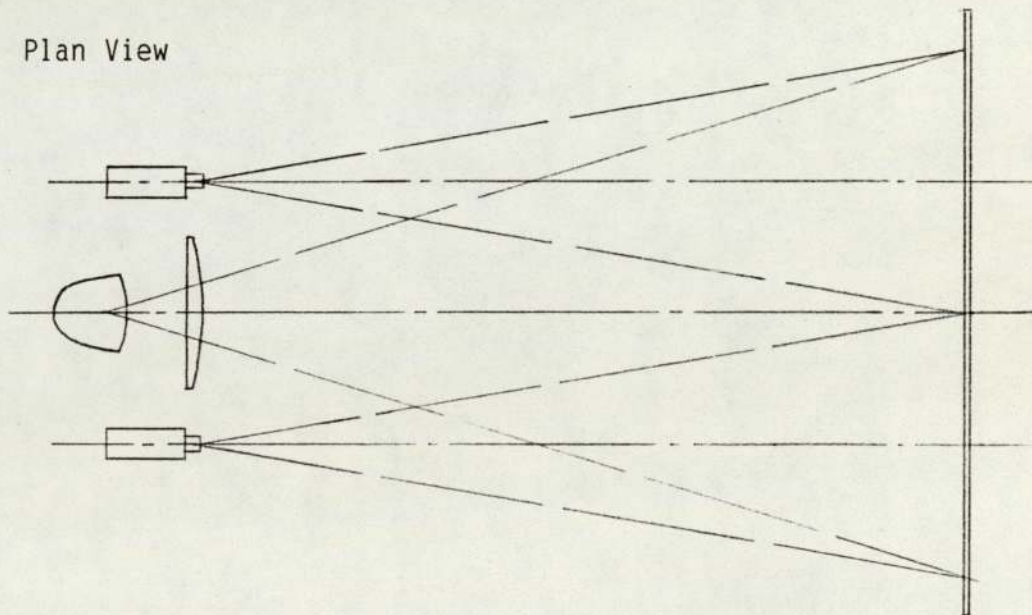


b) Viewing Arrangement (b)

Fig. 7.2 Possible Viewing Arrangements for a Video Photometry System Using a Reflective Screen



c) Viewing Arrangement (c)



d) Viewing Arrangement (d)

Fig. 7.2 Possible Viewing Arrangements for a Video Photometry System Using a Reflective Screen

by its own camera to overcome the problem of the 'wasted' sensor area. A further advantage in viewing only half the total required screen area with a camera is described in section 10.4.2. The method does, however, have the drawback of potential alignment problems and requires either an image processing system with two camera inputs or a camera switching arrangement.

7.4 Screen Pixels

It is assumed in the remainder of this Chapter that:

- a) The reduced-length photometer produces, in the geometrical optics sense, a perfect image i.e.:
 - i) The pencil of light from the lamp which would strike a given point on the far screen (an object point) passes through the lens and converges to a point (the image point) on the near screen.
 - ii) The image points are arranged in an array which is geometrically similar to the object point array.
- b) The camera lens produces, in the geometrical optics sense, a perfect image of the near screen on the camera sensor.
- c) The sensor can be modelled as a two-dimensional array of uniformly-sized, fixed position pixels and that each of these

pixels acts as a completely separate photodetector which is photosensitive over its whole area.

- d) The screen illuminance is produced solely by the lamp under test.

Imaging the near screen with a video camera effectively divides it into a two-dimensional array of elements, which will be referred to as screen pixels; see Fig. 7.3. The shape of these near screen pixels depends on the shape of the sensor pixels, which are normally square or rectangular. The size of the near screen pixels depends not only on the size of the sensor pixels but also on the distance of the near screen to the camera and the focal length of the camera lens; the values of these last two parameters can be chosen to provide the required near screen pixel size.

The near screen pixel illuminance values can be measured by means of the camera and then used to calculate the illuminance values which would have been produced at the far screen, which is also effectively divided into an array of pixels.

The array of far screen pixels is geometrically similar to the array on the near screen; see assumption (a) above. If the co-ordinates of the centre of a given near screen pixel are (x,y) (see Fig. 7.3), then the co-ordinates of the corresponding far screen pixel are $(x/m, y/m)$, where m is the linear magnification of the reduced-length photometer; see section 3.3.2. The dimensions of the effective flux collection area for the far screen pixel are also similarly increased by a factor of $(1/m)$.

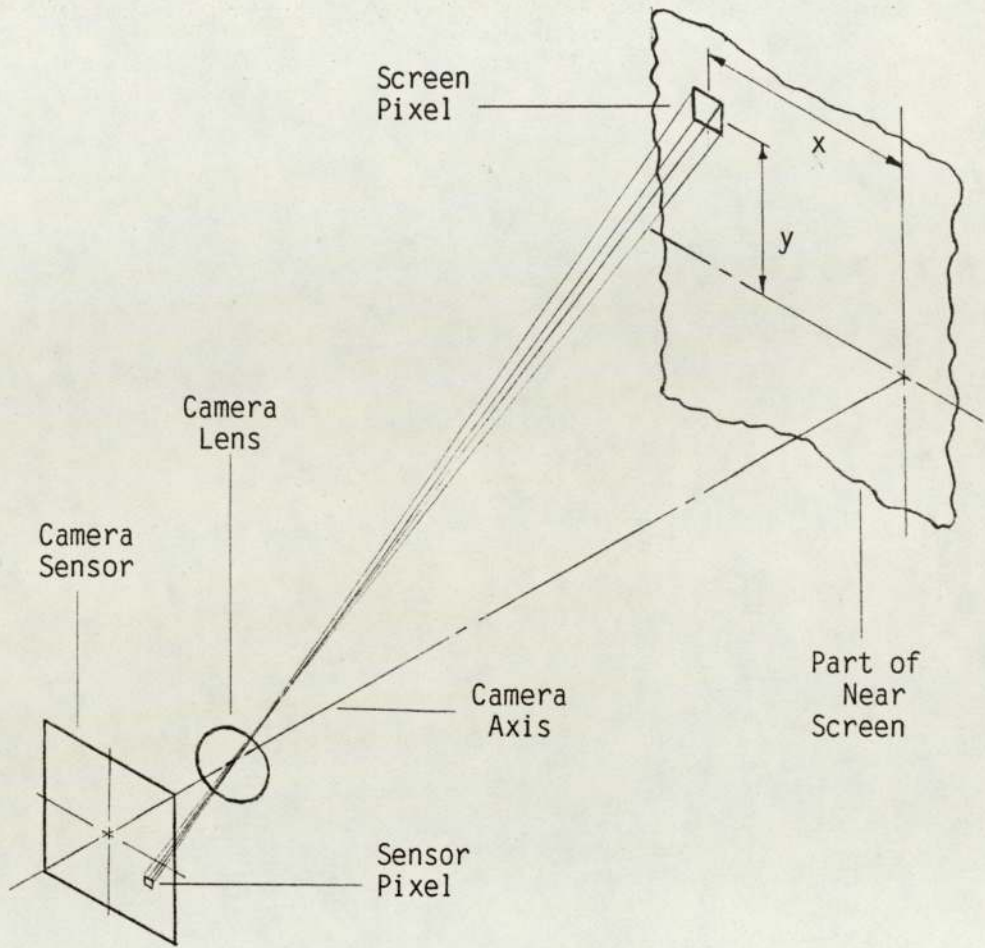


Fig. 7.3 Screen Pixel Imaging in a Video Photometry System

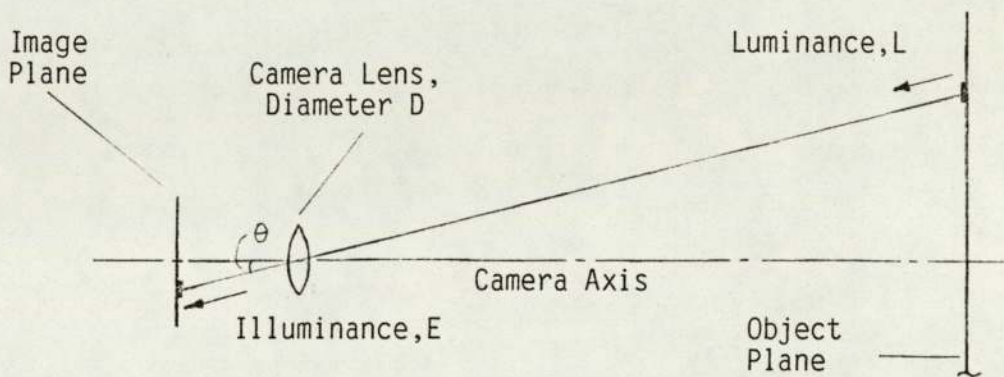


Fig. 7.4 Camera Imaging System Parameters

When discussing screen pixel size, it will normally be the far screen pixel dimensions of the system that will be referred to even though, of course, it is the near screen pixels which are actually viewed by the camera.

7.5 Photometric Analysis of the Proposed Imaging Method

The relationship between the illuminance that would be produced at a given far screen pixel and the voltage output of the corresponding sensor pixel, as measured in the camera's video signal, is considered below.

The following quantities are now defined:

- a) E_{FSCP} - The illuminance that would be produced at a given pixel on on the far screen (Lx).
- b) E_{NSCP} - The illuminance at the corresponding near screen pixel (Lx).
- c) L_{NSCP} - The luminance of the near screen pixel in the direction of its corresponding sensor pixel (Cdm^{-2}).
- d) E_{SEP} - The illuminance at the near screen pixel's corresponding sensor pixel (Lx).
- e) V_{SEP} - The voltage output, measured in the camera's video signal, of the near screen pixel's corresponding sensor pixel (V).

The following relationships must be considered, for all screen pixels:

- a) E_{NSCP} as a function of E_{FSCP}
- b) L_{NSCP} as a function of E_{NSCP}
- c) E_{SEP} as a function of L_{NSCP}
- d) V_{SEP} as a function of E_{SEP}

In order to evaluate E_{FSCP} for all screen pixels in a straightforward manner, it is ideally required that:

a) i)
$$E_{NSCP} = K_1 \cdot E_{FSCP} \quad (7.1)$$

where K_1 is a constant

- ii) K_1 has the same value for all pairs of corresponding far and near screen pixels.

b) i)
$$L_{NSCP} = K_2 \cdot E_{NSCP} \quad (7.2)$$

where K_2 is a constant

- ii) K_2 has the same value for all near screen pixels.

c) i)
$$E_{SEP} = K_3 \cdot L_{NSCP} \quad (7.3)$$

where K_3 is a constant

- ii) K_3 has the same value for all pairs of corresponding near

screen and sensor pixels.

$$d) \quad i) \quad V_{SEP} = K_4 \cdot E_{SEP} \quad (7.4)$$

where K_4 is a constant

ii) K_4 has the same value for all sensor pixels.

If all the above conditions are satisfied then:

$$a) \quad E_{FSCP} = \frac{V_{SEP}}{K_A} \quad (7.5)$$

where K_A is a constant and equals $K_1 \cdot K_2 \cdot K_3 \cdot K_4$.

b) K_A has the same value for all pairs of corresponding far screen and sensor pixels.

If a video photometry system satisfied these two conditions then the measured V_{SEP} values would directly represent the required E_{FSCP} values; K_A could be calculated theoretically and its value checked and adjusted by practical calibration of the system.

7.5.1 Far Screen Pixel and Near Screen Pixel Illuminance Relationship

The illuminance that would be produced at a given pixel on the far screen, E_{FSCP} , is given by:

$$E_{FSCP} = \frac{dF_{FSCP}}{dA_{FSCP}} \quad (7.6)$$

where

dF_{FSCP} = Far screen pixel incident flux (Lm)

dA_{FSCP} = Far screen pixel flux collection area (m^2).

In passing through the reduced-length photometer lens, the flux is decreased, as a result of transmission losses and reflections at the air/glass interfaces, and is imaged onto the corresponding pixel on the near screen:

$$dF_{NSCP} = dF_{FSCP} \cdot T_R \quad (7.7)$$

where

dF_{NSCP} = Near screen pixel incident flux (Lm)

T_R = Transmission of the lens.

The area of the near screen pixel, dA_{NSCP} , is given by:

$$dA_{NSCP} = m^2 \cdot dA_{FSCP} \quad (7.8)$$

where m = Linear magnification of the reduced length photometer. (See section 3.3.2.)

E_{NSCP} , the illuminance at the near screen pixel, is given by:

$$E_{NSCP} = \frac{dF_{NSCP}}{dA_{NSCP}} \quad (7.9)$$

Combining equations 7.6 - 7.9 gives

$$E_{NSCP} = \frac{T_R}{m^2} \cdot E_{FSCP} \quad (7.10)$$

Equation 7.10 is of the same form as equation 7.1, with $K_1 = (T_R / m^2)$.

Since lens losses are essentially constant for visible wavelengths and angles of incidence of up to about 35° (33), then T_R will be a constant. Since m is also a constant (see assumption (a) in section 7.4), then K_1 will have the same value for all pairs of corresponding far and near screen pixels, as required.

7.5.2 Near Screen Pixel Illuminance and Luminance Relationship

In general, the direction of the incident flux and the direction of the corresponding sensor pixel (the viewing direction) are different for each near screen pixel. The direction of the incident flux depends on the position of the screen pixel relative to the lamp; the viewing direction depends on the camera position and will vary with the viewing arrangement used.

Consequently, to satisfy equation 7.2 we require a test screen surface such that the luminance of any small area constituting a screen pixel is independent of the directions of incidence and viewing. Thus, a uniformly diffusing (Lambertian) surface is required; see reference (34).

A uniformly diffusing surface satisfies the equation

$$L = \frac{\rho \cdot E}{\pi} \quad (7.11)$$

where

L = Luminance (Cdm^{-2})

E = Illuminance (Lx)

ρ = Reflection factor

= $\frac{\text{Flux reflected from surface}}{\text{Flux incident on surface}}$

ρ is constant for all angles of flux incidence.

Using this type of surface, therefore, the luminance of a near screen pixel will be given by

$$L_{\text{NSCP}} = \frac{\rho \cdot E_{\text{NSCP}}}{\pi} \quad (7.12)$$

Equation 7.12 is of the same form as equation 7.2, with $K_2 = (\rho/\pi)$.

If ρ is constant over the screen area of interest then K_2 will have the same value for all near screen pixels, as required.

7.5.3 Near Screen Pixel Luminance and Sensor Pixel Illuminance Relationship

We require the relationship between the luminance of any near screen pixel in the direction of its corresponding sensor pixel, L_{NSCP} , and the illuminance produced at this sensor pixel, E_{SEP} . This

can be found by means of the 'camera equation' which appears, in slightly different forms, in many publications; see, for example, references (35) and (36).

The basic form of this equation is:

$$E = \frac{\pi \cdot L \cdot T_c \cdot \cos^4 \theta \left(\frac{D}{v}\right)^2}{4} \quad (7.13)$$

where

E = Image illuminance (Lx)

L = Object luminance in the direction of the camera
(Cdm^{-2})

T_c = Camera lens transmission factor

θ = Off-axis viewing angle

D = Camera lens diameter (m)

v = Distance of the camera lens to the image plane (m).

See also Fig. 7.4.

The derivation of this equation can be found in reference (35).

In the proposed video photometry system, the screen to camera distance, i.e. the camera object distance, u , will be much greater than the image distance, v . Hence v will be approximately equal to the focal length of the camera lens, f .

Thus E_{SEP} and L_{NSCP} will be related by the equation:

$$E_{SEP} = \frac{\pi \cdot L_{NSCP} \cdot T_C \cdot \cos^4 \theta_{SEP}}{4} \left(\frac{D}{f}\right)^2 \quad (7.14)$$

Therefore

$$E_{SEP} = \frac{\pi \cdot L_{NSCP} \cdot T_C \cdot \cos^4 \theta_{SEP}}{4 (f/f)^2} \quad (7.15)$$

where $f/$ = Lens aperture, f/D , i.e. the 'f number'.

For a given screen pixel and its corresponding sensor pixel, θ_{SEP} is constant and hence equation 7.15 is of the same form as equation 7.3, with

$$K_3 = \frac{\pi \cdot T_C \cdot \cos^4 \theta_{SEP}}{4 (f/f)^2} \quad (7.16)$$

However, θ is a function of the sensor pixel position and hence K_3 will not have the same value for all pairs of corresponding near screen and sensor pixels, as required; the $\cos^4 \theta_{SEP}$ term represents an unwanted reduction in sensor image illuminance with increasing off-axis viewing angle. To enable the constant to have the same value for all pairs of pixels, we can write:

$$E_{SEP} = K_{3A} \cdot \cos^4 \theta_{SEP} \cdot L_{NSCP} \quad (7.17)$$

where

$$K_{3A} = \frac{\pi \cdot T_C}{4 (f/f)^2} \quad (7.18)$$

7.5.4 Sensor Pixel Illuminance and Video Output Signal Relationship

The way in which the output voltage signal of a solid-state video camera is related to the illuminance values at the sensor pixels will now be considered. It is assumed here that each V_{SEP} value can be easily identified in the overall video signal.

The basic equations which describe, in photometric terms, the voltage output of each pixel of a solid-state camera are:

$$V_{SEP} = R_{SEP} \cdot X_{SEP} \quad (7.19)$$

where

R_{SEP} = Photometric responsivity of the sensor pixel corresponding to the given far screen pixel for a given spectral composition of incident flux ($VLx^{-1} s^{-1}$)

X_{SEP} = Photometric exposure of the sensor pixel (Lxs)

$$X_{SEP} = E_{SEP} \cdot t_i \quad (7.20)$$

where

t_i = Pixel integration time i.e. the time over which the pixel charge is accumulated (s).

Combining equations 7.19 and 7.20 gives

$$V_{SEP} = R_{SEP} \cdot t_i \cdot E_{SEP} \quad (7.21)$$

For normal camera operation t_i is constant. If R_{SEP} is also constant for all the spectral compositions of incident flux to be measured then equation 7.21 can be written in the form of equation 7.4 with $K_4 = R_{SEP} \cdot t_i$. We also ideally require R_{SEP} , and hence K_4 , to have the same value for all sensor pixels.

7.5.5 Far Screen Pixel Illuminance and Video Output Signal Relationship

Combining equations 7.10, 7.12, 7.15 and 7.21 gives

$$E_{FSCP} = \frac{1}{K_B \cdot \cos^4 \theta_{SEP}} \cdot V_{SEP} \quad (7.22)$$

where

$$K_B = K_1 \cdot K_2 \cdot K_{3A} \cdot K_4$$

If m , t_i and R_{SEP} meet the conditions given in the previous sections, then K_B will have the same value for all pairs of corresponding far screen and sensor pixels, as required. Equation 7.22 is not exactly of the required form, however, owing to the presence of the $\cos^4 \theta_{SEP}$ term; nevertheless, a system which obeys this equation will enable the required E_{FSCP} values to be obtained in a reasonably straightforward manner from the measurement of the V_{SEP}

values. The basic video photometry concept is therefore theoretically feasible.

7.6 Advantages of a Solid-State Camera

The advantages of a solid-state camera over a conventional vacuum tube type camera for this application are as follows:

- a) The discrete nature of a solid-state sensor effectively enables the integration of the flux falling onto a screen pixel, the size and position of which is accurately known as a consequence of the very high accuracy with which the sensor pixels are located.
- b) The digital nature of the scanning mechanism enables, in theory, the output of each sensor pixel to be uniquely identified in the video signal output by the camera.

This contrasts with the electron beam scanning mechanism employed in a conventional vacuum tube camera, for which:

- i) The size of the scanned area is not fixed and careful adjustment is required to avoid over- or under-scanning (37).
- ii) An image reconstructed from its video signal will almost inevitably contain a certain amount of geometric distortion caused by non-linear horizontal and vertical

sweep waveforms and yoke imperfections (37). Furthermore, the amount of geometric distortion produced can vary with factors such as time, temperature and the presence of nearby magnetic fields.

- c) As described in section 7.5.4, a solid-state camera theoretically has a convenient linear sensor illuminance/output voltage characteristic. This is not the case with the vacuum tube type, however, whose output voltage is given by the equation:

$$V = k E^{\gamma} \quad (7.23)$$

where

E = Sensor illuminance (Lx)

V = Sensor output voltage (V)

k & γ are constants.

Further details can be found in reference (38).

- d) With a vacuum tube camera, each image produced is, to a certain extent, contaminated by the ghost of the previous image i.e. a 'residual image' is present. Reference (39) gives details of how this image is formed. Solid-state cameras do not suffer from this problem.
- e) Unlike a vacuum tube camera, a solid-state camera cannot be damaged by over-illumination.

With a vacuum tube camera, it is possible, in an image processing application, to overcome the problems of geometric distortion, non-linear sensor illuminance/voltage output relationship and residual images by careful measurement of the camera's characteristics and the subsequent correction of data acquired by the camera. This process is known as decalibration and is used extensively by NASA to correct the data acquired by the TV cameras used for remote sensing on board spacecraft; see references (39) to (43). This type of scheme, however, has the following problems:

- a) The measurement of a camera's characteristics is a complex and time-consuming process. In general, the characteristics vary from point to point on the sensor and these variations have to be measured and used in the correction procedures if accurate results are to be obtained.
- b) The correction procedures require the manipulation of very large amounts of data, which complicates the design of the system and increases the overall time taken to acquire accurate data from the camera.

Consequently, it was decided that the correction of these characteristics would not be feasible in a practical video photometry system and that only the solid-state type of camera would be studied in detail.

7.7 Comparison of Conventional and Video Photometry Approaches to Illuminance Measurement

- a) With a video photometer, the off-axis imaging performance of the reduced-length photometer influences the accuracy of the data obtained. This is not the case with a conventional goniophotometer, in which all measurements are made on-axis.

- b) The video photometry approach is much more complex than the conventional one. With a goniophotometer, the photodetector directly measures the flux incident on the axis of the measurement surface; with a video photometer, the light is reflected from the whole measurement surface and sampled by the camera lens before being measured by the camera sensor. The properties of the measurement surface (i.e. the screen), the camera's optical system and the camera sensor all influence the performance of the system and constitute potential sources of error.

- c) A conventional goniophotometer effectively produces measurements on a spherical measurement surface; a plane measurement surface is better suited to the video photometry approach.

- d) With a conventional goniophotometer, the operator can make a measurement at any point on the measurement surface, limited only by the mechanical accuracy, resolution and range of movement of the goniometer. With the video photometry approach, however, measurements can only be made at the array

of points corresponding to the centres of the screen pixels. Furthermore, all four viewing arrangements described in section 7.3 cover a relatively limited horizontal field of view in comparison with a conventional goniometer, which can normally be used to measure a field of view of $\pm 90^\circ$ horizontally.

- e) The spacing of the screen pixels determines not only the points at which readings can be made, but also the flux collection area for each reading, which is equal to the area of 1 screen pixel. In a conventional goniophotometer, the flux collection area is independent of the accuracy and resolution with which the measurements points are located.

- f) With a goniophotometer, only the photodetector needs to be totally screened from ambient light, which is relatively straightforward; in a video photometer, the whole of the screen should ideally be kept in darkness, although it would be possible to carry out ambient light correction processing.

8. THE USE OF AN IMAGE PROCESSING SYSTEM FOR VIDEO PHOTOMETRY - FUNDAMENTALS

8.1 Introduction

This Chapter outlines the basic role that an image processing system (IPS) has to play in the type of video photometry system proposed by the author.

It is assumed hereafter that the reader has a detailed knowledge of:

- a) Digital electronics systems; see reference (44), for example.
- b) Types of image processing system architecture; see reference (45).
- c) The theory of analogue to digital conversion, including the concepts of sampling, quantisation and digital coding; see reference (46), for example.
- d) The basic types of analogue to digital converters (ADC's) available i.e. counter (or servo), integrating (or ramp), successive approximation and flash (or parallel); see reference (46), for example.

Since an IPS using pipelined or parallel processors would be unnecessarily complex and prohibitively expensive for this project, it

was assumed at a relatively early stage that a system using a conventional micro or mini-computer as its processing element would be used as the basis of the video photometer design; consequently, only this type of IPS will be considered in this thesis.

The basic role of the IPS is to carry out the following screen illuminance array (SIA) operations; an SIA is defined as a two-dimensional array of numerical data representing the illuminance values which would be produced by a lamp at a specified two-dimensional array of points on the far screen.

- a) The acquisition of an SIA.
- b) The storage of two or more SIA's in the frame store. (This is not necessary if only the conventional tests are to be carried out; see later.)
- c) The display of a pseudo-colour representation of an SIA.
- d) The storage and retrieval of SIA's to and from suitable disk or tape files.

These functions are described in sections 8.2 to 8.6.

8.2 Screen Illuminance Array Acquisition

Acquiring an SIA essentially involves three steps, described in sections 8.2.1. to 8.2.3.

8.2.1 Digitization and Storage of the V_{SEP} Values

The first step involves digitizing the camera's V_{SEP} values and storing the resultant data in the frame store of the IPS; a V_{SEP} value in digital form will be denoted by V_{SEP}' .

There are two fundamental digitization requirements for the video photometry application:

- a) The sampling process carried out by the IPS must be synchronized with the camera to produce 1 sample per sensor pixel.

The ideal frame-grabber for an experimental video photometry system would be capable of being configured to produce 1 sample per sensor pixel for:

- i) Interlaced and non-interlaced video signals
 - ii) Any camera clocking rate
 - iii) Any number of camera pixels per line
 - iv) Any number of lines per frame
- b) The V_{SEP} values must be digitized with sufficient resolution to enable the full range of E_{FSCP} values of interest to be accurately calculated.

As will be seen in Chapter 11, there are problems in meeting both of these requirements with current IPS's; it is assumed here, however, that they can be satisfied.

In addition to the two basic requirements above, a method of removing the noise component of the camera's video signal will probably be required.

8.2.2 Calculation of the E_{FSCP} Values From the V_{SEP} Values

The required E_{FSCP} values will be calculated in digital form from the V_{SEP} values; an E_{FSCP} value in digital form will be denoted by E_{FSCP}' . (Quantisation effects will be considered later.)

If equation 7.5 were obeyed by a practical video photometry system and K_A had the same value for all pairs of corresponding far screen and sensor pixels, then the V_{SEP} values would directly represent the required E_{FSCP} values. It has been shown, however, that, in theory, E_{FSCP} and V_{SEP} are related by the equation

$$E_{FSCP} = \frac{1}{K_B \cdot \cos^4 \theta_{SEP}} \cdot V_{SEP} \quad (7.22)$$

where K_B satisfies the condition given above.

Consequently, if the $\cos^4 \theta_{SEP}$ variations are significant, then the E_{FSCP} values should be calculated using the equation

$$E_{FSCP}' = K_X' \cdot V_{SEP}' \quad (8.1)$$

where K_X' is a suitable digital representation of $1/(K_B \cdot \cos^4 \theta_{SEP})$ and is different for each pair of pixels.

A more complex equation than 8.1 will probably be required in a practical video photometry system in order to correct the effects of non-ideal screen and camera characteristics which result in K_B not having the same value for all pairs of corresponding far screen and sensor pixels; this will be discussed in Chapters 10 and 11.

8.2.3 SIA Generation From the E_{FSCP} ' Values

The array of E_{FSCP} ' values produced by the previous step could be used directly as an SIA for the points corresponding to the centres of the far screen pixels. Other methods of generating an SIA from these values are possible, however, and may have certain advantages; see section 11.3.

8.3 Screen Illuminance Array Storage

Some of the potential applications for the proposed type of system (see Chapter 9) require the acquisition and storage (and subsequent processing) of 2 or more SIA's. Although this could be achieved with a frame-store capable of holding only 1 SIA, by transferring data between the frame-store and the main computer memory or disk, it is obviously more convenient to be able to hold the 2 or more SIA's in the frame-store simultaneously.

In addition to SIA's it may be desirable to use the frame-store to hold the decalibration data used in the SIA acquisition routine; see Chapter 11.

Many IPS's use 8 bit deep frame-stores. As will be seen later, however, more than 8 bits are required to represent the range of illuminance values of interest.

8.4 Screen Illuminance Array Display

A conventional type of iso-lux contour diagram could be produced from an SIA by mathematically deriving and drawing the required contours on the monitor. The use of an IPS, however, enables a pseudo-colour display of an SIA to be produced as follows.

Each SIA element would have a corresponding pixel in the displayed image; this pixel would be assigned a colour (by means of look-up-tables in the display generator) representing which pair of the required illuminance contours the value of the SIA element lay between. For example, blue could represent a value of between 0 and 0.4 lux, red a value of between 0.4 and 0.7 lux and so on. The resulting display would have the appearance of a conventional iso-lux diagram in which the areas between the contour lines had been coloured in. The algorithm for producing this type of display is simpler than that required to find and follow contour lines.

8.5 Screen Illuminance Array Processing

The processing operations to be carried out will depend on the applications that the system is designed for; potential application areas are described in Chapter 9.

The most fundamental operations required would be the addition, subtraction and shifting of SIA's. SIA addition or subtraction would be carried out by adding or subtracting the corresponding elements in the arrays. Shifting on SIA would involve assigning the illuminance values to screen pixels whose positions differ, by given horizontal and/or vertical angular amounts, from those of the points at which the data was actually acquired. The operation is equivalent to physically altering the aim of the lamp and re-acquiring the SIA. For example, an SIA acquired for $\pm 10^\circ$ horizontally, $\pm 8^\circ$ vertically could be shifted 0.5° up to $\pm 10^\circ$ horizontally, $+ 8.5^\circ$, $- 7.5^\circ$ vertically.

8.6 Screen Illuminance Array File Storage

In order to save the acquired data for future use, it is necessary to store it in a disk (or tape) file together with information about the lamp and the test. Since SIA's will contain a large amount of data, the method of long term storage of these files requires careful consideration.

A method of re-loading the frame-store with an SIA from a file is, of course, also required.

9. POTENTIAL APPLICATION AREAS FOR A VIDEO OR HIGH-SPEED PHOTOMETRY SYSTEM

This Chapter describes seven potential application areas within the E&D department for a video or high-speed photometry system capable of acquiring, processing and displaying SIA's in a few tens of seconds or less. Clearly, these types of system also have great potential for production line testing, providing they can be developed to the point where they are simple to operate and calibrate.

9.1 The Conventional Tests

9.1.1 Point to Point Tests

In general, for both the video and high-speed photometers, a point to point test would be carried out by acquiring an SIA and extracting the readings for the required points. An interpolation technique would be necessary if the points for which the data was required did not directly correspond to the points in the SIA.

For the high-speed photometer, a number of discrete photodetectors could be located on the screen at the commonly used test points in order to eliminate the need for mechanical scanning when carrying out a simple point to point test.

9.1.2 Cross-Section Tests

In general, a cross-section test would be carried out by acquiring an SIA and extracting the required one-dimensional array of point readings for display or plotting. Again, interpolation would be used if necessary.

9.1.3 Iso-Lux Tests

An iso-lux test would be carried out by acquiring an SIA and either:

a) Producing a conventional iso-lux diagram by mathematically deriving and drawing the required contours on the monitor or a plotter.

or

b) Displaying a pseudo-colour representation of the SIA on the monitor, as described in section 8.4.

It is for iso-lux tests that the proposed types of system offer the most significant benefits, since the acquisition of the required data by the present Automatic Photometer takes tens of minutes per beam.

9.2 Interactive Design Processing

It will be possible with the proposed types of system to provide an interactive environment for quantitatively investigating the effects of various lamp design features on the beam.

A lamp's beam consists of an infinite number of rays, each originating from a particular point and direction on the filament and directed by the parts of the reflector and lens surfaces it meets. Whilst this is of little relevance when testing a complete lamp, it can be useful to consider the beam as the sum of a finite number of components, each produced by various parts of the filament, reflector and lens. For instance, the reflector can be divided into a number of different areas, each of which, in conjunction with the filament and lens, produces a contribution to the total beam. The beam can, of course, be broken down into an infinite number of such sets of components, but only a few of these will be of interest. Interactive design processing would involve acquiring and manipulating these sets of components.

Two applications have been identified and are described below:

a) Beam Component Study

The basic test procedure would be:

- i) The lamp is covered, leaving only the part of the lens or reflector of interest.

- ii) An SIA for the beam component produced by step (i) is acquired.
- iii) Steps (i) and (ii) are repeated for each beam component of interest.
- iv) The beam components are compared by adding, subtracting, shifting and displaying the SIA's.

For example, the contribution that each facet of a homofocal reflector makes to the total beam could be determined.

b) Beam Synthesis

In the application described above, any beam component to be studied must be physically produced on the test screen by the lamp being tested or be obtainable by performing a combination of addition, subtraction and shifting operations by means of the IPS. In the beam synthesis application, however, the objective would be not only to acquire beam component SIA's, and carry out addition, subtraction and shifting operations, but also to predict the effect of lamp design changes by carrying out more complex SIA processing operations.

The basic test procedure would be:

- i) SIA's are acquired for the beam components of interest.
- ii) One or more of the SIA's is/are processed to simulate

lamp design changes.

iii) A new beam is synthesized by re-combining the SIA's.

In order to carry out this type of work, the ability to predict what changes will be produced in a beam component by a proposed change in the bulb, reflector and lens configuration is required. Some changes in configuration will have more complex effects than others; for example, a simple lens change may merely shift a beam component whereas a change in bulb filament position would produce an effect which would be significantly more difficult to calculate.

The concepts involved in this work are similar to those currently being investigated in the 'Performance Prediction' work (see section 9.6), the basic difference being that the starting point for the calculations would be data acquired physically from a real lamp rather than generated totally from a mathematical model.

9.3 New Methods of Presenting Performance Data

The conventional iso-lux diagram has several drawbacks and the ability to present performance data in the following three additional ways would be very useful:

a) Beam Comparison Diagrams

These would enable the performance of two beams to be compared by means of a single diagram. They would be produced by acquiring an SIA (at the same points) for each beam and either:

i) Subtracting the values of the corresponding elements of the SIA's and producing an iso-lux diagram of the differences by one of the two methods given in section 9.1.3.

or

ii) Dividing the values of the corresponding elements of the SIA's and producing a diagram showing contours of equal ratio values.

b) Road Surface Illuminance Iso-Lux Diagrams

A conventional iso-lux diagram shows the illuminance values obtained on the measurement surface; it would be useful to produce an additional iso-lux diagram showing the values which would be obtained on a plane horizontal surface representing a road; the diagram would show a plane view of this surface. It should be noted, however, that this type of diagram, unlike a conventional iso-lux diagram, cannot show illuminance data for directions above the horizontal axis.

c) Lamp System Iso-Lux Diagrams

A conventional iso-lux diagram shows the performance of a single lamp. In most real systems, two or more lamps are used together. It would therefore be useful to produce a diagram showing the combined effects of the lamps in a system. One problem here is that the conventional methods of specifying points on the measurement surface are based on the position of a single lamp relative to this surface; these test points would have no significance in the context of two or more lamps placed at different positions. Consequently, a different method of specifying test points would have to be developed in order to produce this type of diagram.

These three types of diagram could be produced from the data obtained by a conventional goniophotometer system; they are more suitable for use with a video or high-speed photometry system, however, as a result of their ability to acquire and display large amounts of data quickly.

9.4 Reflector Testing

The optical performance of a headlamp reflector, which is made by moulding or pressing, cannot be fully checked until it has been lacquered and aluminised. Since this takes several hours, many unacceptable reflectors can be produced before a problem is detected. Consequently, there is a need for a method of quickly assessing the optical performance of an untreated reflector.

It was recognised by the author that certain image processing techniques could prove useful in this area. The basic concept is that the image obtained by using a point source in an untreated reflector will contain detailed information about the reflector's form and finish. By studying the differences in the SIA's, or processed versions of the SIA's, produced by good and bad reflectors, a set of criteria for accepting or rejecting a reflector could possibly be established. It is thought that spatial frequency processing techniques (47), such as the use of Fourier Transforms, could be useful here; reflector form variations will produce low spatial frequency components where variations in finish will show as high spatial frequency components. Filtering operations could be used to examine the various components and image features.

9.5 Automatic Aiming

As described in section 3.1, a lamp has to be aimed before the illuminance readings can be taken; the aiming process is currently a manual one. With the video or high-speed photometer, however, there exists the possibility of developing an automatic aiming technique.

With automatic aiming, the basic test procedure would be:

- a) The lamp is roughly aimed by eye or by means of a mechanical fixture.
- b) An SIA is acquired.

- c) The SIA is processed by the computer to determine, by means of a previously defined algorithm, the optimum positions of the horizontal and vertical axes of the measurement surface in relation to the acquired illuminance data.

- d) A new SIA is created using the information generated in step (c); this SIA is equivalent to that which would have been obtained if the optimum aim of the lamp had been found manually.

Automatic aiming would be particularly useful for production line testing since it would reduce the time taken to carry out a test and eliminate the possibility of a good lamp being rejected because of incorrect manual aiming.

For an automatic aiming system to be useful, the aiming algorithms would need to be very sophisticated in order to cope with the many detail differences in beam patterns that are encountered in practice.

9.6 Generation of Data for Development of 'Performance Prediction' Software

The aim of the 'Performance Prediction' work, which is currently being undertaken at the Lucas Group Research Centre, is to provide a mathematical model of a headlamp which can be used to predict the intensity distribution that a given bulb, reflector and lens design will produce without the time and expense involved in building a prototype. This work is very complex and is being carried

out in several stages. An essential part of the development work will be the comparison of theoretically generated photometric data with that acquired by the testing of real lamps; a video or high-speed photometry system would be very useful as a means of acquiring the necessary test data.

9.7 Generation of Data for 'Chess'

'Chess' is a computer model, written by Ford, for predicting how well a given headlamp system, characterised by the positions and intensity distributions of its individual lamps, serves road users' vision needs. It does this by using a mathematical model of human vision to carry out thousands of visibility and glare tests on a standardised test route which simulates a broad range of driving conditions. The ultimate output of the model is a figure-of-merit which is the percentage of distance travelled along the standardised test route for which the lamp system enables certain pre-selected visual performance criterion levels to be met.

The program is being distributed by Ford to the various bodies within the vehicle lighting industry, including lamp manufacturers, with a view to it becoming a standard method of assessing the effectiveness of headlamp systems.

A video or high-speed photometry system would provide a convenient method of acquiring the intensity data required for inputting to the program.

10. MEASUREMENT SURFACE IMAGING WITH A VIDEO CAMERA - FURTHER DETAILS

10.1 Introduction

The basic concepts of measurement surface imaging with a video camera are described in Chapter 7; the four photometric relationships developed in section 7.5 are now considered in more detail. It is shown that there will be many additional factors to be taken into account in a practical video photometry system. The characteristics of a commercially available charge coupled device (CCD) camera are also discussed.

It is assumed in this Chapter that the reader has a detailed knowledge of:

- a) Lens aberrations i.e. spherical aberration, coma, field curvature, astigmatism, distortion and chromatic aberration. See references (48) and (49), for example.
- b) The following topics relating to solid-state sensors and cameras:
 - i) The principles of photon detection and charge generation in silicon by means of a pn junction or MOS (metal oxide silicon) capacitor.
 - ii) The operational principles of the following types of two-dimensional sensors: self-scanned photodiode arrays,

charge coupled devices (parallel/serial, frame transfer and interline transfer types) and charge injection devices.

- iii) The following properties of solid-state sensor arrays: spectral response, dark signal and its non-uniformities, responsivity non-uniformities, noise, cross-talk and blooming.

See references (50) to (58), for example.

10.2 Far Screen Pixel and Near Screen Pixel Illuminance Relationship

As described in section 7.5.1, if a reduced-length photometer produces a geometrically perfect image, the relationship between E_{NSCP} and E_{FSCP} is:

$$E_{\text{NSCP}} = \frac{T_R}{m^2} \cdot E_{\text{FSCP}} \quad (7.10)$$

In practice, however, as a consequence of lens aberrations, each pencil of rays which would converge to a point on the far screen, will, after passing through the lens, form a blur patch, rather than a point, on the near screen. Furthermore, the centre of each patch may not be at the ideal imaging point predicted by the theoretical magnification. In addition, a certain amount of flare, which is discussed in more detail in section 10.4.3 in connection with the camera lens, will occur.

Consequently, departures from equation 7.10 will be experienced in practice; the magnitude of these departures will, in general, vary for each pair of corresponding near and far screen pixels, and will be a function of:

- a) The size of the blur patch.
- b) The illuminance gradients in the area of the beam surrounding the point being measured.
- c) The flux collection area being used to make the illuminance measurement.

The situation is further complicated by the fact that the required far screen pixel illuminance value, E_{FSCP} , is itself a function of factors (b) and (c); see section 3.3.1.

As a result of the complex nature of reduced-length photometer performance, it is not feasible to correct the departures from equation 7.10 which will be produced in any specific situation. Hence a practical video photometry system requires an RLP whose performance can be considered to obey equation 7.10 sufficiently closely for the errors to be ignored. It is, however, very difficult to define a maximum acceptable error, not only because of the many factors which affect RLP performance, but also because, in a video photometry system, the RLP is only one of several potential sources of error. Consequently, whether or not a given departure from equation 7.10 is significant will largely depend on the magnitudes of the errors produced by the other parts of the system, which are themselves

unknown at present.

Reduced-length photometer performance is considered in more detail in Chapters 12 and 13.

10.3 Near Screen Pixel Illuminance and Luminance Relationship

As described in section 7.5.2, a uniformly diffusing surface with a constant reflection factor is ideally required for the screen. In practice, no known surface exhibits perfectly uniform diffuse reflection; many matt-surfaced materials, however, closely approximate the required characteristics over a limited range of incidence and viewing directions (34). It would seem reasonable to assume, therefore, that a matt white screen would be satisfactory for a practical video photometry system, although some variations from equation 7.12 are to be expected in practice; the smaller the deviations of the angles of incidence and viewing from the normal, the better the approximation to a uniform diffuser is likely to be. Thus a maximum off-axis angle of 15° is likely to be more satisfactory than 30° from the aspect of screen pixel luminance characteristics, especially if viewed using arrangement (d) of section 7.3, where the viewing angles involved are smaller than with arrangements (a), (b) and (c).

If the characteristics of the screen were not sufficiently close to those of a uniform diffuser, then the relationship between the E_{NSCP} and L_{NSCP} values could be described by the equation:

$$L_{\text{NSCP}} = K_2 \cdot E_{\text{NSCP}} \cdot C_{\text{NSCP}} \quad (10.1)$$

where

$$K_2 = \rho / \pi$$

C_{NSCP} is a constant, which, in general, has a different value for each pixel.

The C_{NSCP} values for a given screen could be measured and used in the SIA acquisition software to calculate the E_{NSCP} values from the measured L_{NSCP} values; see Chapter 11.

In a practical video photometry system, it would be necessary either to keep the screen very clean, in order that the reflectance characteristics would not significantly change over a period of time, or to carry out periodic measurements of the C_{NSCP} values for inclusion in the correction processing.

10.4 Near Screen Pixel Luminance and Sensor Pixel Illuminance Relationship

10.4.1 Camera Lens Aberrations

It was assumed in section 7.4 that the camera lens produces, in the geometrical optics sense, a perfect image. In practice, this will not be the case, as a result of lens aberrations. Since the effect of these aberrations cannot easily be corrected by subsequent processing,

a practical video photometry system requires them to be sufficiently low that they can be ignored. In view of the fact that the object to be imaged, i.e. the beam pattern on the screen, essentially contains only low spatial frequency components, it is reasonable to assume that a high quality multi-element camera lens would satisfy this condition. (This situation is different to that encountered in many automatic inspection systems, where edges or points in the image have to be detected or measured; in these situations, lens aberrations can be very significant (59).)

10.4.2 Off-Axis Image Illuminance Reduction

It was shown in section 7.5.3 that there is an unwanted reduction in image illuminance with increasing off-axis viewing angles. There are essentially two practical design approaches which can be taken to overcome this problem:

- a) All data acquired from the camera, or cameras, can be processed to compensate for the variations as part of step (b) of the SIA acquisition procedure, as described in section 8.2.2.
- b) The imaging system can be designed such that the variations are sufficiently small to be ignored.

Viewing arrangement (d) clearly has an advantage here over the others since the off-axis viewing angles required to cover any field of view are smaller. For example to cover $\pm 15^\circ$ H, $\pm 7.5^\circ$ V each camera images $\pm 7.5^\circ$ H, $\pm 7.5^\circ$ V. The maximum reduction in image illuminance is therefore:

$$(1 - \cos 7.5^\circ) \times 100\% = 3.4\%$$

With arrangement (c), the camera images the full field resulting in a reduction of 13%. Arrangement (b) requires even greater viewing angles, giving an even greater image illuminance reduction.

This approach is clearly only practical with viewing arrangement (d) if a useful field of view is to be covered; even with this arrangement, however, the variations are probably too high to ignore.

10.4.3 Camera Flare

Equation 7.15 does not take into account the effects of flare i.e. the unwanted light reaching the image plane in addition to the direct image - forming light.

Flare is produced in a camera by light from the subject being reflected at the surfaces of the lens components and the internal camera surfaces; some of this light undergoes multiple reflections and falls more or less evenly all over the image plane, where it has a general fogging effect (60). In a solid-state video camera, the window which is part of the integrated circuit package containing the sensor gives rise to a further two potential reflecting surfaces.

The consequence of flare for the video photometry application is that screen pixels having low luminance values will produce higher than expected sensor pixel illuminance values; the extent of the

departures from equation 7.15 will depend not only on the characteristics of the camera body, lens and sensor package used, but also on the distribution and dynamic range of the screen luminance values being measured, which vary with the type of beam being tested.

The effects of flare cannot easily be corrected by subsequent processing and in a practical video photometry system need to be sufficiently low that they can be ignored. It is very difficult to predict whether or not this is likely to be achieved in practice, however, without making practical measurements; unfortunately, a fully working video photometry system is needed in order to carry out meaningful experimental work.

10.5 Sensor Pixel Illuminance and Video Output Signal Relationship

Equation 7.21 in section 7.5.4 describes the basic theoretical relationship between V_{SEP} and E_{SEP} . In practice, however, the relationship will be far more complex, as a result of various non-ideal camera characteristics.

The main areas of camera performance to be considered for this application are:

- a) Spectral response characteristics
- b) Sensitivity
- c) Clocking characteristics and video signal generation
- d) Dark signal characteristics
- e) Responsivity variations

- f) Noise characteristics
- g) Blooming characteristics
- h) Sensor pixel geometry
- i) Blemishes

The above areas are considered in sections 10.5.1. to 10.5.9.

10.5.1 Spectral Response Characteristics

In order for equation 7.21 to be satisfied, the photometric responsivity, R_{SEP} , must be constant for every spectral composition of incident flux to be measured. For headlamp photometry, this requires a sensor whose spectral response is a reasonably close approximation to the $V(\lambda)$ response, as described in section 4.1. Whereas conventional photodetectors are available which meet this requirement, the situation with solid-state video cameras is not as simple, since they are not sold as photometric measurement instruments and do not, in general, have the required spectral response characteristics; we may therefore have to consider how the response of a given camera can be modified by means of a suitable filter or filters.

There are four basic problem areas, however;

- a) Different types of sensor have different response characteristics, caused by the varying fabrication processes used. A charge coupled device can have a very uneven response characteristic due to interference effects in the polysilicon layers on the surface of the chip (56). Consequently, it could be difficult to obtain the required response with this type of

device. Photodiode arrays are claimed to have a much smoother response which should in theory be easier to modify as required.

- b) Individual sensors of a given type can have widely varying spectral response characteristics (56). There is, therefore, a potential danger in using the 'typical' response characteristics quoted on manufacturers' data sheets.
- c) The practical measurement of sensor spectral response characteristics is a complex task, requiring specialised equipment; not even the National Physical Laboratory are able to carry out such measurements as a matter of routine.
- d) The use of a filter to modify spectral response will also decrease the level of sensor illuminance, thereby effectively decreasing the overall sensitivity of the system.

10.5.2 Sensitivity

The sensitivity of the camera must be sufficiently high to produce a useful range of output voltages for the range of E_{FSCP} values of interest; ideally, the maximum E_{FSCP} value of interest, $E_{FSCP_{MAX}}$, should cause the onset of camera saturation.

Combining equations 7.10, 7.12 and 7.15 gives E_{SEP} as a function of E_{FSCP} :

$$E_{SEP} = \frac{T_R \cdot \rho \cdot T_C \cdot \cos^4 \theta_{SEP}}{4 \cdot m^2 \cdot (f/l)^2} \cdot E_{FSCP} \quad (10.2)$$

The maximum value of E_{SEP} that will be produced, E_{SEPMAX} , is given by:

$$E_{SEPMAX} = \frac{T_R \cdot f \cdot T_C}{4 \cdot m^2 \cdot (f/\lambda)^2} \cdot E_{FSCP_{MAX}} \quad (10.3)$$

If all the system parameters are known, then equations 7.21 and 10.3 can be used to determine whether or not sensor saturation is likely to be achieved. It should be remembered that the effects of any filters used for spectral response modification must also be taken into account.

10.5.3 Clocking Characteristics and Video Signal Signal Generation

As described previously, one of the factors which determines the sensitivity of a solid-state camera is the pixel integration time, t_i , which is determined by the clocking rate of the sensor. Depending on the design of the camera, this rate will be either fixed or variable. A variable clocking rate is a very useful feature, therefore, since it provides a convenient way of accurately controlling the sensitivity of the camera. As will be seen later, a camera with a variable clocking rate also offers a wider range of possibilities for interfacing to an image processing system.

The voltages output from a sensor's pixels are processed in the camera to provide the output video signal. In many cases, this signal is designed to meet one of the existing standards for video signals; information about these standards can be found in references (61) and (62), for example. When the output of a solid state sensor is converted to a video signal of this form, it is often difficult to identify where the output of each sensor pixel appears in the video

signal, particularly when an interlaced output, which introduces the additional complication of half-lines, is used. It is of course, vital for the proposed application that this relationship between the sensor geometry and the video signal is clearly defined.

10.5.4 Dark Signal Characteristics

As described in section 7.5.4, the basic equation governing the output of each sensor pixel is:

$$V_{SEP} = R_{SEP} \cdot X_{SEP} \quad (7.19)$$

In practice, however, the dark signal may also need to be taken into account; this is the component of the output signal voltage produced by thermally generated charge and is present for any level of sensor illuminance. In general, the magnitude of the dark signal is different for each sensor pixel. Hence a more accurate equation is:

$$V_{SEP} = VX_{SEP} + VD_{SEP} \quad (10.4)$$

where

VD_{SEP} = Dark signal component of V_{SEP}

VX_{SEP} = Component of V_{SEP} generated by the exposure X and given by equation 10.5

$$VX_{SEP} = R_{SEP} \cdot t_i \cdot E_{SEP} \quad (10.5)$$

The presence of a dark signal is clearly undesirable when

using a camera to make quantitative photometric measurements and it cannot be ignored unless of a very low level compared to the magnitude of the VX_{SEP} component for the smallest E_{SEP} value of interest; it can, however, be corrected for, as explained later.

10.5.5 Responsivity Variations

As stated in section 10.5.4, the basic theoretical equation describing the relationship between VX_{SEP} and E_{SEP} is:

$$VX_{SEP} = R_{SEP} \cdot t_i \cdot E_{SEP} \quad (10.5)$$

In a real sensor, however, the R_{SEP} values are not necessarily constant:

- a) The relationship between the illuminance of a sensor pixel and the charge packet generated is linear. However, in order to produce a usable signal, an on-chip amplifier converts each charge packet into an output voltage; this stage may be non-linear (51). Furthermore, additional circuitry between the sensor chip and the final video output of the camera may also introduce non-linearities. Consequently, the overall relationship between E_{SEP} and VX_{SEP} can be non-linear. In this case, R_{SEP} in equation 10.5 is not a constant, but a function of illuminance level.

In principle, the effects of non-linearity can be corrected by subsequent processing. For example, a characteristic can be approximated by a series of straight line segments; given

the starting points, end points and slopes of these segments, the X_{SEP} value corresponding to any given V_{SEP} value can be found. This method requires the storage of several parameters per pixel, however; since, in general, these parameters will vary for each pixel (see below), the method is not very feasible for correcting data from an area sensor containing thousands of pixels.

Consequently, the video photometry application requires a sensor that has a substantially linear characteristic, so that the R_{SEP} value for any given pixel can be regarded as constant for any illuminance level.

- b) Even if the R_{SEP} value for any given pixel can be regarded as constant for any illuminance level, this value can vary from pixel to pixel, as a result of processing and materials variations in the chip manufacture (51).

Variations in the R_{SEP} values from pixel to pixel can be corrected for if necessary by the storage of a single parameter per pixel; whilst this type of decalibration is undesirable, since it complicates the system design and calibration, it is not out of the question and is considered in more detail in section 11.3.

If responsivity variations are to be taken into account, then it is convenient to re-write equation 10.5 in the form

$$V_{X_{SEP}} = K_{4A} \cdot \frac{R_{SEP}}{R_{SEPAV}} \cdot E_{SEP} \quad (10.6)$$

where

R_{SEPAV} = Average responsivity of all the sensor pixels

K_{4A} = $t_i \cdot R_{SEPAV}$

K_{4A} has the same value for all sensor pixels.

10.5.6 Noise Characteristics

The video output signal generated by real cameras also contains a random noise element which can cause errors when using a camera to make quantitative measurements:

If V_N is the noise component of the signal, then V_{SEP} is given by:

$$V_{SEP} = V_{X_{SEP}} + V_{D_{SEP}} + V_N \quad (10.7)$$

where V_N is a function of time.

Consequently, when V_{SEP} is digitized the resultant value will include a 'frozen' noise component whose magnitude will depend on that of the noise at the point in time when the sample was taken.

The effects of noise can be reduced by digital filtering; this will be described in section 11.2.

10.5.7 Blooming Characteristics

As will be seen later when methods of interfacing a solid-state camera to an image processing system are considered, the

way in which a sensor performs when part of it is illuminated beyond the level required to produce saturation is an important aspect of performance to be considered for the proposed application.

10.5.8 Sensor Pixel Geometry

It was assumed in Chapter 7 that each sensor pixel acts as an entirely separate photodetector. In practice, this is not the case because of cross-talk (51). Since the effects of cross-talk cannot easily be corrected by subsequent processing, they must be sufficiently low that they can be ignored in a practical video photometry system; in view of the fact that a headlamp beam pattern does not contain high spatial frequency components, it is reasonable to assume that this will be the case.

It was also assumed in the sensor model that the whole of each sensor pixel is photosensitive; this is usually the case, but not for the interline transfer type of CCD sensor, as manufactured by Fairchild. If this type of sensor is to be used, it should be remembered that the effective flux collection area of each screen pixel will be smaller than the total area.

Furthermore, some sensors have pixels whose positions are not fixed, as also assumed in the model; these sensors produce a type of interlaced output by moving the effective pixel positions from one field of the signal to the next; see section 15.6.1 and reference (51).

10.5.9 Blemishes

Blemished sensor pixels are undesirable for the video photometry application because their V_{SEP} values cannot be used to calculate the corresponding E_{FSCP} values. Single pixel blemishes would not cause serious problems because their E_{FSCP} values could be interpolated from the E_{FSCP} values of the surrounding pixels; blemishes which extend over entire rows or columns are less desirable.

10.6 Far Screen Pixel Illuminance and Video Output Signal Relationship

It has been shown that in a practical video photometry system, equation 7.22, describing the relationship between the far screen pixel illuminance and the sensor pixel output voltage, will be modified by the effects of one or more of the following:

- a) Non-ideal reduced-length photometer characteristics
- b) Non-ideal screen diffusion characteristics
- c) Non-ideal camera lens characteristics
- d) Non-ideal camera characteristics:
 - i) Non-photopic spectral response
 - ii) Dark signal
 - iii) Non-linear illuminance/voltage characteristics
 - iv) Pixel to pixel responsivity variations
 - v) Noise
 - vi) Cross-talk

The effects of (a), (c), (d-i) and (d-vi) are complex, depend on the beam characteristics of the lamp being tested and cannot easily be corrected by subsequent processing. The effects of (d-iii) can be corrected in principle but the very large amounts of data that would be necessary for the correction routines do not make this feasible in practice. Consequently, a successful practical video photometry system will require the effects of (a), (c), (d-i), (d-iii) and (d-vi) to be sufficiently low that they can be ignored.

If the effects of (b), (d-ii), (d-iv) and (d-v) are significant, then the relationship between the far screen pixel illuminance and the sensor pixel output voltage is given by equation 10.8 below, which is derived by combining equations 7.10, 10.1, 7.15 and 10.6.

$$E_{FSCP} = \frac{1}{K_C \cdot \cos^4 \theta_{SEP} \cdot C_{NSCP}} \cdot \frac{R_{SEPAV} \cdot VX_{SEP}}{R_{SEP}} \quad (10.8)$$

where

$$VX_{SEP} = V_{SEP} - VD_{SEP} - VN$$

$$K_C = K_1 \cdot K_2 \cdot K_{3A} \cdot K_{4A}$$

$$K_1 = \frac{T_B}{m^2}$$

$$K_2 = \frac{\rho}{\pi}$$

$$K_{3A} = \frac{\pi \cdot T_C}{4 (f')^2}$$

$$K_{4A} = t_i \cdot R_{SEPAV}$$

If m , f and t_i meet the conditions given in sections 7.1, 7.2 and 7.4 respectively, then K_c will have the same value for all pairs of corresponding far screen and sensor pixels, as required, and equation 10.8 can be used to calculate E_{FSCP} from the measured V_{SEP} value; this is discussed in Chapter 11.

10.7 The Fairchild CCD3000 Camera

The solid-state camera characteristics described in section 10.5 are now considered for a modern CCD camera, the Fairchild CCD3000 (63, 64), which uses the CCD222, a 488 x 380 element sensor (65).

Unfortunately, detailed performance information is not always readily available from solid-state camera manufacturers; the information given here is obtained from the Fairchild literature referenced above and is ambiguous, or incomplete in places. The terms 'dark signal', 'dark signal shading non-uniformity (DSSNU)', 'saturation output voltage' (V_{SAT}), 'photoresponse shading non-uniformity (PRSNU)' and 'dynamic range' are used in this section as defined by Fairchild for the CCD222 sensor on page 69 of reference (65).

10.7.1 Spectral Response Characteristics

The sense head of the camera incorporates an infra-red cut-off filter (a 2 mm thick BG38) to give the camera a 'near photopic' response; a typical response curve is given in reference (63), although

no information is provided about the extent of the variation from sample to sample. The response quoted would probably be satisfactory for headlamp photometry (i.e. further filtering would probably not be necessary), although practical tests would be necessary to confirm this.

10.7.2 Sensitivity

Although various sensitivity figures are quoted in photometric terms for the CCD 222 sensor in reference (65), it is not clear how these relate to the CCD3000 camera, because of the infra-red cut-off filter incorporated in the sense head; the sense head illuminance required for saturation is not quoted in photometric terms in the CCD3000 data sheet (63) or operating manual (64). It does, however, state that '20 lux scene illuminance at 2800K will provide 40dB S/N with 50% scene reflectance and an f1.4 lens at 25° C'. An E_{FSCP} value of 50 lux at 25 m and a 4 m reduced-length photometer will produce an E_{NSCP} value of approximately 2500 lux and the screen reflectance will be greater than 50%; there should consequently be little problem in achieving sensor saturation with this camera.

The typical saturation output voltage, V_{SAT} , is quoted in reference (65) as 700 mV on page 71 and 1 V on the graph on page 75.

10.7.3 Clocking Characteristics and Video Signal Generation

The output of the camera is in the form of an EIA RS170 signal (an American standard), which is an undesirable complication for the

present application since it produces a complex sensor geometry/video signal relationship.

The camera has an external master clock input (see reference (64)), but the upper and lower input frequency limits are not stated; it is therefore not clear whether this facility can be used to change the clocking rate by a substantial amount (for example, to half its standard value of approximately 14 MHz), or whether it is intended for 'fine tuning' only.

(Another Fairchild camera, the CCD4000, outputs its data in the form of a 256x256 non-interlaced square pixel scanning format, which is far more attractive for the video photometry application than an RS170 video signal. However, this camera does not in fact use a 256 x 256 sensor with square pixels, as implied in the advertising literature (63); the sensor is actually the CCD222, the output signal being low-pass filtered and re-sampled to simulate a 256 x 256 sensor. This is undesirable for the video photometry application since the direct correspondence between the sensor pixel geometry and the sensor output signal is not reflected in the final camera video output signal.)

10.7.4 Dark Signal Characteristics

The typical dark signal value at 25° C is given on page 75 of reference (65) as 20 mV; the typical V_{SAT} value is given as 1000 mV. This level of dark signal could not be ignored in a video photometry system and would need to be corrected for by subsequent processing.

The typical dark signal shading non-uniformity value at 25° C is given as 1 mV on page 75 of reference (65); this is equivalent to 0.1% V_{SAT} . In the table on page 71 of reference (65), however, the value for this same quantity is given as 1% V_{SAT} ; this table also states that the maximum value is 2% V_{SAT} . If the typical dark signal shading non-uniformity value is only 0.1% V_{SAT} , then it is insignificant and the dark signal can be considered the same for all pixels, which simplifies the correction processing. A larger non-uniformity value, however, would require correction on a pixel by pixel basis.

10.7.5 Responsivity Variations

The gamma value for the camera is quoted as unity (see page 67 of reference (65)) but no tolerances are given.

The typical photoresponse shading non-uniformity is given as 1% V_{OUT} on page 71 of reference (65); the maximum value is given as 10% V_{OUT} . Whether or not correction would be required in practice would depend on whether the values were nearer the 'typical' or 'maximum' figures for the particular sensor being used.

10.7.6 Noise Characteristics

On page 71 of reference (65), the typical saturation output voltage and typical dynamic range at 25° C are given as 700mV and 1000 respectively. Thus, using the Fairchild definitions on page 69 of reference (65), the rms noise is 0.7mV. On page 75 of reference (65), however, the typical rms noise value at 25° C is given as 0.2mV.

Fairchild state that the peak to peak value of the noise is 4 - 6 times the rms value. Thus, assuming on rms noise of 0.7mV and a factor of 6, the peak to peak noise value would be 4.2mV, which, assuming a V_{SAT} value of 700mV, $= 1/167 V_{SAT}$. Thus, even with only 8 bit digitization (see section 11.2), the magnitude of the 'frozen' noise component would be approximately 3 times higher than the quantisation error of $1/512 V_{SAT}$, necessitating the use of a noise reduction method.

10.7.7 Blooming Characteristics

The CCD222 contains a column anti-blooming electrode which reduces the horizontal spreading of the charge generated by a part of the sensor which is saturated; vertical spreading can occur, however, and the camera cannot be considered as an anti-blooming model for the video photometry application.

10.7.8 Sensor Pixel Geometry

No cross-talk performance data is given by Fairchild for this sensor.

The sensor is of the interline transfer type and the whole of each pixel is not photosensitive. If the sensor pixels are considered as contiguous, as in the model described in Chapter 7, then each pixel has a size of $30 \mu\text{m}$ (horizontal) \times $18 \mu\text{m}$ (vertical), of which an area of $12 \mu\text{m}$ (horizontal) \times $18 \mu\text{m}$ (vertical) is photosensitive; see page 69 of reference (65).

10.7.9 Blemishes

The grade of CCD222 sensor used in the CCD3000 camera is specified as having zero blemished columns; the number of blemished rows is not stated, but is presumably also zero. Blemishes are unlikely to be a serious problem with this camera, therefore.

11. THE USE OF AN IMAGE PROCESSING SYSTEM FOR VIDEO PHOTOMETRY - FURTHER DETAILS

11.1 Introduction

This Chapter describes the role of the image processing system in the proposed type of video photometer in more detail.

The most difficult operation to be implemented is SIA acquisition; having acquired an SIA, the other operations are relatively straightforward, at least in principle. Consequently, this Chapter is mainly concerned with the SIA acquisition procedure. The three steps involved, which were briefly described in section 8.2, are considered in more detail in sections 11.2 to 11.4. Section 11.5 considers the effect of ambient light falling on the screen.

Section 11.6 describes the main design considerations involved in using an image processing system for video photometry, taking into account the problems of SIA acquisition and storage.

11.2 Digitization and Storage of the V_{SEP} Values

The following terminology is used in this section in connection with the use of an analogue to digital converter to digitize a video signal, and the interpretation of the digital data as illuminance values:

- $E_{FSCP\text{MIN}}$ - The minimum E_{FSCP} value to be measured for a given beam type
- $E_{FSCP\text{MAX}}$ - The maximum E_{FSCP} value to be measured for a given beam type
- V_{SEPSAT} - The saturation output voltage of the camera
- V_{NPP} - The peak to peak voltage of the noise in the camera's video signal
- V_{ADC} - The analogue to digital converter input voltage
- V_{ADCFS} - The V_{ADC} value required to produce full scale output; it is assumed that the system is designed so that $V_{SEPSAT} = V_{ADCFS}$
- n - The number of analogue to digital converter bits
- Q_V - The analogue to digital converter bit size, expressed as an input voltage; $Q_V = V_{ADCFS} / 2^n$. The maximum quantisation error = $Q_V/2$.

There are difficulties in satisfying both of the fundamental requirements given in Chapter 8 with current image processing systems:

- a) Virtually all current IPS's are designed for use with conventional tube type video cameras. With this type of camera, the part of the video signal representing the sensor

illuminance does not present any special sampling requirements since the signal does not originate from discrete elements, as in a solid-state camera. Hence currently available IPS's cannot be used for the video photometry application without modification of the sampling circuitry of the frame-grabber.

- b) It is not possible to digitize video rate signals (from either type of camera) with the same resolution as slower signals. Most current IPS's use 6 or 8 bit converters; a commonly used 8 bit device is the TRW 1007J (66), which costs several hundred pounds. Higher resolution video rate converters are available, but are primarily aimed at military applications and are very expensive. Analogue Devices, for instance, produce a 12 bit 10MHz converter, the CAV-1210 (67), but this costs several thousand pounds and the use of such a device is clearly not feasible for the video photometry project.

The use of 8 bit digitization for the video photometry application will now be considered.

We will consider the case of a headlamp dipped beam and assume that $E_{FSCP_{MIN}} = 0.25$ lux at 25 m and $E_{FSCP_{MAX}} = 50$ lux at 25 m. Thus, when the E_{FSCP} ' value is calculated from the V_{SEP} ' value, the resolution will be $50/256$ lux i.e. approximately 0.2 lux. The maximum quantisation error will correspond to 0.1 lux.

A quantisation error of 0.1 lux is acceptable when the value being measured is at the upper end of the 0.25 lux to 50 lux range since it is insignificant in relation to the overall

error associated with the measurement; see section 4.1. When measuring values at the bottom end of this range, however, then this level of quantisation error is unacceptable since it represents a large percentage of the value being measured.

There is therefore, a fundamental problem in using a standard image processing system with an 8 bit analogue to digital converter to make measurements over the dynamic range of illuminance values of interest.

In theory, this problem can be overcome by one of two basic approaches, which are described later.

As stated in Chapter 8, a method of removing the noise in the camera's video signal, i.e. the VN term in equation 10.7, will also probably be required; this is now considered.

If $V_{N_{pp}}$ is less than $Q_v/2$ then its effect will be masked by the quantisation error. In this case therefore, the camera noise can be disregarded and the required end result of step (a) of the SIA acquisition procedure is a frame of V_{SEP} ' data.

If $V_{N_{pp}}$ is greater than $Q_v/2$, then a noise reduction technique is required. As will be seen in section 11.3, it is possible to remove the effects of dark current and responsivity variations from a single frame of V_{SEP} ' data acquired from a camera; this is possible because the above characteristics can be measured in advance. Noise in the camera's video signal cannot be removed in the same way, however, since it is random in nature and its value at the instant the

video signal is sampled cannot be known in advance. The noise level can be reduced, however, by using a digital filtering technique to combine several frames of digitized data obtained from a stationary image; these techniques are described in reference (68). The largest improvement in signal to noise ratio is obtained using an averaging filter; the noise reduction obtained is proportional to the square root of the number of frames averaged. Some image processing systems have hardware to enable this averaging operation to be performed at a much faster rate than is possible by using the computer.

If digital noise filtering is used, then the required end result of step (a) of the SIA acquisition procedure is a frame of data representing, in digital form, the $(V_{SEP} - VN)$ values; these will be denoted by $(V_{SEP} - VN)'$. The noise component of the $(V_{SEP} - VN)'$ data must be reduced to the level where it is equivalent to a VN_{pp} of $Q_V/2$ or less, so that the noise is insignificant compared to the quantisation error.

Methods of overcoming the dynamic range problem described earlier and producing a frame of V_{SEP}' or $(V_{SEP} - VN)'$ values with sufficiently low quantisation errors are now considered. The two basic approaches which can be adopted are:

- a) Slowing down the rate at which the analogue to digital conversion is carried out, thereby enabling a higher resolution ADC to be used; this approach will be known as the single range approach, since it aims to cover the illuminance values of interest for a given beam type in a single range, using a high resolution converter.

A 10 bit converter, giving a maximum quantisation error of approximately 0.025 lux when used over a 0-50 lux range would be acceptable; 11 or 12 bits would be more satisfactory. (The Automatic Photometer uses a 12 bit converter, covering a range of 0-100 lux for dipped beams; this gives a maximum quantisation error of 0.012 lux.)

- b) Using a conventional 8 bit video rate converter, but arranging for the V_{SEP} values to be converted to be always at a sufficiently high level for the quantisation error to be acceptably small; this approach will be known as the multiple range approach since it effectively breaks down the range of illuminance values to be measured for any given beam type into a series of ranges.

It should be noted that for both approaches we are only considering the range of illuminance values of interest for any given beam type (in this case the dipped beam) and that an additional mechanism for changing the sensitivity of the system to cater for the various beam types is necessary.

Methods of implementing the single and multiple range approaches are described and evaluated in sections 11.2.1 and 11.2.2 respectively.

11.2.1 Single Range Digitization Methods

Two possible single range digitization methods are described and evaluated here; for both methods, the system would be designed so

that $E_{FSCPMAX}$ produces a camera output of V_{SEPSAT} .

11.2.1.1 Method (a)

The required reduction in digitization rate would be achieved by reducing the clocking rate of the camera and the ADC; the method obviously requires a camera with a variable clocking rate facility and could be used with or without digital filtering to produce V_{SEP} ' or $(V_{SEP} - VN)$ ' values.

11.2.1.2 Method (b)

This method is based on the use of more than one frame of camera data to build up 1 frame of V_{SEP} ' data in the frame-store; only some of the pixels in each line of camera data would be digitized, thereby allowing more time for each conversion than would normally be available. (The method does, of course, rely on the sensor image not changing from one frame to the next.)

For example, if each line of the camera's video signal contains the output from 256 pixels, then pixel numbers 1, 5, 9, 13 etc. could be digitized from the first frame; numbers 2, 6, 10, 14 etc. from the second frame, and so on; 4 frames of data provide 1 frame of V_{SEP} ' data.

The above process must be repeated several times if noise

reduction is required, to produce a frame of $(V_{SEP} - VN)$ ' data.

Since the camera would be operated at normal video rate in this method, it does not need a camera with a variable clocking rate facility.

11.2.1.3 Evaluation

The single range approach has the attraction of simplicity; no range switching is necessary during the measurement of a given beam and only one frame of V_{SEP} ' or $(V_{SEP} - VN)$ ' data is required. The approach does, however, have two serious drawbacks.

- a) A custom-designed frame-grabber, which would be costly and time-consuming to develop, is required.

Even allowing for the slower sampling speed used with the single range approach, the converter is required to operate at about 1-2 MHz if the time taken to acquire a frame of data is not to be reduced to an unreasonable level. The design of a suitable frame-grabber would require a detailed knowledge of high-speed analogue circuit design and the camera and image processing system to be used.

- b) A high degree of noise reduction is required, which would result in long data acquisition times.

Although the use of a high-resolution analogue to digital converter would reduce the quantisation error to an acceptably

low level, it also means that a higher degree of noise reduction would be required, so that the noise component of the $(V_{SEP} - VN)$ ' data would be masked by the quantisation error. Furthermore, the time taken to acquire each frame of data would be longer, since the single range approach increases the resolution at the expense of a reduced conversion rate.

A comparison of the use of 8 and 10 bit digitization is now made for the CCD3000 camera discussed earlier; it is assumed that V_{NPP} is $V_{SEPSAT} / 167$ (see section 10.7.6).

With 8 bit digitization, the noise must be reduced to a level where it is equivalent to a V_{NPP} of $V_{SEPSAT} / 512$ or less, which requires a reduction factor of at least 3, which would be obtained by averaging 9 or more frames. At 30 frames per second (corresponding to a pixel rate of 7.16 MHz) the total data acquisition time would be approximately 0.3 seconds, which would be perfectly acceptable.

For 10 bit digitization, the noise must be reduced to a level where it is equivalent to a V_{NPP} of $V_{SEPSAT} / 2048$ or less, which requires a reduction factor of at least 12, which would be obtained by averaging 144 or more frames. At, say, 4 frames per second (corresponding to a pixel rate of about 1MHz) this would take approximately 36 seconds. Since two cameras would be required in a practical video photometry system to cover a field of view of $\pm 15^\circ$ H, $\pm 8^\circ$ V (see Chapter 15), the total time to carry out step (a) of the SIA acquisition procedure would be approximately 72 seconds; this is considerably longer than the

corresponding data acquisition time for the high-speed photometer (see Chapter 17). Furthermore, there would be frame-store overflow problems in attempting to average this number of frames of 10 bit data. 12 bit digitization is, of course, even less feasible.

The single range approach will not be a practical proposition, therefore, unless cameras with significantly lower noise levels become available.

11.2.2 Multiple Range Digitization Methods

It was shown earlier that the quantisation error produced by an 8 bit analogue to digital converter only becomes significant for the very low illuminance values; if we can arrange for the V_{SEP} values representing these low illuminance values to be amplified before conversion then the maximum quantisation error can be reduced by the same factor.

Since it is not possible to know in advance which pixels the gain should be applied to, the basic approach is to digitize a whole frame of camera data several times, each time using a different effective sensitivity setting, and subsequently select the most appropriate V_{SEP} ' reading for each pixel; each frame of data can itself be the average of several frames, in order to reduce noise.

Two ways in which this could be achieved will now be considered. It is assumed that:

- a) Only two sensitivity settings are being used i.e. two frames of V_{SEP} ' or $(V_{SEP} - VN)$ ' data are acquired; the principle can be extended to three or more settings.
- b) An 8 bit analogue to digital converter is being used.

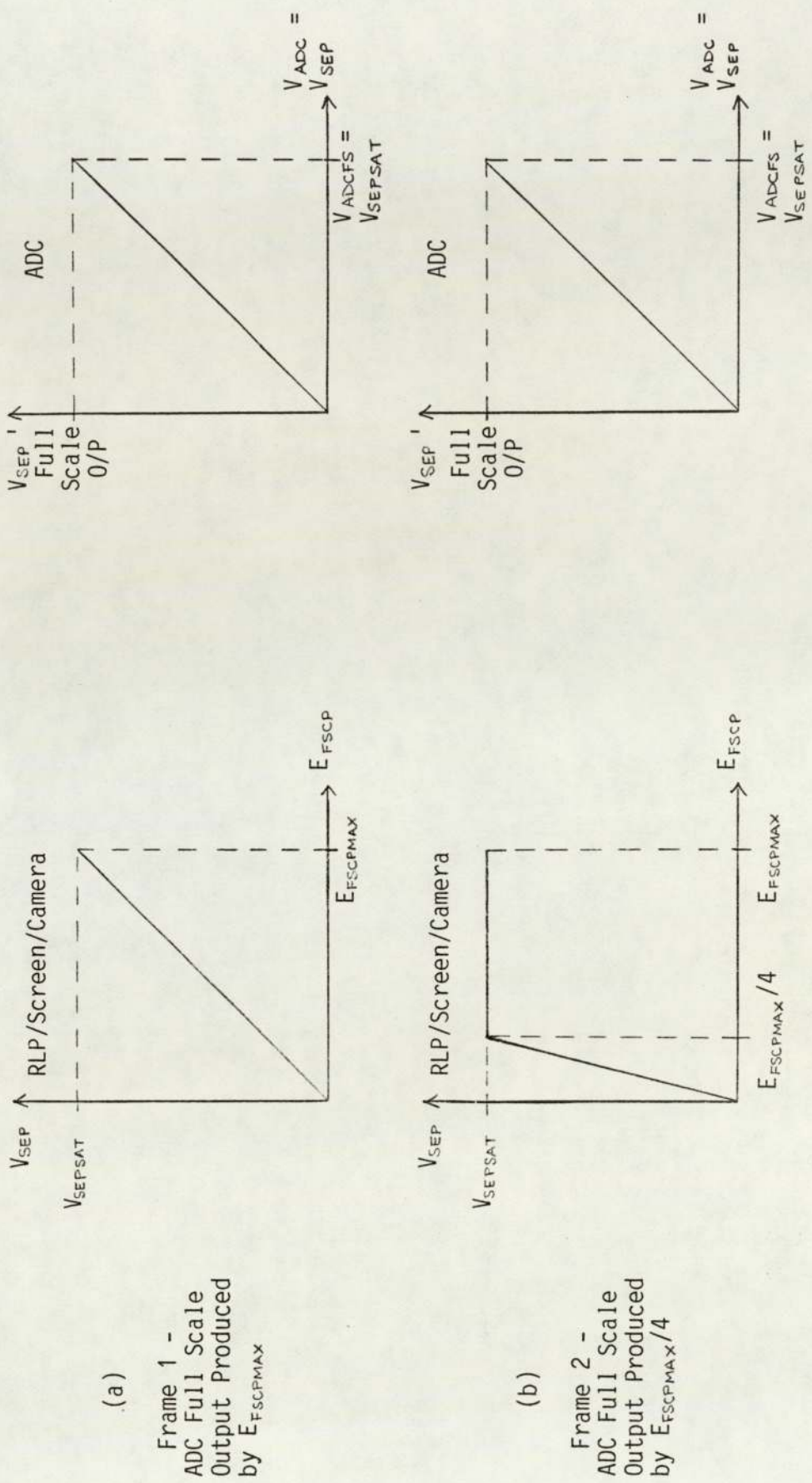
11.2.2.1 Method (a)

In this method the required variation in system sensitivity would be produced by altering the E_{FSCP} value at which V_{SEPSAT} occurred; this could be achieved by means of the camera lens aperture, neutral density filters and, for some cameras, the sensor clocking rate.

For the first frame of data, it would be arranged for V_{SEPSAT} to be produced by $E_{FSCP_{MAX}}$, as shown in Fig. 11.1a; if the V_{SEP} value for each pixel were converted to 8 bit resolution, then the maximum quantisation error in the resulting V_{SEP} ' (or $(V_{SEP} - VN)$ ' value) would be equivalent to $E_{FSCP_{MAX}}/512$.

For the second frame it would be arranged for V_{SEPSAT} to be produced by a much smaller value of E_{FSCP} , say $E_{FSCP_{MAX}}/4$, as shown in Fig. 11.1b. V_{SEP} values of 0 to V_{SEPSAT} would now represent E_{FSCP} values of 0 to $E_{FSCP_{MAX}}/4$. In order for this frame of data to be valid, the V_{SEP} values produced by the non-saturated pixels must not be affected by the sensor pixels which are saturated; i.e. an anti-blooming camera would be required.

If the V_{SEP} value for each pixel were again converted to 8 bit



(a)

Frame 1 -
ADC Full Scale
Output Produced
by E_{FSCP}^{MAX}

(b)

Frame 2 -
ADC Full Scale
Output Produced
by E_{FSCP}^{MAX}/4

Fig. 11.1 Video Signal Digitization - Multiple Range Method (a)

resolution, then the maximum quantisation error for E_{FSCP} values of between 0 and $E_{FSCP_{MAX}}/4$ would be $E_{FSCP_{MAX}}/2048$; this would be equivalent to using a 10 bit ADC.

Having digitized the two frames of data, the appropriate V_{SEP}' (or $(V_{SEP} - V_N)'$) value for each pixel would then be chosen. For $0 < E_{FSCP} < E_{FSCP_{MAX}}/4$, the value from the second frame would be chosen; for $E_{FSCP_{MAX}}/4 < E_{FSCP} < E_{FSCP_{MAX}}$, the value from the first frame would be chosen. Each value could be stored in the form of an 8 bit magnitude and a range code, indicating how the magnitude was to be interpreted. Alternatively, each value could be converted into a 10 bit word.

11.2.2.2 Method (b)

In this method, the required variation in system sensitivity would be produced by using a variable gain voltage amplifier between the output of the camera and the input of the ADC. (Only the part of the video signal representing the sensor illuminance would be amplified; a means of extracting this from the overall video signal would be required.) The camera would be operated at a single sensitivity, with $E_{FSCP_{MAX}}$ corresponding to V_{SEPSAT} .

For the first frame of V_{SEP}' (or $(V_{SEP} - V_N)'$) data to be acquired, the amplifier gain, G , would be set to 1 (or bypassed); the output of the ADC would represent an illuminance range of 0 to $E_{FSCP_{MAX}}$ with a maximum quantisation error of $E_{FSCP}/512$. See Fig. 11.2a.

For the second frame, the gain of the amplifier would be set to

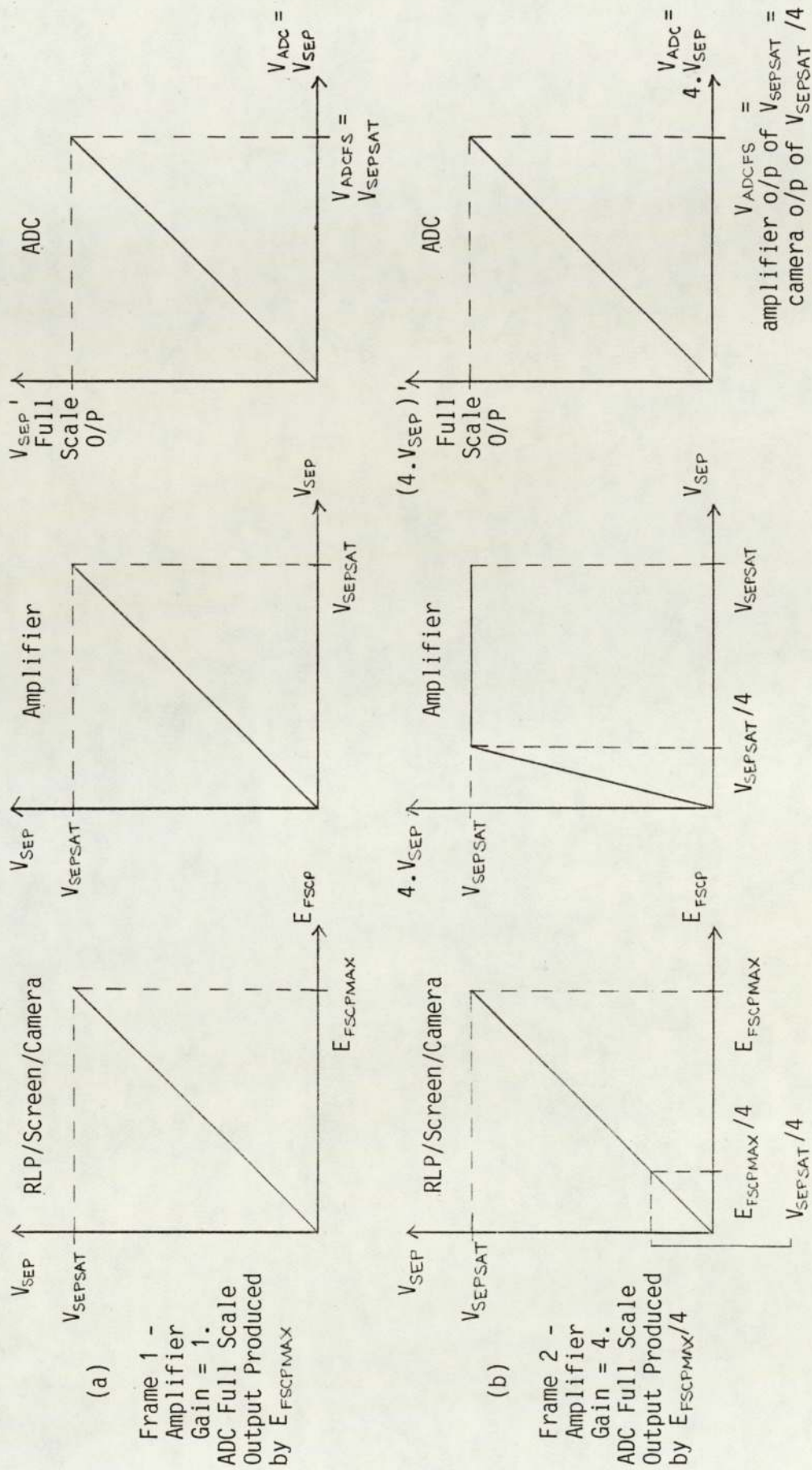


Fig. 11.2 Video Signal Digitization - Multiple Range Method (b)

greater than 1; a gain of 4 is assumed here. (The input voltage range of the ADC would be left unchanged.) The output range of the ADC would now represent an E_{FSCP} range of 0 to $E_{FSCP_{MAX}}/4$ with a maximum quantisation error of $E_{FSCP}/2048$. See Fig. 11.2b.

The appropriate V_{SEP} ' (or $(V_{SEP} - V_N)$ ') values would then be chosen as in method (a).

11.2.2.3 Evaluation

The multiple range approach, although more complex in principle than the single range approach, since it requires a mechanism for changing the sensitivity of the system during the beam measurement process and the acquisition and storage of two (or more) sets of data, has the significant advantage of enabling a standard 8 bit video rate analogue to digital converter to be used as the basis of the frame-grabber.

Method (a), is considerably more attractive than method (b), because:

- i) Fewer frame-grabber modifications would be required.

Method (a) would essentially use a standard frame-grabber; the only modifications required would be those for synchronizing the camera clocking and frame-grabber sampling. Method (b) requires a frame-grabber incorporating a high-performance video rate variable gain amplifier, and its implementation would not be straightforward.

- ii) The data acquisition time would be much shorter.

For both methods the noise component of the $(V_{SEP} - VN)'$ data must be reduced to a level where it is equivalent to a VN_{PP} of $V_{SEPSAT} / 512$ or less, assuming that an 8 bit converter is being used.

For method (a), assuming that the camera has a noise level of $V_{SEPSAT} / 167$, then the acquisition time for each frame of $(V_{SEP} - VN)'$ data would be about 0.3 seconds; see section 11.2.1.3. The total time for step (a) of the SIA acquisition procedure, for two cameras, would therefore be approximately 1.2 seconds, which would be perfectly acceptable.

For method (b) the acquisition time for the first frame of $(V_{SEP} - VN)'$ data would again be approximately 0.3 seconds. When acquiring the second frame, however, the noise in the camera's video signal would also be amplified together with the required signal component. (In practice, the amplifier itself would add further noise to the system.) The amount of noise reduction required would therefore be increased. With a gain of 4, the averaging of at least 16 times more frames would be required. Assuming that 144 frames are to be averaged, the time taken to acquire the second frame of $(V_{SEP} - VN)'$ data would be approximately 4.8 seconds, giving a total time for step (a) of the SIA acquisition procedure, for two cameras, of approximately 10.2 seconds; this is higher than for method (a) and the high speed photometer (see Chapter 17).

11.2.3 Conclusions

The most attractive method of all those considered, therefore, is multiple range method (a), since it would be the easiest to implement, from the aspect of the image processing system modifications required, and the only one which would produce acceptable data acquisition times, with present solid-state camera noise levels. The method does, however, require a camera with a high degree of anti-blooming performance.

11.3 Calculation of the E_{FSCP} ' Values From the V_{SEP} ' Values

This section considers the calculation of the E_{FSCP} ' values from the measured V_{SEP} ' or $(V_{SEP} - VN)$ ' values in a practical video photometry system when the following effects are to be taken into account:

- a) Non-ideal screen diffusion characteristics.
- b) Non-ideal sensor characteristics:
 - i) Dark Signal
 - ii) Pixel to Pixel Responsivity Variations
 - iii) Noise

It will be assumed that E_{FSCP} and V_{SEP} are related by equation 10.8 and that K_C has the same value for all pairs of corresponding far screen and sensor pixels; see section 10.6. If a multiple range

digitization method is being used, then each sensitivity setting will have a different K_C value; the value for each sensitivity is assumed to apply to all pairs of pixels.

In order to use equation 10.8 for calculating an E_{FSCP} ' value, we need to:

- a) Calculate VX_{SEP} ' (i.e. VX_{SEP} in digital form) from the measured V_{SEP} ' or $(V_{SEP} - VN)$ ' values; this involves the removal of the dark signal component, stored in digital form, VD_{SEP} '. In general, each sensor pixel will have a different VD_{SEP} ' value; these values would be measured beforehand and stored in the computer or frame-store. If a multiple range digitization method is being used, then the value of VD_{SEP} ' may also depend on the sensitivity setting used to obtain the V_{SEP} ' or $(V_{SEP} - VN)$ ' value. This is determined by the way in which the multiple range method is implemented.
- b) Multiply the VX_{SEP} ' value obtained from (a) above by K_Y ', where K_Y ' is a digital representation of K_Y which is given by:

$$K_Y = \frac{1}{K_C \cdot \cos^4 \theta_{SEP} \cdot C_{NSCP}} \cdot \frac{R_{SEPAV}}{R_{SEP}}$$

In general, each pair of corresponding far screen and sensor pixels will have a different K_Y value; the K_Y values would be measured beforehand and stored in the computer or frame-store. If a multiple range digitization method is being used then K_Y will also depend on the sensitivity setting used to acquire the V_{SEP} ' or $(V_{SEP} - VN)$ ' value.

It should be noted that the stored VD_{SEP}' and K_Y' values need not represent the absolute values of VD_{SEP}' and K_Y' ; any suitable digital representation could be used to make the optimum use of storage available in the computer or frame-store. For example, a representation of the amount by which each pixel's VD_{SEP}' value varied from the average VD_{SEP}' value could be used; the software to carry out calculations (a) and (b) above would incorporate the processing steps to carry out any necessary format conversions.

Calculations (a) and (b) above are considered in more detail in sections 11.3.1. and 11.3.2.

11.3.1 Calculation of VX_{SEP}' from V_{SEP}'

If V_N is sufficiently small to be ignored then VX_{SEP}' and V_{SEP}' are related by the equation:

$$VX_{SEP}' = V_{SEP}' - VD_{SEP}' \quad (11.1)$$

i.e. the required VX_{SEP}' value is produced by subtracting the VD_{SEP}' value from the V_{SEP}' value produced as the result of step (a) of the SIA acquisition procedure.

If V_N is not sufficiently small to be ignored, then it can be removed by digital filtering as part of step (a) to give a set of $(V_{SEP} - V_N)'$ values; see section 11.2. VX_{SEP}' and $(V_{SEP} - V_N)'$ are related by the equation:

$$VX_{SEP}' = [(V_{SEP} - V_N)' - VD_{SEP}'] \quad (11.2)$$

The required VX_{SEP}' value is again produced by subtracting the VD_{SEP}' value from the result of step (a).

The VD_{SEP}' values to be used in the calculation can be found as follows. A lens cap is placed over the camera lens (thereby setting E_{SEP} and hence VX_{SEP} to zero for all pixels) and the resultant VD_{SEP}' values stored. If a multiple range digitization method is being used, and the VD_{SEP} values are a function of the sensitivity setting, then it will be necessary to store an array of VD_{SEP}' data for each sensitivity. Since dark signal is a function of temperature (it approximately doubles for a $10^{\circ}C$ rise), it would be desirable to carry out the VD_{SEP} measurement process prior to every lamp testing session.

11.3.2 Calculation of E_{FSCP}' from VX_{SEP}'

In order to calculate the K_{γ} value for each pair of corresponding far screen and sensor pixels, the values of the following quantities are required:

- a) $\cos^4 \theta_{SEP}$
- b) C_{NSCP}
- c) R_{SEPAV} / R_{SEP}
- d) K_C

Methods of obtaining these values are considered below.

a) $\cos^4 \theta_{SEP}$

A sensor pixel's $\cos^4 \theta_{SEP}$ value can be calculated from a knowledge of the pixel's location in relation to the optical axis of the camera.

b) C_{NSCP}

The C_{NSCP} value for a screen pixel could be measured by means of a suitable light source and luminance photometer; since a video photometer's screen would be divided into many thousands of pixels, however, it would clearly not be feasible to individually measure the C_{NSCP} value for each one. In practice, however, the values are unlikely to vary significantly from one pixel to the next and sufficient accuracy would probably be obtained by dividing the screen into a number of zones, each consisting of a block of adjacent pixels, and obtaining a single correction factor value for each zone; the measured value would then be used as the C_{NSCP} value for every pixel in the zone. In this way, the number of measurements required is considerably reduced.

c) R_{SEPAV} / R_{SEP}

The R_{SEPAV} / R_{SEP} values could be measured as follows. The camera lens is removed and the sensor uniformly illuminated; the illuminance level should be such that the resultant V_{SEP} values are around 80-90% of the saturation output voltage of the sensor, V_{SEPSAT} . The V_{SEP} or $(V_{SEP} - V_N)$ values are obtained

and the corresponding VX_{SEP} values calculated. The ratio VX_{SEPAV} / VX_{SEP} is then calculated for each sensor pixel, where VX_{SEPAV} is the digital representation of the average of all the VX_{SEP} values. Since VX_{SEP} is equal to $R_{SEP} \cdot t_i \cdot E_{SEP}$ and t_i and E_{SEP} are constant for all the pixels, then the VX_{SEPAV} / VX_{SEP} values are equivalent to the required R_{SEPAV} / R_{SEP} values.

As will be seen later, it is also possible to reduce the effect of responsivity variations when producing an SIA from the E_{FSCP} values.

d) K_C

$$K_C = K_1 \cdot K_2 \cdot K_{3A} \cdot K_{4A}$$

$$K_C = \frac{T_R \cdot P \cdot T_C \cdot R_{SEPAV} \cdot t_i}{4 \cdot m^2 \cdot (f/\lambda)^2} \quad (11.3)$$

The value of K_C can be theoretically calculated and adjusted, if necessary, by practical measurements.

If a multiple range digitization method is being used, then the value of K_C will be different for each sensitivity setting.

11.4 SIA Generation From the E_{FSCP} Values

Three possible methods of producing an SIA from the E_{FSCP} values are described in sections 11.4.1. to 11.4.3.

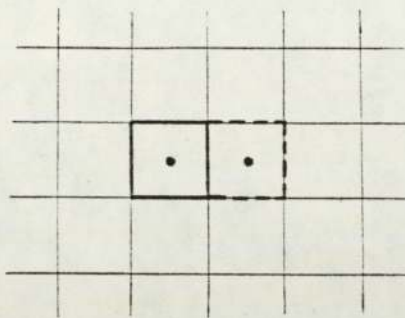
11.4.1 Method (a)

The E_{FSCP} ' values are used directly as SIA elements for the points corresponding to the centres of the screen pixels, as shown in Fig. 11.3a. This method has the attraction of simplicity but has the following drawbacks:

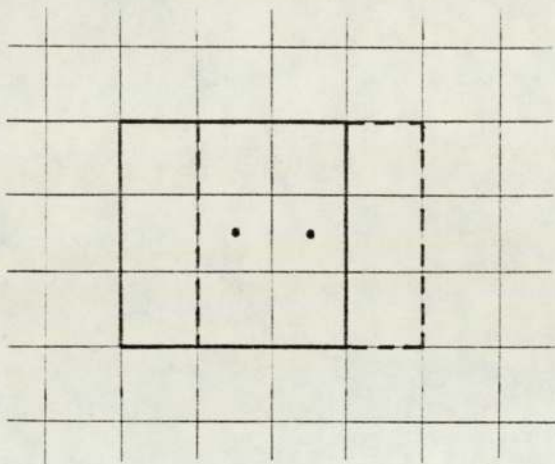
- a) The flux collection area and the measurement point spacings of the array of screen pixels represented by the E_{FSCP} ' values are not independent (see section 7.7); the SIA's measurement points will have the same characteristics.
- b) Any remaining differences between the calculated E_{FSCP} ' values and the true illuminance values of the screen pixels will be directly reproduced in the SIA element values.
- c) SIA element values will not be directly available for those screen pixels which are imaged by blemished sensor pixels; these values would have to be produced by interpolation of surrounding E_{FSCP} ' values.

11.4.2 Method (b)

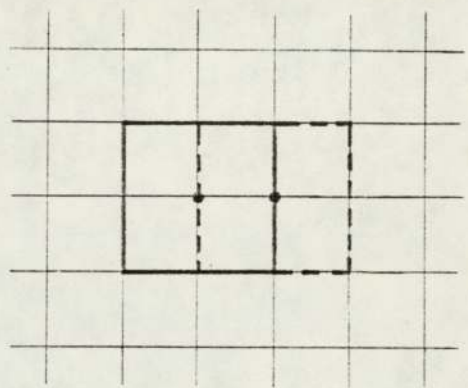
The average value of the E_{FSCP} ' values for a contiguous block of screen pixels is taken (by means of the computer), to produce a number representing a measurement point reading for the central point in the block, with an effective flux collection area equal to the total area of the block. The resultant value is used as the SIA element for the central point.



(a) Method a
Effective Flux
Collection
Area = $x \times y$



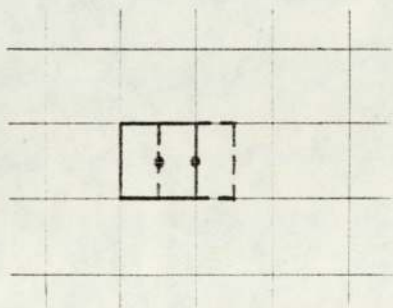
Effective Flux Collection Area = $3x \times 3y$
i) Odd Number of Pixels



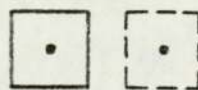
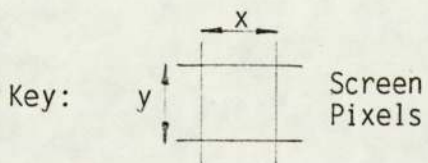
Effective Flux
Collection Area = $2x \times 2y$

ii) Even Number of Pixels

(b) Method b



(c) Method c
Effective Flux
Collection
Area = $x \times y$



Effective Measurement
Points and Flux
Collection Areas
for the SIA Elements

Fig. 11.3 SIA Generation Methods - Effective Measurement Points and Flux Collection Areas

In practice, a rectangular block of screen pixels would be used; this would contain either an even or an odd number of pixels. If the number is odd, then the effective measurement point is at the centre of the central pixel in the block; if, however, the number is even, then the effective measurement point is where the central four pixels meet. See Fig. 11.3b.

This method has several attractions:

- a) It allows a choice of effective flux collection areas for a given screen pixel size. Using an even number of pixels gives possible effective flux collection area values of $2x \times 2y$, $4x \times 4y$ etc. whereas an odd number gives possible values of $3x \times 3y$, $5x \times 5y$ etc; see Fig. 11.3b.
- b) Any remaining errors in the E_{FSCP} ' values tend to be averaged out in producing the SIA element values.
- c) If one or more of the E_{FSCP} ' values required to produce an SIA element value is not available (owing to the corresponding sensor pixel or pixels being blemished), the remaining values can be averaged with little loss in accuracy.

The drawback of this method is that it complicates and slows down the overall SIA acquisition procedure.

11.4.3 Method (c)

The E_{FSCP} ' values are interpolated to produce data for

effective measurement points lying between those at the centres of the screen pixels; see Fig. 11.3c.

This method allows the effective resolution of the system to be increased; it has the following drawbacks, however:

- a) The effects of any remaining errors are not averaged out, as in method (b).
- b) E_{FSCP} ' values not available must themselves be interpolated before the process can be carried out.
- c) It complicates and slows down the overall SIA acquisition process.

11.5 Ambient Light Correction

In a practical video photometry system, some form of ambient lighting will be necessary for the operator to control the equipment; it should be possible to arrange this lighting in such a way that any ambient light reaching the screen is insignificantly small compared to the light from the lamp under test. If this is not the case, however, then the method of eliminating the effects of ambient light described in Appendix C can be used.

11.6 Main Video Photometry System Design Considerations

The five main factors to be taken into account when considering the use of an image processing system for the proposed 11.6 type of video photometer are:

- a) The method of digitizing the camera's video signal
- b) SIA size
- c) Frame store utilisation
- d) The method of representing the SIA element values
- e) Software

These factors are discussed in sections 11.6.1 to 11.6.5.

11.6.1 The Method of Digitizing the Camera's Video Signal

In designing a video photometry system, it must be decided which digitization method will be used and whether or not digital filtering will be necessary to reduce noise. These decisions greatly influence the IPS hardware requirements.

11.6.2 SIA Size

In a practical video photometry system, the SIA size to be used will be a compromise based on the many conflicting requirements

and equipment limitations and costs; the main factors to be considered are: the required field of view, RLP performance, the required screen pixel size, the viewing arrangement, the number of camera pixels, the method of producing SIA's from the E_{FSCP} ' values, available frame-store sizes, the number of SIA's to be stored and the transient processing area requirements (see next section).

11.6.3 Frame Store Utilisation

It is proposed that the frame store is divided into 2 logical areas; the transient processing area (TPA) and the SIA storage area. The TPA will be used to store the array of V_{SEP} ' or $(V_{SEP} - VN)$ ' values and convert them into an SIA, to be held in the SIA storage area; as stated in section 8.3, it is highly desirable to be able to store 2 or more SIA's simultaneously. Part of the TPA will ideally be used to store some or all of the decalibration data used in the SIA acquisition procedure in order to avoid continually reading it from disk, which will slow down the overall SIA acquisition process.

In order to display an SIA by the method described in 8.3, it may be necessary to produce an intermediate array of data, since the SIA's will require more than 8 bits per element (see next section) but most image processing systems have look-up-tables designed to accept only 8 bits of input data; this intermediate array could be produced in part of the TPA. The use of this technique also enables other information to be provided in the display, such as legends, test point data and headings.

The above factors influence the number of frame-store pixels

required; commonly available frame store sizes are 256 x 256, 512 x 256, 512 x 512, 1024 x 512 and 1024 x 1024.

11.6.4 The Method of Representing the SIA Element Values

As described in section 11.1, 10-12 bits are required to represent the range of illuminance values encountered for a given beam type; depending on the method of digitizing the camera's video signal chosen, this data could be produced in the form of a single 10-12 bit quantity or an 8 bit magnitude and 2 bit gain code. However, we also need to cater for:

- a) The total range of illuminance values for all beam categories.
- b) The higher illuminance values which may be produced when SIA's are subtracted.
- c) 'Negative illuminance' values which may be produced when SIA's are subtracted.

These requirements can be met by a 16 bit word, using 15 bits for magnitude and 1 bit for sign. Alternatively, a gain and magnitude coding method could be used. Three possible storage methods are given in Table 11.1. It should be noted that the storage method affects the number of frame-store pixels required to store a given size of SIA.

11.6.5 Software

Various image processing software packages are commercially

| METHOD | DATA CODING FORMAT | FRAME-STORE PIXEL MEMORY REQUIREMENTS | BENEFITS | DRAWBACKS |
|--------|---|---------------------------------------|--|--|
| a | 15 bits magnitude and 1 bit sign, stored as a 16 bit word. | 16 bits | Makes SIA processing straightforward. | Cannot be implemented with conventional 8 bit frame-stores. |
| b | 8 bits magnitude, 3 bits gain and 1 bit sign, stored as a 12 bit word. | 12 bits | Uses less memory than method (a), which may increase range of suitable equipment and/or reduce cost. | <ul style="list-style-type: none"> i) Cannot be implemented with conventional 8 bit frame-stores. ii) Makes SIA processing more complex and slower than with method (a). |
| c | 15 bits magnitude and 1 bit sign, stored as 2 bytes, with separate addresses. | 8 bits | Can be implemented with conventional 8 bit frame-stores. | <ul style="list-style-type: none"> i) Requires 2 pixels per SIA element. ii) Makes SIA processing more complex and slower than with method (a). |

Table 11.1 Possible Frame-Store Data Coding Formats for SIA Elements

available; most are written by system manufacturers for their own equipment, the remainder being general purpose packages which can theoretically be implemented on a variety of systems. An example of the latter type of package is SEMPER (69).

These packages are not very suitable as the basis of the software required for the proposed video photometry system, however, because:

- a) They are not directly capable of carrying out the specialised processing operations to be implemented.
- b) They contain many facilities which are not required for this application.

Consequently, custom-written software is required; the development effort that will be required to produce this software can be reduced if low level routines, to carry out functions such as look-up-table programming or grabbing a frame of data, are available from the equipment manufacturer.

12. REDUCED-LENGTH PHOTOMETER ANALYSIS METHOD

12.1 Introduction

As described in section 10.2, there are many difficulties involved in determining and evaluating reduced-length photometer performance, and, as described in section 5.1, it was more convenient, for the purposes of this project, to carry out a theoretical study rather than a practical one.

The following method of analysis, intended to provide an overall appreciation of RLP imaging performance, was used:

- a) The sizes and positions of the blur patches produced at various off-axis angles by a given RLP configuration and given lamp size are determined, by means of a two-dimensional RLP model and a ray tracing technique.

(A two-dimensional analysis method was chosen in order to limit the work to a reasonable level; the three-dimensional method described in reference (70) was considered but not used.)

- b) A RLP's performance at a given off-axis angle is considered acceptable if the rays which would have converged to a given point on the far screen:
 - i) pass through the lens, i.e. if the system does not act as a field stop

and

- ii) fall on the part of the near screen corresponding to the ideal image point and a surrounding flux collection area equivalent to a square of side 65mm on a far screen at 25 m i.e. the maximum flux collection area permitted by the ECE regulations.

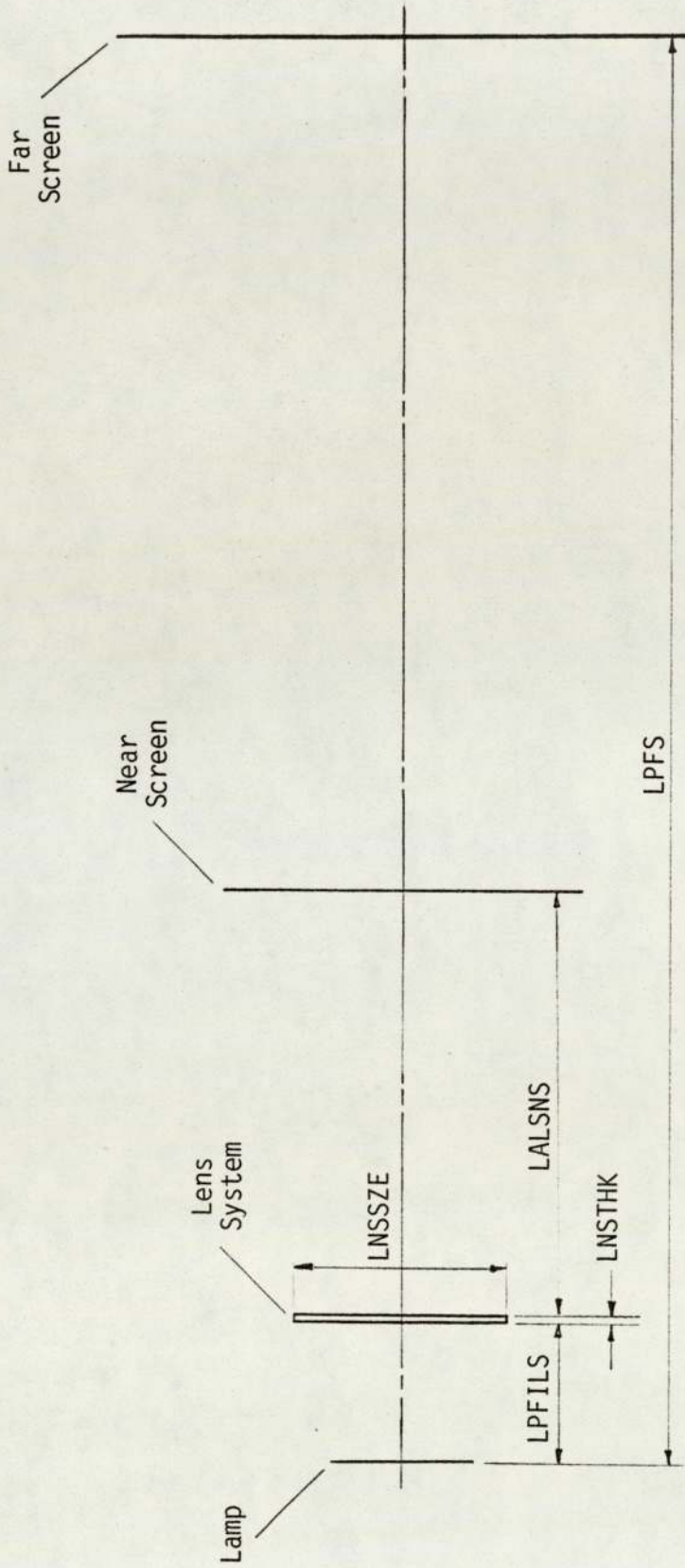
If these criteria are met, then it is reasonable to assume that the measurement error produced by the RLP is unlikely to be greater than the variations which would be obtained when directly measuring the far screen illuminance values with the range of flux collection areas permitted by the ECE regulations.

The RLP model and the full analysis procedure are described in sections 12.2 and 12.3 respectively.

12.2 The Reduced-Length Photometer Model

The basic RLP model used is shown in Fig. 12.1a. The overall configuration is defined in the model by means of the five following parameters, which take positive values only:

- a) LPFS - Distance from the lamp to the far screen (m)
- b) LPFILS - Distance from the lamp to the first lens surface (m)
- c) LNSTHK - Lens system thickness (m)
- d) LNSSZE - Lens system size (m)
- e) LALSNS - Distance from the last lens surface to near screen (m)



Note: All overall configuration parameters are positive

Fig. 12.1a Reduced-Length Photometer Model - Overall Configuration

The details of the lens system are specified by means of a separate set of parameters, which will be described later.

The model can be used to represent both the horizontal and vertical planes through the axis of the RLP system. LPFS, LPFILS, LNSTHK and LALSNS remain the same for both planes. If the lens used is circular (or square) then LNSSZE is also the same and a single set of RLP parameters can be used for analysing both the horizontal and vertical planes. If a rectangular shaped lens is used, however, then two sets of parameters are required.

The overall size and shape of the pencil of rays reaching a point on the far screen clearly depends on the size and shape of the lamp being considered. These pencil characteristics also vary, however, with the position of the point on the far screen being considered, as follows.

Points on or close to the axis receive light from the whole frontal area of the lamp. In moving off-axis, however, the effective size of the source decreases. The way in which this happens depends on the design of the lamp; in particular, the lens, with its many zones, plays an important role in determining how the rays will be distributed on the screen.

For any given point on the far screen, therefore, the 'effective lamp size', ELPS, rather than its true physical size, is used. The 'effective lamp size' becomes the 'effective lamp width', ELPW, in the horizontal plane and the 'effective lamp height', ELPH,

in the vertical plane. The relationship between the 'effective lamp size' of a lamp at any off-axis angle and the physical size of its reflector is very complex and varies with the type of lamp. For the purposes of this study, the simplified relationships given in Table 12.1, which were derived from discussions with the lamp designers, were used; the maximum off-axis angles of interest for the reduced-length photometer study were 30° horizontally and 12° vertically.

The way in which the model is used in the analysis is shown in Fig. 12.1b. An odd-numbered pencil of rays converges to the point POIWFS. The central ray in the pencil is at an off-axis angle of OAAC. The effective lamp size used as the source of the rays is ELPS; the starting points are a distance of RSPINC apart. A general ray in the pencil (ray number R) is shown in Fig. 12.1c. It starts at a point RSPR on the lamp and has an off-axis angle of OAAR. It intersects the near screen at the point POIWNS; in general, each ray will have a different value of POIWNS. The model's equivalent of the blur patch formed by a real RLP is a blur line, whose position can be calculated from the POIWNS values.

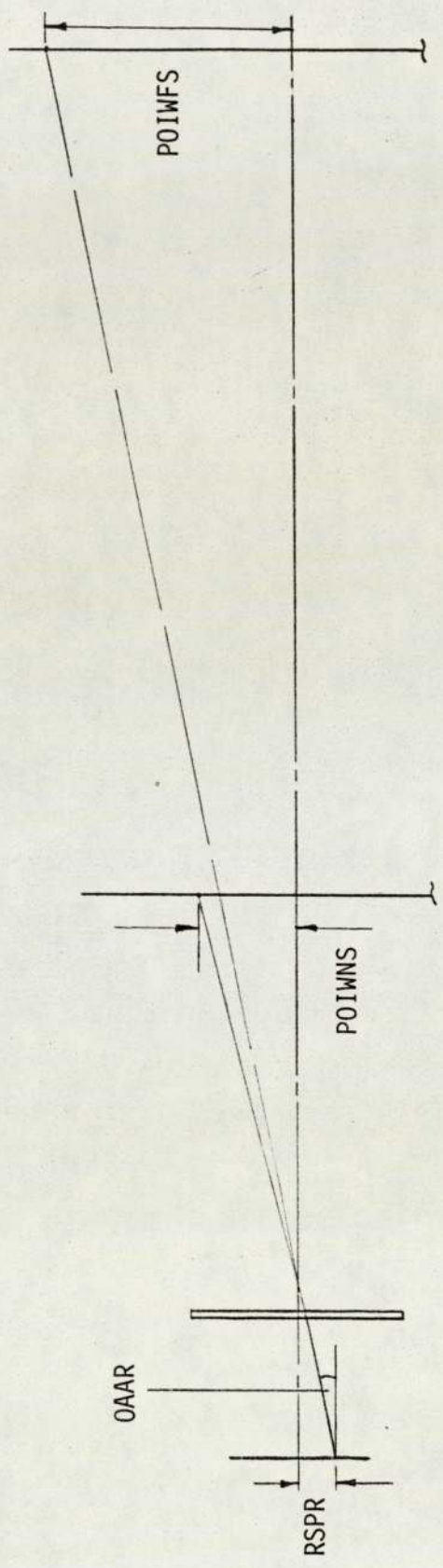
Two conditions have been assumed above:

a) $OAAC \leq LOAAC$

where LOAAC is the limiting value of OAAC; this is the configuration's maximum value of OAAC for which a point source can be imaged without the system acting as a field stop. See Fig. 12.1d.

| HORIZONTAL PLANE | |
|---------------------------------|--------------------------------|
| OFF-AXIS ANGLE (OAAC) | EFFECTIVE LAMP WIDTH (ELPW) |
| 0° - 10° | 1 x PRW |
| 10° - 20° | $\frac{2}{3}$ x PRW |
| 20° - 30° | $\frac{1}{3}$ x PRW |
| PRW = Physical Reflector Width | |
| VERTICAL PLANE | |
| OFF-AXIS ANGLE (OAAC) | EFFECTIVE LAMP HEIGHT (ELPH) |
| 0° - 12° | 1 x PRH |
| PRH = Physical Reflector Height | |

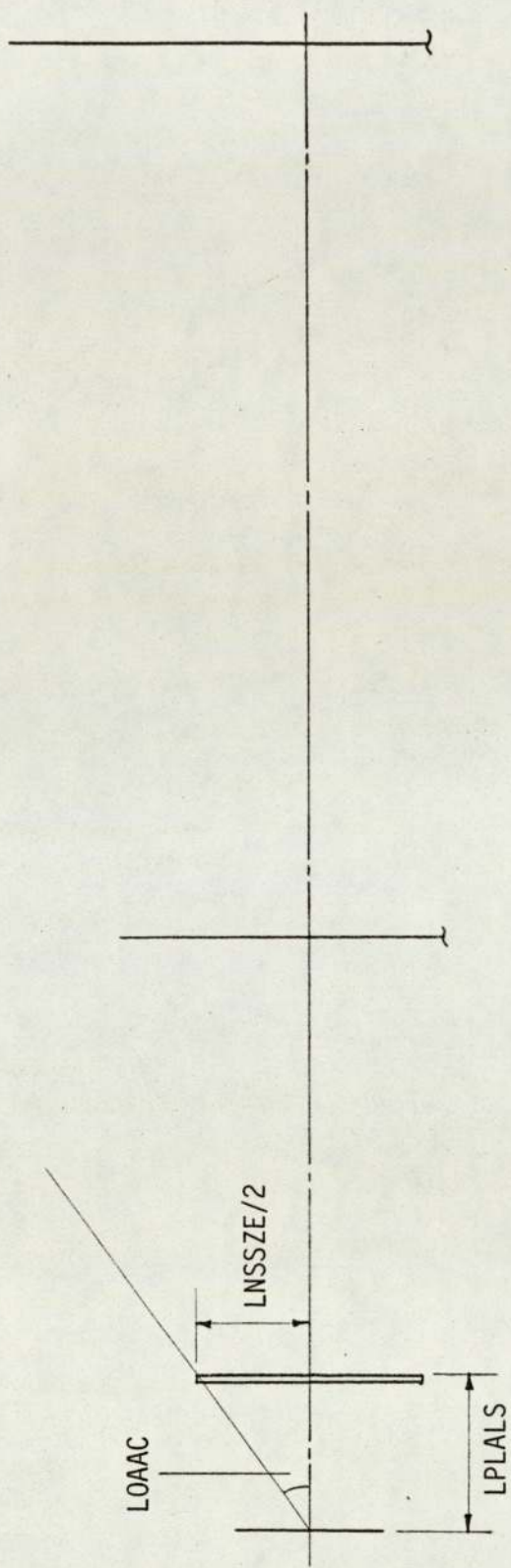
Table 12.1 Relationship Between Physical and Effective Lamp Sizes for Reduced-Length Photometer Analysis



- RSPR - Starting Point of Ray Number R
- OAAR - Off-Axis Angle of Ray Number R
- POIWS - Point of Intersection with Near Screen of Ray Number R

Notes: i) POIWS and RSPR are specified by their perpendicular distances from the axis; these distances are positive if above the axis, negative if below.
 ii) OAAR is positive if the ray must be moved anti-clockwise to reach the axis.

Fig. 12.1c Reduced-Length Photometer Model - A Single Ray in the Pencil



Notes: i) $LPLALS = LPFILS + LNSTHK$
 ii) $LOAAC = \pm \tan^{-1} (LNSSZE / (2 \cdot LPLALS))$

Fig. 12.1d Reduced-Length Photometer Model - Limiting Off-Axis Angle

b) $ELPS \leq LTELPS$

where LTELPS is the limiting value of ELPS; this is the maximum value of ELPS which can be used for a given OAAC (\leq LOAAC) without the system acting as a field stop. See Figs. 12.1e and 12.1f.

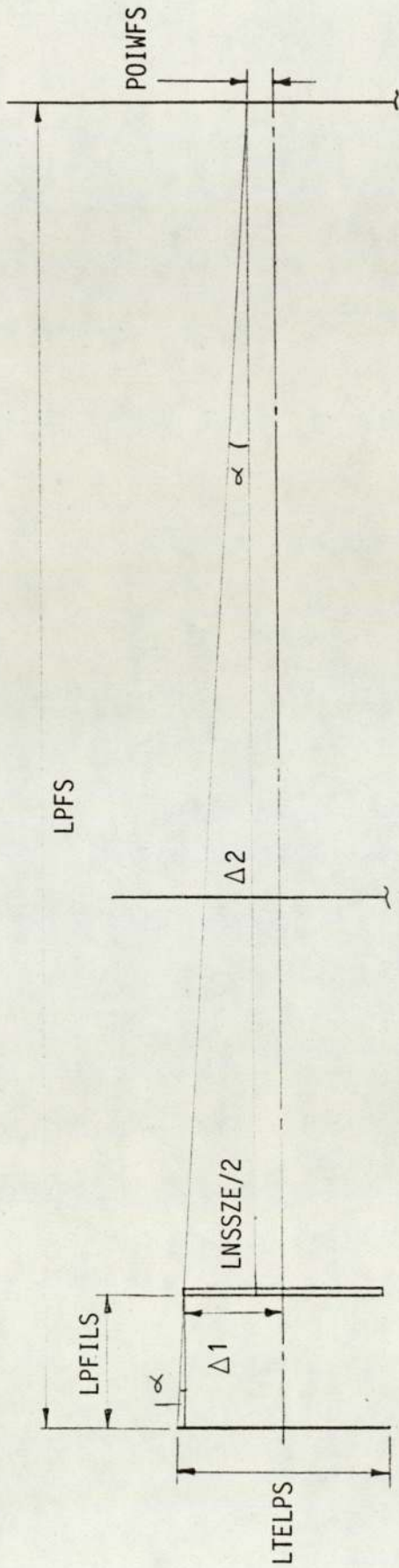
A Fortran computer program, RLP, was written to carry out the ray tracing calculations; it was written to enable the effects of using more than one lens element to be studied if required. The role of this program in the analysis procedure is described in the next section, its internal details being described in Appendix D. For the sake of consistency, the names of the variables used in this Chapter are the same as in the RLP program.

12.3 The Analysis Procedure

The full procedure for analysing the performance of a given reduced-length photometer configuration with a given lamp by means of the RLP program consists of seven steps, which are described below:

- 1) The overall configuration parameters and lens system parameters of the proposed configuration are determined and input to the RLP program; details of how this is carried out are given in Appendix D.

If a circular (or square) lens is proposed, then the parameters are the same for both the vertical and horizontal planes and



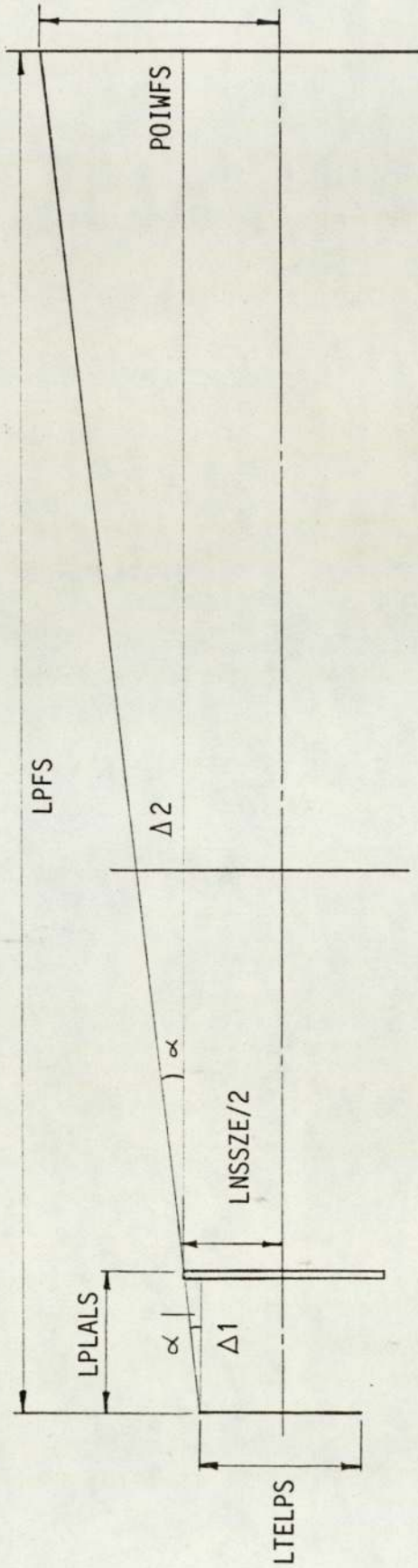
In $\Delta 1$: $\tan \alpha = \frac{(LTELPS/2) - (LNSSZE/2)}{LPFALS}$

In $\Delta 2$: $\tan \alpha = \frac{(LNSSZE/2) - |POIWFS|}{LPFS - LPFALS}$

Combining above equations gives $LTELPS = LNSSZE + 2 \cdot \frac{LPFALS \cdot ((LNSSZE/2) - |POIWFS|)}{LPFS - LPFALS}$

Note: The above equations are true for both positive and negative values of $POIWFS$. Only positive values of $POIWFS$ are used in the RLP program, however.

Fig. 12.1e Reduced-Length Photometer Model - Limiting Effective Lamp Size ($|POIWFS| \leq LNSSZE/2$)



In $\Delta 1$: $\tan \alpha = \frac{(LNSSZE/2) - (LTELPS/2)}{LPLALS}$

In $\Delta 2$: $\tan \alpha = \frac{|POIWFS| - (LNSSZE/2)}{LPFS - LPLALS}$

Combining above equations gives $LTELPS = LNSSZE - 2 \cdot \frac{LPLALS \cdot (|POIWFS| - (LNSSZE/2))}{LPFS - LPLALS}$

- Notes: i) It is assumed that $|POIWFS| < |(LPFS \cdot \tan \text{LOAAC})|$
 ii) The above equations are true for both positive and negative values of POIWFS.
 Only positive values of POIWFS are used in the RLP program, however.

Fig. 12.1f Reduced-Length Photometer Model - Limiting Effective Lamp Size ($|POIWFS| > LNSSZE/2$)

the program output for these parameters can be used to determine the performance for both planes. Otherwise, two separate sets of output data are required.

a) The overall configuration parameters

The overall configuration parameters were defined in section 12.2. LNSTHK and LNSSZE depend on the lens system parameters chosen (see below).

LALSNS is normally calculated as follows:

i) Equation B3 (see Appendix B) is used to calculate v , with $d = LPFS$ and $x = (LPFILS + LNSTHK/2)$

ii) $LALSNS = (v - LNSTHK/2)$

(The effects of using slightly different values of LALSNS can, of course, be studied by means of the program; see Chapter 13.)

All the overall configuration parameters are specified in the program as positive, real numbers.

b) The lens system parameters

The required lens system parameters, i.e. the number of surfaces and their characteristics, are as follows:

- i) NUMSRF (Integer) - Number of surfaces

- ii) C(J) (Real Array) - Curvature of surface J (m^{-1})

J = Surface number. Range = 1 to NUMSRF

C is positive if the centre of the curvature is to the right of the surface.

- iii) N (J) (Real Array) - Refractive index of medium to the left of surface J

J = Surface number. Range = 1 to NUMSRF

- iv) N\$(J) (Real Array) - Refractive index of medium to the right of surface J.

J = Surface number. Range = 1 to NUMSRF

- v) T (J) (Real Array) - Vertex spacing between surfaces J and (J+1)

J = Surface number. Range = 1 to (NUMSRF - 1)

- 2) The program is run (see Appendix D). It performs operations 2.1 to 2.5 described below.

2.1) Outputs the overall configuration and lens system

parameters for reference.

2.2) Calculates and outputs LOAAC for the configuration.

2.3) Inputs the following parameters from the user, via the console, to determine the characteristics of the pencils to be generated. All are input as positive real numbers.

a) OAACIN - The required angular increment between central rays of successive pencils (Degrees)

b) MOAACI - The maximum value of OAAC of interest (Degrees)

(Only negative values of OAAC are used in the program i.e. OAAC is decremented from 0 to (-MOAACI) in steps of (-OAACIN). The corresponding POIWFS values are positive.)

The value of MOAACI specified by the user must be:

i) \leq LOAAC

ii) A multiple of OAACIN

c) RSPINC - The ray starting point increment (m)

d) MELPSI - The maximum effective lamp size of interest (m)

The value of MELPSI specified by the user must be:

- i) \leq LNSSZE
- ii) An even numbered multiple of RSPINC. (This is to generate an odd number of rays.)

It is the user's responsibility to ensure that the values specified for the above parameters meet the conditions stated; they are not checked by the program. The program is, however, written so that the inexact way in which some real values are represented in the computer will not cause any problems.

2.4) Calculates the number of pencils, NOPEN, to be generated:

$$\text{NOPEN} = \frac{\text{MOAACI} + 1}{\text{OAACIN}}$$

2.5) Performs the following for each pencil, P, where P is assigned values from 1 to NOPEN;

a) Calculates OAAC, POIWFS and LTELPS for the pencil:

- i) $\text{OAAC} = (P-1) \cdot \text{OAACIN}$
- ii) $\text{POIWFS} = -\text{LPFS} \cdot \tan \text{OAAC}$ (see Fig. 12.1b)
- iii) The formula used to calculate LTELPS depends on whether or not ($\text{POIWFS} \leq \text{LNSSZE}/2$); see Figs. 12.1e and 12.1f.

b) Prints the values of P, OAAC, POIWFS and LTELPS.

- c) Calculates the value of ELPS to be used for the pencil:

If LTELPS > MELPSI then ELPS is assigned the value of MELPSI. Otherwise, ELPS is assigned the value of the largest even numbered multiple of RSPINC which is \leq LTELPS. This produces the same ray starting points for all pencils.

- d) Calculates the number of rays in the pencil, NORINP, to be generated:

$$\text{NORINP} = \frac{\text{ELPS}}{\text{RSPINC}} + 1$$

- e) Prints the heading for the ray results table.
- f) Performs the following for each ray in the pencil, R, where R is assigned values from 1 to NORINP:

- i) Calculates RSPR and OAAR:

$$\text{If NORINP} = 1, \text{ RSPR} = \frac{-\text{ELPS}}{2} + (\text{R}-1) \cdot \text{RSPINC}$$

$$\text{If NORINP} = 1, \text{ RSPR} = 0$$

$$\text{OAAR} = -\tan^{-1} \left(\frac{\text{POIWFS} - \text{RSPR}}{\text{LPFS}} \right)$$

Note that the formula for OAAR applies to both positive and negative values of RSPR; see Figs.

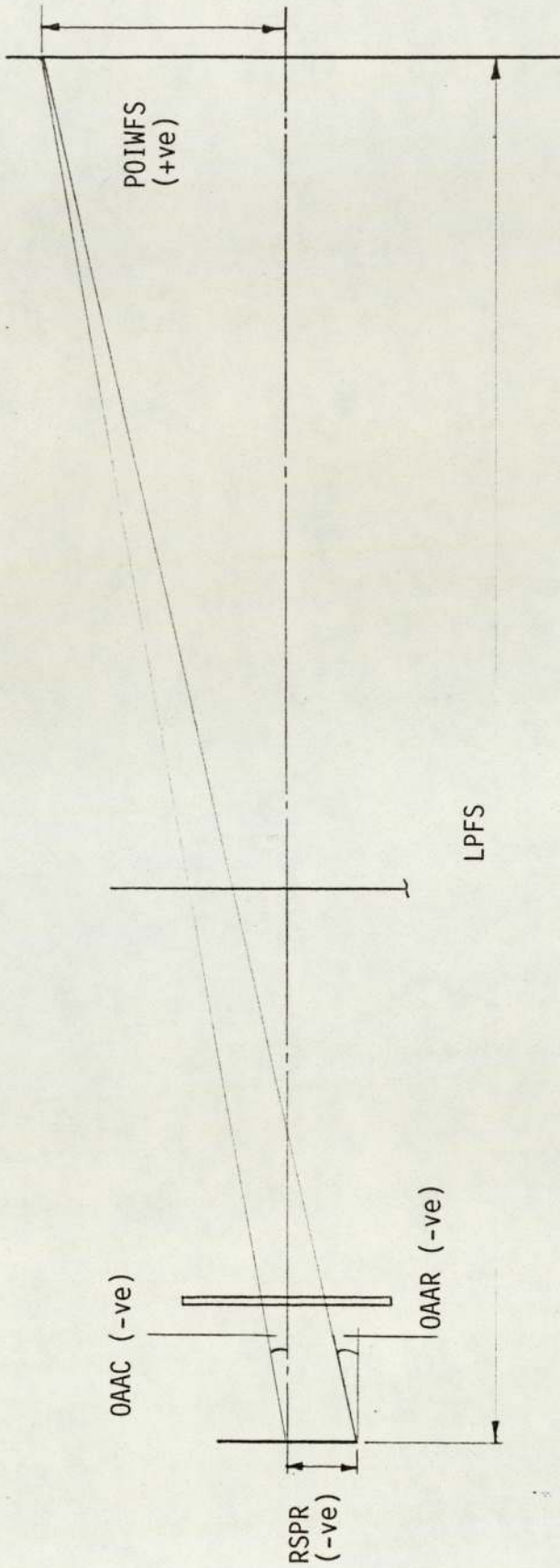
12.1g and 12.1h.

- ii) Calculates POIWNS for the ray by applying Snell's law at each surface of the lens system.
- iii) Prints the values of RSPR, OAAR and POIWNS.
- g) Calculates and prints the magnification of the system for the central ray of the pencil, MAG; this is only carried out if POIWFS = 0.

$$\text{MAG} = \frac{\text{POIWNS for central ray in pencil}}{\text{POIWFS for the pencil}}$$

A sample of the printout obtained for 1 pencil is shown in Table 12.2.

- 3) The ELPS data for the lamp size of interest are calculated, using Table 12.1.
- 4) The data output by the program is now used to determine, for both the horizontal and vertical planes, whether or not the ELPS of the lamp exceeds the LTELPS value of the configuration for each OAAC value of interest. If it does then the configuration is clearly unsuitable since it acts as a field stop.
- 5) If the configuration does not act as a field stop for the range of OAAC values of interest, then its imaging performance can be



$$|\tan \text{OAAR}| = \frac{|\text{POIWFS}| + |\text{RSPR}|}{\text{LPFS}}$$

$$\therefore \text{OAAR} = -\tan^{-1} \frac{\text{POIWFS} - \text{RSPR}}{\text{LPFS}}$$

Fig. 12.1h Reduced-Length Photometer Model - Off-Axis Angle of Ray (RSPR < 0)

PENCIL NUMBER = 2

ANGLE OF CENTRAL RAY (OACD) = -1.0000 DEG

PT. OF INTERSECTION WITH FAR SCREEN (POIWF) = 0.4364 M

LIMITING EFFECTIVE LAMP SIZE (LELPS) = 0.4730 M

| STARTING PT. ON LAMP (RSPR) | ANGLE OF RAY (OARD) | PT. OF INTERSECTION WITH NEAR SCREEN (POIWN) |
|---------------------------------------|----------------------------|--|
| -0.1500 | -1.3436 | 0.0613 |
| -0.1400 | -1.3207 | 0.0611 |
| -0.1300 | -1.2978 | 0.0610 |
| -0.1200 | -1.2749 | 0.0609 |
| -0.1100 | -1.2520 | 0.0608 |
| -0.1000 | -1.2291 | 0.0607 |
| -0.0900 | -1.2062 | 0.0607 |
| -0.0800 | -1.1833 | 0.0606 |
| -0.0700 | -1.1604 | 0.0606 |
| -0.0600 | -1.1375 | 0.0606 |
| -0.0500 | -1.1146 | 0.0606 |
| -0.0400 | -1.0916 | 0.0607 |
| -0.0300 | -1.0687 | 0.0607 |
| -0.0200 | -1.0458 | 0.0607 |
| -0.0100 | -1.0229 | 0.0608 |
| 0.0000 | -1.0000 | 0.0608 |
| 0.0100 | -0.9771 | 0.0609 |
| 0.0200 | -0.9542 | 0.0609 |
| 0.0300 | -0.9313 | 0.0610 |
| 0.0400 | -0.9084 | 0.0610 |
| 0.0500 | -0.8854 | 0.0610 |
| 0.0600 | -0.8625 | 0.0611 |
| 0.0700 | -0.8396 | 0.0611 |
| 0.0800 | -0.8167 | 0.0611 |
| 0.0900 | -0.7938 | 0.0611 |
| 0.1000 | -0.7709 | 0.0611 |
| 0.1100 | -0.7480 | 0.0611 |
| 0.1200 | -0.7250 | 0.0611 |
| 0.1300 | -0.7021 | 0.0611 |
| 0.1400 | -0.6792 | 0.0610 |
| 0.1500 | -0.6563 | 0.0609 |

MAGNIFICATION = 0.1393

Table 12.2 Example of Data Produced by 'RLP' Program

examined more closely.

The paraxial magnification (i.e. the magnification obtained for an OAAC value of, say, 1°) can be obtained from the program output. (This value will differ slightly from that predicted by equation B4 in Appendix B. This difference is of no consequence, however; it is the actual paraxial magnification obtained which is of interest). The POIWNS values which would be obtained if the paraxial magnification was maintained for all OAAC values are calculated from the equation:

$$\text{Required POIWNS} = \text{Paraxial Magnification} \times \text{POIWFS}$$

- 6) Blur patch data tables for both the horizontal and vertical planes are compiled. These list the following parameters for each OAAC value of interest:
 - a) Required POIWNS value, as calculated in step 5.
 - b) Minimum POIWNS value, as output by the program, for the appropriate ELPS value.
 - c) Maximum POIWNS value, as output by the program, for the appropriate ELPS value.
 - d) (Maximum POIWNS - Minimum POIWNS), i.e. the length of the blur line.
 - e) (Minimum POIWNS - Required POIWNS)

f) (Maximum POIWNS - Required POIWNS)

The values of the above quantities for the example output data shown in Table 12.2 are given below; it is assumed that the paraxial magnification of the system is 0.1393 and that ELPS = 0.3 m.

a) Required POIWNS = $0.1393 \times 0.4364 = 0.0608$ m

b) Minimum POIWNS = 0.0606 m

c) Maximum POIWNS = 0.0613 m

d) (Maximum POIWNS - Minimum POIWNS) = 0.0007 m

e) (Minimum POIWNS - Required POIWNS) = - 0.0002 m

f) (Maximum POIWNS - Required POIWNS) = 0.0005 m

(Examples of blur patch data tables for a series of OAAC angles can be found in Appendix E.)

- 7) The blur patch data tables produced in the previous step are now used to compare the performance of the configuration with that of an ideal reduced-length photometer and to determine its acceptability using the criterion proposed in section 12.1.

For the configuration and lamp combination to satisfy this criterion requires:

a) (Minimum POIWNS - Required POIWNS)

$$\leq \frac{(65 \times \text{Paraxial Magnification})}{2} \text{ mm}$$

and

b) (Maximum POIWNS - Required POIWNS)

$$\leq \frac{(65 \times \text{Paraxial Magnification})}{2} \text{ mm}$$

For the example data given above, $(65 \times \text{Paraxial Magnification} / 2) = 0.0045 \text{ m}$. This criterion is easily satisfied, therefore, which is to be expected since the off-axis angle is only 1° .

13. FOUR METRE REDUCED-LENGTH PHOTOMETER PERFORMANCE

13.1 Introduction

This Chapter describes the performance of various single-element 4 m reduced-length photometer configurations, using the analysis method described in Chapter 12; a 4 m configuration was the most suitable choice for a prototype video photometry system to be implemented in the E&D department darkroom.

To simplify the presentation of the results, a single set of worst-case physical lamp size data is used here. The horizontal analyses are based on the use of a physical reflector width, PRW, of 300 mm; the widest reflector currently produced (for the 35FR lamp fitted to the Austin Maestro) is approximately 290 mm wide. (Twin pocket lamps have wider reflectors but are treated as two separate lamps for testing purposes.) A physical reflector height, PRH, of 160 mm is used for the vertical analysis; this is the aperture size of a standard seven inch round lamp, which is currently the tallest lamp produced. The resultant effective lamp sizes, based on the data given in Table 12.1, are given in Table 13.1

Since the maximum ELPW of interest is greater than the maximum ELPH of interest (300 mm compared to 160 mm) and the horizontal off-axis imaging angles of interest are greater than the vertical ones (up to 30° compared to 12°) then the horizontal plane is clearly the one which must be considered the more closely.

| HORIZONTAL PLANE | |
|-------------------------|--------------------------------|
| OFF-AXIS ANGLE (OAAC) | EFFECTIVE LAMP WIDTH (ELPW) |
| 0° - 10° | 300 mm |
| 10° - 20° | 200 mm |
| 20° - 30° | 100 mm |
| VERTICAL PLANE | |
| OFF-AXIS ANGLE (OAAC) | EFFECTIVE LAMP HEIGHT (ELPH) |
| 0° - 12° | 160 mm |

Table 13.1 Effective Lamp Size Information for Reduced Length Photometer Study

Four basic configurations, some described by more than one set of parameters (when the value of LNSSZE is different for the horizontal and vertical planes and when the performance for light of different colours is to be studied), are considered. For each configuration, the sets of parameters are given in Appendix E. Owing to the volume of data generated by running the RLP program, the printouts have been combined into a separate document (71) rather than included in this thesis. The blur patch data tables generated using the worst case ELPS data given in Table 13.1 are also contained in Appendix E.

13.2 Performance Study

The E&D department Automatic Photometer configuration will be considered first; this uses a rectangular-shaped crown glass plano-convex lens of 4 m focal length. The lamp is placed behind the plane surface of the lens. The size of the lens is 460 mm x 360 mm but the mounting frame reduces the effective size to 436 mm x 336 mm. It is referred to here as configuration 1a for the horizontal plane and configuration 1b for the vertical plane. The standard refractive index value for crown glass (i.e. that for the sodium D line) is used. The program output for the horizontal plane (71) shows that this configuration acts as a field stop for horizontal off-axis angles of greater than 7° and would not therefore enable a useful field of view to be covered when used in a video photometer. Blur patch data tables for this configuration are not given.

In order to cover a wider field of view, a smaller LPFILS value

and/or greater LNSSZE value is required.

A configuration based on the use of a slightly larger 4 m focal length crown glass plano-convex lens and a smaller LPFILS value will now be considered. The lamp is again placed behind the plane surface of the lens. The lens is assumed to be circular and have a diameter of 0.5 m, reduced to an effective diameter of 0.48 m by the mounting frame. The LNSTHK value used is 35 mm. (As will be seen later, these are the parameters of the actual lens purchased for the video photometer.) LPFILS is 400 mm, which was the estimated value of the smallest practical distance which could be used with a conventional goniometer; as will be seen later, the use of a conventional goniometer is desirable with a video photometer even though the normal point to point movement is not required to take measurements. The LALSNS value used was calculated using equation B3, as described in section 12.3.

Configuration 2a uses these parameters and the standard D line refractive index value. The program printout shows that the configuration acts as a field stop for angles in the horizontal plane of $18^\circ - 20^\circ$ as a result of the LTELPS values for these angles. As will be seen later, however, the imaging performance ceases to be acceptable before this limit is reached. The paraxial magnification for the system (for this refractive index value) is 0.1393.

Blur patch data tables for both the horizontal and vertical planes for configuration 2a are given in Appendix E; both are generated from the same program printout since the system is symmetrical.

In order to satisfy the criterion of acceptability given in Chapter 12, the following conditions must be met:

$$(\text{Minimum POIWNS} - \text{Required POIWNS}) \leq 4.5\text{mm}$$

$$(\text{Maximum POIWNS} - \text{Required POIWNS}) \leq 4.5\text{mm}$$

It can be seen from the horizontal plane blur patch data table that the above conditions are satisfied for 0° to 10° . (It should be remembered that only one side of the axis is being considered; the results, of course, apply equally to the other side of the axis i.e. an acceptable range of 0° to x° off-axis means that a total field of view of $\pm x^\circ$ can be imaged satisfactorily.) For 10° to 13° the length of the blur patch, i.e. the value of (Maximum POIWNS - Minimum POIWNS), is still smaller than the 9 mm near screen flux collection area diameter but the blur patch does not fall on the required part of the screen because of the distortion in the image; the magnification at 13° , for example, is 0.1383 which is 0.7% lower than the paraxial magnification. (The distortion does, of course, gradually increase in moving off-axis; it is not until 11° , however, that it is sufficiently high to cause the blur patch to fall outside the screen area corresponding to the ideal imaging point and its surrounding flux collection area.) Thus the performance can be considered satisfactory for the horizontal plane over a range of 0° to 13° if this small amount of distortion is acceptable. Beyond 13° , the size of the blur patch and the amount of distortion rise sharply. At 18° , for example, the blur patch size is 16.5mm and the magnification is 1.5% lower than the paraxial magnification.

It can be seen from the vertical plane blur patch data table

for this configuration that the above conditions are satisfied for 0° to 10° ; the blur patch size remains smaller than the 9 mm near screen flux collection area diameter for 10° to 12° .

The effect of placing the lens with the convex side towards the lamp will now be considered; configuration 3 is the same as 2a except for this change in lens orientation. It can be seen from the blur patch data table for the horizontal plane that the blur patch sizes produced are larger than for configuration 2a. The conditions of acceptability are met for 0° to 6° compared with 0° to 10° , or 0° to 7° compared with 0° to 13° , if the small amount of distortion is acceptable. It is clearly more satisfactory, therefore, to place the lens with the plane side towards the lamp as in configuration 2a.

The effects of chromatic aberration will now be studied. Since the refractive index of glass varies with wavelength, the focal plane for each spectral component of the white light to be imaged lies at a different distance from the lens. The imaging performance for the red and blue components can be studied by using the appropriate refractive index values.

Configurations 2b and 2c represent the same physical arrangement as configuration 2a; they differ in that they use the refractive indices for red light (the hydrogen C line) and blue light (hydrogen F line) respectively.

The blur patch data tables shows that the required conditions are satisfied for 0° to 11° horizontally and vertically for red light, but only 0° to 7° horizontally and 0° to 9° vertically for blue light.

The relatively poor performance for blue light is caused by the focal plane lying some distance in front of the screen position; it effectively limits the acceptable performance range of the system for white light to 0° to 7° horizontally and 0° to 9° vertically.

The overall blur patch size for white light (calculated using the smallest of the three 'Minimum POIWNS' values and the largest of the three 'Maximum POIWNS' values for a given off-axis angle) remains smaller than the 9 mm flux collection area diameter for 0° to 8° horizontally and 0° to 12° vertically. Consequently, if a small amount of distortion is acceptable, then the performance can be considered satisfactory over these ranges.

The imaging performance characteristics of the configuration can be significantly modified by changing the position of the near screen, since the focal planes are actually curved surfaces, as shown in Fig. 13.1. Hence moving the screen closer to the lens increases the sizes of the blur patches for points close to the axis but decreases them for points further off-axis. Hence the off-axis imaging performance can be improved at the expense of a slightly inferior performance for points close to the axis. Moving the screen position also enables a more acceptable compromise between the imaging performance for the yellow, red and blue components than achieved above to be obtained.

Configurations 4a, b and c are the same as 2a, b and c except that they use a LALSNS value of 3.995 m in order to increase the acceptable field of view. The paraxial magnification of this configuration for yellow light is 0.1384, which again gives the

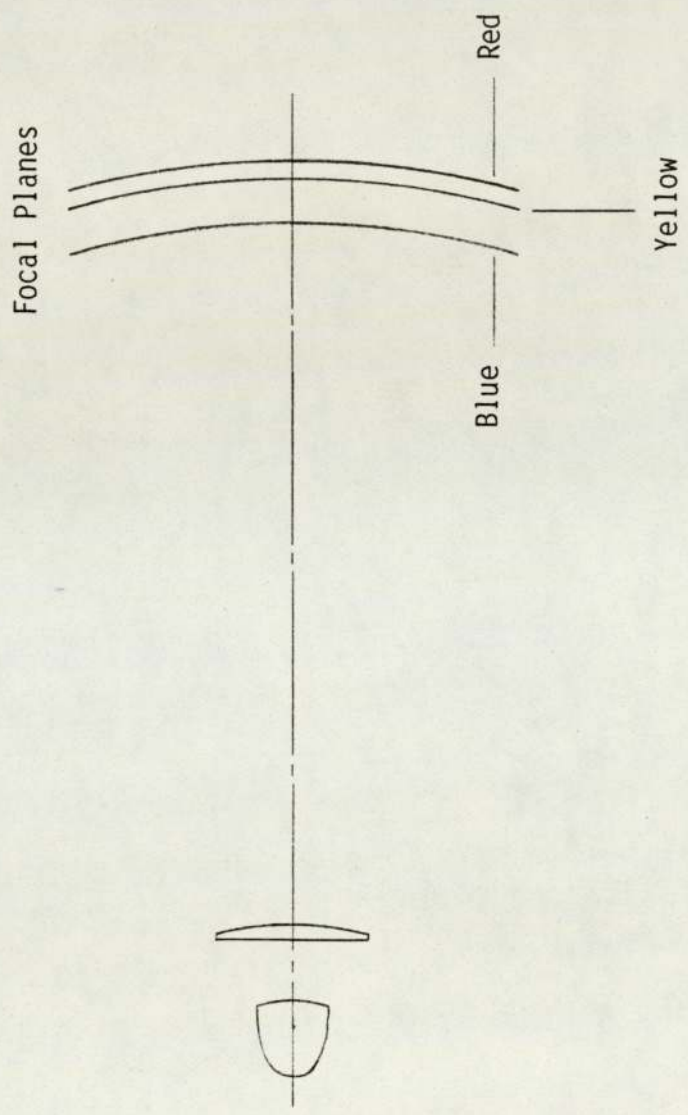


Fig. 13.1 Focal Planes for a Single-Element Reduced Length Photometer Imaging a Flat Far Screen

expression $(65 \times \text{Paraxial Magnification})/2$ a value of 4.5 mm.

It can be seen from the blur patch data tables that the required conditions are now satisfied for 0° to 11° horizontally and vertically for both yellow and red light and 0° to 9° horizontally and vertically for blue light. Consequently, the overall performance for this configuration for white light can be considered satisfactory for 0° to 9° horizontally and 0° to 9° vertically.

If a small amount of distortion is acceptable, then the performance can be considered satisfactory over ranges of 0° to 13° horizontally and 0° to 12° vertically, since these are the ranges over which the overall blur patch size for white light remains smaller than the 9 mm flux collection area diameter.

13.3 Conclusions

It has been estimated by means of the devised model and analysis procedure that a suitably configured single-element 4 m reduced-length photometer can provide a satisfactory imaging performance, providing a small amount of distortion is acceptable, for angles:

- a) Up to approximately 13° off-axis in the horizontal plane.
- b) Up to and beyond the maximum off-axis angle of interest in the vertical plane of 12° .

It should be remembered, however, that:

- a) The true three-dimensional imaging situation has been represented by a two-dimensional model which has been used to analyse independently the horizontal and vertical axes of the system. In practice, a point which is, say, 12° left and 8° up is likely to produce larger blur patch sizes than predicted here.
- b) The effects of reflections at the lens surfaces, giving rise to flare, have been ignored.
- c) A single set of worst case effective lamp size data has been used. For most lamps, the true effective lamp size values, and hence the blur patch sizes, will be smaller than predicted here; this will tend to compensate for (a) above.
- d) It has been assumed that a blur patch size smaller than a near screen flux collection area equivalent to a square of side 65 mm at 25 m is necessary to prevent unacceptably large illuminance measurement errors. In practice, however, the error produced will depend on the illuminance gradients at the point being measured; consequently, in areas where these gradients are low, the error may often be acceptably small even when the blur patch size exceeds the above limit.

As a consequence of the above factors, the results produced should be regarded as approximate; in practice the performance of a given reduced-length photometer configuration will depend on the size

and beam pattern characteristics of the lamp being measured.

14. AN INTEGRATED PHOTOMETRIC DATA PROCESSING SCHEME

A basic introduction to this scheme, and the reasons why it is necessary, are given in section 5.1.6. This Chapter provides further information on the author's proposals and the extent to which they have so far been implemented.

14.1 Description

The author proposed that:

- a) A central computer, to which all the computer-based photometers would be linked, should be used as the basis of the facilities.
- b) The central computer should be used to:
 - i) Store data acquired by computer-based photometers; the data from each lamp tested should be stored in a single file, known as a Photometric Data File (PDF).

The PDF structure should enable the storage of many different types of photometric data, obtained from one or more beams per lamp.

- ii) Execute the performance prediction software and store the results, again in PDF's.

- iii) Execute a general purpose suite of software for processing the contents of PDF's; this software should be used to carry out operations such as iso-lux diagram plotting and test point data tabulation.

This type of operation is essentially independent of the techniques and equipment used to produce the data. For example, an iso-lux diagram is produced from a two-dimensional array of illuminance values; it is irrelevant whether these values have been measured by a photometer or theoretically calculated by performance prediction software. Consequently, this type of operation can be implemented in such a way that it can be used with data from a variety of sources.

- iv) Execute 'Chess' using suitable PDF data as input.

- v) Enter manually acquired data into a PDF.

- c) The primary role of a computer-based photometer should be to acquire data for transmission to the central computer for processing and long-term storage; see section 14.2.1.

The advantages of this scheme are:

- a) The problems of transferring data between the required facilities are minimised.
- b) There is only one main filing system to maintain and search

when the data from any given lamp is required.

- c) The design and construction of new computer-based photometers will not involve the re-implementation of standard processing operations, such as iso-lux diagram plotting, thereby enabling optimum use to be made of the limited software development resources available.
- d) The modification or decommissioning of computer-based photometers will not affect the PDF filing system or PDF processing software.
- e) The PDF processing software can be modified without affecting the operation of the computer-based photometers. Furthermore, a common set of software development tools (editor, compiler etc) can be used.

Further information about the roles of the computer-based photometers, PDF's and the PDF processing software are given in sections 14.1.1 to 14.1.3; a diagram of the scheme is given in Fig. 14.1.

14.1.1 Computer-Based Photometers

As stated above, the primary purpose of a computer-based photometer in this scheme is to acquire data for transmission to the central computer for processing and long-term storage.

It is important that the actual acquisition of data is carried

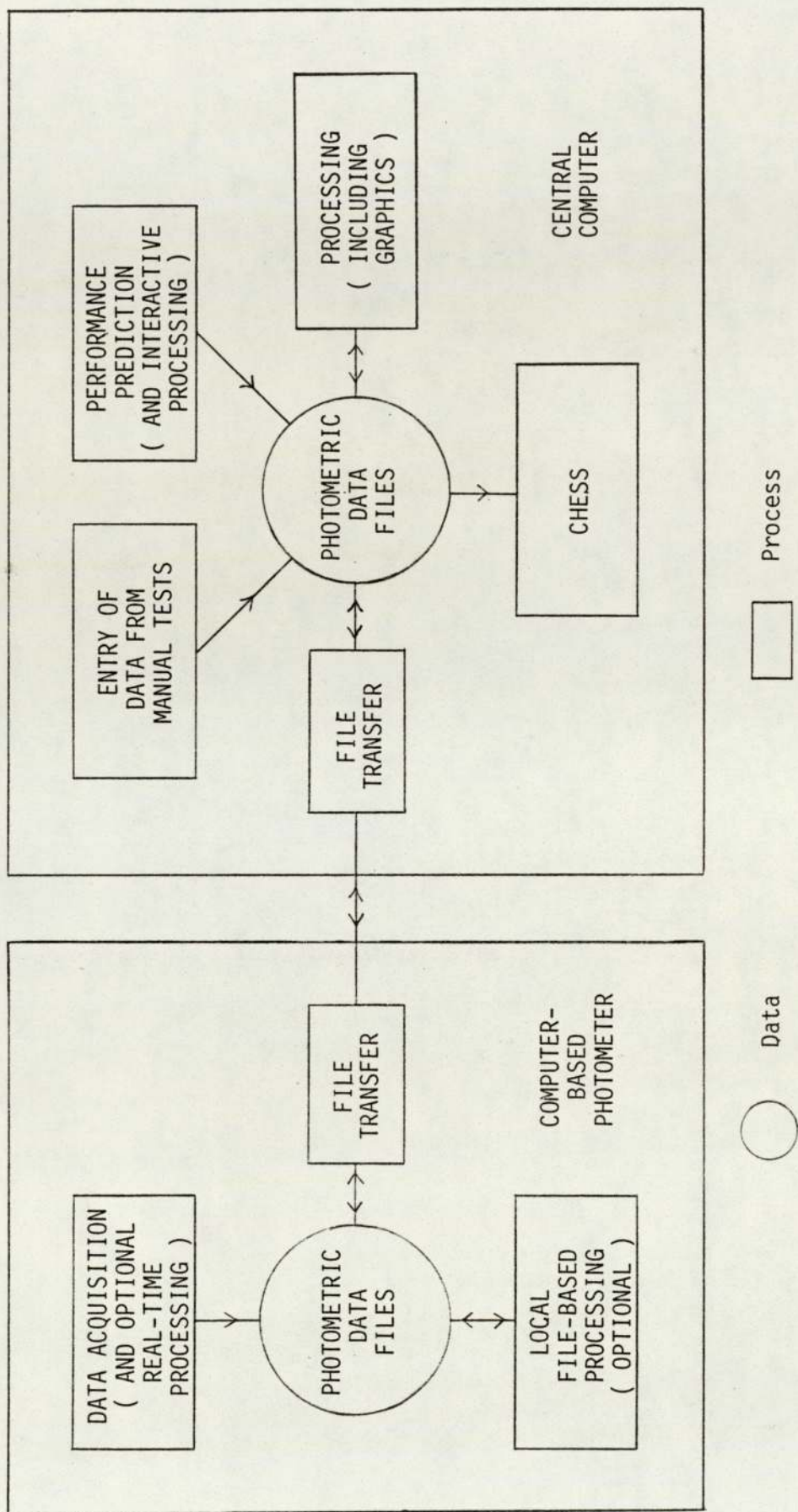


Fig. 14.1 Photometric Data Processing Scheme

out solely by the photometer with the transfer of data to the central computer being a separate operation. This makes the most efficient use of the central computer and enables data to be acquired even if the computer, or link to it, is not operational. The photometer, therefore, should acquire the data and store it in a file on a local storage system for subsequent transmission to the central computer.

In addition to acquiring data, the ability to carry out some local processing operations on the photometer is highly desirable for those occasions when a 'quick look' at the data is required, either in advance of or instead of, its permanent storage on the central computer. This can be accomplished in two ways:

a) 'Real-Time' Processing

Software to carry out the required processing operations could be combined with the data acquisition routines.

(This technique was used in the Automatic Photometer; for example, the routine which acquires and files test point data also outputs it to the console.)

b) File-Based Processing

The PDF's could be processed on the photometer, eliminating the immediate need for transfer to the central computer.

In general, the type and extent of the local real-time and file-based processing desirable will depend on the techniques and

equipment used in any particular design of photometer. With careful design and choice of equipment and computer languages it should be possible to run many of the routines written for the central computer on the photometer's computer.

To summarise, although the primary purpose of a photometer in this scheme is to acquire data for processing on the central computer, certain stand-alone processing capabilities are desirable for ease and flexibility of operation.

14.1.2 Photometric Data Files

A PDF will contain photometric data produced by a computer-based photometer or the performance prediction software. Various types and amounts of data will need to be stored in PDF's; two examples of the many possible types of data which might occur are:

- a) Illuminance values at discrete points on a flat screen.
- b) A two-dimensional array of intensity values.

Each PDF will need to contain information describing the type of data stored in it to enable the data to be processed correctly.

14.1.3 Photometric Data File Processing Software

The main operations for which software will be required are:

- a) Plotting and displaying iso-lux and iso-candela contour diagrams from two dimensional arrays of spherical test surface illuminance data.
- b) Plotting and displaying cross-section diagrams for one- or two-dimensional arrays of spherical test surface illuminance data.
- c) Listing test point readings.
- d) Tabulating test point readings from several lamps.

Many other operations, for example those described in section 9.3, are also desirable.

The PDF processing software should be implemented in a modular form, using a library of standard procedures. This would simplify the software development process and minimise the effort required to implement new processing operations. A standard language should be used so that the difficulties involved in duplicating the software on the computer-based photometers, to provide a stand-alone processing capability, will also be minimised.

14.2 Implementation

The proposed scheme has been adopted in principle by the department, although its full implementation will take a considerable amount of time and effort and this task was clearly outside the scope

of the project.

The only feasible choice for the central computer was the Lucas Group Computer, situated at Shirley, about 30 miles from Cannock; its use for this scheme has the following benefits and drawbacks:

a) Benefits

- i) Terminals for this computer are currently in use in the department; a keyboard/printer, graphics terminal and flat-bed plotter are available.
- ii) The running of the system places no load on the manpower resources of the E&D department.
- iii) Extensive mass storage is available, ideal for archiving a large number of files.
- iv) Graphics support software is available.

b) Drawbacks

- i) Peripheral connection is complicated by the need for a communications link between the two sites.
- ii) This link can limit the speed at which data can be transmitted to, or received from, any peripheral, which can slow down response time.

- iii) The large number of users can also slow down response time.
- iv) CPU time is expensive.
- v) Technical support is not always easily obtainable.

Some of these drawbacks can be alleviated to a certain extent, as follows:

- i) It is hoped in future to connect all peripherals, including computer-based photometers, to the Group Computer via the Cannock Management Services department's mini-computer, which will simplify the problems involved.
- ii), iii) and iv)

The amount of data to be transmitted between the two sites and the CPU time required can be reduced by the use of intelligent terminals and/or the use of one or more smaller computers connected to the Group Computer. For example, the performance prediction software will involve a very large number of mathematical operations and will be expensive to run. It might be possible, however, to use a 16 bit microcomputer to run these routines, whilst retaining the advantages of the mainframe for archiving the results and generating graphical output. The combination of the Group Computer and one or more additional computers can still be regarded as the

'central computer' for the purposes of this scheme.

The author has carried out the following tasks towards the implementation of the scheme:

- a) A file transfer system between the Automatic Photometer and the Group Computer has been established; see Appendix G.
- b) A PDF storage format has been defined, based on the use of the Group Computer and Fortran 77; see Appendix H.
- c) An example of PDF processing software has been written; see Appendix H.

15. THE PROPOSED VIDEO PHOTOMETRY SYSTEM

15.1 Introduction

This Chapter describes the proposed prototype video photometry system.

Section 15.2 provides an overall description of the system, with the 'front-end' i.e. the reduced-length photometer, cameras and screen system, being described in more detail in section 15.3.

Although the system could not be implemented, a certain amount of construction work was carried out, and is described in section 15.4.

Section 15.5 discusses the image processing system requirements and the equipment evaluation work which led to the selection of the 'Gems System 33'.

The camera requirements, equipment evaluation work and the reasons why none of the cameras was considered suitable are given in section 15.6.

The conclusions reached from the work described in this Chapter are given in section 15.7.

15.2 Overall Description

The system was designed in accordance with the photometric data processing scheme described in Chapter 14, and was to be capable of being used as a stand-alone unit, or in conjunction with the Group Computer.

The system was to cover the seven application areas given in Chapter 9 to the following extent:

a) The Conventional Tests

As stated in section 9.1.3, the potential increased speed of data acquisition is most significant for iso-lux tests. It was therefore decided that the ability to display a pseudo-colour representation of an SIA on a colour monitor was the main priority in this category. The plotting of iso-lux and cross-section diagrams (i.e. hard copy) and the listing of test point values were to be carried out by software on the Group Computer.

b) Interactive Design Processing

It was decided that the system should be capable of carrying out, on a stand-alone basis, the processing required for the 'Beam Component Study' application i.e. the ability to add, subtract and shift SIA's is required. The 'Beam Synthesis' work was to be considered at a later date.

c) New Methods of Presenting Performance Data

The SIA's acquired by the proposed system will enable the types of diagrams described in section 9.3 to be produced; this does, of course, require the development of the appropriate software. It was intended that this software should initially be developed for the Group Computer (see Chapter 14) and later implemented on the video photometer to take advantage of the colour display facilities.

d) Reflector Testing

It was considered that this was a large area of work that could not be tackled realistically until a basic video photometry system was in operation. Consequently, it was decided that the role of the prototype system in this area should be that of a research tool; spatial frequency processing software is available on the Group Computer.

e) Automatic Aiming

This was to be treated as a future development.

f) Generation of Data for Performance Prediction Software

This was to be catered for by transferring data files to the Group Computer; see Chapter 14.

g) Generation of Data for 'Chess'

This was also to be catered for by transferring data files to the Group Computer.

The system was to be capable of simultaneously storing 2 SIA's in the frame-store and carrying out the following operations:

- a) Acquiring an SIA
- b) Displaying a pseudo-colour representation of an SIA
- c) Adding, subtracting and shifting SIA's
- d) Transferring an SIA from the frame-store to a disk file
- e) Loading an SIA into the frame-store from a disk file
- f) Transferring disk files to the Group Computer

These operations are shown in Fig. 15.1a.

The video photometer was to consist of 2 main parts: the front-end and a modified image processing system. The purpose of the front-end is to convert the near screen illuminance distribution into analogue electrical video signals for input to the modified image processing system. It uses viewing arrangement (d) (see section 7.3) and a 4 m reduced-length photometer. Thus the proposed system is essentially as shown in Fig. 5.2, with the addition of a second

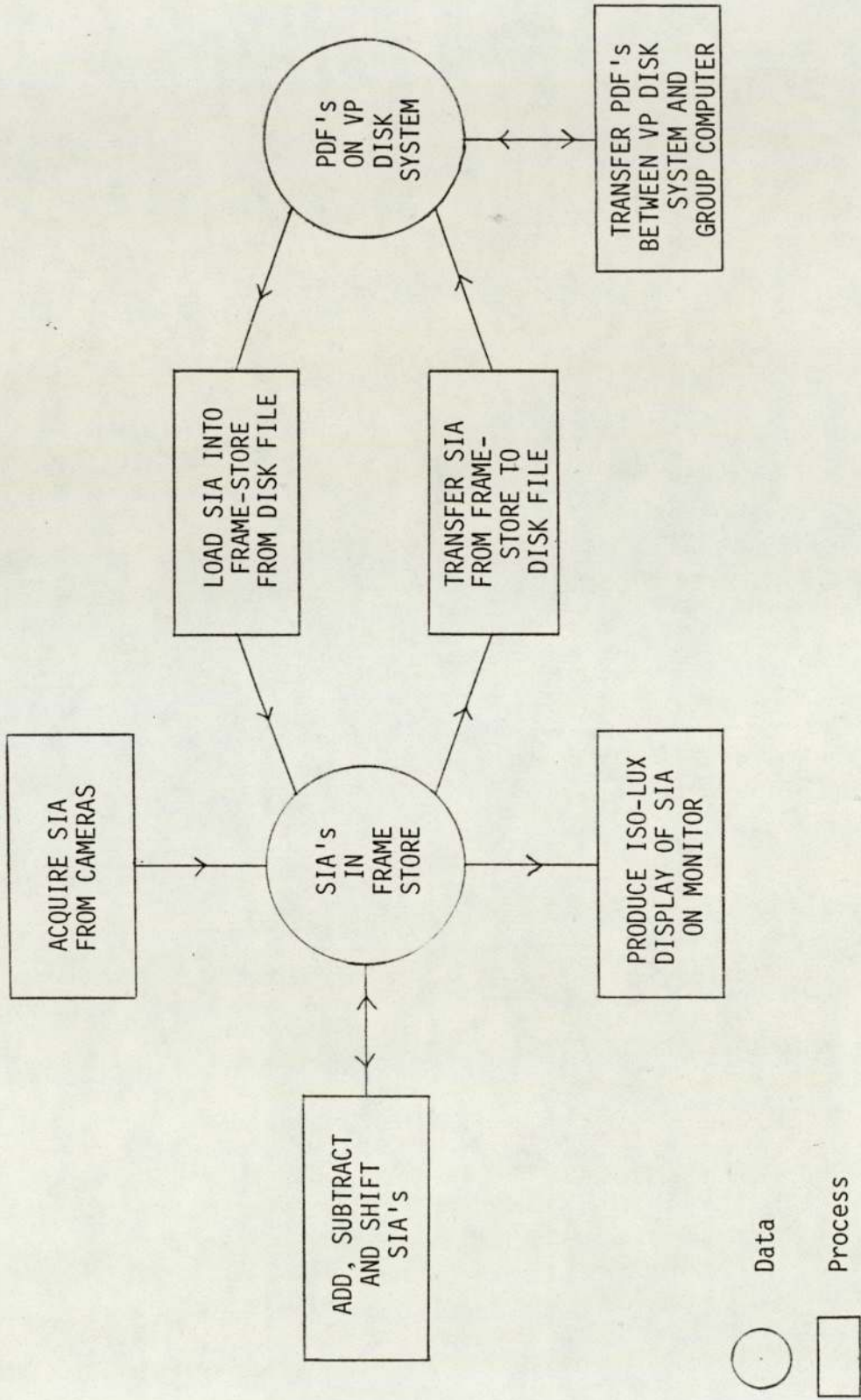


Fig. 15.1a Proposed Video Photometry System - SIA Processing Operations

camera, positioned as shown in Fig. 7.2d.

It was decided that the equipment would be constructed in the 'General Testing Room' of the E&D darkroom; the other possible locations in this darkroom were discounted because they would have required substantial reconstruction work. A cubicle was constructed (by the Works Engineers department) to re-house the signal lamp test equipment normally used in the 'General Testing Room'.

The system was to measure a range of illuminance values corresponding to 0-50 lux at 25 m, this being suitable for measuring headlamp dipped beams and foglamps. Main beams and spotlamps would be measured by using neutral density filters over the camera lenses to produce further measurement ranges of 0-200 and 0-400 lux at 25 m.

It was originally hoped to use 2 Fairchild cameras with 256 x 256 square pixels and anti-blooming characteristics, although the use of other makes of camera was not ruled out. The use of these Fairchild cameras would produce an SIA size of 512 x 256; they were to be interfaced to the image processing system by multiple range digitization method (a) using a standard 8 bit video ADC. Measurements over the 0-50 lux range were to be made by acquiring 2 arrays of data, as described in section 11.2.2.1, with full-scale sensitivities of 12.5 lux and 50 lux. It was hoped to switch sensitivities by altering the clocking rate of the cameras.

Provision was to be made for digital filtering to reduce noise. It was considered that corrections for the camera's dark signals and responsivity variations, the \cos^4 law variations and

possibly non-ideal screen reflectance characteristics would be necessary in calculating the E_{FSCP} values; practical measurements were to be carried out using the system in order to determine the extent of the decalibration processing required.

A screen pixel size of 25 mm x 25 mm (at 25 m) was to be used, assuming the use of a camera with square pixels. This size offers the following benefits:

- a) It is sufficiently small to enable high resolution iso-lux diagrams to be produced (25 mm corresponds to approximately 0.05°).
- b) 512 x 256 screen pixels of this size produce a field of view of $\pm 14.4^\circ$ H, $\pm 7.2^\circ$ V, which is a convenient size. (The system was designed to allow a larger field of view to be covered if required; see later.)
- c) The positions of all but 2 of the ECE test points can be made to correspond exactly to the effective measurement points produced by using an array of 25 mm x 25 mm screen pixels. The positional error of the two points which do not correspond (25L and 25R) is only 0.25%

It was planned to use method (b) of generating an SIA from the E_{FSCP} values (see section 11.4.2); the average of 4 pixels was to be used, giving an effective measurement area of 50 mm x 50 mm at 25 m.

Ambient light correction was to be applied if necessary; see

section 11.5 and Appendix C.

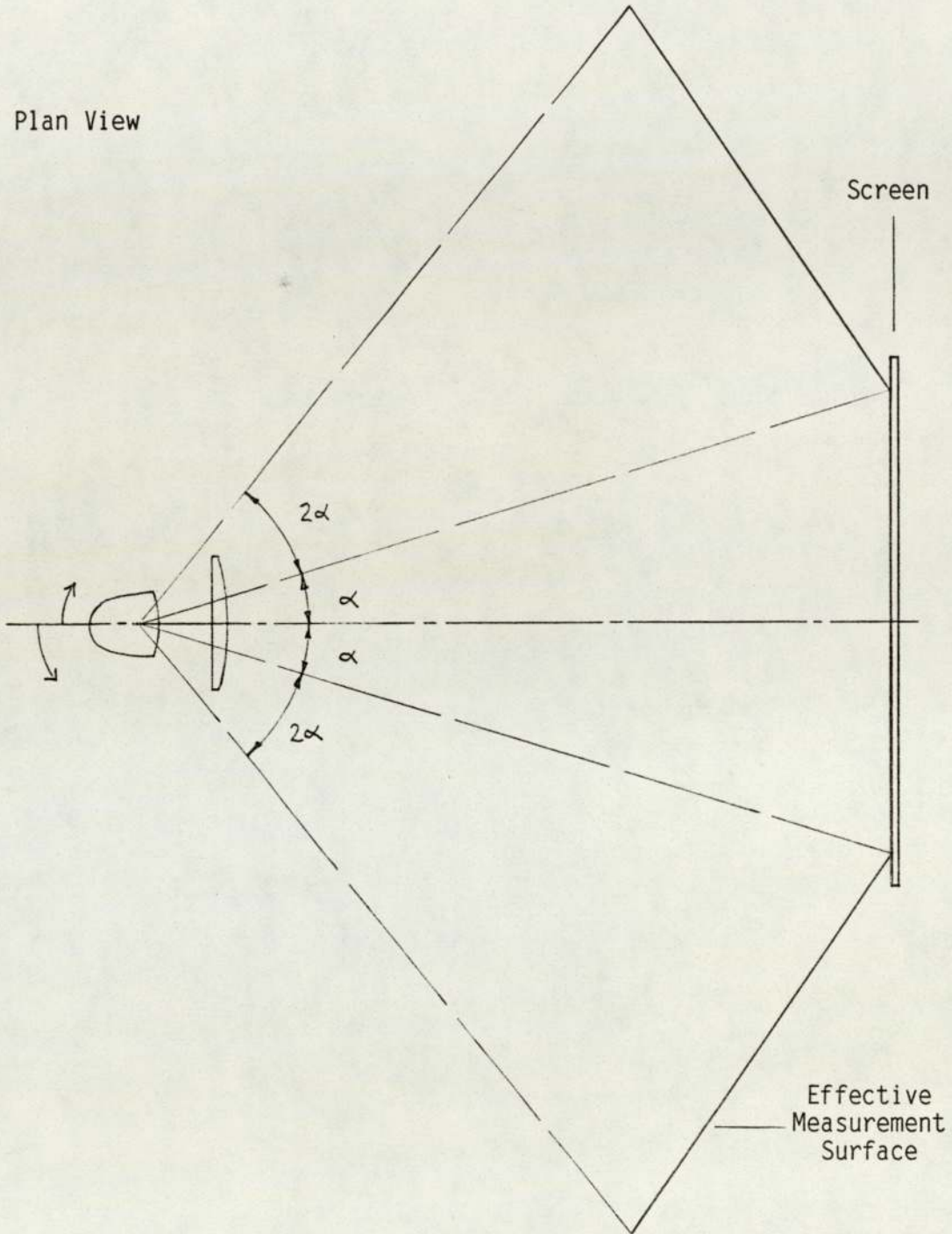
The basic field of view to be imaged by the cameras was to be $\pm 14.4^\circ$ H, $\pm 7.2^\circ$ V. Some tests, however, require data to be acquired over a larger field of view. This was to be catered for by providing the facility to build-up a large SIA from several smaller ones, each acquired with the lamp set to a different initial position by means of a conventional goniometer. For example, a lamp could be aimed and an SIA obtained for $\pm 10^\circ$ H, $\pm 7.2^\circ$ V. If the lamp is now rotated 20° clockwise, then the readings which would have been obtained between -30° H and -10° H will now again be obtained between -10° H and $+10^\circ$ H and a second SIA can be acquired. Similarly, a third SIA for $+10^\circ$ H to $+30^\circ$ H can be obtained. An SIA covering $\pm 30^\circ$ H $\pm 7.2^\circ$ V could then be produced by combining these SIA's in the image processing system. The method does have the disadvantage that the effective measurement surface is neither a conventional plane nor a spherical one, but a combination of the two, as shown in Fig. 15.1b. This surface can, however, be considered approximately equivalent to a spherical surface.

The front-end and the image processing system are considered in more detail in sections 15.3 and 15.5 respectively.

15.3 The Front-End

It was proposed to use reduced-length photometer configuration 4 of Chapter 13; the range of off-axis angles for which it was estimated that satisfactory imaging performance would be obtained is approximately equal to the system's field of view. It was not

Plan View



Acquiring and combining SIA's with the lamp (a) as shown (b) rotated clockwise by $2\alpha^\circ$ and (c) rotated anti-clockwise by $2\alpha^\circ$, produces an effective measurement surface as shown.

Fig. 15.1b Proposed Video Photometry System - Measurement Surface for Extended Field of View

feasible to use either a longer focal length system, because of space restrictions, or one with more lens elements, because the manufacturing costs would be excessive.

The proposed outline design of the front-end is shown in Fig. 15.1c.

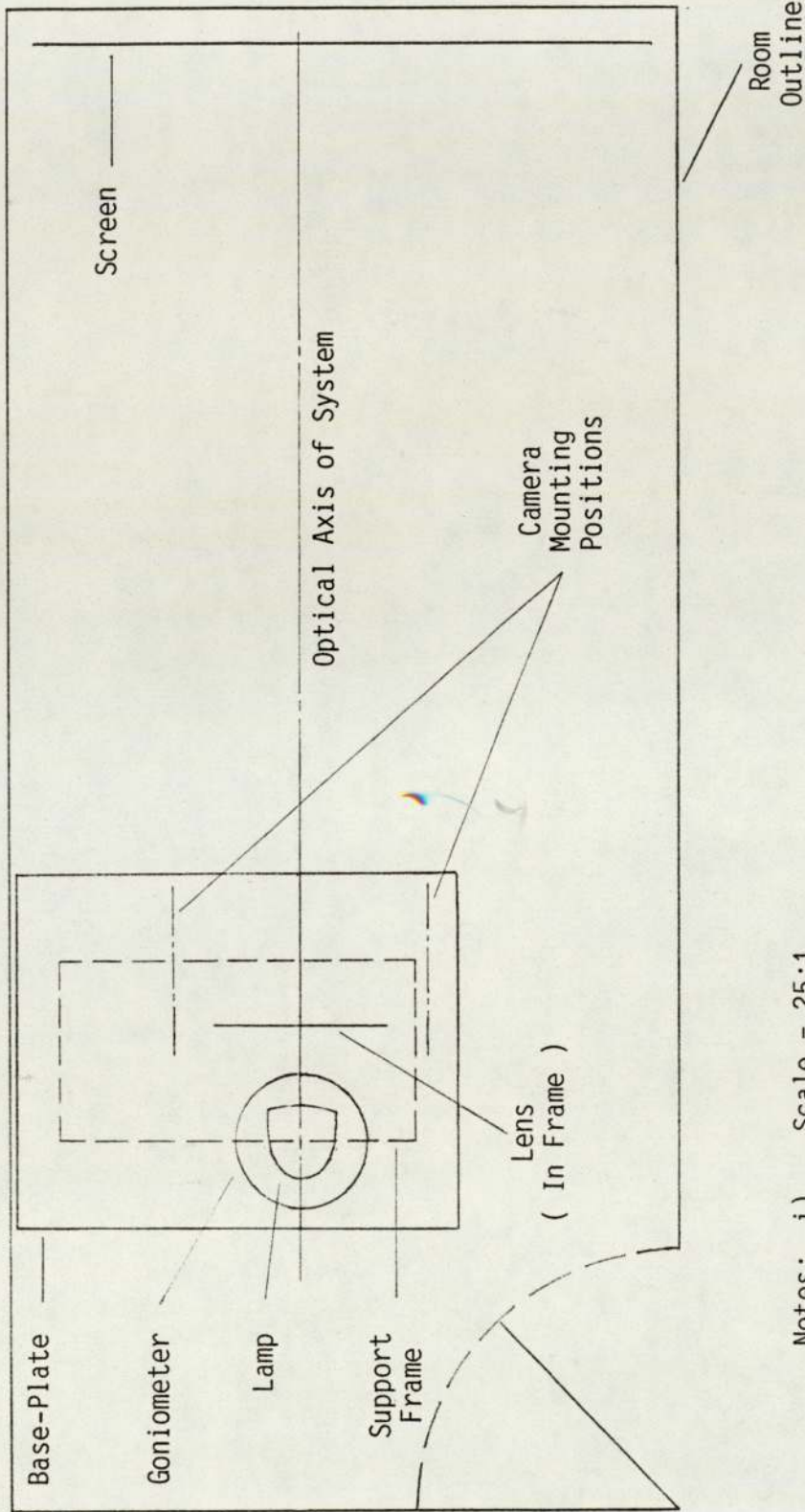
The correct operation of a video photometry system relies on the components of the front-end being accurately located with respect to each other and the methods of mechanically supporting the components have to be carefully considered. Since the goniometer, condensing lens and camera were to be positioned relatively close to each other, it was decided to mount them on a common base-plate. Two methods of maintaining the position of this plate relative to the screen were considered:

- a) Mounting the base-plate and the screen to a large frame system.
- b) Mounting the base-plate on a suitable stand and the screen to the wall of the room.

The second method was chosen because it would be simpler to construct, have a better appearance and provide easier access to the components of the system.

The following requirements were formulated for the screen mounting system:

- a) It should accurately locate and rigidly support the screen in



- Notes:
- i) Scale = 25:1
 - ii) Size of Room = 5.14 m x 2.29 m
 - iii) Height of Optical Axis from Floor = 1.18 m
 - iv) For Reduced Length Photometer Details see Configuration 4, Chapter 13

Fig. 15.1c Proposed Video Photometry System - Outline Layout of Front-End

relation to the base-plate.

- b) It should allow the screen to be easily changed; it may be necessary to experiment with screens of different surface finish or prepare a special screen for aligning the cameras.
- c) It should provide a gap of at least 80 mm between the wall and the screen for mounting a conventional photodetector, which may be necessary for calibrating the system.

The screen design used is described in section 15.4.

It has been assumed so far that the parts of the screen imaged by the two cameras do not overlap. It was felt that in practice, however, it may be more satisfactory to arrange for these two areas to overlap slightly; the E_{FSCP} data for the overlapping regions would be produced by taking an average of the values from each camera, thereby tending to reduce any remaining errors. The desirability of this was to be assessed by practical work after the basic system had been implemented.

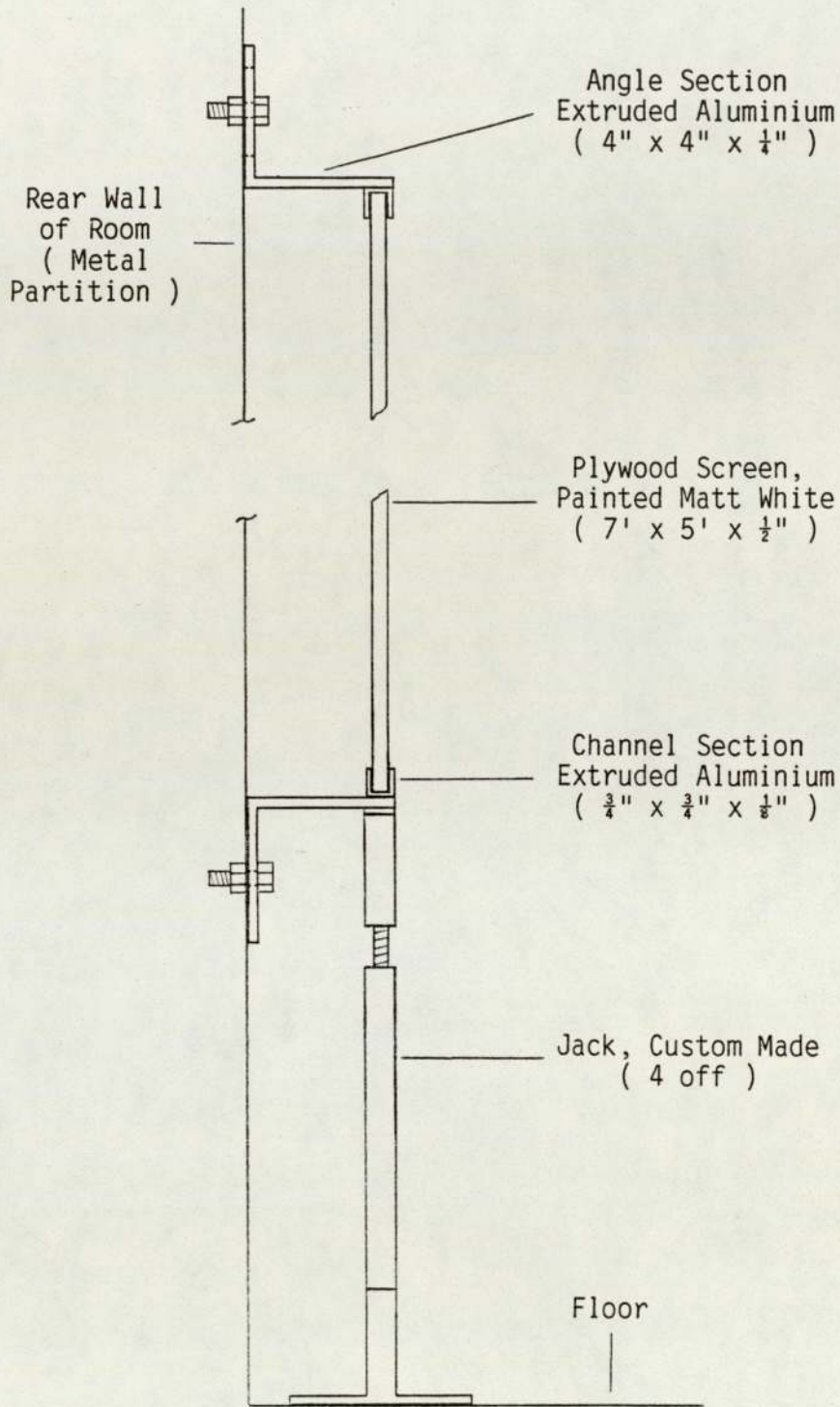
The camera requirements are described in section 15.6.1.

15.4 System Construction

Despite the fact that a suitable camera for use with the proposed system had not been found when the work described in this Chapter was being carried out, it was decided to construct as much of

the front-end as possible to save time later on. As mentioned in section 15.2, the 'General Testing Room' of the E&D darkroom was made available for this project by re-locating the equipment previously used there. The work which was carried out is outlined below; the Prototype department made the mechanical components and carried out the machining work, to the author's specifications.

- a) An existing manual goniometer was available for the system; modifications were made to enable large modern lamps to be mounted.
- b) A set of guides for mounting the goniometer on were produced; these enable the goniometer to be moved sideways to bring either pocket of a twin-pocket lamp onto the optical axis of the reduced-length photometer, whilst maintaining the correct distance from the lens.
- c) A 0.5 m diameter, 4 m focal length lens (with anti-reflection coating) was bought-in from Optical Surfaces, Surrey; the lens parameters are those used in reduced-length photometer configurations 2 and 4 in Chapter 13.
- d) A frame for mounting the above lens was produced.
- e) A 5' x 4' cast aluminium plate was bought in and drilled with a 2 dimensional array of holes. A support frame for the plate was made from an unused steel table.
- f) A screen and support system which met the requirements given in



- Notes: i) The top and bottom supports are bolted to the rear wall. The top support has elongated holes which allow it to slide up for easy removal of the screen. The bottom support remains in a fixed position.
- ii) Scale = 5:1.
- iii) Centre of screen is 1.18 m from floor.

Fig. 15.1d Proposed Video Photometry System - Screen and Supports

the previous section was produced; the basic design is shown in Fig. 15.1d. The screen consisted of a 7' x 5' sheet of plywood and was painted matt white.

15.5 The Image Processing System

15.5.1 Introduction

The main design considerations described in section 11.6 are now discussed for the proposed prototype system.

a) The Method of Digitizing the Camera's Video Signal

It was intended to use multiple range digitization method (a) for the reasons given in section 11.2.3. It was not possible to produce a firm specification for the frame-grabber, however, since it was not known which camera would be used. Provision was to be made for digital filtering to reduce noise.

b) SIA Size

The proposed SIA size, based on the use of the Fairchild cameras, was 512 x 256; this is a convenient size for storing in the frame-store. The use of different cameras, however, could produce other SIA sizes.

c & d) Frame-Store Utilization and Method of Representing the SIA Values

It was hoped to use method (a) of storing the SIA element values, since it is the most elegant and minimises the complexity of the system design and processing software. The use of one of the other methods was not ruled out, however.

The choice of storage method determines the size of the frame store area required to hold two 512 x 256 SIA's. It was calculated that a minimum TPA size (see section 11.6.3) of 512 x 512 would be required for efficient SIA generation and processing.

The total frame store sizes required for the three storage methods are:

Method (a): 1024 x 512 x 16 (TPA = 512 x 512 x 16)

Method (b): 1024 x 512 x 12 (TPA = 512 x 512 x 12)

Method (c): 3 x (512 x 512 x 8) (TPA = 512 x 512 x 8)

The above sizes were essentially the minimum requirements, since, as stated previously, an SIA size other than 512 x 256 could be used. It was therefore highly desirable to select a system which allows memory sizes larger than those above to be installed.

e) Software

It was hoped to use a system in which an extensive set of

low-level routines was available.

The main requirements for the image processing system were as follows:

- a) The equipment should be designed and manufactured in Britain because of the need for detailed technical liaison with the manufacturers and custom modification of the equipment.
- b) The supplier should be able to supply a complete system. (Buying separate modules from different manufacturers provides the opportunity to custom-build a system and reduce the capital expenditure but requires a considerable amount of work in designing and building interfaces, putting together racks, wiring harnesses etc. which would be very time consuming.)
- c) The system should be modular and flexible to allow for modification and future upgrading.
- d) The micro/mini-computer used as the processing element should be capable of being operated as a stand-alone computer and running a conventional operating system.

In particular, it should be possible to:

- i) Use the system to develop the custom software required to carry out the operations described in section 15.2.
- ii) Run a standard communications software package for

linking the system to the Group Computer. No firm decisions could be made regarding the method of effecting this link, since there were many uncertainties relating to the planned extension of the communications network between the Cannock and Shirley sites. It was assumed at this stage that a relatively simple file transfer protocol, such as IBM 2780 or 3780 emulation (72) would be used.

- e) The frame-store should allow SIA's to be stored by one of the methods described in section 11.6 and meet the corresponding minimum size requirements given earlier in this section; method (a) is the preferred choice. It is also highly desirable that larger memory sizes can be configured if desired.
- f) The system should enable video rate digital filtering to be carried out if required to reduce camera noise.
- g) The manufacturers should be prepared to carry out custom modifications to the frame-grabber, the specifications for which were to be produced as the project progressed.
- h) The system should allow displayed images to be annotated by means of a graphics overlay.
- i) Low level software routines should be available to aid the development of the custom software required to implement the processing operations.

15.5.2 Evaluation of Commercially Available Image Processing Systems

Selecting image processing equipment is not a straightforward task because of the following factors:

- a) There is a wide variety of equipment available, ranging from board-level modules for use with custom built systems to fully integrated image processing systems. New items are continually being introduced and the typical price/performance ratio is constantly changing.

- b) The use of stand-alone image processing equipment in industry is a relatively recent development and there are no established guidelines for choosing the type of equipment required. First-time buyers will often not know what features they should be looking for and will only discover the drawbacks of equipment after they have bought and used it.

The task was particularly complex for the video photometry project because:

- a) The basic video photometry principles had not been tried in practice.

- b) Current image processing systems are not ideally suited to the video photometry application. As explained previously, the main problems are:

- i) Current image processing systems are designed for use with conventional video cameras and do not satisfy the ideal video signal sampling requirements given in section 8.2.1.
- ii) Current image processing systems use 8 bit (or lower resolution) analogue to digital converters and, in many cases, 8 bit frame-stores; a higher resolution is required for headlamp photometry.
- iii) The operations to be implemented require custom-written software.

Information on many different image processing systems, hardware modules and software packages had been gathered and studied by the author since the start of the project; these are listed in Appendix F. In addition, at the author's request, the Company subscribed to a SIRA group-sponsored project whose aims were to provide information on how to select image processing equipment and on the range of equipment available. Unfortunately, however, this project did not prove as helpful as expected, since the final report (73) was not issued until June 1984, eighteen months after the date of completion envisaged at the start of the project.

Three of the systems studied were shortlisted and detailed discussions were held with the manufacturers. A comprehensive document (74) describing the proposed video photometry system and the image processing system requirements was prepared by the author and supplied to the manufacturers.

The three systems were:

- i) Gresham - Lion 'Supervisor 214' ; see references (75-76)
- ii) Microconsultants 'Intellect' Systems ; see references (77-79)
- iii) Gems Ltd 'Gems System 33' ; see references (80-82)

All three systems use 8 bit frame-grabbers and are designed for use with conventional video cameras.

Each of these systems is now discussed with reference to the requirements given in section 15.5.1; in all cases it is assumed that the reader is familiar with the basic architectures of the systems, as described in the above references.

- i) Gresham-Lion 'Supervisor 214'.

The system satisfies requirements a, b, c, d, h and i. The other requirements are discussed below:

- e) The frame-store is organised as bit planes, each of 1024 x 512 pixels, enabling a memory of up to 32 bits deep to be configured. However, the maximum size word which can be transferred between the image memory and the computer is 12 bits; see reference (76). Consequently, methods (b) & (c), but not the preferred method (a), can be used for storing SIA's.
- f) There is no provision for video rate digital filtering.

g) The manufacturers were not prepared to carry out custom modifications to the frame-grabber.

ii) Microconsultants 'Intellect' Systems

Microconsultants produce two Intellect systems; the 100, a single frame-store system, and the 200, a more sophisticated multi-frame-store system.

Both systems satisfy requirements a, b, d and i. The other requirements are discussed below.

c) The 100 is a low-cost system which does not have much potential for expansion; the frame-store size is $512 \times 512 \times 8$ and cannot be increased. The 200 system has more potential for expansion; one feature of this system is that hardware processing modules are available to enable operations such as Fourier Transforms to be carried out at much higher speeds than are possible when using the computer.

e) The frame-store in the 100 system is not sufficiently large for the proposed video photometer. Up to 12 frame-stores of $512 \times 512 \times 8$ can be accommodated in the 200 system; all possible configurations are limited to 8 bits depths, however. Thus only SIA storage method (c) could be used.

f) Both the 100 and 200 systems have a recursive video

processor, for carrying out noise reduction, as standard; it only produces 8 bit results, however.

- g) The manufacturers were not prepared to carry out custom modifications to the frame-grabber.
- h) No separate graphics overlay planes are available in these systems; graphics overlays can be produced by using one or more bits of the frame-store, however. Creating overlays in this way does, of course, reduce the number of bits available for storing the image data and the method is not satisfactory for the proposed application.

It should also be noted that both systems are designed to display rectangular pixels of a fixed 4:3 aspect ratio and the square pixel format of the proposed camera would create problems.

iii) Gems Ltd 'Gems System 33'

This system basically satisfies all of the requirements; c, e, f, g and h are discussed below:

- c) The Gems system is particularly flexible; all of the major application dependant parameters are controlled by software programmable registers. This includes the system clocking rate, which can be reduced to accommodate slow scan inputs.

- e) Up to 8 frame-store modules, each containing an image memory of size 1024 x 1024 x 8, can be accommodated. The modules can be configured in a variety of ways; it is possible to configure a 1024 x 1024 x 16 memory, which enables the preferred method of SIA storage (method (a)) to be used.

- f) A real-time video processor is available for digital filtering; this outputs a 16 bit result and can be used at TV or slow-scan input rates.

- g) The manufacturers are prepared to carry out custom modifications for customers with special requirements and have experience in designing and interfacing non-standard input devices.

- h) Graphics overlays are easily achieved since each memory module contains a 1 bit overlay plane in addition to the 8 bit image memory.

15.5.3 Conclusions

Of the three systems, the 'Gems System 33' was clearly the most suitable as a result of its versatile architecture and the willingness and ability of the manufacturers to carry out custom modifications. This system was therefore chosen to form the basis of the proposed prototype system and a number of technical liaison meetings were held.

It was agreed that the design of the system should be based on

multiple range digitization method (a), for the reasons given in section 11.2; modifications to synchronize the camera and digitization circuitry to produce 1 sample per camera pixel would be required.

15.6 The Camera

15.6.1 Introduction

A camera to be used with the proposed system and multiple range digitization method (a) must have the following basic characteristics:

- a) A spectral response approximately equal to the photopic curve; see section 10.5.1. (A suitable external filter can be used if necessary.)
- b) A level of anti-blooming performance which will allow parts of the sensor to be illuminated at a level of at least four times that required to produce the onset of saturation, without affecting the outputs of the non-saturated parts of the sensor; see sections 10.5.7 and 11.2.2.
- c) A sufficiently high sensitivity to enable a headlamp and a 4 m reduced-length photometer, producing a near screen illuminance equivalent to 12.5 lux at 25 m, to saturate the camera, taking into account any filters used for spectral response modification; see section 10.5.2.
- d) A clearly defined relationship between the sensor geometry and

the video signal output by the camera; see section 10.5.3.

- e) A very high degree of linearity; see section 10.5.5.
- f) Negligible camera flare; see section 10.4.3.

If the above basic requirements are met, then the following areas are to be considered:

- a) Possible mechanisms for varying the E_{FSCP} value at which V_{SEPSAT} is produced; see section 11.2.2.
- b) The magnitudes of the dark signal and responsivity variations from pixel to pixel (see sections 10.5.4 and 10.5.5); these determine whether or not dark signal and responsivity correction processing is necessary (see section 11.3).
- c) The magnitude of the noise component of the video signal; this determines whether or not digital filtering is required and over how many frames; see sections 10.5.6 and 11.2. (Ideally the camera will have a peak to peak noise level of less than $V_{SEPSAT} / 512$ i.e. less than the quantisation error. This is unlikely to be the case, however.)
- d) The number of sensor blemishes; see sections 10.5.9 and 11.4.

At the time that this work was being carried out, cameras with some degree of anti-blooming capability were available from three manufacturers: General Electric, Raticon and I2S. The models which

were considered the most promising for use with the proposed video photometry system, based on a Gems image processing system and multiple range digitization method (a), are briefly described below:

a) General Electric (GE) TN2506

This camera is designed and manufactured in America and sold in the UK by Adrian March Electronics of Bordon, Hants; see references (83, 84). It uses a GE charge injection device (CID) with 290 x 416 rectangular pixels; the non-square format means that a screen pixel format other than the convenient size of 25 mm x 25 mm (at 25 m) would have to be used.

The camera has an 'extended integration' mode of operation (84) which would theoretically provide a convenient way of varying the E_{FSCP} value at which V_{SEPSAT} is produced, which is necessary for multiple range digitization method (a).

b) Reticon MC9256

This camera is also designed and manufactured in America and sold in the UK via their own sales office, in Wokingham, Berkshire; see references (85, 86). It uses a Reticon solid-state photodiode array sensor, type number RA256 x 256A (87), having 256 x 256 square pixels, which is convenient for this application.

It has an external clock input facility which would

theoretically provide a convenient way of varying the E_{FSCP} value at which V_{SEPSAT} is produced. The permissible range of input frequencies is only 1.9 to 8 MHz, however.

c) Imagerie Industrie Systeme (I2S) IS200

This camera is designed and manufactured in France and sold in the UK by G V Planer of Sunbury on Thames, Middlesex and Industrial Monitoring Equipment (IME), of Rickmansworth, Herts; see reference (88). It uses a Thomson-CSF anti-blooming CCD sensor, type number TH7852 (89).

This sensor is different to those considered previously in that the positions of the sensor pixels do not remain fixed; the positions of the charge collection zones are shifted by half a pixel to produce different information for the even and odd fields of the interlaced video signal. Thus, although the sensor produces a video signal having 288 lines, there are in fact only 144 rows of sensor pixels, each containing 208 rectangular photosensitive elements.

This interlacing system is an unnecessary complication for the video photometry application and means that the screen pixels would effectively overlap.

It would, of course, be possible to use only one field of the signal; in this case, the sensor model described in section 7.4 would still apply (except for the fact that a small area of each pixel is not photosensitive). Using only one field of the

signal does mean, however, that the number of rows of screen pixels is limited to 144.

The camera has a 'single-shot' mode (88), which would theoretically produce a convenient way of varying the E_{FSCP} value at which V_{SEPSAT} is produced.

Purchasing these cameras solely for evaluation purposes could not be justified because of their high cost. Consequently, the performance of each camera was assessed by studying the manufacturer's literature and by carrying out a few practical measurements on the UK distributor's demonstration model; comprehensive practical tests were not possible because each camera was only available for a few hours. The tests were carried out in conjunction with Gems Ltd, on their premises at Cambridge, since they had better test facilities and previous experience in evaluating cameras.

The practical tests concentrated on the following three aspects of performance: sensitivity, anti-blooming capability and linearity. Measurements of the video output signal magnitude were made using an oscilloscope. The basic test procedures were as follows:

a) Sensitivity

The camera sensitivity was measured by viewing a white screen illuminated by a headlamp with a known maximum intensity. The camera lens aperture required to cause the onset of saturation when using a headlamp producing a 4 m reduced-length photometer near screen illuminance equivalent to 12.5 lux at 25 m, was

calculated.

b) Anti-Blooming Capability

This was assessed by removing the camera lens and covering part of the sensor window with opaque tape. The remaining part of the sensor was illuminated with various levels of illuminance beyond that required to cause the onset of saturation and the effects on the video output from the covered part of the sensor noted.

c) Linearity and Pixel Responsivity Variations

These characteristics were measured by removing the camera lens and directly illuminating the sensor. Neutral density filters were used to provide different levels of illuminance.

The characteristics of these three cameras, as assessed from the manufacturers' literature and the tests outlined above are discussed in sections 15.6.2 to 15.6.4 in relation to camera requirements (a) to (e) given earlier in this section; it was not possible to determine whether or not requirement (f), negligible camera flare, could be met since no information was available from the manufacturers and meaningful practical tests were not possible with the limited time and resources available. It is assumed in sections 15.6.2 to 15.6.4 that the reader has a basic familiarity with the manufacturers' literature referenced above.

15.6.2 General Electric TN2506

Owing to the fact that a demonstration model of this camera was not available in the UK, the practical tests were carried out with a TN2505, which is a similar model but is designed for use with the American 525 line video signal format rather than the European 625 line format.

- a) The typical spectral response characteristics of the devices used in the TN2505 and the TN2506 are given in reference (84); the response extends from approximately 400 nm to 1100 nm and an infra-red cut-off filter would be required. A near photopic response may be difficult to achieve since none of the readily available filters has the required response characteristics; in addition there are the general problems described in section 10.5.1. No details of the variation in characteristics from sample to sample are given in the manufacturers's literature.
- b) The manufacturers state that these cameras have 'an extremely good anti-blooming performance' (84) but provide no quantitative data. The practical measurements showed that illuminating part of the sensor at a level of four times that required to produce the onset of saturation affected the outputs of approximately 4 adjacent pixels. This level of anti-blooming performance would probably be acceptable.
- c) Reference (84) states that full output is obtained at 0.8 footcandles (8.6 lux) faceplate illuminance, with the 'gain boost' facility not used. Setting E_{SEPMAX} in equation 10.3 to

8.6 lux, and assuming $m = 0.1384$, $\rho = 0.9$, $T_R = 0.9$, $T_C = 0.9$ and $E_{FSCPMAX} = 12.5$ lux, gives a required camera lens aperture of approximately $f/4$. The practical tests gave approximately the same result. This is a convenient value and, assuming a maximum lens aperture of, say, $f/2$, means that the proposed system should give about four times the minimum illuminance required. However, this does not take into account the infra-red cut-off filter needed to meet requirement (a), which could reduce the overall sensitivity by more than this factor and therefore cause sensitivity problems. It would be possible, however; to increase the camera's sensitivity if necessary, either by using the 'gain-boost' facility (which would increase noise) or by operating it in the 'extended integration mode' (which would increase dark current); see reference (84).

- d) The information about the sensor geometry/video signal relationship given in the user's manual (84) is incomplete and unclear. For example, taking the values for the TN2506 model in the 'vertical interval timing' diagram (Fig. 13 in reference (84)), it would appear that there are $(286 + 0.5 + 0.5) = 287$ active lines in the odd field and 288 active lines in the even field; it is not stated how these are derived from the 290 rows of pixels in the sensor. Similarly, in the 'horizontal interval timing' diagram (Fig. 14 in reference (84)), it would appear that there are 400 'active panels' in a line, the first representing a 'half pixel'; the meaning of 'half pixel' and an explanation of how the 400 'active panels' are derived from the 416 columns of the sensor are not given.

e) No quantitative information on sensor linearity is given in the manufacturers literature. The practical tests showed that the TN2505 demonstration model was very non-linear; reducing the illuminance from that required to cause the onset of saturation to 50% of this value reduced the magnitude of the output signal to approximately 10% of V_{SEPSAT} . Moreover, there was a severe pixel responsivity variation problem. With uniform sensor illuminance, the magnitude of the video signal decreased with position along each line; with the sensor illuminated so that the first pixel of each line produced an output of V_{SEPSAT} , the output of the last pixel was only about 75% V_{SEPSAT} . Furthermore, the way in which the signal decreased varied with alternate lines. This level of variation was clearly unacceptable. In addition, the video signal lens was also found to have a significant noise content, some of it of a periodic nature, possibly originating from the dc to dc converter used in the camera.

The camera suppliers were asked various questions relating to the measured performance and the problems experienced, which were possibly being caused by an internal fault or incorrect adjustment. No satisfactory answers were received, however, leaving the author (and the staff of Gems Ltd) with little confidence in the product or the suppliers.

15.6.3 Reticon MC9256

A demonstration model of this camera was not available in the UK. Consequently, the tests were carried out with an MC9128, which is

a similar camera, but has a 128 x 128 pixel sensor, model number RA128x128A.

a) The typical spectral response of the RA256x256A sensor is given in reference (87). The response extends from approximately 400 nm to approximately 1100 nm and an infra-red cut-off filter would be required. Again, a near-photopic response may be a difficult to achieve in practice.

b) The RA128x128A and RA256x256A sensors are not specifically designed as anti-blooming sensors, but the blooming effect is generally less severe in solid state photodiode arrays than in CCD's because the sensor elements are separate and distinct PN junctions; however, since there are common video lines for each column of diodes, a vertical blooming effect is observed caused by excess charge collected on the column video line.

The practical tests on the MC9128 showed that the magnitude of the effect was too high for multiple range digitization method (a) to be used successfully. Furthermore, reference (86) shows that blooming is more severe with the RA256x256A than with the RA128x128A.

c) Since the camera could not be used with multiple range digitization method (a), requirement (c) is not relevant. The practical tests showed, however, that the MC9256, whose sensor is only 0.4 times as sensitive as that in the MC9128, would probably not have sufficient sensitivity, even at its slowest clocking rate, when used with a suitable infra-red cut-off

filter.

- d) Reference (86) shows that the video signal presents the sensor pixel outputs in a relatively straightforward non-interlaced format; a detailed practical study of the signal was not possible, however, because of the limited time that the camera was available.

- e) Reference (86) shows that the RA128x128A and RA256x256A sensors have a linear exposure/output voltage relationship. It is stated, however, that this relationship is dependent on the proper electrode potentials being applied to the sensor, and that improper potentials can cause substantial non-linearity. The practical measurements on the MC9128 demonstration model showed that it had a high degree of linearity.

15.6.4 I2S IS200

The camera tested was a demonstration model belonging to IME.

- a) The typical spectral response of the TH7852 sensor is given in reference (89). The response extends from approximately 400 nm to 1100 nm and an infra-red cut-off filter would be required. Again, a near photopic response may be difficult to achieve in practice.

- b) The sensor appears to offer a high degree of anti-blooming capability; see reference (89).

However, carrying out the test described in section 15.6.1 on the demonstration model resulted in the output video signal derived from the non-illuminated part of the sensor increasing as the level of illuminance on the other part of the sensor increased beyond that required for saturation; a four times overload caused an increase of about 10-15% in the magnitude of the signal from the non-illuminated area, which is too high to allow multiple range digitization method (a) to be used successfully.

- c) The sensitivity information given in reference (89) is somewhat ambiguous and no detailed practical tests were carried out through lack of time.
- d) The sensor geometry/video signal relationship is complex because of the interlacing mechanism described in section 15.6.1. The detailed information which would be necessary to determine the positions of the screen pixels when using this camera in the proposed type of system is not given in the manufacturers literature.
- e) Reference (89) states that the sensor's gamma value is 1, although no tolerance is given. The practical tests on the IS200 demonstration model showed that it had a high degree of linearity.

IME were informed of the disappointing anti-blooming capability exhibited by the demonstration model and more information about this and other aspects of the camera's performance, and the internal

circuitry of the camera, were requested.

They replied that the observed increase in output signal voltage derived from the non-illuminated areas of the sensor was not caused by the sensor itself, but was a consequence of the camera's video board. This was of little consolation, however, since the end result was the same: an insufficient overall level of anti-blooming performance to enable multiple range digitization method (a) to be used successfully. IME were unable to supply much of the other information requested because of the fact that the camera had largely been developed for military applications and many of the circuit details were of a confidential nature. This lack of detailed information would make it very difficult to use the camera for the proposed type of system.

IME stated that the design of the video board had been improved in the IS400 camera (90). This camera has a sensor with 288 rows of sensor pixels, each consisting of 384 pixels, and produces a video signal having 576 lines, by means of the same interlacing technique used in the IS200. A detailed study of this camera's characteristics was not carried out, however, because of the following reasons:

- a) It was not available with the 'single shot' facility, without which there would be no convenient way of altering the E_{FSCP} value at which V_{SEPSAT} occurred.
- b) Detailed technical information would again not be available from the manufacturers.

- c) The cost of this camera, with an anti-blooming version of the sensor, was over £4000. Since the proposed video photometry system requires two of these, the cost of the front-end components would be higher than for the proposed 'high-speed photometer', which also offers many technical advantages; see Chapters 16 and 17.

15.6.5 Conclusions

At the end of the camera evaluation work, it was concluded that it would not be possible to implement a video photometry system using one of these cameras and multiple range digitization method (a) because:

- a) None of the cameras had the required characteristics.
- b) The documentation and the level of technical support available from the suppliers, particularly in the case of the General Electric and I2S models, was not sufficiently good for this application, where very detailed information about the performance and internal circuitry of the camera is necessary in order to be able to interface it to the image processing system and make accurate quantitative photometric measurements.

15.7 Conclusions

The conclusions reached from the work described in this Chapter were:

- a) The Gems image processing system, unlike the others examined, was suitable as the basis of the proposed type of video photometry system, given the fundamental limitations described in Chapter 11.
- b) The available cameras did not have the required characteristics to enable their use with multiple range digitization method (a).
- c) The level of technical support available from the camera suppliers was not considered sufficiently good for the proposed application.

Consequently, an alternative approach to high-speed photometry, also based on the use of an image processing system, was suggested by the author; this is described in the next Chapter.

16. AN ALTERNATIVE APPROACH TO HIGH-SPEED PHOTOMETRY

16.1 Overall Description

This approach, which was briefly described in Chapter 5, is based on the type of system shown in Fig. 16.1.

The system, which will be referred to as a 'high-speed photometer', uses a one-dimensional array of discrete photodiodes mounted vertically in the centre of the test screen. These photodiodes are connected, via transimpedance amplifiers and a custom interface, to a micro-computer and image processing system, to enable their outputs to be digitized and stored as a one-dimensional array of data in a specified column of the frame-store memory. The lamp is mounted on a motorised rotary table, which is also interfaced to the micro-computer and image processing system, and which enables the beam to be scanned over the photodiode array. Data acquisition software controls the scanning of the beam and the digitization and storage of the photodiode outputs and produces a two-dimensional array of data in the frame-store. Various decalibration operations are performed on the acquired data in order to produce a second array, which will again be referred to as a Screen Illuminance Array (SIA); in this system the SIA will represent the illuminance values which would be produced by the lamp at a specified two-dimensional array of points on a spherical measurement surface at a specified distance from the lamp (see section 16.3).

Such a system would be capable of producing an SIA for a field

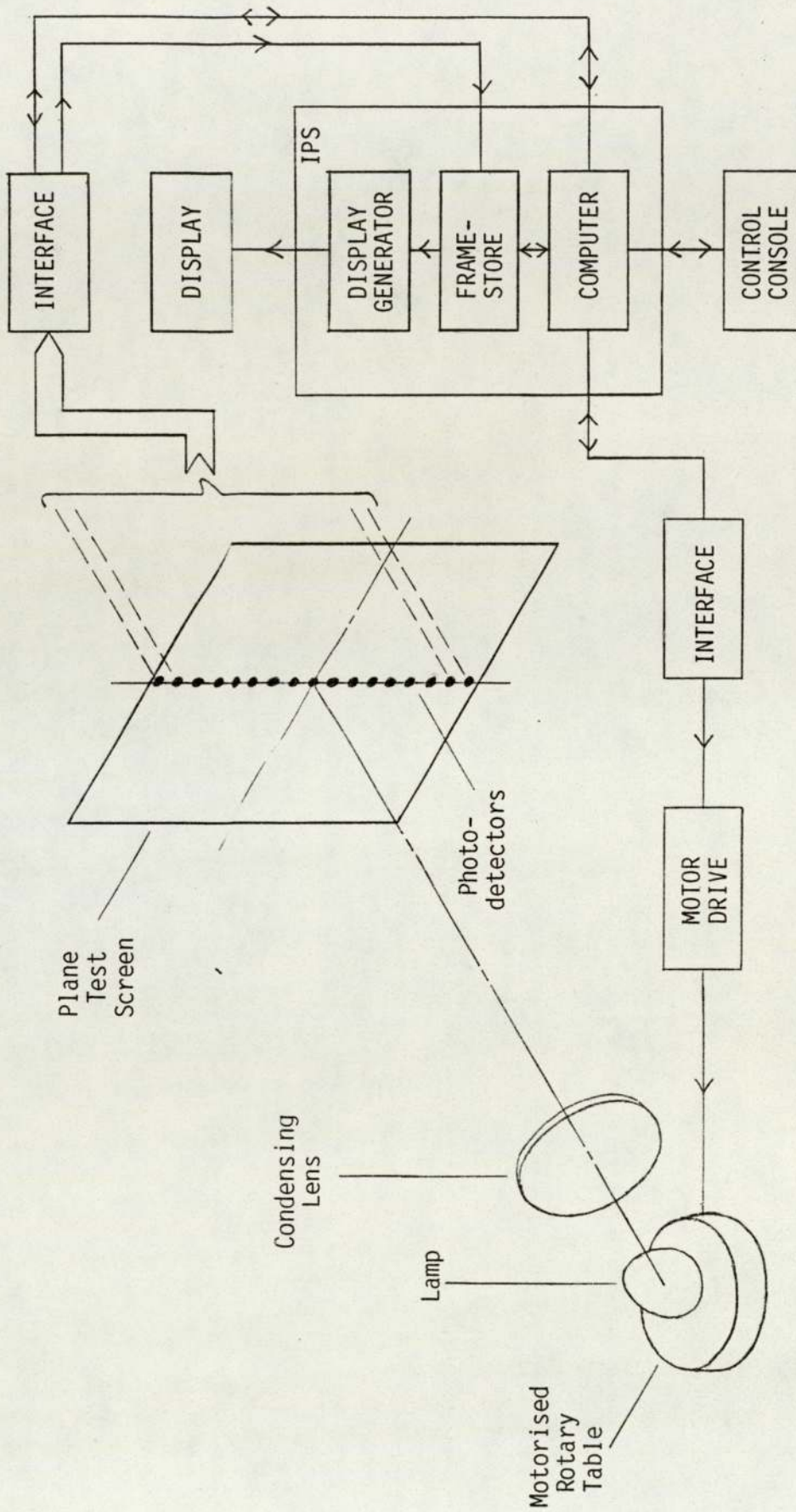


Fig. 16.1 Basic Concept of the 'High-Speed Photometer'

of view of, say, $\pm 15^\circ$ H, $\pm 8^\circ$ V in approximately ten seconds. This is a significant improvement over the existing Automatic Photometer, which takes approximately ten minutes to acquire data over the same field of view. Thus the time taken to acquire data for both the dipped and main beams of a headlamp would be reduced from about twenty minutes to about twenty seconds. This SIA acquisition time is unlikely to be much longer than, and may even be shorter than, the corresponding time for a practical implementation of the proposed video photometry system, when the following factors are taken into account:

- a) The need to digitize data from two cameras, probably at several different sensitivity settings and reduced camera clocking rates.
- b) The probable need to:
 - i) Average over several frames to reduce noise
 - ii) Carry out processing to remove the effects of sensor dark current, responsivity variations and blemishes.

Like a video photometer, a high-speed photometer will require a custom interface to the micro-computer/image processing system. This interface will be costly to develop because its operation will be very different from that of a conventional frame-grabber. However, high resolution digital data can more easily be obtained from discrete photodiodes than from a video camera, because:

- a) A much slower conversion rate can be used

A conversion time of between 10 and 100 μ s per diode would be a reasonable design aim.

- b) The noise level is lower

The noise produced by a photodiode and transimpedance amplifier is significantly lower than that produced by a video camera.

Furthermore, the problems relating to the lack of available camera information would not arise.

16.2 Comparison With The Video Photometry Approach

Compared to the video photometry approach, the technique proposed here is better suited to the task of acquiring accurate quantitative photometric data, for the following reasons:

- a) Unlike a video photometer, a high-speed photometer can easily be designed to have a measurement surface which is effectively spherical, and hence produce readings which are directly equivalent to those of a conventional goniophotometer, as explained in section 16.3.
- b) The RLP imaging performance is less critical; only the performance in the vertical line of the photodiodes will affect

the measurements made. As shown in Chapter 13, an RLP's vertical performance is better than its horizontal performance because the effective lamp height is generally smaller than the effective lamp width and the range of off-axis angles of interest is smaller.

- c) The photodetectors directly measure beam illuminance; the screen characteristics are unimportant and the problems of lens aberrations, camera flare and \cos^4 law image illuminance reduction, which occur with a video camera, do not arise.
- d) With the proposed video photometry system, it could be difficult to obtain (and maintain) the correct relative positions of the two video cameras and the test screen. This problem will not arise with a high-speed photometer; the correct positioning of the photodetectors will be a relatively straight forward operation.
- e) Photodiodes having photopic, or near photopic, spectral response characteristics are readily available.
- f) Unlike solid state sensor arrays, discrete photodiodes cannot produce cross-talk or blooming.
- g) A photodiode and transimpedance amplifier combination having a very high degree of linearity over many decades of incident illuminance, negligible noise and zero dark current can be produced relatively easily. Such a circuit enables the range of illuminance values of interest for all beam types to be

covered in a single range.

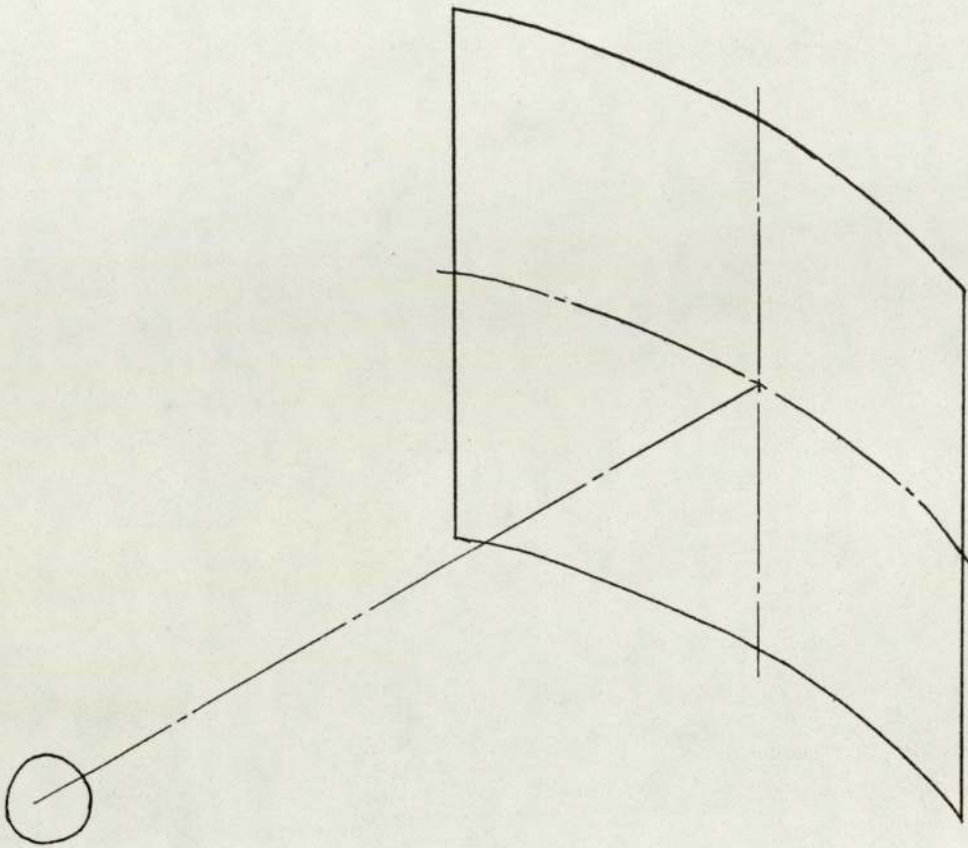
- h) The SIA acquisition procedure will require fewer decalibration operations. Furthermore, those that are necessary will be easier to implement, since the amount of decalibration data to be acquired, stored and manipulated will be much smaller, as a consequence of using a one-dimensional array of photodetectors instead of a two-dimensional array.
- i) The operation of lamp aiming will be easier to carry out. In the high-speed photometer, the output of the photodiode at the centre of the screen (i.e. at the 'HV point') can (in addition to being fed to the image processing system) be displayed on a DVM, to enable the operator to aim a lamp in the same way as with a conventional goniophotometer. In a video photometer, a complete frame of V_{SEP} or $(V_{SEP} - VN)$ data must be obtained to find the illuminance at the HV point, which could take many tens of seconds; see section 11.2.1.
- j) No special mechanism will be required to acquire data over an extended horizontal field of view; the angular movement of the rotary table can simply be increased, via the control software.
- k) The system will have a better long term stability because:
 - i) Changes in the screen characteristics will not affect the measurement accuracy.

- ii) The photodiode amplifier circuitry is much simpler than the sensor amplifier circuitry in a video camera and will be less susceptible to drift of its characteristics.

16.3 The Measurement Surface

The measurement surface produced by the configuration of Fig. 16.1 is shown in Fig. 16.2; it is different from both the plane and spherical measurement surfaces conventionally used as the basis of headlamp performance specification and measurement. However, by multiplying the values of the digitized transimpedance amplifier output voltages by the appropriate correction factors, the data can be made equivalent to that which would have been obtained by using a spherical measurement surface at the full imaging distance. By mounting the photodetectors in the vertical plane and rotating the lamp in the horizontal plane, the resultant spherical co-ordinate system is the same as that produced by a type A goniometer, which gives compatibility with the SAE regulations and the Automatic Photometer.

Using the terminology developed earlier for the video photometer, the array of photodetectors can be considered as a one-dimensional array of near screen pixels on a plane measurement surface; see Fig. 16.3. The flux collection area of each near screen pixel will be smaller than its overall area, because of the fact that the photosensitive area of a photodiode is smaller than its overall size, but this is of little consequence. Assuming a perfect RLP, the far screen pixels will have the same format, with the linear



The use of a horizontal rotary table and a vertical array of photo-detectors on a plane screen produces an effective measurement surface as shown. As described in the text, however, this arrangement can be used to produce data which is equivalent to that obtained by using a type A goniometer.

Fig. 16.2 Measurement Surface for the 'High-Speed Photometer'

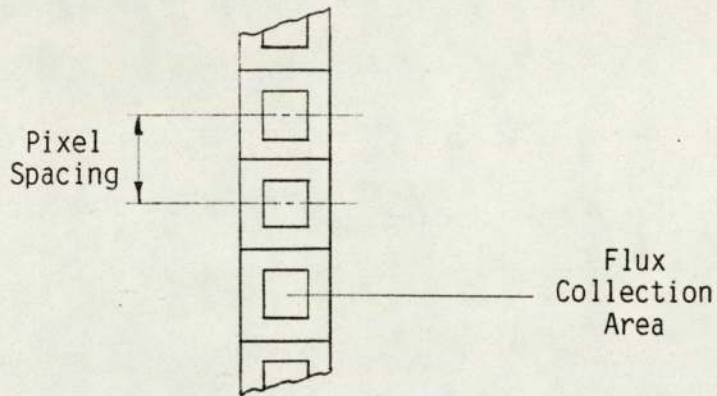


Fig. 16.3 Near Screen Pixel Array for the 'High-Speed Photometer'

dimensions increased in size by a factor of $1/m$. The equivalent far screen illuminance for each near screen pixel will be given by:

$$E_{FSCP} = \frac{m^2 \cdot E_{NSCP}}{T_R} \quad (16.1)$$

The illuminance values which would be obtained using a line of pixels on the zero meridian of a spherical measurement surface at the full imaging distance will be referred to as the $E_{FSCPSMS}$ values.

The relationship between an $E_{FSCPSMS}$ value and the corresponding E_{FSCP} value, obtained by using equation 3.5 with $\alpha = 0$ is:

$$E_{FSCPSMS} = \frac{E_{FSCP}}{\cos^3 \beta} \quad (16.2)$$

Using equations 16.1, 16.3, 4.3 (with $E_{PD} = E_{NSCP}$) and 4.4, gives:

$$E_{FSCPSMS} = \frac{m^2 \cdot (V_{OUT} - V_{OS})}{T_R \cdot \cos^3 \beta \cdot R_{PD} \cdot I} \quad (16.3)$$

The $E_{FSCPSMS}$ values can therefore be obtained from the measured V_{OUT} values; details of the procedure are given in the next section.

16.4 SIA Acquisition Procedure

The proposed SIA acquisition procedure is as follows:

- a) The lamp's beam is scanned across the photodiodes by means of

the rotary table. For each horizontal angle at which data is required, the voltage outputs of the transimpedance amplifiers, the V_{OUT} values, are digitized and stored in the frame-store, by means of the custom interface, the computer and the image processing system; a digitized V_{OUT} value will be represented by V_{OUT}' . The readings will preferably be taken 'on-the-fly', but, if necessary, the table can be stopped at each position for which data is required. Each one-dimensional array of V_{OUT}' values will be stored in successive columns of the frame-store memory, thereby producing a two-dimensional array of V_{OUT}' data.

b) Each column of V_{OUT}' data is now processed as follows:

i) The amplifier V_{OS}' values, which are the digitized V_{OS} values, previously acquired and stored as a one-dimensional array (see below), are subtracted from the corresponding V_{OUT}' values.

(It is simpler to carry out a software correction than to adjust a large number of trimmer resistors.)

ii) The $(V_{OUT}' - V_{OS}')$ values are multiplied by previously acquired factors (see below), stored as a one-dimensional array, representing the $(m^2 / (T_R \cdot \cos^3 \beta \cdot R_{PD} \cdot r))$ value for each photodiode and amplifier.

The two-dimensional array of data produced by this procedure is an SIA representing the $E_{FSCPSMS}$ values. If necessary, a

correction for ambient light can be carried out by means of a similar scheme to that described in Appendix C for a video photometer. (It will be necessary, however, to design the system so that the amount of light from the headlamp reaching the photodetectors by means of reflections from the walls remains negligible as the lamp is rotated.)

The V_{0S} ' values required for the above procedure can be obtained by covering the photodiodes and digitizing the resultant V_{OUT} values.

The scaling factors representing the $(m^2 / (T_R \cdot \cos^3 \beta \cdot R \cdot r))$ values can be obtained as follows:

- a) A lamp whose maximum intensity is accurately known is mounted on the table and positioned such that the central photodetector is in line with the direction of maximum intensity.
- b) The required digital representation of the $E_{FSCPSMS}$ value corresponding to the intensity of the lamp is divided by the actual V_{OUT} ' value obtained from the central photodetector. (The transimpedance amplifier feedback resistor, r , will be chosen so that these quantities have the same nominal value.) This result of this calculation, which should be carried out in floating point form, represents the $(m^2 / (T_R \cdot \cos^3 \beta \cdot R_{PD} \cdot r))$ factor to be used for that photodetector.
- c) The vertical orientation of the lamp is adjusted until one of the adjacent photodetectors is in line with the direction of maximum intensity and step (b) is repeated.

- d) The lamp adjustment, digitization and calculation procedure is repeated for all of the photodetectors to give the required one-dimensional array of factors.

17. THE PROPOSED HIGH-SPEED PHOTOMETRY SYSTEM

17.1 Introduction

It was apparent from the image processing system evaluation work undertaken that it would be possible to implement a high-speed photometer using currently available equipment and that, unlike planning the implementation of a video photometer, it could confidently be predicted in advance that the system would be capable of making accurate measurements over the required range of illuminance values. It was also clear that the Gems system would provide a very good basis for the system.

Consequently, an overall system design was produced, based on the work carried out previously for the proposed video photometry system:

- a) The system was designed in accordance with the photometric data processing scheme described in Chapter 14 and was to be capable of being used as a stand-alone unit or in conjunction with the Group Computer.
- b) The application areas, and the extent to which these were to be covered, remain the same as for the proposed video photometry system; see section 15.2.
- c) The system was to be capable of simultaneously storing 2 (or more) SIA's in the frame-store and carrying out the same six

SIA processing operations as the video photometer; see section 15.2.

- d) It uses a 4 m reduced-length photometer.
- e) It was designed to be constructed in the 'General Testing Room' of the E&D darkroom, and to use most of the mechanical components made for the proposed video photometry system.

17.2 System Description

The system will use a one-dimensional array of 160 photodiodes covering a vertical range of $\pm 8^\circ$, with a resolution of 0.1° . This resolution is not as high as that proposed for the prototype video photometry system, but is the same as the maximum resolution available with the Automatic Photometer, which has proved satisfactory. It is proposed to take horizontal samples every 0.1° giving SIA sizes of 300×160 for a $\pm 15^\circ$ horizontal scan and 600×160 for a $\pm 30^\circ$ scan. This horizontal resolution is twice as high as available with the Automatic Photometer. The proposed scanning speed is 4° per second; the acquisition of the V_{OUT} values (see Chapter 16) for a $\pm 15^\circ$ horizontal scan will take 7.5 seconds. (The total SIA acquisition time will be longer, because of the need to carry out the offset and gain corrections described in section 16.4.)

RLP configuration 2 described in section 13.2 will be used; the vertical performance of this configuration satisfies the criterion given in section 12.1 to beyond 8° off-axis. (With the proposed video

photometry system, it was thought that it would be necessary to improve the off-axis performance of the RLP; this would be achieved at the expense of the paraxial performance. This trade-off should not be necessary with the proposed high-speed photometer, since the off-axis performance is not so critical; see section 16.2.)

The system will be designed to measure an illuminance range of 0-400 lux at 25 m.

The following work was carried out:

- a) A more detailed system design was produced in conjunction with Gems Ltd.

The proposed system, shown in Fig. 17.1, essentially consists of the following:

- i) A Gems System 33 and auxiliary hardware; see section 17.3
- ii) A microcomputer and peripherals; see section 17.3
- iii) A photodiode sub-system; see section 17.4
- iv) An analogue input sub-system for interfacing items (i) and (ii) with item (iii); see section 17.5
- v) A rotary table sub-system; see section 17.6
- vi) System software; see section 17.7

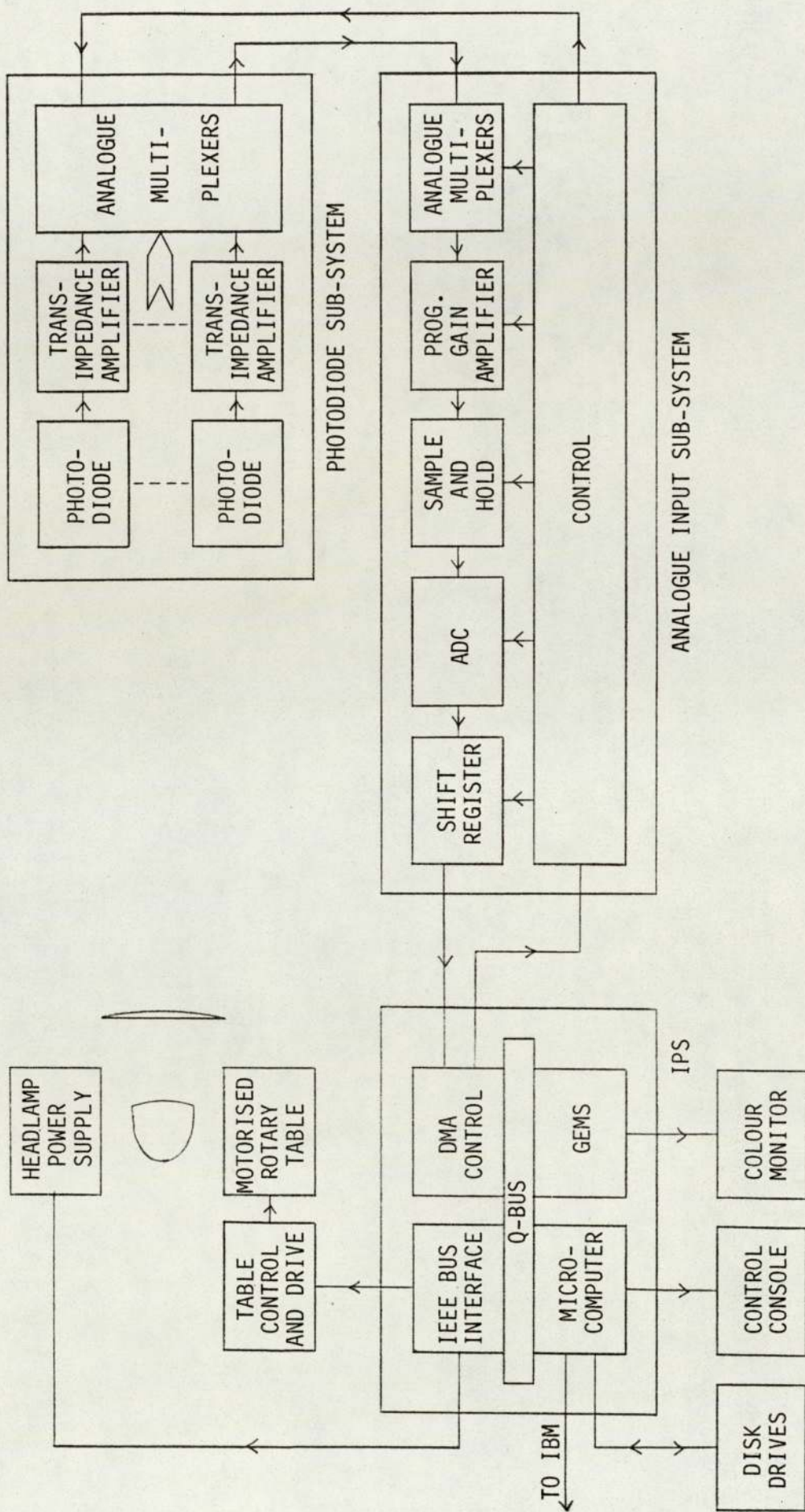


Fig. 17.1 The 'High-Speed Photometer' - Functional Block Diagram

- vii) Ancillary hardware; see section 17.8

- b) A suitable photodiode was chosen; see section 17.4

- c) Rotary tables and associated electronic control and drive modules from various suppliers were assessed. The Ealing-Beck 'System 5' was found to be the most suitable; see section 17.6.

17.3 The Gems and the Microcomputer

The Gems system will essentially consist of the following:

- a) One Gemsystem 33 controller. (This will be built to enable TV input and video processor modules to be added at a later date if required, to carry out a practical investigation of the video photometry concepts; see Chapter 18.)

- b) Two 1024 x 1024 x (8+1) memory modules

- c) Three TV output modules

- d) A fixed oscillator module

- e) A Gems Q-bus interface

- f) A VDU

- g) A colour monitor

- h) A cabinet to house the Gems and the microcomputer

The microcomputer will be a DEC Micro-PDP11 (91) or an equivalent Arrow system.

17.4 The Photodiode Sub-System

This will essentially consist of the following:

- a) A linear array of 160 discrete photodiodes mounted vertically on the test screen. The mounting positions, measured in metres from the optical axis, are given by the expression $(0.1393 \times 25 \times \tan \beta)$, where $\beta = -8^\circ$ to $+8^\circ$, in 0.1° steps.
- b) Several additional photodiodes mounted at the commonly used test points to enable the readings for these points to be acquired without the need for lamp movement.
- c) A set of printed circuit boards containing:
 - i) The transimpedance amplifiers for the photodiodes. These will be designed to produce a full scale output corresponding to 400 lux at 25 m.
 - ii) A set of analogue multiplexers to reduce the number of connections required between the transimpedance amplifiers and the analogue input sub-system. A 256 to

16 multiplexing system will probably be used.

- d) A mechanical assembly for mounting items (a) and (c).

Since 160 photodiodes are required, spaced approximately 6 mm apart, it will not be possible to use the UDT PIN 10AP device (24), as used in the Automatic Photometer, since it is too large and too expensive. Consequently, a much cheaper and smaller device, the Centronics OSD 1-E (92), costing approximately £3-50, was evaluated. The spectral response of this device does not match the photopic curve as accurately as the UDT device does, but can still be considered satisfactory, taking into account the considerations given in section 4.1; practical tests with a sample device confirmed that the errors that would be produced in this application were acceptably small. Further practical tests showed that, when measuring light of a fixed spectral composition, the linearity of this device and the UDT PIN 10AP matched to within 1%.

The characteristics of various op-amps, varying in cost from a few tens of pence to tens of pounds, were also studied; it was thought that the required level of performance could be achieved for about £6 per channel; the Burr-Brown OPA 2111AM (93), a dual device costing approximately £12, will probably be used.

17.5 The Analogue Input Sub-System

This sub-system will, upon the receipt of a software initiated command, digitize the transimpedance amplifier outputs and transmit

the data to the Gems for storage in the frame-store as a one-dimensional column of data; the area of the frame-store to be used will be software selectable. The sub-system will be housed in a cabinet beneath the test screen and will be interfaced to the Gems via the microcomputer's Q-bus, using a DMA controller, and to the photodetector sub-system. It will essentially consist of the following:

- a) A set of analogue multiplexers to carry out a further stage of multiplexing on the transimpedance amplifier outputs to produce a single channel signal.
- b) A programmable gain amplifier. This will enable the transimpedance amplifier outputs to be amplified by a software-selectable gain of 1, 2 or 4 before analogue to digital conversion, to produce effective full scale values of 409.6, 204.8 or 102.4 lux at 25 m, as required by the operator.
- c) A 12 bit analogue to digital converter. This will produce a resolution ranging from 0.1 lux, for the 409.6 lux full scale range, to 0.025 lux, for the 102.4 lux range.
- d) A programmable shift register to enable the 12 bit data produced by the analogue to digital converter to be extended to a 16 bit word to compensate for the different gain factors used and provide a common overall format for storing data in the frame-store. The 16 bits of data will be used as 15 bits magnitude and 1 bit sign; these will be used to represent +819.2 lux with a resolution of 0.025 lux. This format will

enable the required SIA addition and subtraction operations to be carried out.

- e) A control section for the above.

17.6 The Rotary Table Sub-System

This will essentially consist of the following:

- a) A motorised rotary table.
- b) Control and drive units for the table.
- c) A fixture for mounting the lamp on the table, and enabling its vertical aim to be easily adjusted.

Rotary tables and electronic drive and control units sold by Ealing-Beck, (94), Laser Lines (95), Time and Precision (96) and Unimatic (97) were evaluated; the Ealing-Beck 'System Five' was far more suitable than the others for this application and offered the following benefits:

- a) It is a convenient size.
- b) It has a high accuracy.
- c) It uses a five-phase stepper motor, which avoids many of the problems which are associated with four-phase motors.

- d) The control unit has an IEEE-488 interface (98), which simplifies the connection to the computer system.
- e) The table's position at any instant can be read from the control unit.
- f) A hand controller is available; this will enable the lamp aiming process to be easily carried out.
- g) A position display, with LED readout (important for darkroom use) and a zeroing facility is available.

A lamp mounting fixture was made from part of the goniometer built for the proposed video photometer; a base plate for mounting this on the Ealing-Beck rotary table was designed and made.

17.7 The System Software

This will essentially consist of the following:

- a) The DEC RT-11 operating system and Fortran Compiler (99).
- b) Special purpose programs to acquire, display, process, store and retrieve SIA's. These will make use of the following:
 - i) GEMLIB2. This is a library of subroutines which interfaces a user's Fortran program to the Gems system hardware (82).

- ii) Special purpose routines, written by Gems, to:
 - a) Control the rotary table, analogue input and photodiode sub-systems.
 - b) Add and subtract arrays of data in the frame-store.
- c) Software for transferring the SIA files to the Group Computer. This will probably be a DEC 2780/3780 emulator (72).

17.8 Ancillary Hardware

The system will use the base plate and support frame, the reduced length photometer lens and frame and the test screen and support system constructed for the proposed video photometer.

A programmable power supply (100), which can be interfaced to the computer via the IEEE bus, will be used to energise the lamp under test.

17.9 Implementation

The implementation of the system will require:

- a) A capital expenditure of approximately £80,000, divided as follows:

| | | |
|------|---|----|
| i) | The Gems and auxiliary hardware | 20 |
| ii) | The microcomputer and peripherals (including interfaces to the analogue input and rotary table sub-systems) | 11 |
| iii) | The photodiode sub-system (including some design work by Gems Ltd) | 4 |
| iv) | The analogue input sub-system (including design work by Gems Ltd) | 29 |
| v) | The rotary table sub-system | 3 |
| vi) | Software: RT11, Fortran Compiler, GEMLIB2, special purpose routines by Gems Ltd | 11 |
| vii) | Headlamp power supply system | 2 |

b) The tasks listed below to be carried out; the way in which the work will be divided between Lucas and Gems is also indicated.

- i) The finalisation of the system specification, including the interfaces between the various parts of the system

Lucas/Gems

- ii) The design and construction of the photodiode sub-system

Mainly Lucas

- iii) The design and construction of the analogue input sub-system

Mainly Gems

- iv) The interfacing of the photodiode and analogue input sub-systems to the Gems and microcomputer

Lucas/Gems

- v) The specification and writing of a software routine to transfer data from the analogue input sub-system to the frame-store.

Mainly Gems

- vi) The interfacing of the rotary table sub-system to the Gems and the microcomputer

Gems

- vii) The specification and writing of a software routine to carry out a complete scanning and data acquisition sequence, using (v) above

Mainly Gems

- viii) The specification and writing of a software routine to acquire an SIA, using (vii) above

Lucas

- ix) The specification and writing of software routines to display, add, subtract, store and retrieve SIA's

Lucas

- x) System integration and testing

Lucas/Gems

- xi) The implementation of a system for transferring SIA files to the Group computer

Lucas.

18. DISCUSSION

18.1 Introduction

Two new types of headlamp photometer have been considered; both are based on the use of a digital image processing system and are designed for acquiring data significantly more quickly than is possible using the currently available equipment. The 'video photometer' uses two video cameras to measure the beam illuminance data, whilst the 'high-speed photometer' has a one-dimensional array of photodiodes and a one-dimensional mechanical scanning system.

The high-speed photometer can be implemented using currently available technology, and, whilst requiring a large amount of custom work, it can be predicted with a high degree of confidence that the system will be capable of making accurate measurements over the wide range of illuminance values of interest. A video photometer capable of the same performance cannot be implemented using presently available equipment.

It is therefore recommended that the high-speed photometry approach is the one which should be adopted. The proposed system will enable:

- a) A colour iso-lux display of a lamp's beam to be produced in approximately 10-20 seconds.
- b) Measurements at the commonly used test points to be made

without the need for any mechanical movement.

- c) The contributions which are made to a lamp's beam by the various lens and reflector zones to be quantitatively assessed.
- d) The rapid acquisition of data for the development of the performance prediction and 'Chess' software.
- e) A practical investigation of the video photometry technique to be carried out; see section 18.5.

In addition, it is recommended that all future photometric data processing software is implemented in accordance with the integrated scheme described earlier.

Despite the complications of the video photometry approach, it is considered that it may have a part to play in the future, particularly in applications where the dynamic range of illuminance values to be measured is limited, such as a production line system solely for testing the 'SAE' type of dipped beam. Consequently, sections 18.2 - 18.4 consider the following problem areas in relation to possible future developments:

- a) Video rate analogue to digital conversion
- b) Camera evaluation and performance
- c) Other potential problem areas.

Section 18.5 describes the recommended approach to further work in the video photometry area.

18.2 Video Rate Analogue to Digital Conversion

Current image processing system frame-grabbers do not have the 10 (or more) bits resolution required for headlamp photometry; most systems use 6 or 8 bit analogue to digital converters.

Although this problem can be overcome by means of the multiple range digitization approach described earlier, the availability of a high-resolution video rate frame-grabber would provide more design options; it should be remembered, however, that such a frame-grabber would only be of use if the camera noise level were sufficiently low; see section 11.2.1.

Since the architecture of the Gems means that a 12 bit bus from the frame-grabber to the frame-store can be implemented fairly readily, the feasibility of a 12 bit frame-grabber mainly depends on whether or not the cost of 12 bit video rate analogue to digital converters falls from its present level of several thousand pounds to a more reasonable figure. The general trends in this field suggest that this could happen. For example, 6 bit flash converters, which cost several hundred pounds a few years ago, are now available for less than £50. The required price reduction is only likely to occur, however, if there is a sufficiently large demand for high resolution video rate analogue to digital converters; unfortunately it would appear that this demand will not exist, at least in the near future,

in the fields of television broadcasting and image processing.

Digital techniques are becoming increasingly important in television broadcasting, but the video signals, both luminance and chrominance components, are normally stored in 8 bit form; see reference (101).

Image processing system manufacturers are likely to continue to use 8 bit converters in the near future as a result of the following factors:

- a) Most image processing applications do not require high resolution conversion; many utilise binary images, in which each pixel is assigned a value of 0 or 1, depending on whether the video signal is lower or higher than a given threshold, and for those which do require grey scale information, 4, 6 or 8 bits is usually sufficient.
- b) Most image processing systems have 8 bit deep frame-stores and would not be able to store data from a higher resolution converter.
- c) There is normally little point, unless using a noise reduction technique, in quantising a video signal to more than 8 bits resolution, since the additional bits would only represent 'frozen noise'.

As a result of the above considerations, there may be little incentive for analogue to digital converter manufacturers to develop

low cost, high resolution video rate devices, and costs may remain high for many years.

18.3 Camera Evaluation and Performance

There are two main problem areas:

- a) There is a lack of in-depth technical support available in the United Kingdom from solid-state camera manufacturers, most of whom are based abroad.
- b) The technical performance of currently available cameras is not sufficiently good for the proposed prototype video photometry system.

These areas are considered in sections 18.3.1 and 18.3.2.

18.3.1 Evaluation

The level of technical support available in the United Kingdom is unlikely to improve until the market for solid-state cameras expands significantly, which will take several years. Furthermore, since most users do not require detailed performance information about parameters such as spectral response and linearity tolerances, there will be little incentive for manufacturers to make such data available; in many cases, in-depth studies of such parameters may not even have been carried out.

Ideally, the prototype video photometry system would be implemented with the close assistance of a solid-state camera manufacturer; it is unlikely that such collaboration would be of interest to a manufacturer, however, since the number of cameras which would be purchased by Lucas, even if the system were a total success, would not be sufficiently large.

Consequently, the problems involved in assessing cameras for this application are unlikely to diminish significantly over the next few years.

18.3.2 Performance

The main camera requirements are in the areas of spectral response, sensitivity, sensor geometry/video signal relationship and linearity. In addition, anti-blooming is required if a standard 8 bit frame-grabber is to be utilised. Of the other parameters to be considered, noise is the most important, as this dictates whether or not digital noise filtering is required, and if so, the number of frames to be averaged.

These areas are considered below:

a) Spectral Response

Most of the solid-state cameras currently available, including those examined for the proposed video photometry system, would require their spectral response to be modified by means of a suitable infra-red cut-off filter, or combination of filters,

in order to produce the required approximation to the photopic response. As solid-state camera and filter technology improves, it is possible that manufacturers will be capable of producing models which have a closer match to the photopic response. However, since cameras are not generally sold as photometric measurement devices, and most users do not require such a response, there will probably be little incentive for them to do so.

Ideally, a measurement of the response of the camera to be used, including any filters which are required, would be carried out by an independent test house, such as the National Physical Laboratory, to verify that the response was suitable. Unfortunately, such measurements cannot presently be carried out as a matter of routine and would be very expensive to commission; this situation may alter over the next few years as solid-state cameras and sensors become more widely used in industry.

b) Sensitivity

There would probably be sensitivity problems with the cameras examined, in view of the need to use an infra-red cut-off filter to obtain the required spectral response, and this situation is likely to be encountered in the future. It should be possible to overcome the problem, however, providing the camera has a variable clocking rate facility, or some other mechanism by which the sensor pixel integration time can be increased.

c) Sensor Geometry/Video Signal Relationship

In most cases, the type of detailed information required to fully define the relationship between the sensor geometry and the video signal, which is necessary to design a video photometry system, is not readily available from camera manufacturers and it seems unlikely that this situation will change significantly in the near future.

d) Linearity

Theoretically, the sensor illuminance/output voltage relationship for a solid-state camera is linear, but in practice, as a result of the various stages of amplification used, this is not always the case. Unfortunately, linearity tolerance information is not generally available from the camera manufacturers, and must be assessed by practical measurements. As solid-state camera technology improves, then the degree of linearity obtainable will hopefully increase. Of the cameras examined, the Reticon and I2S exhibited a reasonably high degree of linearity.

e) Anti-Blooming

Of the cameras examined, only the GE model displayed a degree of anti-blooming performance which could be considered acceptable for the proposed data acquisition method. (Unfortunately, various other aspects of the camera's performance were unsatisfactory.) Nevertheless, as solid-state

sensor technology improves, anti-blooming capability is likely to become more common, and the level of effectiveness will probably increase. It should be remembered, however, that the primary reason anti-blooming capability is provided is to prevent image spread on a monitor, and that this can be achieved with a lower level of anti-blooming performance than is required to enable accurate quantitative illuminance measurements to be made using the proposed scheme.

Consequently, it will continue to be necessary to evaluate carefully the level of performance provided by a given camera; since manufacturers do not generally provide detailed anti-blooming performance data of the form required for this application, the evaluation must be carried out by practical tests.

f) Noise

Noise is a significantly greater problem with solid-state cameras than discrete photodiodes, and presently restricts the range of illuminance values which can be measured, without the aid of a noise reduction technique, to typically 200:1, compared to typically 10^6 :1 for a photodiode. Future cameras can be expected to have lower noise levels than current models, as a consequence of general improvements in the technology, but is highly unlikely that their performance in this area will ever approach that of discrete photodiodes.

18.4 Other Potential Problem Areas

If a suitable camera and digitization method are identified, then the feasibility of the system will depend on the reduced length photometer performance and the effects of non-uniform screen characteristics and camera flare.

Reduced-length photometer performance is more critical with the video photometry technique than the conventional and high speed photometry approaches. The theoretical work undertaken indicates that the performance of a 4 m system will be satisfactory for moderate off-axis angles. The situation is very complex, however, since the imaging performance depends on the illuminance gradients in the beam and the lamp size as well as the lens characteristics. The implementation of the proposed high-speed photometry system will enable practical results to be obtained and compared with the theoretical data.

The effects of non-uniform screen characteristics, which are unimportant in the conventional and high-speed photometry approaches, can be corrected; although this is straightforward in principle, however, it is likely to be tedious in practice.

Camera flare is a more serious problem, and its effects cannot easily be corrected since they will depend on the illuminance characteristics of the lamp being measured. Consequently, even if all the other problems can be overcome, the video photometry principle may still be unworkable in practice.

18.5 Recommended Approach to Further Video Photometry Work

In view of all the uncertainties surrounding the practical viability of the video photometry concept, it is considered that the best approach to future work in this area is as follows:

a) The Implementation of the High-Speed Photometer

As described above, this will provide a powerful facility with little risk of failure. It will also enable a practical study of the characteristics of the reduced-length photometer to be carried out.

b) Monitoring Camera and Analogue to Digital Converter Development

Progress in the areas of video rate analogue to digital conversion and solid-state camera development should be monitored to determine the future feasibility of implementing a camera/frame-grabber sub-system capable of satisfying the basic requirements.

c) Camera/Frame-Grabber Sub-System Implementation

When it appears that a camera/frame-grabber capable of satisfying the basic requirements can be implemented, this should be carried out for use with the high-speed photometer's image processing system and computer.

d) Practical Measurements

Practical measurements with the above system will enable the viability of the video photometry method to be determined and compared to the high-speed photometry approach.

This program will eliminate the high financial risk of attempting to implement a complete video photometry system from scratch without having first carried out a practical evaluation of the techniques involved.

18.6 Epilogue

Following the author's recommendations, the Company decided to implement the high-speed photometer described in Chapter 17 and the necessary expenditure was approved in February 1986. The work is being carried out by the author and Gems of Cambridge, as planned, and is scheduled for completion in December 1986.

LIST OF CONTENTS OF APPENDICES

| Appendix | Page |
|---|------|
| A THE CONCEPT OF HEADLAMP INTENSITY | 317 |
| B REDUCED-LENGTH PHOTOMETERS | 320 |
| C AMBIENT LIGHT IN A VIDEO PHOTOMETRY SYSTEM | 324 |
| D REDUCED-LENGTH PHOTOMETER ANALYSIS PROGRAM (RLP) | 327 |
| D.1 Introduction | 327 |
| D.2 Program Listing | 328 |
| D.3 Notes on the Program | 340 |
| D.3.1 Block Data Sub-Program | 340 |
| D.3.2 Main Program | 341 |
| D.3.3 Subroutine RAY | 343 |
| D.3.4 Subroutine REFRCT | 345 |
| D.4 Instructions for Using the Program | 345 |
| D.5 Glossary of Main Program Variables | 346 |
| E FOUR METRE REDUCED-LENGTH PHOTOMETER PERFORMANCE: BLUR PATCH DATA TABLES | 347 |
| E.1 Configuration 1 | 347 |
| E.1.1 Configuration 1h | 347 |
| E.1.1.1 Parameters | 347 |
| E.1.1.2 Blur Patch Data | 348 |

| | | |
|---------|------------------|-----|
| E.1.2 | Configuration 1v | 348 |
| E.1.2.1 | Parameters | 348 |
| E.1.2.2 | Blur Patch Data | 348 |
| E.2 | Configuration 2 | 348 |
| E.2.1 | Configuration 2Y | 349 |
| E.2.1.1 | Parameters | 349 |
| E.2.1.2 | Blur Patch Data | 349 |
| E.2.2 | Configuration 2R | 350 |
| E.2.2.1 | Parameters | 350 |
| E.2.2.2 | Blur Patch Data | 350 |
| E.2.3 | Configuration 2B | 350 |
| E.2.3.1 | Parameters | 350 |
| E.2.3.2 | Blur Patch Data | 350 |
| E.2.4 | Notes | 350 |
| E.3 | Configuration 3Y | 351 |
| E.3.1 | Parameters | 351 |
| E.3.2 | Blur Patch Data | 351 |
| E.3.3 | Notes | 352 |
| E.4 | Configuration 4 | 352 |
| E.4.1 | Configuration 4Y | 352 |
| E.4.1.1 | Parameters | 352 |
| E.4.1.2 | Blur Patch Data | 352 |
| E.4.2 | Configuration 4R | 352 |
| E.4.2.1 | Parameters | 352 |
| E.4.2.2 | Blur Patch Data | 353 |
| E.4.3 | Configuration 4B | 353 |
| E.4.3.1 | Parameters | 353 |
| E.4.3.2 | Blur Patch Data | 353 |
| E.4.4 | Notes | 353 |

| | | |
|---|---|-----|
| F | IMAGE PROCESSING EQUIPMENT CONSIDERED | 367 |
| G | THE AUTOMATIC PHOTOMETER/GROUP COMPUTER FILE TRANSFER SYSTEM | 369 |
| | G.1 Introduction | 369 |
| | G.2 Implementation | 371 |
| H | PHOTOMETRIC DATA FILES AND THEIR PROCESSING | 376 |
| | H.1 Photometric Data File (PDF) Structure | 376 |
| | H.1.1 Overview of PDF Structure | 376 |
| | H.1.2 Detailed Structure | 379 |
| | H.1.2.1 PDF Identification Section | 379 |
| | H.1.2.2 Main Body Header | 380 |
| | H.1.2.3 Block Header | 381 |
| | H.1.2.4 Sub-Block Header | 382 |
| | H.1.3 PDF Naming System | 391 |
| | H.2 PDF Processing Software | 393 |
| | H.2.1 Introduction | 393 |
| | H.2.2 Program PDFLC | 395 |
| | H.2.3 Subroutine PDFI | 402 |
| | H.2.4 Subroutine RECRD | 410 |
| | H.2.5 Subroutine RDERR | 414 |
| | H.2.6 Example of Printout Produced by PDFLC | 417 |

LIST OF FIGURES IN APPENDICES

| Fig. | | Page |
|------|---|------|
| B1 | Reduced Length Photometer Configuration | 323 |
| H1 | Overall Photometric Data File Structure | 378 |

LIST OF TABLES IN APPENDICES

| Table | | Page |
|----------|--|------|
| E1 - E13 | Reduced Length Photometer Study - Blur Patch Data Tables: | |
| E1 | Configuration 2Y - Horizontal Plane | 354 |
| E2 | Configuration 2Y - Vertical Plane | 355 |
| E3 | Configuration 2R - Horizontal Plane | 356 |
| E4 | Configuration 2R - Vertical Plane | 357 |
| E5 | Configuration 2B - Horizontal Plane | 358 |
| E6 | Configuration 2B - Vertical Plane | 359 |
| E7 | Configuration 3Y - Horizontal Plane | 360 |
| E8 | Configuration 4Y - Horizontal Plane | 361 |
| E9 | Configuration 4Y - Vertical Plane | 362 |
| E10 | Configuration 4R - Horizontal Plane | 363 |
| E11 | Configuration 4R - Vertical Plane | 364 |

| | | |
|---------|---|-----|
| E12 | Configuration 4B - Horizontal Plane | 365 |
| E13 | Configuration 4B - Vertical Plane | 366 |
| H1 | Photometric Data File Structure Details | 384 |
| H2 - H7 | PDF Structure: | |
| H2 | PDF Identification Section, Record 1 | 385 |
| H3 | Main Body Header, Record 1 | 386 |
| H4 | Main Body Header, Record 2 | 387 |
| H5 | Block Header, Record 1 | 388 |
| H6 | Block Header, Record 2 | 389 |
| H7 | Sub-Block Header, Record 1 | 390 |

APPENDIX A

THE CONCEPT OF HEADLAMP INTENSITY

This Appendix describes how the concept of luminous intensity, which is normally defined in terms of a point source, can be applied to a headlamp.

Intensity, I , is normally defined as the luminous flux, dF , emitted by a point source into a small solid angle, $d\omega$, in a particular direction:

$$I = \frac{dF}{d\omega}$$

From this definition can be derived the well known inverse-square and cosine laws of illumination, which enable the calculation of the illuminance at a specified point on a specified plane produced by a point source.

A headlamp is not, however, a point source; it is an optical system consisting of a bulb, a reflector and a lens and the overall size of the light-emitting area will typically be about 300 cm^2 . The concept of intensity as defined above clearly has little meaning for a source of this type.

It is, however, possible to re-define intensity in a way which allows it to be used with non-point sources, such as a headlamp:

$$I = \lim_{d \rightarrow \infty} Ed^2$$

where

E = Illuminance measured at the point which is a distance d from the lamp in the direction of interest and lies on the plane perpendicular to the direction of interest.

Further details about this concept are given in reference (102). It should be noted that in the case of a point source, the two definitions given above become equivalent.

This alternative definition allows the intensity of a non-point source to be calculated from practical measurements of the illuminance values it produces; in practice, Ed^2 generally reaches a value sufficiently close to its limiting value at a convenient measurement distance, the actual value of which depends on the type of source, its dimensions and the accuracy acceptable.

Having found a way to define the concept of intensity for a non-point source and to measure it in practice, we can also use the inverse-square and cosine laws to accurately calculate the illuminance values produced at various points of interest, providing their distances are greater than or equal to the distance at which Ed^2 reaches the practical approximation to its limiting value.

The minimum distance from the source at which the illuminance should be measured to enable the intensity to be calculated to a given accuracy can be determined theoretically for various types of source, although the mathematics can become complex (103).

In the case of a diffuse, circular source, it can be shown that for an error of less than 1%, the minimum distance is 5 times the source diameter and for an error of less than 0.1%, 16 times the source diameter.

In the case of projector sources, such as headlamps and searchlights, which use a basic light source in conjunction with reflecting and refracting surfaces, then the minimum distance for a given accuracy depends on 2 criteria. Firstly, the distance must be greater than that at which the 'cross-over point' for the lamp occurs (104); beyond this point a projector functions as a luminous disc and so, secondly, the same considerations as for a true diffuse radiating source apply. For a headlamp, the cross-over point normally occurs between about 7 m and 15 m and consequently a measurement distance of greater than 15 m is required; this will be at least 40 times the largest dimension of the light-emitting area of the lamp and hence the difference between the value of E_d^2 at this distance and at infinity is negligible.

APPENDIX B

REDUCED-LENGTH PHOTOMETERS

This Appendix analyses the reduced-length photometer configuration (the basic principle of which was described in section 3.3.2), by means of the standard thin lens equation.

Let d = Distance of lamp to far screen
 x = Distance of lamp to lens
 f = Focal length of the lens
 v = Distance of lens to near screen
 m = Magnification i.e. $\frac{\text{size of near screen image}}{\text{size of far screen image}}$

See Fig. B1.

The lens equation will be used to calculate v and m , given d and x .

The standard thin lens equation is:

$$\frac{1}{u} + \frac{1}{v} = \frac{1}{f} \tag{B1}$$

where

u = Distance of object from lens

v = Distance of image from lens

f = Focal length of lens.

The sign convention used here is:

The distance from the lens to a real object or image is +ve

The distance from the lens to a virtual object or image is -ve

The focal length of a convex lens is +ve

The focal length of a concave lens is -ve

The magnification, m , produced by a thin lens is given by

$$m = \frac{-v}{u} \quad (B2)$$

For a reduced-length photometer:

The 'object' is the beam pattern which would have been produced on the far screen and is therefore virtual. Consequently, 'u' is the distance from the lens to the far screen and is -ve. i.e. $u = -(d-x)$.

The 'image' is the beam pattern produced on the near screen and is therefore real. Consequently, v is +ve.

The lens is convex and its focal length is therefore +ve.

Using equation B1:

$$\frac{-1}{(d-x)} + \frac{1}{v} = \frac{1}{f}$$

Therefore

$$\frac{1}{v} = \frac{1}{f} + \frac{1}{(d-x)} \quad (B3)$$

Using equation B2:

$$m = \frac{-v}{-(d-x)}$$

Therefore

$$m = \frac{v}{(d-x)} \quad (B4)$$

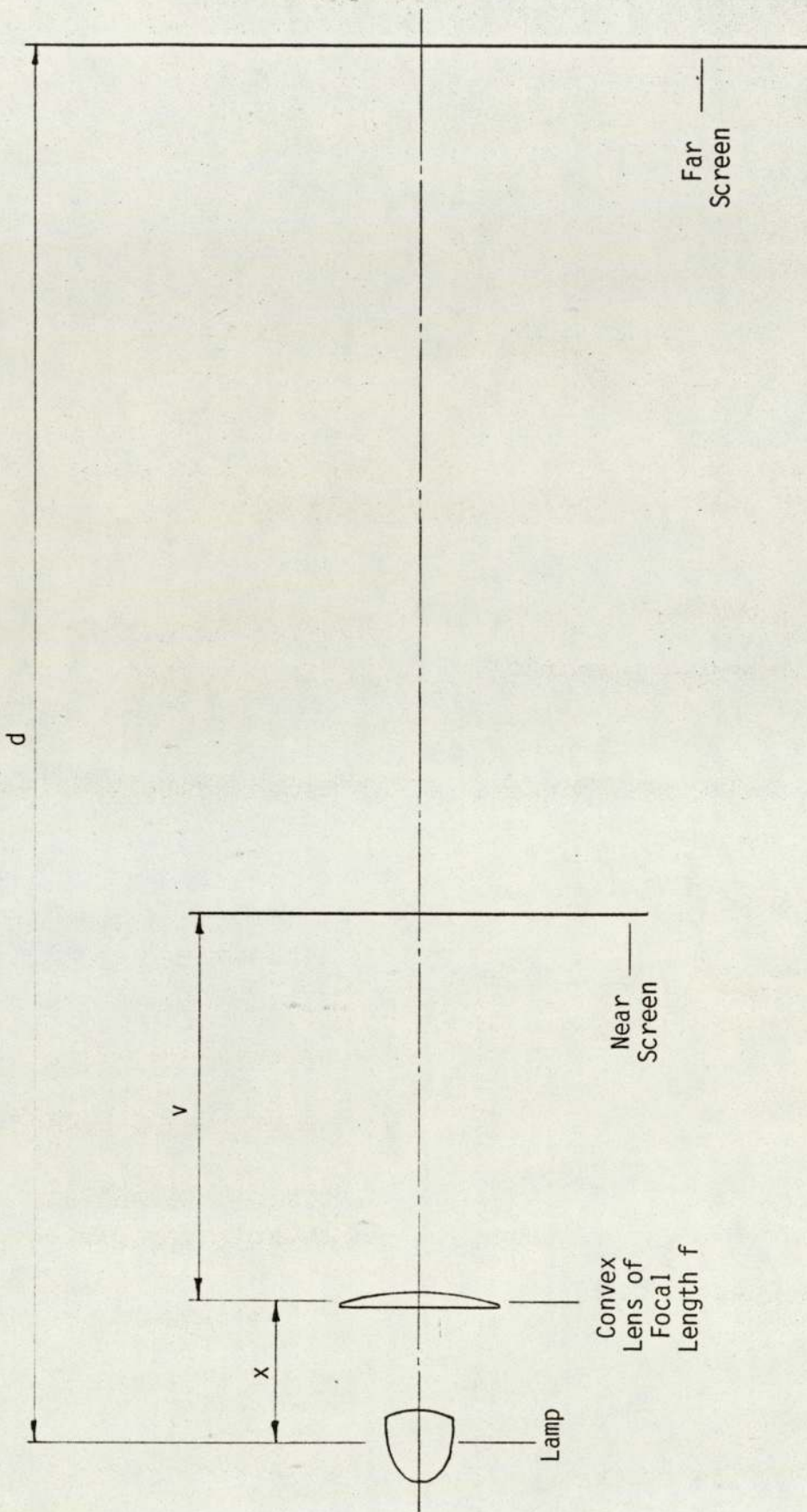


Fig. B1 Reduced Length Photometer Configuration

APPENDIX C

AMBIENT LIGHT IN A VIDEO PHOTOMETRY SYSTEM

As stated in Chapter 11, it should be possible to ignore the effects of the test screen illuminance produced by ambient light. If this is not the case, however, then the following correction method can be applied.

The screen illuminance will consist of two components:

$$E_{FSCP} (T) = E_{FSCP} (L) + E_{FSCP} (A) \quad (C1)$$

where

$E_{FSCP} (T)$ = Total screen illuminance, referred to the far screen

$E_{FSCP} (L)$ = Screen illuminance produced by the lamp, referred to the far screen

$E_{FSCP} (A)$ = Screen illuminance produced by ambient light, referred to the far screen

If an ambient light correction is to be made, then the quantity to be produced by step (b) of the SIA acquisition procedure, and subsequently used by step (c), becomes $E_{FSCP} (L)$.

The procedure to be performed for acquiring an SIA is modified to the following:

- a) The V_{SEP}' or $(V_{SEP} - VN)'$ values produced by $E_{FSCP}(A)$, i.e. $V_{SEP}'(A)$ or $(V_{SEP} - VN)'(A)$, are measured and the VD_{SEP}' values subtracted to give $VX_{SEP}'(A)$ values.
- b) The $E_{FSCP}'(A)$ values are calculated from the $VX_{SEP}'(A)$ values.
- c) The V_{SEP}' or $(V_{SEP} - VN)'$ values produced by $E_{FSCP}(T)$, i.e. $V_{SEP}'(T)$ or $(V_{SEP} - VN)'(T)$, are measured and the VD_{SEP}' values subtracted to give $VX_{SEP}'(T)$ values.
- d) The $E_{FSCP}'(T)$ values are calculated from the $VX_{SEP}'(T)$ values.
- e) The $E_{FSCP}'(A)$ values are subtracted from the $E_{FSCP}'(T)$ values to give the required $E_{FSCP}'(L)$ values.
- f) The SIA element values are calculated from the $E_{FSCP}'(L)$ values.

The same result can be achieved more quickly by the following procedure:

- a) The $V_{SEP}'(A)$ or $(V_{SEP} - VN)'(A)$ values are acquired; these are equivalent to $[VX_{SEP}'(A) + VD_{SEP}']$ values.
- b) The $V_{SEP}'(T)$ or $(V_{SEP} - VN)'(T)$ values are acquired; these are equivalent to $[VX_{SEP}'(T) + VD_{SEP}']$ values.

- c) The $V_{SEP}'(A)$ or $(V_{SEP} - VN)'$ (A) values are subtracted from the $V_{SEP}'(T)$ or $(V_{SEP} - VN)'$ (T) values to give $[VX_{SEP}'(T) - VX_{SEP}'(A)]$ values, which are equivalent to $VX_{SEP}'(L)$ values.
- d) The $VX_{SEP}'(L)$ values are used to calculate the $E_{FSCP}'(L)$ values.
- e) The SIA element values are calculated from the $E_{FSCP}'(L)$ values.

APPENDIX D

REDUCED-LENGTH PHOTOMETER ANALYSIS PROGRAM (RLP)

D.1 Introduction

This program was written to analyse the imaging performance of a given reduced-length photometer configuration. It is used as part of the overall procedure given in Chapter 12. The program originally used for the research was written in Fortran 66, the only version of Fortran available at the time on the IBM Group Computer. The program was re-written in Fortran 77 for presentation in this thesis. This section assumes a detailed knowledge of IBM Fortran; see references (105 - 107).

The program is written in the form of a main program, two subroutines and a block data subprogram for initialising the variables. It follows the basic concepts of top-down design and structured programming; see reference (108), for example.

The program listing is given in section D.2. Notes about the program and the calculations carried out are contained in section D.3. Section D.4 describes the method of initialising and running the program.

D.2 Program Listing

REDUCED-LENGTH PHOTOMETER ANALYSIS PROGRAM

00100 C
00200 C
00300 C
00400 C
00500 C
00600 C
00700 C
00800 C
00900 C
01000 C
01100 C
01200 C
01300 C
01400 C
01500 C
01600 C
01700 C
01800 C
01900 C
02000 C
02100 C
02200 C
02300 C
02400 C
02500 C
02600 C
02700 C
02800 C
02900 C
03000 C
03100 C

NAME

RLP

VERSION

V2.4

AUTHOR

S. J. CARTWRIGHT

DESCRIPTION

SEE CHAPTER 12 AND APPENDIX D OF THESIS

SUBROUTINES CALLED

RAY, REFRACT

PART 1

03200 C
 03300 C
 03400 C
 03500 C
 03600
 03700 C
 03800
 03900 C
 04000
 04100 C
 04200
 04300
 04400
 04500
 04600
 04700
 04800 C
 04900
 05000 C
 05100
 05200
 05300
 05400
 05500
 05600 C
 05700
 05800 C
 05900 C

ASSIGNMENT OF RLP CONFIGURATION PARAMETERS

BLOCK DATA

REAL LPFS,LPFILS,LNSTHK,LNSSZE,LALSNS,N,N#
 COMMON /RLPOCP/ LPFS,LPFILS,LNSTHK,LNSSZE,LALSNS

1 PARAMETER (NUMSUR = 2)
 2 DATA LPFS /25.0/
 3 DATA LPFILS /0.4/
 4 DATA LNSTHK /0.035/
 5 DATA LNSSZE /0.48/
 6 DATA LALSNS /3.42271/

COMMON /RLPLSP/ NUMSRF,C(NUMSUR),N(NUMSUR),N#(NUMSUR),T(NUMSUR-1)

DATA NUMSRF /NUMSUR/
 7 DATA C(1),C(2) /0,-0.4780114/
 8 DATA N(1),N(2) /1.00000,1.52300/
 9 DATA N#(1),N#(2) /1.52300,1.00000/
 10 DATA T(1) /0.035/

END

```

06000 C
06100 C
06200 C
06300 C
06400 C
06500 C
06600
06700
06800 C
06900
07000
07100
07200 C
07300
07400
07500 C
07600 C
07700 C
07800 C
07900
08000
08100 C
08200
08300
08400
08500
08600
08700
08800
08900
09000
09100
09200
09300
09400
09500

PART 2
MAIN PROGRAM

2.1 DATA DECLARATION

11 PARAMETER ( NUMSUR = 2 )
PARAMETER ( DGTORD = 1.745329E-2 )

REAL LPFS,LPFILS,LNSTHK,LNSSZE,LALSNS,N,N#
COMMON /RLPOCF/ LPFS,LPFILS,LNSTHK,LNSSZE,LALSNS
COMMON /RLPLSP/ NUMSRF,C(NUMSUR),N(NUMSUR),N#(NUMSUR),T(NUMSUR-1)

REAL MELPSI,LTELPS,LFLALS,MAG,MOAACI,LOAACR,LOAACD
INTEGER NORINP,R,P

2.2 OUTPUT OF RLP CONFIGURATION DETAILS

PRINT *, 'REDUCED-LENGTH PHOTOMETER ANALYSIS PROGRAM V2.4'
PRINT *, '
PRINT *, 'OVERALL CONFIGURATION PARAMETERS'
PRINT *, '
FORMAT (' LPFS = ',F9.5,' M')
PRINT 2000, LPFS
FORMAT (' LPFILS = ',F9.5,' M')
PRINT 2010, LPFILS
FORMAT (' LNSTHK = ',F9.5,' M')
PRINT 2020, LNSTHK
FORMAT (' LNSSZE = ',F9.5,' M')
PRINT 2030, LNSSZE
FORMAT (' LALSNS = ',F9.5,' M')
PRINT 2040, LALSNS
PRINT *, '
PRINT *, '

```

```

09600 C
09700 PRINT X, 'LENS SYSTEM PARAMETERS'
09800 PRINT *, '
09900 FORMAT (' NUMSRF = ', I3 )
10000 PRINT 2050, NUMSRF
10100 PRINT *, '
10200 DO 200 J = 1, NUMSRF
10300 FORMAT (' C(', I1, ') = ', F9.5)
10400 PRINT 2060, J, C(J)
10500 FORMAT (' N(', I1, ') = ', F9.5)
10600 PRINT 2070, J, N(J)
10700 FORMAT (' N#(', I1, ') = ', F9.5)
10800 PRINT 2080, J, N#(J)
10900 IF ( J.NE. NUMSRF ) THEN
11000 FORMAT (' T(', I1, ') = ', F9.5)
11100 PRINT 2090, J, T(J)
11200 END IF
11300 PRINT *, '
11400 200 CONTINUE
11500 PRINT *, '
11600 PRINT *, '
11700 C
11800 C
11900 C
12000 C
12100 C
12200
12300 LPLALS = LPFILS + LNSTHK
12400 LOAACR = ATAN ( LNSSZE / (2*LPLALS) )
12500 FORMAT (' LIMITING OFF-AXIS ANGLE (LOAAC) = ', F9.1, ' DEG. ')
12600 LOAACD = LOAACR/DGTORD
12700 PRINT 2100, LOAACD
12800 PRINT *, '
12900 C

```

```

13000 C      INPUT PENCIL SPECIFICATION PARAMETERS FROM CONSOLE
13100 C
13200      PRINT *, 'ENTER ANGULAR INCREMENT FOR CENTRAL RAYS (OAACIN)'
13300      READ (5,*) OAACIN
13400      PRINT *, 'ENTER MAX. OFF-AXIS ANGLE OF INTEREST (MOAACI)'
13500      READ (5,*) MOAACI
13600      PRINT *, 'ENTER RAY STARTING PT. INCREMENT (RSPINC)'
13700      READ (5,*) RSPINC
13800      PRINT *, 'ENTER MAX. EFFECTIVE LAMP SIZE OF INTEREST (MELPSI)'
13900      READ (5,*) MELPSI
14000 C
14100 C      CALCULATE NUMBER OF PENCILS
14200 C
14300      NOPEN = NINT (MOAACI/OAACIN) + 1
14400 C
14500 C      DO TO 220 FOR EACH PENCIL
14600 C
14700      DO 220 P = 1, NOPEN
14800          OAACD = - ((P-1) * OAACIN)
14900          OAACR = OAACD * DGTORD
15000          POIWFS = - (LPFS * TAN (OAACR))
15100 C
15200 C      CALCULATE LTELPS
15300 C
15400      IF ( POIWFS .LE. (LNSSZE/2) ) THEN
15500          LTELPS=LNSSZE+(2*LPLALS*((LNSSZE/2)-POIWFS)/(LPFS-LPFILS))
15600      ELSE
15700          LTELPS=LNSSZE-(2*LPLALS*(POIWFS-(LNSSZE/2))/(LPFS-LPLALS))
15800      END IF

```

```

15900 C
16000 C
16100 C
16200
16300
16400
16500
16600 2110
16700
16800
16900 2120
17000
17100 2130
17200 &
17300
17400 2140
17500
17600
17700
17800 C
17900 C
18000 C
18100
18200
18300
18400
18500
18600
18700 C
18800 C
18900 C
19000
19100 C

      OUTPUT PENCIL DETAILS
      PRINT *, ' '
      PRINT *, ' '
      PRINT *, ' '
      PRINT *, ' '
      FORMAT (' PENCIL NUMBER = ', I3)
      PRINT 2110, P
      PRINT *, ' '
      FORMAT (' ANGLE OF CENTRAL RAY (OACD) = ', F9.4, ' DEG')
      PRINT 2120, OACD
      FORMAT (' PT. OF INTERSECTION WITH FAR SCREEN (POIWF) = ',
      F9.4, ' M')
      PRINT 2130, POIWF
      FORMAT (' LIMITING EFFECTIVE LAMP SIZE (LTELPS) = ', F9.4, ' M')
      PRINT 2140, LTELPS
      PRINT *, ' '
      PRINT *, ' '

      CALCULATE ELPS
      IF ( LTELPS .GE. MELPSI ) THEN
        ELPS = MELPSI
      ELSE
        MNOI = INT ( LTELPS / ( 2 * RSPINC ) )
        ELPS = MNOI * ( 2 * RSPINC )
      END IF

      CALCULATE NUMBER OF RAYS IN PENCIL
      NORINP = NINT ( ELPS/RSPINC ) + 1

```

```

19200 C      OUTPUT TABLE HEADING
19300 C
19400 2150  FORMAT ( '      STARTING PT.      ' , '      ANGLE OF RAY      ' ,
19500 &      ' FT. OF INTERSECTION ' )
19600 2160  FORMAT ( '      ON LAMP      ' ,
19700 &      ' WITH NEAR SCREEN ' )
19800      PRINT 2150
19900      PRINT 2160
20000      PRINT *, ' '
20100 2170  FORMAT ( '      (RSPR)      ' , '      (OAAARD)      ' ,
20200 &      ' (POIWNs)      ' )
20300      PRINT 2170
20400      PRINT *, ' '
20500 C
20600 C      DO 10 210 FOR EACH RAY
20700 C
20800      DO 210 R = 1, NORINF
20900      IF (NORINF .NE. 1) THEN
21000          RSPR = ((R-1) * RSPINC) - (ELPS/2)
21100      ELSE
21200          RSPR = 0
21300      END IF
21400      OAAARD = - ( ATAN ( (POIWFs-RSPR)/LPFS) )
21500      CALL RAY (OAAARD, RSPR, POIWNs)
21600      OAAARD = OAAARD/DGTORD
21700 2180  FORMAT (F12.4, F20.4, F20.4)
21800      PRINT 2180, RSPR, OAAARD, POIWNs
21900 210  CONTINUE
22000 C

```

```

22100 C          CALCULATE MAGNIFICATION
22200 C
22300 C          IF (POIWFS.NE.0) THEN
22400 C              RSFR = 0
22500 C              OAARR = - ( ATAN ( (POIWFS-RSPR)/LPFS) )
22600 C              CALL RAY (OAARR,RSPR,POIWNS)
22700 C              MAG = FOIWNS / POWIFS
22800 C              PRINT *,
22900 C              FORMAT (' MAGNIFICATION = ',F9.4 )
23000 C              PRINT 2190 ,MAG
23100 C              END IF
23200 C
23300 C          NEXT PENCIL, UNLESS FINISHED
23400 C
23500 C          220 CONTINUE
23600 C
23700 C          STOP
23800 C          END
23900 C
24000 C
24100 C          PART 3
24200 C
24300 C          SUBROUTINE RAY (OAARR,RSPR,POIWNS)
24400 C
24500 C
24600 C          CALCULATES PATH OF 1 RAY
24700 C
24800 C          INPUTS - OAARR,RSPR
24900 C          OUTPUT - FOIWNS
25000 C
25100 C          CALLS SUBROUTINE REFRACT
25200 C
25300 C

```

```

25400 C      3.1 DATA DECLARATION
25500 C      3.2 "OPENING" RAY CALCULATIONS
25600 C      3.3 "REFRACTION" & "TRANSFER" RAY CALCULATIONS
25700 C      (USING SUBROUTINE "REFRCT")
25800 C      3.4 "CLOSING" RAY CALCULATIONS
25900 C
26000 C
26100 C      3.1 DATA DECLARATION
26200 C
26300 C      12 PARAMETER ( NUMSUR = 2 )
26400 C      REAL LPFS,LPFILS,LNSTHK,LNSSZE,LALSNS,N,N#
26500 C      COMMON /RLPOCF/ LPFS,LPFILS,LNSTHK,LNSSZE,LALSNS
26600 C      COMMON /RLPLSP/ NUMSRF,C (NUMSUR),N (NUMSUR),N# (NUMSUR),T (NUMSUR-1)
26700 C
26800 C      REAL UR (NUMSUR),U#D (NUMSUR),U#R (NUMSUR),
26900 C      &Q (NUMSUR),Q# (NUMSUR),ID (NUMSUR),IR (NUMSUR),
27000 C      &I#D (NUMSUR),I#R (NUMSUR),X (NUMSUR),Y (NUMSUR)
27100 C      REAL NJ,N#J,IRJ,I#RJ
27200 C
27300 C      3.2 "OPENING" RAY CALCULATIONS
27400 C
27500 C      H = RSPR
27600 C      S = -LPFILS
27700 C      S# = LALSNS
27800 C      UR(1) = OAARR
27900 C
28000 C      Q(1) = H * COS ( UR(1) ) + S * SIN ( UR(1) )
28100 C
28200 C
28300 C

```

```

28400 C      3.3  "REFRACTION" & "TRANSFER" CALCULATIONS
28500 C
28600 C      FOR FIRST (NUMSRF - 1) SURFACES
28700 C      "REFRACTION" & "TRANSFER"
28800 C
28900 C      DO 300 J = 1, (NUMSRF-1)
29000 C
29100 C          "REFRACTION"
29200 C
29300 C          QJ = Q(J)
29400 C          URJ = UR(J)
29500 C          CJ = C(J)
29600 C          NJ = N(J)
29700 C          N#J = N$(J)
29800 C
29900 C          CALL REFRCT (QJ,URJ,CJ,NJ,N#J,IRJ,I#RJ,Q#J,U#RJ,XJ,YJ)
30000 C
30100 C          IR(J) = IRJ
30200 C          I#R(J) = I#RJ
30300 C          Q$(J) = Q#J
30400 C          U#R(J) = U#RJ
30500 C          X(J) = XJ
30600 C          Y(J) = YJ
30700 C
30800 C          "TRANSFER"
30900 C
31000 C          Q(J+1) = Q$(J) - ( T(J) * SIN(U#R(J)) )
31100 C          UR(J+1) = U#R(J)
31200 C
31300 C          300 CONTINUE
31400 C

```

```

31500 C FINAL SURFACE - "REFRACTION" ONLY
31600 C
31700 C J = NUMSRF
31800 C
31900 C QJ = Q(J)
32000 C URJ = UR(J)
32100 C CJ = C(J)
32200 C NJ = N(J)
32300 C N#J = N#(J)
32400 C
32500 C CALL REFRACT (QJ,URJ,CJ,NJ,N#J,IRJ,I#RJ,Q#J,U#RJ,XJ,YJ)
32600 C
32700 C IR(J) = IRJ
32800 C I#R(J) = I#RJ
32900 C Q#(J) = Q#J
33000 C U#R(J) = U#RJ
33100 C X(J) = XJ
33200 C Y(J) = YJ
33300 C
33400 C
33500 C 3.4 "CLOSING" CALCULATIONS
33600 C
33700 C
33800 C J = NUMSRF
33900 C H# = ( Q#(J) - S# * SIN (U#R(J)) ) / ( COS (U#R(J)) )
34000 C POIWNS = H#
34100 C
34200 C
34300 C RETURN
34400 C END
34500 C
34600 C

```

34700 C
34800 C
34900 C
35000 C
35100 C
35200 C
35300 C
35400 C
35500 C
35600 C
35700 C
35800 C
35900
36000
36100
36200
36300
36400
36500
36600 C
36700
36800

PART 4

SUBROUTINE REFRCT (QJ,URJ,CJ,NJ,N#J,IRJ,I#RJ,Q#J,U#RJ,XJ,YJ)

"REFRACTION" CALCULATIONS FOR SURFACE NO. J

INPUTS - QJ,URJ,CJ,NJ,N#J

OUTPUTS - IRJ,I#RJ,Q#J,U#RJ,XJ,YJ

REAL NJ,N#J,IRJ,I#RJ

IRJ = ARSIN (QJ * CJ - SIN (URJ))

I#RJ = ARSIN ((NJ / N#J) * SIN (IRJ))

U#RJ = URJ + IRJ - I#RJ

G = QJ / (COS (URJ) + COS (IRJ))

Q#J = G * (COS (U#RJ) + COS (I#RJ))

XJ = G * SIN (URJ + IRJ)

YJ = G * (1 + COS (URJ + IRJ))

RETURN

END

D.3 Notes on the Program

This section contains notes on the program and the calculations carried out and should be read in conjunction with Chapter 12, which describes the basic operations performed by the program.

The program is divided into 4 main parts:

- 1) The Block Data subprogram for assigning the configuration parameters; see section D.3.1.
- 2) The Main Program; see section D.3.2.
- 3) Subroutine 'RAY'; see section D.3.3.
- 4) Subroutine 'REFRCT'; see section D.3.4.

D.3.1 Block Data Subprogram

- a) Two named common blocks of variables, RLPOCP and RLPLSP, are set up for the overall configuration and lens system parameters respectively. The required values of these variables, with the exception of NUMSRF, are defined directly by means of DATA statements (numbered 2 - 10). The number of surfaces is specified by means of the constant NUMSUR, assigned in the PARAMETER statement (numbered 1). This is used primarily as a convenient way of defining the dimensions of the various arrays (including C, T, N and N\$) used in the

program. NUMSUR must also be assigned in the MAIN program (statement no. 11) and in the RAY subroutine (statement no. 12).

- b) The program is used to analyse different configurations by altering statement numbers 1 - 12 and re-compiling; see section D.4.

(In the early versions of this program the parameters were assigned when the program was run by reading in values from the console. However, since many of these parameters remained unchanged every time the program was run, this method became very tedious and was changed to the one used here. It is still not ideal, however, since it involves the user in modifying the source code which could easily lead to a corrupted program. A more satisfactory method than either of the above would be one which stored default values in a file and enabled the operator to change these as required by means of a set of commands. Work was started on this; since the program had provided the information required, however, it was decided that the additional work could not be justified and the program was left in the form given here.)

D.3.2 Main Program

- a) The main program consists of 3 sections:
 - 2.1) Data Declaration
 - 2.2) Output of RLP Configuration Details

2.3) Calculations

- b) The names of the variables used in the program are the same as in Chapter 12. The names of all the angular variables, however, are followed by either D or R indicating degrees or radians respectively. Calculations are carried out in degrees where possible; those using Fortran functions, however, have to be carried out in radians. All distances are expressed in metres.

- c) Section 2.1 of the program is straightforward and can be understood from the listing. Note that statement 11 must be modified if the number of surfaces in the lens system is changed when the parameters are defined.

- d) Section 2.2 of the program prints the overall configuration parameters and lens system parameters for reference. Again, this section is straightforward and can be understood from the listing.

- e) Section 2.3 of the program carries out the calculations listed in step 2 of the analysis procedure, described in Chapter 12. Again, most of the program is straightforward; the following notes provide additional information.
 - i) The use of the NINT function in the calculation of NOPEN ensures that no errors are caused by the inexact way in which the values of MOAACI and OAACIN will be represented as real variables. (This function is also

used in the calculation of NORINP later in the program.)

- ii) For the calculation of ELPS when LTELPS < MELPSI, MNOI is the maximum number of increments of (2 x RSPINC) that can be fitted in LTELPS. It is found by truncating (LTELPS / (2 x RSPINC)). ELPS is then set to MNOI x (2 x RSPINC).
- iii) POIWNS is calculated by subroutine RAY from RSPR and OAAR; see section D.3.3.

D.3.3 Subroutine 'RAY'

- a) This subroutine calculates the POIWNS value for a ray from its OAAR and RSPR values by tracing the ray's path through the lens system.
- b) The ray paths have been defined by means of the (Q, U) method; this is one of several trigonometrical ray tracing methods that have been devised over the years. A description of the method can be found in references (109, 110); it is assumed here that the reader is familiar with this material.
- c) The subroutine is divided into four parts:
 - 3.1) Data Declaration
 - 3.2) 'Opening' Ray Calculations
 - 3.3) 'Refraction' and 'Transfer' Calculations

3.4) 'Closing' Ray Calculations

- d) The names of the variables used correspond to those given in reference (109), with the prime in the primed symbols replaced with a \$; for example Q\$ represents Q'. In addition, J is used to represent the surface number.
- e) Statement no. 12 in section 3.1 must be modified if the number of surfaces in the lens system is changed when the RLP parameters are defined.
- f) The opening, refraction, transfer and closing equations used correspond to those given in references (109, 110).
- g) In the opening ray calculations section, RSPR, LPFILS, LALSNS and OAAR are assigned to the appropriate variables using (Q,U) terminology.
- h) The refraction calculations are carried out by means of subroutine REFRCT; see section D.3.4. Note that the values of I, I\$, X and Y returned by REFRCT are not used in the version of the program given here.
- i) The closing calculations produce the value of H\$ which corresponds to the POIWNS value required; this value is returned to the main program.
- j) All of the values calculated for each surface are stored in arrays so that their values are still available after they

have been used to trace the ray's path through to the near screen. The program was written in this way in order that graphics subroutines for producing a ray-tracing plot could easily be added. Work was started on this but since the program had provided the required information, it was decided that the additional work could not be justified.

D.3.4 Subroutine 'REFRCT'

- a) This subroutine carries out the refraction calculations for a single ray at a single surface. It inputs the values of QJ, URJ, CJ, NJ and N\$J and returns the values of IRJ, I\$RJ, Q\$J, U\$RJ, XJ and YJ.
- b) The equations used for the calculations correspond to those given in references (109, 110).

D.4 Instructions for Using the Program

In order to run the program under TSO on the Group Computer, the user should carry out the following operations:

- a) Edit statement numbers 1 - 12 (using EDIT or SPF) in the source program (RLP.FORT) to change the reduced-length photometer parameters to the required values.
- b) Compile and link the program using the CLINKNW command.
- c) Run the program using the RUNFORT command.

D.5 Glossary of Main Program Variables

| | |
|--------|--|
| C(J) | Curvature of lens surface J |
| ELPS | Effective lamp size |
| LALSNS | Distance from last lens surface to near screen |
| LNSSZE | Lens system size |
| LNSTHK | Lens system thickness |
| LOAAC | Limiting value of OAAC |
| LPFILS | Distance from lamp to first lens surface |
| LPFS | Distance from lamp to far screen |
| LTELPS | Limiting value of ELPS |
| MAG | Magnification for central ray in pencil |
| MELPSI | Maximum ELPS of interest |
| MOAACI | Maximum OAAC of interest |
| N(J) | Refractive index of medium to left of lens surface J |
| N\$(J) | Refractive index of medium to right of lens surface J |
| NOPEN | Number of pencils |
| NORINP | Number of rays in pencil |
| NUMSRF | Number of lens surfaces |
| OAAC | Off-axis angle of central ray in pencil |
| OAACIN | Angular increment between central rays of successive pencils |
| OAAR | Off-axis angle of ray R in pencil |
| P | Pencil number |
| POIWFS | Point of intersection of pencil with far screen |
| POIWNS | Point of intersection of ray with near screen |
| R | Ray number |
| RSPINC | Ray starting point increment |
| RSPR | Starting point of ray number R |
| T(J) | Vertex spacing between lens surfaces J and (J+1) |

APPENDIX E

FOUR METRE REDUCED-LENGTH PHOTOMETER PERFORMANCE: BLUR PATCH DATA

TABLES

This Appendix contains the parameters and the blur patch data tables for the RLP configurations discussed in Chapter 13. The tables are produced from the printouts generated by running the RLP program; these printouts are given in reference (71).

E.1 Configuration 1

This is the configuration used in the E&D Automatic Photometer. Configuration lh and lv represent the horizontal and vertical planes respectively.

E.1.1 Configuration lh

E.1.1.1 Parameters

LPFS = 25.0 m
LPFILS = 0.56 m
LNSTHK = 0.022 m
LNSSZE = 0.436 m
LALSNS = 3.4262 m

NUMSRF = 2

$$C (1) = 0$$

$$N (1) = 1.0$$

$$N\$ (1) = 1.523$$

$$T (1) = 0.022$$

$$C (2) = -0.4780114$$

$$N (2) = 1.523$$

$$N\$ (2) = 1.0$$

E.1.1.2 Blur Patch Data

Configuration lh acts as a field stop for angles greater than 7° ; blur patch data tables are consequently not given.

E.1.2 Configuration lv

E.1.2.1 Parameters

As configuration lh except LNSSZE = 0.336 m

E.1.2.2 Blur Patch Data

Blur patch data is not given for this configuration.

E.2 Configuration 2

This is similar to configuration 1 but uses a larger, circular lens and a smaller LPFILS value. 2Y, 2R and 2B represent the same physical configuration but use the refractive indices for yellow light

(sodium D line), red light (hydrogen C line) and blue light (hydrogen F line) respectively. The parameters are the same for both the horizontal and vertical planes.

E.2.1 Configuration 2Y

E.2.1.1 Parameters

LPFS = 25.0 m
LPFILS = 0.4 m
LNSTHK = 0.035 m
LNSSZE = 0.48 m
LALSNS = 3.42271

NUMSRF = 2
C (1) = 0
N (1) = 1.0
N\$ (1) = 1.523
T (1) = 0.035

C (2) = -0.4780114
N (2) = 1.523
N\$ (2) = 1.0

E.2.1.2 Blur Patch Data

Blur patch data for the horizontal and vertical planes is given in tables E1 and E2 respectively.

E.2.2 Configuration 2R

E.2.2.1 Parameters

As configuration 2Y, except $N(1)$ and $N(2) = 1.52036$

E.2.2.2 Blur Patch Data

Blur patch data for the horizontal and vertical planes is given in tables E3 and E4 respectively.

E.2.3 Configuration 2B

E.2.3.1 Parameters

As configuration 2Y, except $N(1)$ and $N(2) = 1.52929$

E.2.3.2 Blur Patch Data

Blur patch data for the horizontal and vertical planes is given in tables E5 and E6 respectively.

E.2.4 Notes

- a) LALSNS is calculated using the method given in section 12.3.
- b) Paraxial magnification = 0.1393 for yellow light; this value is used to calculate the 'Required POIWNS' values for all three colours.

E.3 Configuration 3Y

This is the same as configuration 2Y, but with the convex surface of the lens facing the lamp.

E.3.1 Parameters

LPFS = 25.0 m
LPFILS = 0.4 m
LNSTHK = 0.035 m
LNSSZE = 0.48 m
LALSNS = 3.42271

NUMSRF = 2
C(1) = 0.4780114
N(1) = 1.0
N\$(1) = 1.523
T(1) = 0.035

C(2) = 0
N(2) = 1.523
N\$(2) = 1.0

E.3.2 Blur Patch Data

Only the blur patch data for the horizontal plane is given; see table E7.

E.3.3 Notes

a) Paraxial magnification = 0.1400

E.4 Configuration 4

Configurations 4Y, 4R and 4B are the same as 2Y, 2R and 2B except that they use a smaller LALSNS value.

E.4.1 Configuration 4Y

E.4.1.1 Parameters

As configuration 2Y, except LALSNS = 3.395 m

E.4.1.2 Blur Patch Data

Blur patch data for the horizontal and vertical planes is given in tables E8 and E9 respectively.

E.4.2 Configuration 4R

E.4.2.1 Parameters

As configuration 2R, except LALSNS = 3.395 m

E.4.2.2 Blur Patch Data

Blur patch data for the horizontal and vertical planes is given in tables E10 and E11 respectively.

E.4.3 Configuration 4B

E.4.3.1 Parameters

As configuration 2B, except LALSNS = 3.395 m

E.4.3.2 Blur Patch Data

Blur patch data for the horizontal and vertical planes is given in tables E12 and E13 respectively.

E.4.4 Notes

- a) Paraxial magnification = 0.1384 for yellow light; this value is used to calculate the 'Required POIWNS' values for all three colours.

| OAAC | REQD POIWNS | MIN POIWNS | MAX POIWNS | MAX POIWNS -MIN POIWNS | MIN POIWNS -REQD POIWNS | MAX POIWNS -REQD POIWNS |
|------|-------------|------------|------------|---------------------------|----------------------------|----------------------------|
| 0 | 0.0000 | -0.0003 | 0.0003 | 0.0006 | -0.0003 | 0.0003 |
| -1 | 0.0608 | 0.0606 | 0.0613 | 0.0007 | -0.0002 | 0.0005 |
| -2 | 0.1216 | 0.1215 | 0.1225 | 0.0010 | -0.0001 | 0.0009 |
| -3 | 0.1825 | 0.1825 | 0.1839 | 0.0014 | 0.0000 | 0.0014 |
| -4 | 0.2435 | 0.2434 | 0.2453 | 0.0019 | -0.0001 | 0.0018 |
| -5 | 0.3047 | 0.3044 | 0.3070 | 0.0026 | -0.0003 | 0.0023 |
| -6 | 0.3660 | 0.3655 | 0.3688 | 0.0033 | -0.0005 | 0.0028 |
| -7 | 0.4276 | 0.4266 | 0.4309 | 0.0043 | -0.0010 | 0.0033 |
| -8 | 0.4894 | 0.4878 | 0.4932 | 0.0054 | -0.0016 | 0.0038 |
| -9 | 0.5516 | 0.5490 | 0.5557 | 0.0067 | -0.0028 | 0.0041 |
| -10 | 0.6141 | 0.6104 | 0.6185 | 0.0081 | -0.0037 | 0.0044 |
| -11 | 0.6769 | 0.6720 | 0.6777 | 0.0057 | -0.0049 | 0.0008 |
| -12 | 0.7402 | 0.7337 | 0.7406 | 0.0069 | -0.0065 | 0.0004 |
| -13 | 0.8040 | 0.7956 | 0.8038 | 0.0082 | -0.0084 | -0.0002 |
| -14 | 0.8683 | 0.8577 | 0.8674 | 0.0097 | -0.0106 | -0.0009 |
| -15 | 0.9331 | 0.9200 | 0.9312 | 0.0112 | -0.0131 | -0.0019 |
| -16 | 0.9986 | 0.9826 | 0.9955 | 0.0129 | -0.0160 | -0.0031 |
| -17 | 1.0647 | 1.0454 | 1.0601 | 0.0147 | -0.0193 | -0.0046 |
| -18 | 1.1315 | 1.1086 | 1.1251 | 0.0165 | -0.0229 | -0.0064 |

Table E1 Blur Patch Data for RLP Configuration 2Y, Horizontal Plane

| OAAC | REQD POIWNS | MIN POIWNS | MAX POIWNS | MAX POIWNS -MIN POIWNS | MIN POIWNS -REQD POIWNS | MAX POIWNS -REQD POIWNS |
|------|-------------|------------|------------|---------------------------|----------------------------|----------------------------|
| 0 | 0.0000 | -0.0003 | 0.0003 | 0.0006 | -0.0003 | 0.0003 |
| -1 | 0.0608 | 0.0606 | 0.0611 | 0.0005 | -0.0002 | 0.0003 |
| -2 | 0.1216 | 0.1215 | 0.1220 | 0.0005 | -0.0001 | 0.0004 |
| -3 | 0.1825 | 0.1825 | 0.1828 | 0.0003 | 0.0000 | 0.0003 |
| -4 | 0.2435 | 0.2434 | 0.2438 | 0.0004 | -0.0001 | 0.0003 |
| -5 | 0.3047 | 0.3044 | 0.3051 | 0.0007 | -0.0003 | 0.0004 |
| -6 | 0.3660 | 0.3655 | 0.3665 | 0.0010 | -0.0005 | 0.0005 |
| -7 | 0.4276 | 0.4266 | 0.4281 | 0.0015 | -0.0010 | 0.0005 |
| -8 | 0.4894 | 0.4878 | 0.4899 | 0.0021 | -0.0016 | 0.0005 |
| -9 | 0.5516 | 0.5491 | 0.5519 | 0.0028 | -0.0025 | 0.0003 |
| -10 | 0.6141 | 0.6105 | 0.6141 | 0.0036 | -0.0036 | 0.0000 |
| -11 | 0.6769 | 0.6721 | 0.6766 | 0.0045 | -0.0048 | -0.0003 |
| -12 | 0.7402 | 0.7339 | 0.7393 | 0.0054 | -0.0063 | -0.0009 |

Table E2 Blur Patch Data for RLP Configuration 2Y, Vertical Plane

| OAAC | REQD POIWNs | MIN POIWNs | MAX POIWNs | MAX POIWNs -MIN POIWNs | MIN POIWNs -REQD POIWNs | MAX POIWNs -REQD POIWNs |
|------|-------------|------------|------------|---------------------------|----------------------------|----------------------------|
| 0 | 0.0000 | -0.0007 | 0.0007 | 0.0014 | -0.0007 | 0.0007 |
| -1 | 0.0608 | 0.0603 | 0.0616 | 0.0013 | -0.0005 | 0.0008 |
| -2 | 0.1216 | 0.1213 | 0.1226 | 0.0013 | -0.0003 | 0.0010 |
| -3 | 0.1825 | 0.1824 | 0.1836 | 0.0012 | -0.0001 | 0.0011 |
| -4 | 0.2435 | 0.2435 | 0.2448 | 0.0013 | 0.0000 | 0.0013 |
| -5 | 0.3047 | 0.3046 | 0.3065 | 0.0019 | -0.0001 | 0.0018 |
| -6 | 0.3660 | 0.3658 | 0.3684 | 0.0026 | -0.0002 | 0.0024 |
| -7 | 0.4276 | 0.4270 | 0.4304 | 0.0034 | -0.0006 | 0.0028 |
| -8 | 0.4894 | 0.4883 | 0.4927 | 0.0044 | -0.0011 | 0.0033 |
| -9 | 0.5516 | 0.5497 | 0.5553 | 0.0056 | -0.0019 | 0.0037 |
| -10 | 0.6141 | 0.6112 | 0.6181 | 0.0069 | -0.0029 | 0.0040 |
| -11 | 0.6769 | 0.6728 | 0.6777 | 0.0049 | -0.0041 | 0.0008 |
| -12 | 0.7402 | 0.7345 | 0.7406 | 0.0061 | -0.0057 | 0.0004 |
| -13 | 0.8040 | 0.7964 | 0.8038 | 0.0072 | -0.0076 | -0.0002 |
| -14 | 0.8683 | 0.8586 | 0.8674 | 0.0088 | -0.0097 | -0.0009 |
| -15 | 0.9331 | 0.9210 | 0.9313 | 0.0103 | -0.0121 | -0.0018 |
| -16 | 0.9986 | 0.9836 | 0.9956 | 0.0120 | -0.0150 | -0.0030 |
| -17 | 1.0647 | 1.0465 | 1.0602 | 0.0137 | -0.0182 | -0.0045 |
| -18 | 1.1315 | 1.1097 | 1.1253 | 0.0156 | -0.0218 | -0.0062 |

Table E3 Blur Patch Data for RLP Configuration 2R, Horizontal Plane

| OAAC | REQD POIWNS | MIN POIWNS | MAX POIWNS | MAX POIWNS -MIN POIWNS | MIN POIWNS -REQD POIWNS | MAX POIWNS -REQD POIWNS |
|------|-------------|------------|------------|---------------------------|----------------------------|----------------------------|
| 0 | 0.0000 | -0.0006 | 0.0006 | 0.0012 | -0.0006 | 0.0006 |
| -1 | 0.0608 | 0.0603 | 0.0615 | 0.0012 | -0.0005 | 0.0007 |
| -2 | 0.1216 | 0.1213 | 0.1224 | 0.0011 | -0.0003 | 0.0008 |
| -3 | 0.1825 | 0.1824 | 0.1833 | 0.0009 | -0.0001 | 0.0008 |
| -4 | 0.2435 | 0.2435 | 0.2442 | 0.0007 | 0.0000 | 0.0007 |
| -5 | 0.3047 | 0.3046 | 0.3051 | 0.0005 | -0.0001 | 0.0004 |
| -6 | 0.3660 | 0.3658 | 0.3664 | 0.0006 | -0.0002 | 0.0004 |
| -7 | 0.4276 | 0.4270 | 0.4280 | 0.0010 | -0.0006 | 0.0004 |
| -8 | 0.4894 | 0.4883 | 0.4898 | 0.0015 | -0.0011 | 0.0004 |
| -9 | 0.5516 | 0.5497 | 0.5518 | 0.0021 | -0.0019 | 0.0002 |
| -10 | 0.6141 | 0.6112 | 0.6141 | 0.0029 | -0.0029 | 0.0000 |
| -11 | 0.6769 | 0.6728 | 0.6766 | 0.0038 | -0.0041 | -0.0003 |
| -12 | 0.7402 | 0.7346 | 0.7393 | 0.0047 | -0.0056 | -0.0009 |

Table E4 Blur Patch Data for RLP Configuration 2R, Vertical Plane

| OAAC | REQD POIWNS | MIN POIWNS | MAX POIWNS | MAX POIWNS -MIN POIWNS | MIN POIWNS -REQD POIWNS | MAX POIWNS -REQD POIWNS |
|------|-------------|------------|------------|---------------------------|----------------------------|----------------------------|
| 0 | 0.0000 | -0.0017 | 0.0017 | 0.0034 | -0.0017 | 0.0017 |
| -1 | 0.0608 | 0.0593 | 0.0627 | 0.0034 | -0.0015 | 0.0019 |
| -2 | 0.1216 | 0.1202 | 0.1239 | 0.0037 | -0.0014 | 0.0023 |
| -3 | 0.1825 | 0.1811 | 0.1852 | 0.0041 | -0.0014 | 0.0027 |
| -4 | 0.2435 | 0.2420 | 0.2466 | 0.0046 | -0.0015 | 0.0031 |
| -5 | 0.3047 | 0.3029 | 0.3082 | 0.0053 | -0.0018 | 0.0035 |
| -6 | 0.3660 | 0.3638 | 0.3699 | 0.0061 | -0.0022 | 0.0039 |
| -7 | 0.4276 | 0.4247 | 0.4319 | 0.0072 | -0.0029 | 0.0043 |
| -8 | 0.4894 | 0.4857 | 0.4941 | 0.0084 | -0.0037 | 0.0047 |
| -9 | 0.5516 | 0.5468 | 0.5566 | 0.0098 | -0.0048 | 0.0050 |
| -10 | 0.6141 | 0.6080 | 0.6193 | 0.0113 | -0.0061 | 0.0052 |
| -11 | 0.6769 | 0.6700 | 0.6779 | 0.0079 | -0.0069 | 0.0010 |
| -12 | 0.7402 | 0.7317 | 0.7407 | 0.0090 | -0.0085 | 0.0005 |
| -13 | 0.8040 | 0.7935 | 0.8039 | 0.0104 | -0.0105 | -0.0001 |
| -14 | 0.8683 | 0.8555 | 0.8673 | 0.0118 | -0.0128 | -0.0010 |
| -15 | 0.9331 | 0.9177 | 0.9311 | 0.0134 | -0.0154 | -0.0020 |
| -16 | 0.9986 | 0.9802 | 0.9952 | 0.0150 | -0.0184 | -0.0034 |
| -17 | 1.0647 | 1.0429 | 1.0597 | 0.0168 | -0.0218 | -0.0050 |
| -18 | 1.1315 | 1.1059 | 1.1246 | 0.0187 | -0.0256 | -0.0069 |

Table E5 Blur Patch Data for RLP Configuration 2B, Horizontal Plane

| OAAC | REQD POIWNS | MIN POIWNS | MAX POIWNS | MAX POIWNS -MIN POIWNS | MIN POIWNS -REQD POIWNS | MAX POIWNS -REQD POIWNS |
|------|-------------|------------|------------|---------------------------|----------------------------|----------------------------|
| 0 | 0.0000 | -0.0005 | 0.0005 | 0.0010 | -0.0005 | 0.0005 |
| -1 | 0.0608 | 0.0602 | 0.0614 | 0.0012 | -0.0006 | 0.0006 |
| -2 | 0.1216 | 0.1210 | 0.1223 | 0.0013 | -0.0006 | 0.0007 |
| -3 | 0.1825 | 0.1818 | 0.1832 | 0.0014 | -0.0007 | 0.0007 |
| -4 | 0.2435 | 0.2426 | 0.2443 | 0.0017 | -0.0009 | 0.0008 |
| -5 | 0.3047 | 0.3034 | 0.3055 | 0.0021 | -0.0013 | 0.0008 |
| -6 | 0.3660 | 0.3643 | 0.3669 | 0.0026 | -0.0017 | 0.0009 |
| -7 | 0.4276 | 0.4253 | 0.4284 | 0.0031 | -0.0023 | 0.0008 |
| -8 | 0.4894 | 0.4864 | 0.4901 | 0.0037 | -0.0030 | 0.0007 |
| -9 | 0.5516 | 0.5476 | 0.5520 | 0.0044 | -0.0040 | 0.0004 |
| -10 | 0.6141 | 0.6089 | 0.6141 | 0.0052 | -0.0052 | 0.0000 |
| -11 | 0.6769 | 0.6704 | 0.6765 | 0.0061 | -0.0065 | -0.0004 |
| -12 | 0.7402 | 0.7321 | 0.7392 | 0.0071 | -0.0081 | -0.0010 |

Table E6 Blur Patch Data for RLP Configuration 2B, Vertical Plane

| OAAC | REQD POIWNs | MIN POIWNs | MAX POIWNs | MAX POIWNs -MIN POIWNs | MIN POIWNs -REQD POIWNs | MAX POIWNs -REQD POIWNs |
|------|-------------|------------|------------|---------------------------|----------------------------|----------------------------|
| 0 | 0.0000 | -0.0004 | 0.0004 | -0.0008 | -0.0004 | 0.0004 |
| -1 | 0.0611 | 0.0606 | 0.0616 | 0.0010 | -0.0005 | 0.0005 |
| -2 | 0.1222 | 0.1216 | 0.1229 | 0.0013 | -0.0006 | 0.0007 |
| -3 | 0.1834 | 0.1823 | 0.1844 | 0.0021 | -0.0011 | 0.0010 |
| -4 | 0.2447 | 0.2430 | 0.2461 | 0.0031 | -0.0017 | 0.0014 |
| -5 | 0.3062 | 0.3037 | 0.3081 | 0.0044 | -0.0025 | 0.0019 |
| -6 | 0.3679 | 0.3642 | 0.3702 | 0.0060 | -0.0037 | 0.0023 |
| -7 | 0.4297 | 0.4247 | 0.4326 | 0.0079 | -0.0050 | 0.0029 |
| -8 | 0.4919 | 0.4851 | 0.4953 | 0.0102 | -0.0068 | 0.0034 |
| -9 | 0.5543 | 0.5455 | 0.5583 | 0.0128 | -0.0088 | 0.0040 |
| -10 | 0.6171 | 0.6059 | 0.6215 | 0.0156 | -0.0112 | 0.0044 |
| -11 | 0.6803 | 0.6695 | 0.6819 | 0.0124 | -0.0108 | 0.0016 |
| -12 | 0.7439 | 0.7304 | 0.7453 | 0.0149 | -0.0135 | 0.0014 |
| -13 | 0.8080 | 0.7914 | 0.8089 | 0.0175 | -0.0166 | 0.0009 |
| -14 | 0.8726 | 0.8524 | 0.8728 | 0.0204 | -0.0202 | 0.0002 |
| -15 | 0.9378 | 0.9135 | 0.9371 | 0.0236 | -0.0243 | -0.0005 |
| -16 | 1.0036 | 0.9746 | 1.0017 | 0.0271 | -0.0290 | -0.0019 |
| -17 | 1.0701 | 1.0358 | 1.0666 | 0.0308 | -0.0343 | -0.0035 |
| -18 | 1.1372 | 1.0970 | 1.1319 | 0.0349 | -0.0402 | -0.0053 |

Table E7 Blur Patch Data for RLP Configuration 3Y, Horizontal Plane

| OAAC | REQD POIWNS | MIN POIWNS | MAX POIWNS | MAX POIWNS -MIN POIWNS | MIN POIWNS -REQD POIWNS | MAX POIWNS -REQD POIWNS |
|------|-------------|------------|------------|---------------------------|----------------------------|----------------------------|
| 0 | 0.0000 | -0.0011 | 0.0011 | 0.0022 | -0.0011 | 0.0011 |
| -1 | 0.0604 | 0.5596 | 0.0617 | 0.0021 | -0.0008 | 0.0013 |
| -2 | 0.1208 | 0.1201 | 0.1222 | 0.0021 | -0.0007 | 0.0014 |
| -3 | 0.1813 | 0.1807 | 0.1828 | 0.0021 | -0.0006 | 0.0015 |
| -4 | 0.2419 | 0.2414 | 0.2433 | 0.0019 | -0.0005 | 0.0014 |
| -5 | 0.3027 | 0.3021 | 0.3038 | 0.0017 | -0.0006 | 0.0011 |
| -6 | 0.3636 | 0.3629 | 0.3650 | 0.0021 | -0.0007 | 0.0014 |
| -7 | 0.4248 | 0.4238 | 0.4266 | 0.0028 | -0.0010 | 0.0018 |
| -8 | 0.4862 | 0.4847 | 0.4884 | 0.0037 | -0.0015 | 0.0022 |
| -9 | 0.5480 | 0.5457 | 0.5505 | 0.0048 | -0.0023 | 0.0025 |
| -10 | 0.6101 | 0.6068 | 0.6129 | 0.0061 | -0.0033 | 0.0028 |
| -11 | 0.6725 | 0.6680 | 0.6721 | 0.0041 | -0.0045 | -0.0004 |
| -12 | 0.7354 | 0.7292 | 0.7346 | 0.0054 | -0.0062 | -0.0008 |
| -13 | 0.7988 | 0.7907 | 0.7973 | 0.0066 | -0.0081 | -0.0015 |
| -14 | 0.8627 | 0.8524 | 0.8604 | 0.0080 | -0.0103 | -0.0023 |
| -15 | 0.9271 | 0.9143 | 0.9238 | 0.0095 | -0.0128 | -0.0033 |
| -16 | 0.9921 | 0.9764 | 0.9876 | 0.0112 | -0.0157 | -0.0045 |
| -17 | 1.0578 | 1.0388 | 1.0518 | 0.0130 | -0.0190 | -0.0060 |
| -18 | 1.1242 | 1.1015 | 1.1163 | 0.0148 | -0.0227 | -0.0079 |

Table E8 Blur Patch Data for RLP Configuration 4Y, Horizontal Plane

| QAAC | REQD POIWNs | MIN POIWNs | MAX POIWNs | MAX POIWNs -MIN POIWNs | MIN POIWNs -REQD POIWNs | MAX POIWNs -REQD POIWNs |
|------|-------------|------------|------------|---------------------------|----------------------------|----------------------------|
| 0 | 0.0000 | -0.0009 | 0.0009 | 0.0018 | -0.0009 | 0.0009 |
| -1 | 0.0604 | 0.0596 | 0.0613 | 0.0017 | -0.0008 | 0.0009 |
| -2 | 0.1208 | 0.1201 | 0.1217 | 0.0016 | -0.0007 | 0.0009 |
| -3 | 0.1813 | 0.1807 | 0.1822 | 0.0015 | -0.0006 | 0.0009 |
| -4 | 0.2419 | 0.2414 | 0.2426 | 0.0012 | -0.0005 | 0.0007 |
| -5 | 0.3027 | 0.3021 | 0.3031 | 0.0010 | -0.0006 | 0.0004 |
| -6 | 0.3636 | 0.3629 | 0.3636 | 0.0007 | -0.0007 | 0.0000 |
| -7 | 0.4248 | 0.4238 | 0.4244 | 0.0006 | -0.0010 | -0.0004 |
| -8 | 0.4862 | 0.4847 | 0.4858 | 0.0011 | -0.0015 | -0.0004 |
| -9 | 0.5480 | 0.5457 | 0.5473 | 0.0016 | -0.0023 | -0.0007 |
| -10 | 0.6101 | 0.6068 | 0.6091 | 0.0023 | -0.0033 | -0.0010 |
| -11 | 0.6725 | 0.6680 | 0.6711 | 0.0031 | -0.0045 | -0.0014 |
| -12 | 0.7354 | 0.7293 | 0.7334 | 0.0041 | -0.0061 | -0.0020 |

Table E9 Blur Patch Data for RLP Configuration 4Y, Vertical Plane

| OAAC | REQD POIWNS | MIN POIWNS | MAX POIWNS | MAX POIWNS - MIN POIWNS | MIN POIWNS - REQD POIWNS | MAX POIWNS - REQD POIWNS |
|------|-------------|------------|------------|-------------------------------|--------------------------------|--------------------------------|
| 0 | 0.0000 | -0.0017 | 0.0017 | 0.0034 | -0.0017 | 0.0017 |
| -1 | 0.0604 | 0.0590 | 0.0623 | 0.0033 | -0.0014 | 0.0019 |
| -2 | 0.1208 | 0.1197 | 0.1229 | 0.0032 | -0.0011 | 0.0021 |
| -3 | 0.1813 | 0.1804 | 0.1835 | 0.0031 | -0.0009 | 0.0022 |
| -4 | 0.2419 | 0.2412 | 0.2440 | 0.0028 | -0.0007 | 0.0021 |
| -5 | 0.3027 | 0.3021 | 0.3046 | 0.0025 | -0.0006 | 0.0019 |
| -6 | 0.3636 | 0.3630 | 0.3652 | 0.0022 | -0.0006 | 0.0016 |
| -7 | 0.4248 | 0.4239 | 0.4262 | 0.0023 | -0.0009 | 0.0014 |
| -8 | 0.4862 | 0.4850 | 0.4880 | 0.0030 | -0.0012 | 0.0018 |
| -9 | 0.5480 | 0.5461 | 0.5502 | 0.0041 | -0.0019 | 0.0022 |
| -10 | 0.6101 | 0.6073 | 0.6125 | 0.0052 | -0.0028 | 0.0024 |
| -11 | 0.6725 | 0.6686 | 0.6720 | 0.0034 | -0.0039 | -0.0005 |
| -12 | 0.7354 | 0.7301 | 0.7345 | 0.0044 | -0.0053 | -0.0009 |
| -13 | 0.7988 | 0.7916 | 0.7973 | 0.0057 | -0.0072 | -0.0015 |
| -14 | 0.8627 | 0.8533 | 0.8604 | 0.0071 | -0.0094 | -0.0023 |
| -15 | 0.9271 | 0.9152 | 0.9239 | 0.0087 | -0.0119 | -0.0032 |
| -16 | 0.9921 | 0.9774 | 0.9877 | 0.0103 | -0.0147 | -0.0044 |
| -17 | 1.0578 | 1.0399 | 1.0519 | 0.0120 | -0.0179 | -0.0059 |
| -18 | 1.1242 | 1.1026 | 1.1165 | 0.0139 | -0.0216 | -0.0077 |

Table E10 Blur Patch Data for RLP Configuration 4R, Horizontal Plane

| OAAC | REQD POIWNs | MIN POIWNs | MAX POIWNs | MAX POIWNs -MIN POIWNs | MIN POIWNs -REQD POIWNs | MAX POIWNs -REQD POIWNs |
|------|-------------|------------|------------|---------------------------|----------------------------|----------------------------|
| 0 | 0.0000 | -0.0012 | 0.0012 | 0.0024 | -0.0012 | 0.0012 |
| -1 | 0.0604 | 0.0593 | 0.0617 | 0.0024 | -0.0011 | 0.0013 |
| -2 | 0.1208 | 0.1198 | 0.1221 | 0.0023 | -0.0010 | 0.0013 |
| -3 | 0.1813 | 0.1805 | 0.1826 | 0.0021 | -0.0008 | 0.0013 |
| -4 | 0.2419 | 0.2412 | 0.2431 | 0.0019 | -0.0007 | 0.0012 |
| -5 | 0.3027 | 0.3021 | 0.3036 | 0.0015 | -0.0006 | 0.0009 |
| -6 | 0.3636 | 0.3630 | 0.3641 | 0.0011 | -0.0006 | 0.0005 |
| -7 | 0.4248 | 0.4239 | 0.4248 | 0.0009 | -0.0009 | 0.0000 |
| -8 | 0.4862 | 0.4850 | 0.4857 | 0.0007 | -0.0012 | -0.0005 |
| -9 | 0.5480 | 0.5461 | 0.5473 | 0.0012 | -0.0019 | -0.0007 |
| -10 | 0.6101 | 0.6073 | 0.6091 | 0.0018 | -0.0028 | -0.0010 |
| -11 | 0.6725 | 0.6686 | 0.6711 | 0.0025 | -0.0039 | -0.0014 |
| -12 | 0.7354 | 0.7301 | 0.7334 | 0.0033 | -0.0053 | -0.0020 |

Table E11 Blur Patch Data for RLP Configuration 4R, Vertical Plane

| OAAC | REQD POIWNS | MIN POIWNS | MAX POIWNS | MAX POIWNS -MIN POIWNS | MIN POIWNS -REQD POIWNS | MAX POIWNS -REQD POIWNS |
|------|-------------|------------|------------|---------------------------|----------------------------|----------------------------|
| 0 | 0.0000 | -0.0005 | 0.0005 | 0.0010 | -0.0005 | 0.0005 |
| -1 | 0.0604 | 0.0601 | 0.0611 | 0.0010 | -0.0003 | 0.0007 |
| -2 | 0.1208 | 0.1206 | 0.1218 | 0.0012 | -0.0002 | 0.0010 |
| -3 | 0.1813 | 0.1810 | 0.1827 | 0.0017 | -0.0003 | 0.0014 |
| -4 | 0.2419 | 0.2414 | 0.2436 | 0.0022 | -0.0005 | 0.0017 |
| -5 | 0.3027 | 0.3018 | 0.3048 | 0.0030 | -0.0009 | 0.0021 |
| -6 | 0.3636 | 0.3623 | 0.3661 | 0.0038 | -0.0013 | 0.0025 |
| -7 | 0.4248 | 0.4229 | 0.4276 | 0.0047 | -0.0019 | 0.0028 |
| -8 | 0.4862 | 0.4835 | 0.4894 | 0.0059 | -0.0027 | 0.0032 |
| -9 | 0.5480 | 0.5441 | 0.5514 | 0.0073 | -0.0039 | 0.0034 |
| -10 | 0.6101 | 0.6049 | 0.6137 | 0.0088 | -0.0052 | 0.0036 |
| -11 | 0.6725 | 0.6661 | 0.6723 | 0.0062 | -0.0064 | -0.0002 |
| -12 | 0.7354 | 0.7273 | 0.7347 | 0.0074 | -0.0081 | -0.0007 |
| -13 | 0.7988 | 0.7886 | 0.7973 | 0.0087 | -0.0102 | -0.0015 |
| -14 | 0.8627 | 0.8502 | 0.8603 | 0.0101 | -0.0125 | 0.0024 |
| -15 | 0.9271 | 0.9120 | 0.9237 | 0.0117 | -0.0151 | 0.0034 |
| -16 | 0.9921 | 0.9740 | 0.9873 | 0.0133 | -0.0181 | 0.0048 |
| -17 | 1.0578 | 1.0363 | 1.0514 | 0.0151 | -0.0215 | 0.0064 |
| -18 | 1.1242 | 1.0989 | 1.1158 | 0.0169 | -0.0253 | 0.0084 |

Table E12 Blur Patch Data for RLP Configuration 4B, Horizontal Plane

| OAAC | REQD POIWNS | MIN POIWNS | MAX POIWNS | MAX POIWNS -MIN POIWNS | MIN POIWNS -REQD POIWNS | MAX POIWNS -REQD POIWNS |
|------|-------------|------------|------------|---------------------------|----------------------------|----------------------------|
| 0 | 0.0000 | -0.0001 | 0.0001 | 0.0002 | -0.0001 | 0.0001 |
| -1 | 0.0604 | 0.0602 | 0.0605 | 0.0003 | -0.0002 | 0.0001 |
| -2 | 0.1208 | 0.1206 | 0.1208 | 0.0002 | -0.0002 | 0.0000 |
| -3 | 0.1813 | 0.1810 | 0.1813 | 0.0003 | -0.0003 | 0.0000 |
| -4 | 0.2419 | 0.2414 | 0.2420 | 0.0006 | -0.0005 | 0.0001 |
| -5 | 0.3027 | 0.3018 | 0.3027 | 0.0009 | -0.0009 | 0.0000 |
| -6 | 0.3636 | 0.3623 | 0.3636 | 0.0013 | -0.0013 | 0.0000 |
| -7 | 0.4248 | 0.4229 | 0.4247 | 0.0018 | -0.0019 | -0.0001 |
| -8 | 0.4862 | 0.4835 | 0.4860 | 0.0025 | -0.0027 | -0.0002 |
| -9 | 0.5480 | 0.5443 | 0.5474 | 0.0031 | -0.0037 | -0.0006 |
| -10 | 0.6101 | 0.6052 | 0.6091 | 0.0039 | -0.0049 | -0.0010 |
| -11 | 0.6725 | 0.6663 | 0.6711 | 0.0048 | -0.0062 | -0.0014 |
| -12 | 0.7354 | 0.7275 | 0.7333 | 0.0058 | -0.0079 | -0.0021 |

Table E13 Blur Patch Data for RLP Configuration 4B, Vertical Plane

APPENDIX F

IMAGE PROCESSING EQUIPMENT CONSIDERED

The image processing equipment which was considered, and from which the short list of equipment given in section 15.5.2 was produced, is given below. The addresses of the manufacturers can be found in reference (73).

- a) Analog Devices IVS-100 Vision System
- b) British Robotic Systems Ltd Autoview Systems
- c) Colorado Video Inc Frame Stores
- d) Compression Labs Inc Vicom System
- e) Computer Recognition Systems Ltd Series 4000 Frame Stores
- f) Data-Sud Systemes VME Bus Boards
- g) Dindima Group Proprietary Ltd Arlunya TF4000 Series Frame Stores
- h) Gems of Cambridge Ltd Gems System 33
- i) General Automation Erascop 600 System
- j) Gould Inc DeAnza Systems

- k) Gresham Lion (PPL) Ltd Supervisor 214 System
- l) Grinell Graphics Systems
- m) Hakuto MV Series Frame Stores
- n) Hamamatsu TV Europa Digitizer HTV-C 1500
- o) Hughes Aircraft Company Anaram 90 Series System
- p) International Imaging Systems Model 75 System
- q) Microconsultants Intellect Systems
- r) Nihon Regulator Co Ltd Luzex 500 Image Analyser

APPENDIX G

THE AUTOMATIC PHOTOMETER/GROUP COMPUTER FILE TRANSFER SYSTEM

G.1 Introduction

It is assumed here that the reader is familiar with the concepts of data communications; see reference (111), for example.

The file transfer facility was required for the photometric data processing scheme described in Chapter 14; the basic requirement was the ability to create a dataset on the IBM mainframe at the Shirley site, using the Time Sharing Option (TSO), containing the data from an Automatic Photometer 'result' file (see section 6.2).

It was decided to use a simple teletype emulation protocol (running at 1200 baud) for transmitting the data to the mainframe since this could be implemented with minimal modifications to the existing communications link; more sophisticated protocols or higher speeds would have required a second private wire between the Cannock and Shirley sites, which was ruled out by cost and time considerations. Despite the use of a simple protocol, a sophisticated error checking and correction capability was provided by means of the intelligent multiplexers used in the communications link.

Unlike the data originating from a real teletype, the data bytes contained in the Automatic Photometer 'result' files can have any value from 00H to FFH, where H represents a hexadecimal number. Not all of these values can be accepted by the mainframe as valid

characters, and a method of recoding the data was required. The method chosen by the author was to split each data byte into two four-bit 'nibbles', each represented by an acceptable byte value i.e. one corresponding to a printable ASCII character. A further consequence of the fact that the data to be transmitted does not originate from a real teletype is that it is not organised in lines terminated by line-end characters.

The following were required to implement the system:

- a) Modifications to the communications link between the two sites.
- b) Teletype emulation software for the Automatic Photometer microcomputer, the purpose of this being to transmit stored data to the mainframe as though it were being sent from a teletype. A standard CP/M based package, modified to suit the application (by the suppliers) was to be purchased.
- c) Software for the mainframe to receive and store the data.
This was to consist of 4 parts:
 - i) The software which runs on the mainframe's front-end-processor. This was IBM's 'TCAM' at the start of the project but was later changed to 'NTO'; see later.
 - ii) An application program to receive the characters from TCAM and store them in an intermediate dataset, containing 2 characters for every one in the original

Automatic Photometer file. A modified version of an existing TSO program (YJPWPIN) was to be used.

- iii) A program to input the data from the intermediate dataset and produce an output dataset equivalent to the original Automatic Photometer file by re-combining each pair of bytes into a single byte in accordance with the data coding scheme. This was to be custom written.
- iv) A command list (i.e. a CLIST) to run the programs described in (ii) and (iii).

G.2 Implementation

A summary of the work which was carried out to implement the file transfer system is given below; the work was undertaken by the author unless stated otherwise.

- a) The communications link was modified by Group Computing.
- b) The link was interfaced to the RS232C port on the SBC-104 board of the Automatic Photometer's micro-computer by the author and Group Computing.
- c) The 'YJPWPIN' program was modified for use with the Automatic Photometer by Group Computing.

- d) A specification for the teletype emulator software required for the Automatic Photometer was written.

The main requirements were:

- i) It should enable the console of the Automatic Photometer to be operated as a conventional TSO terminal.
- ii) It should enable non-character files (i.e those in which the data bytes can have any value from 00H to FFH and are not organised in lines with line-end characters) to be transmitted by sending each byte as two printable ASCII characters in accordance with the devised data coding scheme and in records of a convenient length (128 bytes was used in the final system).
- iii) It should allow file transmission to be aborted if required; the transmission time can be up to 1 hour because of the lengths of the files and the relatively slow transmission speed of 1200 baud.
- e) Various commercially available teletype emulator software packages for CP/M systems were assessed. The 'TTY' package was chosen because its producers, Systematica, were British and were prepared to carry out the modifications required to transmit non-character data files at a reasonable cost.

- f) The modified 'TTY' package was supplied by Systematica and was tested with 'YJPWIN' and 'TCAM' to produce intermediate TSO datasets from the Automatic Photometer files. Various problems were found. Most of these were clearly caused by 'bugs' in TTY; Systematica found these and supplied details of the required object code patches for implementation by the author. They were unable to find the cause of the most serious problem, however, this being that large files would only be partially transmitted; the system would simply 'hang-up' before all of the records in the file had been sent. It was not clear at this stage whether the problem was being caused by 'TTY', the communications link, 'YJPWIN' or 'TCAM'.
- g) Extensive testing, carried out in conjunction with Group Computing, established that the fault was almost certainly being caused by 'TTY'.
- h) Systematica were still unable to find the reason why TTY was causing the problem, but supplied a simplified file transfer package ('SEND') complete with assembly language listing for testing. This did not handshake correctly with the mainframe as supplied but various modifications were made (by the author) and a working version produced; this enabled large files to be transmitted successfully, thereby proving that this problem was being caused by 'TTY'.
- i) Further extensive testing revealed a new problem, however; occasionally, a few records, although apparently received and

acknowledged by TSO, would not be present when the stored dataset was examined. This time, the problem appeared to lie with 'TCAM'. Unfortunately, the Group Computing programmers were not sufficiently familiar with this software to understand the exact failure mechanism or suggest how it could be overcome. TCAM was scheduled for replacement, however, by the more modern and sophisticated 'NTO' as part of a general systems upgrade and it was suggested that work was suspended until NTO had been installed.

- j) Work continued when 'NTO' had been commissioned. The combination of 'SEND', 'YJPWPIN' and 'NTO' worked successfully; replacing 'TCAM' with 'NTO' had solved the missing record problem.

- k) 'SEND' was now patched into 'TTY', to provide the full range of facilities required. ('SEND' replaced the section of code in 'TTY' which had not worked correctly.) The modified version of 'TTY' now worked satisfactorily, except when using the facility to transmit more than one file without having to exit and restart the program. Systematica supplied further patches for implementation by the author, which solved the problem; the intermediate TSO datasets could now be created successfully.

- l) A program to input the data from an intermediate dataset and produce an output dataset equivalent to the original Automatic Photometer file, and a CLIST for running the TSO programs,

were written by the author and A. Ball.

At the end of the above work, the file transfer scheme functioned as required.

APPENDIX H

PHOTOMETRIC DATA FILES AND THEIR PROCESSING

Section H.1. describes the 'Photometric Data File' (PDF) structure developed by the author to be used in conjunction with the Group Computer and 'VS Fortran' as part of the photometric data processing scheme described in Chapter 14. It provides a flexible method of storing photometric data produced by a computer-based photometer or performance prediction software and will enable software modules for processing the data to be written.

An example of PDF processing software is given in section H.2.

H.1 PDF Structure

H.1.1 Overview of PDF Structure

The two following assumptions have been made in defining the structure:

- a) A PDF will contain data for a single lamp.
- b) Once a file has initially been created, the most commonly performed operations will involve reading the data from the file, rather than modifying it or adding to it.

Consequently, a simple sequential file structure has been used. However, a mechanism by which additional data can be appended

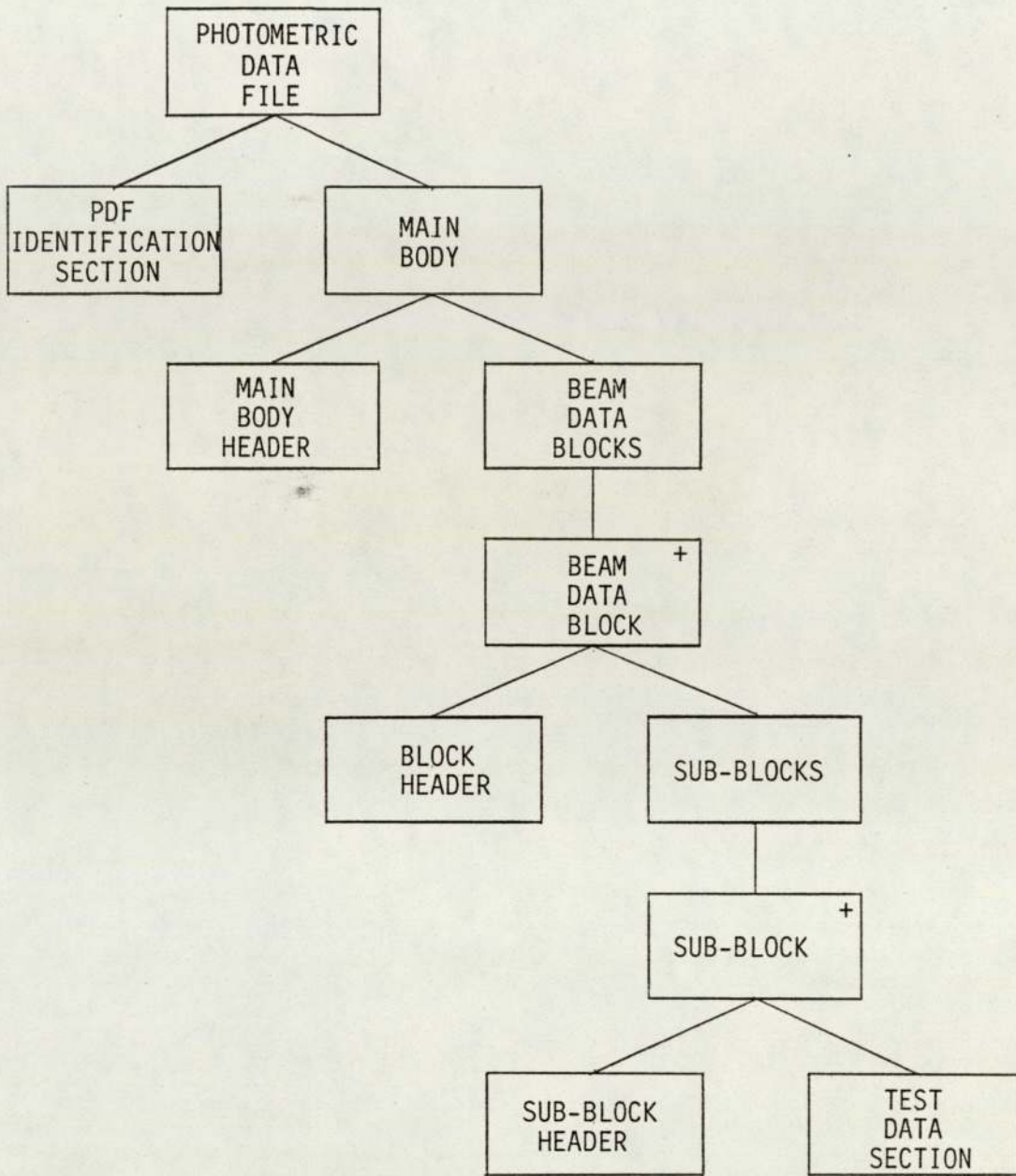
to a file and referenced to existing data is provided. Each record in the file has a length of 128 bytes; this value was chosen for compatibility with the existing Automatic Photometer CP/M result files.

The overall structure is shown in Fig. H.1. Each file consists of an identification section, which enables the processing software to determine whether or not the file specified by the operator is a PDF, and the main body. The main body consists of a header, containing information about the lamp and the structure of the main body, and one or more data blocks, each containing data relating to one beam of the lamp. The facility to store several blocks per lamp enables data from multifunction lamps to be stored. For example, the dipped, main, sidelamp and direction indicator functions of a lamp can be tested and the data stored in four separate blocks.

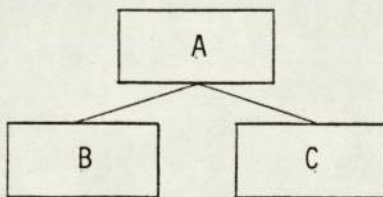
Each block consists of a header, containing information about the beam and the block structure, and one or more sub-blocks. The facility to store several sub-blocks per block enables more than one set of data to be stored for each beam. For example, test point values and a two-dimensional array of data for iso-lux contouring could be acquired and stored in 2 separate sub-blocks.

Each sub-block consists of a header, containing information about the type of test data and the sub-block structure, and the test data section, which contains the photometric data itself.

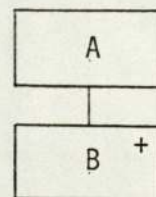
The overall structure of the identification section, the main body header, a block header and a sub-block header are given in Table H.1. The detailed structure of each of these sections is described in



Notation:



Data component A consists of data component B followed by data component C



Data component A consists of 1 or more occurrences of data component B

Fig. H1 Overall Photometric Data File Structure

section H.1.2.

The structure of the test data section will depend on the type of data to be stored; detailed storage formats will be developed as the scheme is introduced and are not covered here.

H.1.2 Detailed Structure

H.1.2.1 PDF Identification Section

See Table H.2.

Notes:

a) PDFID

This enables the processing software to confirm that the file to be processed is a PDF.

b) PDFPVC

PDFPVC identifies this PDF structure (or 'picture'). It may be necessary in the future to modify this picture, or produce a completely different one; in this case new version codes can be assigned and the processing software written to identify which picture was used to construct the file and process the contents accordingly. This version of the file structure is defined as 'V1.00'.

H.1.2.2 Main Body Header

See Tables H.3 and H.4

Notes:

a) STFFCD

Certain specific constructions based on the use of this general file picture could be formulated for convenience of file creation and processing. For example, when transferring data from Automatic Photometer 'Iso-lux result' files, there will always be either 1 or 2 blocks, each containing one sub-block. Furthermore, there will be no block or sub-block comments records. These conditions can be identified with a suitable standard file format code, to simplify the software required to process the data. (NBLKS, NSBLKS, NBCR and NSBCR should still be assigned their appropriate values to provide compatibility with all PDF processing software.)

b) NBLKS

Valid range = 1-9999

c) NFCR

Valid range = 0-9999

H.1.2.3 Block Header

See Tables H.5 and H.6

Notes:

a) BLKCNO

This is included to enable the processing software to check that the calculated starting address of the block is correct.

b) STBFCD

The purpose of STBFCD is similar to that of STFFCD; it enables specific block constructions to be formulated for convenience of file creation and processing.

c) NSBLKS

Valid range = 1-9999

d) NBCR

Valid range = 0-9999

e) LNKREF

It may be required on occasions to append additional data to an existing PDF and to logically associate this data with an

existing block. This can be achieved by placing the additional data in a new block at the end of the file, and entering the number of the new block in the LNKREF field of the existing block with which the data is to be associated. Valid range, if used, = 1-9999; it should be set to 0 if not used.

- f) The VOLTGE and CURRNT values can be stored in either of the two forms given below; both are read correctly using F.6.3 in the format statement.

'NN.NNN'

' NNNNN'

H.1.2.4 Sub-Block Header

See Table H.7

Notes:

- a) SBCNO

This is included to enable the processing software to check that the calculated starting address of the sub-block is correct.

- b) STSFCD

The purpose of STSFCD is similar to that of STFFCD and STBFCD;

it enables specific sub-block constructions to be formulated for convenience of file creation and processing.

c) NSBCR

Valid range = 0-9999

d) NTDSR

Valid range = 1-9999

e) DTYP CD

This is used to identify the type of data stored in the test data section.

f) DSTO CD

This is used to identify the format in which the data is stored in the test data section.

g) DSRCCD

This is used to identify the source of the data stored in the test data section.

| SECTION | SUB-SECTION | CONTENTS | RECORD NUMBERS |
|--------------------|--------------|---|------------------|
| PDF Identification | 1 | PDF Identification and Picture Version Number | 1 |
| Main Body Header | 1 | General File Structure Details | 1 |
| | 2 | Lamp Information - Fixed Format | 2 |
| | 3 (Optional) | File/Lamp Information - Free Format | 3 + (if present) |
| Block Header | 1 | General Block Structure Details | 1 |
| | 2 | Beam Information - Fixed Format | 2 |
| | 3 (Optional) | Block/Beam Information - Free Format | 3 + (if present) |
| Sub-Block Header | 1 | General Sub-Block Structure Details | 1 |
| | 2 (Optional) | Sub-Block/Data Information - Free Format | 2 + (if present) |

Table H1 Photometric Data File Structure Details

| FIELD | BYTE NO'S | CONTENTS | STORAGE FORMAT | CORRESPONDING PROGRAM VARIABLE | |
|-------|---------------------|---------------------------------------|----------------|--------------------------------|----------------|
| | | | | NAME | TYPE |
| 1 | 1 - 19 | 'PHOTOMETRICDATAFILE' | A19 | PDFID | CHARACTER * 19 |
| 2 | 20 - 24 25 - 128 | File Picture Version Code Not Used | A5 | PDFPVC | CHARACTER * 5 |

Table H2 PDF Structure - PDF Identification Section, Record 1

| FIELD | BYTE NO' s | CONTENTS | STORAGE FORMAT | CORRESPONDING PROGRAM VARIABLE | |
|-------|------------|--------------------------------|-------------------|--------------------------------|----------------|
| | | | | NAME | TYPE |
| 1.1 | 1 - 3 | PDF Identifier) | A3 | NAMEFI | CHARACTER * 3 |
| 1.2 | 4 | Data Source Code) | A1 | NAMEDS | CHARACTER * 1 |
| 1.3 | 5 - 8 | File Number) | A4 | NAMENO | CHARACTER * 4 |
| 1.4 | 9 - 11 | Year Code) | A3 | NAMEYR | CHARACTER * 3 |
| 1.5 | 12 - 14 | Month Code) | A3 | NAMEMO | CHARACTER * 3 |
| 1.6 | 15 - 16 | Lamp Manufacturer Code) | A2 | NAMEMA | CHARACTER * 2 |
| 1.7 | 17 - 24 | Lamp Type Code) | A8 | NAMEY | CHARACTER * 8 |
| 2 | 25 - 32 | Date of Test) | A8 | DATETS | CHARACTER * 8 |
| 3 | 33 - 48 | Standard File Format Code | A16 | STFFCD | CHARACTER * 16 |
| 4 | 49 - 52 | Number of Blocks | I4 | NBLKS | INTEGER * 4 |
| 5 | 53 - 56 | Number of File Comment Records | I4 | NFCR | INTEGER * 4 |
| | 57 -128 | Not Used | | | |

Table H3 PDF Structure - Main Body Header, Record 1

| FIELD | BYTE NO' s | CONTENTS | STORAGE FORMAT | CORRESPONDING PROGRAM VARIABLE | |
|-------|---------------------|------------------------------------|-------------------|--------------------------------|----------------|
| | | | | NAME | TYPE |
| 1 | 1 - 16 | Lamp Manufacturer | A16 | LMPMAN | CHARACTER * 16 |
| 2 | 17 - 32 | Lamp Type | A16 | LMPTYP | CHARACTER * 16 |
| 3 | 33 | Lamp Rule of Road | A1 | LMPROR | CHARACTER * 1 |
| 4 | 34 | Lamp Hand | A1 | LMPHND | CHARACTER * 1 |
| 5 | 35 - 50 51 - 128 | Lamp Sample Identifier Not Used | A16 | LMPSID | CHARACTER * 16 |

Table H4 PDF Structure - Main Body Header, Record 2

| FIELD | BYTE NO' s | CONTENTS | STORAGE FORMAT | CORRESPONDING PROGRAM VARIABLE | |
|-------|------------|---------------------------------|-------------------|--------------------------------|----------------|
| | | | | NAME | TYPE |
| 1 | 1 - 4 | Block Check Number | I4 | BLKCNO (BLK) | INTEGER * 4 |
| 2 | 5 - 20 | Standard Block Format Code | A16 | STBFCD (BLK) | CHARACTER * 16 |
| 3 | 21 - 24 | Number of Sub-Blocks in Block | I4 | NSBLKS (BLK) | INTEGER * 4 |
| 4 | 25 - 28 | Number of Block Comment Records | I4 | NBCR (BLK) | INTEGER * 4 |
| 5 | 29 - 32 | Link Reference | I4 | LNKREF (BLK) | INTEGER * 4 |
| | 33 - 128 | Not Used | | | |

Table H5 PDF Structure - Block Header, Record 1

| FIELD | BYTE NO'S | CONTENTS | STORAGE FORMAT | CORRESPONDING PROGRAM VARIABLE | |
|-------|-----------|------------------------|-------------------|--------------------------------|----------------|
| | | | | NAME | TYPE |
| 1 | 1 - 48 | Beam Description | A48 | BEAMDS (BLK) | CHARACTER * 48 |
| 2 | 49 - 64 | Bulb Manufacturer | A16 | BLBMAN (BLK) | CHARACTER * 16 |
| 3 | 65 - 80 | Bulb Type | A16 | BLBTYP (BLK) | CHARACTER * 16 |
| 4 | 81 - 96 | Bulb Sample Identifier | A16 | BLBSID (BLK) | CHARACTER * 16 |
| 5 | 97 - 102 | Test Voltage | F6.3 | VOLTGE (BLK) | REAL * 4 |
| 6 | 103 - 108 | Current Consumption | F6.3 | CURRNT (BLK) | REAL * 4 |
| | 109 - 128 | Not Used | | | |

Table H6 PDF Structure - Block Header, Record 2

| FIELD | BYTE NO' s | CONTENTS | STORAGE FORMAT | CORRESPONDING PROGRAM VARIABLE | |
|-------|------------|-------------------------------------|-------------------|--------------------------------|----------------|
| | | | | NAME | TYPE |
| 1 | 1 - 4 | Sub-Block Check Number | I4 | SBCNO (BLK, SBLK) | INTEGER * 4 |
| 2 | 5 - 20 | Standard Sub-Block Format Code | A16 | STSFCD (BLK, SBLK) | CHARACTER * 16 |
| 3 | 21 - 24 | Number of Sub-Block Comment Records | I4 | NSBCR (BLK, SBLK) | INTEGER * 4 |
| 4 | 25 - 28 | Number of Test Data Section Records | I4 | NTDSR (BLK, SBLK) | INTEGER * 4 |
| 5 | 29 - 44 | Data Type Code | A16 | DTYPCD (BLK, SBLK) | CHARACTER * 16 |
| 6 | 45 - 60 | Data Storage Code | A16 | DSTOCD (BLK, SBLK) | CHARACTER * 16 |
| 7 | 61 - 76 | Data Source Code | A16 | DSRCCD (BLK, SBLK) | CHARACTER * 16 |
| | 77 - 128 | Not Used | | | |

Table H7 PDF Structure - Sub-Block Header, Record 1

H.1.3 PDF Naming System

Each PDF will be stored in the departmental dataset storage area and assigned a name consisting of 8 fields; this will enable the CAT LIST command (112), to provide a powerful facility for searching for an individual PDF, or group of PDF's, from the overall catalogue.

The structure of the name is:

@81221@.PDF.DATASOURCE.FILENUMBER.YEAR.MONTH.LAMPMANUFACTURER.LA
MPTYPE

where

@81221@ = TSO Departmental Profile

PDF = File Type Identifier

DATASOURCE = Data Source Identifier
(One letter code e.g. A = E&D Automatic
Photometer)

FILENUMBER = File Number Identifier
(One letter followed by three digits e.g.
A001)

DATASOURCE and FILENUMBER together form a
unique identifier for each PDF

- YEAR = Year of Lamp Test Identifier
(Y followed by two digits e.g. Y85 for 1985)
- MONTH = Month of Lamp Test Identifier
(M followed by two digits e.g. M01 for January)
- LAMPMANUFACTURER = Lamp Manufacturer Identifier
(Two letter code e.g. LU for Lucas)
- LAMPTYPE = Lamp Type Identifier
(One to eight characters, the first of which must be a letter e.g. FR35)

Three examples of the way in which the CAT LIST command can be used to search for PDF's are given below.

- a) Find all the PDF's created from Automatic Photometer data in 1984.

```
CAT L @81221@.PDF.A.*.Y84
```

- b) Find the PDF created from Automatic Photometer file number A872.

```
CAT L @81221@.PDF.A.A872
```

- c) Find all PDF's containing data acquired from Lucas 35FR lamps.

H.2 PDF Processing Software

H.2.1 Introduction

The type of PDF processing software which will be required for the implementation of the photometric data processing scheme is given in Chapter 14.

A program to list the contents of a PDF which has been created in accordance with the structure described in the previous section is given here as an example of how processing software can access PDF data. The program follows the basic concepts of top-down design and structured programming; see reference (108), for example. It consists of a main routine (PDFLC) and three subroutines (PDFI, RECRD and RDERR); these subroutines have been written so that they can also be used by other PDF processing software. RECRD is used to read the contents of a specified record of a PDF. RDERR is for use if RECRD fails to read a record successfully, to print a message giving details of the error which occurred. PDFI is a general purpose initialisation routine.

It was originally planned to use the 'direct access read' facility in 'VS Fortran' for reading the data from PDF's, but it was found that the time taken to format and process large files using this method was unacceptably long. Consequently, it is now intended to use the 'sequential access read' facility only. However, subroutine

RECRD, whilst using only 'sequential read' statements, enables the calling program to access a PDF as though it were a direct access file, by specifying the record to be read by means of its record number.

The full listings of the main routine and the subroutines are given in sections H.2.2 to H.2.5. Section H.2.6 gives an example of the printout produced by running PDFLC.

PHOTOMETRIC DATA FILE PROCESSING SOFTWARE

PROGRAM TO LIST CONTENTS OF A PDF

NAME

PDFLC

VERSION

V1.1

AUTHOR

S. J. CARTWRIGHT

DESCRIPTION

THIS PROGRAM LISTS A DESCRIPTION OF THE CONTENTS OF
A PHOTOMETRIC DATA FILE

SUBROUTINES CALLED

PDFI, RECRD, RDERR

00100 C
00200 C
00300 C
00400 C
00500 C
00600 C
00700 C
00800 C
00900 C
01000 C
01100 C
01200 C
01300 C
01400 C
01500 C
01600 C
01700 C
01800 C
01900 C
02000 C
02100 C
02200 C
02300 C
02400 C
02500 C
02600 C
02700 C
02800 C
02900 C
03000 C
03100 C
03200 C
03300 C

```

03400 C DEFINE MAXIMUM NUMBER OF BLOCKS IN A FILE
03500 C
03600 C PARAMETER (MHOBIF = 4)
03700 C
03800 C DEFINE MAXIMUM NUMBER OF SUB-BLOCKS IN A BLOCK
03900 C
04000 C PARAMETER (MHOSIB = 4)
04100 C
04200 C DECLARE VARIABLES CORRESPONDING TO DATA IN FILE
04300 C
04400 C (A) FDF IDENTIFICATION SECTION VARIABLES
04500 C
04600 C CHARACTER*19 PDFID
04700 C CHARACTER*5 PDFPVC
04800 C
04900 C (B) MAIN BODY HEADER VARIABLES
05000 C
05100 C CHARACTER*3 NAMEFI
05200 C CHARACTER*1 NAMEDS
05300 C CHARACTER*4 NAMENO
05400 C CHARACTER*3 NAMEYR
05500 C CHARACTER*3 NAMEMO
05600 C CHARACTER*2 NAMEMA
05700 C CHARACTER*8 NAMEYI
05800 C
05900 C CHARACTER*8 DATETS
06000 C CHARACTER*16 STFFCD
06100 C INTEGER NBLKS,NFCR
06200 C
06300 C CHARACTER*16 LMPMAN,LMPYYP
06400 C CHARACTER*1 LMPROR,LMPHND
06500 C CHARACTER*16 LMPSID
06600 C

```

```

06700 C      (C) BLOCK HEADER VARIABLES
06800 C
06900      INTEGER      BLKNO (MNOBIF)
07000      CHARACTER*16 STBFC (MNOBIF)
07100      INTEGER      NSBLKS (MNOBIF), NBCR (MNOBIF), LNKREF (MNOBIF)
07200 C
07300      CHARACTER*48 BEAMDS (MNOBIF)
07400      CHARACTER*16 BLEMAN (MNOBIF), BLBTYP (MNOBIF), BLESID (MNOBIF)
07500      REAL          VOLTGE (MNOBIF), CURRNT (MNOBIF)
07600 C
07700 C      (D) SUB-BLOCK HEADER VARIABLES
07800 C
07900      INTEGER      SECHO (MNOBIF, MNOSIB)
08000      CHARACTER*16 STSFC (MNOBIF, MNOSIB)
08100      INTEGER      NSBCR (MNOBIF, MNOSIB), NTDSR (MNOBIF, MNOSIB)
08200      CHARACTER*16 DTYP (MNOBIF, MNOSIB), DSTOCD (MNOBIF, MNOSIB)
08300      CHARACTER*16 DSRCCD (MNOBIF, MNOSIB)
08400 C
08500 C
08600 C      DECLARE COMMON BLOCKS FOR ABOVE DATA
08700 C
08800      COMMON /MBHV/  NAMEFI, NAMEDS, NAMENO, NAMEYR, NAMEMO, NAMEMA, NAMEY,
&
08900      DATEIS, STFFCD, NBLKS, NFCR,
&
09000      LMPMAN, LMPTYP, LMPROR, LMPHND, LMPSID
09100 C
09200      COMMON /BLKHV/  BLKNO, STBFC, NSBLKS, NBCR, LNKREF,
&
09300      BEAMDS, BLBMAN, BLBTYP, BLESID, VOLTGE, CURRNT
09400 C
09500      COMMON /SBLKHV/  SBCNO, STSFC, NTDSR, NSBCR, DTYP, DSTOCD, DSRCCD
09600 C
09700 C

```

```

09800 C DECLARE BLOCK AND SUB-BLOCK ADDRESS VARIABLES
09900 C
10000 C INTEGER BSA(MNOBIF),SBSA(MNOBIF,MNOSIB)
10100 C
10200 C BSA (MNOBIF) - BLOCK STARTING ADDRESSES
10300 C SBSA (MNOBIF,MNOSIB) - SUB-BLOCK STARTING ADDRESSES
10400 C
10500 C DECLARE COMMON BLOCKS FOR ABOVE DATA
10600 C
10700 C COMMON /ADDR/ BSA,SBSA
10800 C
10900 C
11000 C DECLARE VARIABLES FOR SUBROUTINE RECD
11100 C
11200 C INTEGER UN,REC,RETCOD,RETREC
11300 C CHARACTER*128 RECDAT
11400 C
11500 C
11600 C DECLARE VARIABLES USED IN THIS PROGRAM
11700 C
11800 C INTEGER BLK,SBLK
11900 C
12000 C BLK - BLOCK CURRENTLY BEING PROCESSED
12100 C SBLK - SUB-BLOCK CURRENTLY BEING PROCESSED
12200 C
12300 C CHARACTER*30 FNAME
12400 C
12500 C
12600 C INITIALISE VARIABLES
12700 C
12800 C
12900 C DATA UN / 7 /
13000 C
13100 C
13200 C

```

```

13300 C
13400 C
13500 C
13600 C
13700
13800 C
13900
14000
14100 C
14200
14300
14400
14500
14600
14700
14800
14900
15000
15100
15200
15300
15400
15500 C
15600
15700
15800
15900
16000
16100
16200
16300
16400
16500
16600 C

PROCESSING STARTS HERE

CALL PDFI

FNAME = NAMEFI/'.'///NAMEDS/'.'///NAMENO/'.'///NAMEYR/'.'///
& NAMEMO/'.'///NAMEMA/'.'///NAMEY

PRINT *, ' '
PRINT *, 'PDF CONTENTS LISTING ROUTINE V1.1'
PRINT *, ' '
PRINT *, 'FILE NAME - ', FNAME
PRINT *, ' '
PRINT *, 'LAMP DETAILS - '
PRINT *, 'MANUFACTURER : ', LMPMAN, ' ', 'TYPE : ', LMPTYP
PRINT *, 'RULE OF ROAD : ', LMPROR, ' '
& 'HAND : ', LMPHND
PRINT *, 'SAMPLE : ', LMPSID
PRINT *, ' '
PRINT *, 'DATE OF TEST - ', DATETS
PRINT *, ' '

IF ( NFCR.NE.0 ) THEN
  PRINT *, 'COMMENTS - '
  DO 100 REC = 4, (4 + NFCR - 1)
    CALL RECRD (UN,REC,RECDAT,RETCOD,RETREC)
    IF (RETCOD.NE.0) CALL RDERR (RETCOD,RETREC)
    PRINT *, RECDAT(1:64)
    PRINT *, RECDAT(65:128)
  100 CONTINUE
  PRINT *, ' '
END IF

```

```

16700 C
16800 C
16900
17000 C
17100
17200
17300
17400
17500
17600
17700
17800
17900
18000
18100
18200
18300
18400
18500
18600
18700
18800
18900 C
19000
19100
19200
19300
19400
19500
19600
19700
19800
19900
20000 C

DO FOR ALL BLOCKS

DO 500 BLK = 1,NBLKS

  PRINT 1, BLK
  FORMAT (' BLOCK ',I4,' -')
  PRINT *, ' '
  PRINT *, ' ', 'BEAM - ', BEAMDS(BLK)
  PRINT *, ' '
  PRINT *, ' ', 'BULB DETAILS - '
  PRINT *, ' ', 'MANUFACTURER : ', BLBMAN(BLK), ' '
  PRINT *, ' ', 'TYPE : ', BLBTYP(BLK)
  PRINT *, ' ', 'SAMPLE : ', BLBSID(BLK)
  PRINT *, ' '
  IF (CURRENT(BLK).EQ.0) THEN
    PRINT 2, VOLTGE(BLK)
    FORMAT (3X,' VOLTAGE - ',F6.3)
  ELSE
    PRINT 3, VOLTGE(BLK), CURRNT(BLK)
    FORMAT (3X,' VOLTAGE - ',F6.3,10X,' CURRENT - ',F6.3)
  END IF
  PRINT *, ' '

  IF (NBCR(BLK).NE.0) THEN
    PRINT *, ' ', 'COMMENTS - '
    DO 200 REC = (BSA(BLK) + 2), (BSA(BLK) + 2 + NBCR(BLK) - 1)
      CALL RECRD (UN,REC,RECDAT,RETCOD,RETREC)
      IF (RETCOD.NE.0) CALL RDERR (RETCOD,RETREC)
      PRINT *, ' ', RECDAT(1:64)
      PRINT *, ' ', RECDAT(65:128)
    CONTINUE
    PRINT *, ' '
  END IF
END IF

```

```

20100 C      DO FOR ALL SUB-BLOCKS
20200 C
20300 C      DO 400 SBLK = 1, NSBLKS(BLK)
20400 C
20500 C          PRINT *, ' '
20600 C          PRINT 4, SBLK
20700 C          FORMAT (3X, ' SUB-BLOCK ', I4, ' - ')
20800 C          PRINT *, ' '
20900 C          PRINT X, ' ', 'DATA TYPE - ', DTYPCD(BLK, SBLK)
21000 C          PRINT *, ' '
21100 C          PRINT X, ' ', 'DATA SOURCE - ', DSRCCD(BLK, SBLK)
21200 C          PRINT *, ' '
21300 C
21400 C      IF (NSBCR(BLK, SBLK).NE.0) THEN
21500 C          PRINT *, ' ', 'COMMENTS - '
21600 C          DO 300 REC = (SBSA(BLK, SBLK) + 1),
21700 C              (SBSA(BLK, SBLK) + 1 + NSBCR(BLK, SBLK) - 1)
21800 C              CALL RECD (UN, REC, RECDAT, RETCOD, RETREC)
21900 C              IF (RETCOD.NE.0) CALL RDERR (RETCOD, RETREC)
22000 C              PRINT *, ' ', RECDAT(1:64)
22100 C              PRINT *, ' ', RECDAT(65:128)
22200 C              CONTINUE
22300 C              PRINT *, ' '
22400 C              END IF
22500 C          NEXT SUB-BLOCK
22600 C
22700 C      400 CONTINUE
22800 C
22900 C          NEXT BLOCK
23000 C
23100 C      500 CONTINUE
23200 C
23300 C          PRINT *, ' '
23400 C          PRINT *, 'END OF LISTING'
23500 C          STOP
23600 C          END
23700 C

```

H.2.3 Subroutine PDFI

PHOTOMETRIC DATA FILE PROCESSING SOFTWARE

SUBROUTINE PDFI

VERSION

V1.3

AUTHOR

S. J. CARTWRIGHT

DESCRIPTION

PDFI IS AN INITIALISATION SUBROUTINE FOR USE BY 'PHOTOMETRIC DATA FILE' PROCESSING SOFTWARE. IT CALCULATES AND STORES THE STARTING ADDRESSES OF ALL BLOCKS AND SUB-BLOCKS AND READS THE CONTENTS OF THE MAIN BODY, BLOCK AND SUB-BLOCK HEADERS (EXCEPT THE COMMENT RECORDS).

INPUT PARAMETERS

NONE

OUTPUT PARAMETERS

NONE

00100 C
 00200 C
 00300 C
 00400 C
 00500 C
 00600 C
 00700 C
 00800 C
 00900 C
 01000 C
 01100 C
 01200 C
 01300 C
 01400 C
 01500 C
 01600 C
 01700 C
 01800 C
 01900 C
 02000 C
 02100 C
 02200 C
 02300 C
 02400 C
 02500 C
 02600 C
 02700 C
 02800 C
 02900 C
 03000 C
 03100 C
 03200 C
 03300 C
 03400 C
 03500 C

| | | |
|-------|---|---|
| 03600 | C | SUBROUTINES CALLED |
| 03700 | C | |
| 03800 | C | RECRD, RDERR |
| 03900 | C | |
| 04000 | C | |
| 04100 | C | USAGE |
| 04200 | C | |
| 04300 | C | THE VARIABLES READ FROM THE PDF ARE PASSED TO THE CALLING ROUTINE |
| 04400 | C | BY MEANS OF 4 NAMED COMMON AREAS; THE CALLING PROGRAM MUST |
| 04500 | C | DUPLICATE THE DECLARATIONS GIVEN IN LINES 5100 - 12400 |
| 04600 | C | |
| 04700 | C | |
| 04800 | C | SUBROUTINE PDFI |
| 04900 | C | |
| 05000 | C | |
| 05100 | C | DEFINE MAXIMUM NUMBER OF BLOCKS IN A FILE |
| 05200 | C | |
| 05300 | C | PARAMETER (MNOBIF = 4) |
| 05400 | C | |
| 05500 | C | DEFINE MAXIMUM NUMBER OF SUB-BLOCKS IN A BLOCK |
| 05600 | C | |
| 05700 | C | PARAMETER (MNOSIB = 4) |
| 05800 | C | |
| 05900 | C | DECLARE VARIABLES CORRESPONDING TO DATA IN FILE |
| 06000 | C | |
| 06100 | C | (A) PDF IDENTIFICATION SECTION VARIABLES |
| 06200 | C | |
| 06300 | C | CHARACTER*19 PDFID |
| 06400 | C | CHARACTER*5 PDFPVC |
| 06500 | C | |

| | | |
|-------|---|--|
| 06600 | C | (B) MAIN BODY HEADER VARIABLES |
| 06700 | C | |
| 06800 | | CHARACTER*3 NAMEFI |
| 06900 | | CHARACTER*1 NAMEDS |
| 07000 | | CHARACTER*4 NAMEO |
| 07100 | | CHARACTER*3 NAMEYR |
| 07200 | | CHARACTER*3 NAMEO |
| 07300 | | CHARACTER*2 NAMEMA |
| 07400 | | CHARACTER*8 NAMEY |
| 07500 | C | |
| 07600 | | CHARACTER*8 DATETS |
| 07700 | | CHARACTER*16 STFFCD |
| 07800 | | INTEGER NBLKS,NFCR |
| 07900 | C | |
| 08000 | | CHARACTER*16 LMPMAN,LMPY |
| 08100 | | CHARACTER*1 LMPROR,LMPHND |
| 08200 | | CHARACTER*16 LMPSID |
| 08300 | C | |
| 08400 | C | (C) BLOCK HEADER VARIABLES |
| 08500 | C | |
| 08600 | | INTEGER BLKCNO (MNOBIF) |
| 08700 | | CHARACTER*16 STBFCD (MNOBIF) |
| 08800 | | INTEGER NSBLKS (MNOBIF), NBCR (MNOBIF), LNKREF (MNOBIF) |
| 08900 | C | |
| 09000 | | CHARACTER*48 BEAMDS (MNOBIF) |
| 09100 | | CHARACTER*16 BLBMAN (MNOBIF), BLBTYP (MNOBIF), BLBSID (MNOBIF) |
| 09200 | | REAL VOLTGE (MNOBIF), CURRNT (MNOBIF) |
| 09300 | C | |
| 09400 | C | (D) SUB-BLOCK HEADER VARIABLES |
| 09500 | C | |
| 09600 | | INTEGER SBCNO (MNOBIF,MNOSIB) |
| 09700 | | CHARACTER*16 STSFCD (MNOBIF,MNOSIB) |
| 09800 | | INTEGER NSBCR (MNOBIF,MNOSIB), NTDSR (MNOBIF,MNOSIB) |
| 09900 | | CHARACTER*16 DTYPCD (MNOBIF,MNOSIB), DSTOCD (MNOBIF,MNOSIB) |
| 10000 | | CHARACTER*16 DSRCCD (MNOBIF,MNOSIB) |
| 10100 | C | |

```

10200 C
10300 C
10400 C
10500
10600
10700
10800 C
10900
11000
11100 C
11200
11300 C
11400 C
11500 C
11600 C
11700
11800 C
11900 C
12000 C
12100 C
12200 C
12300 C
12400
12500 C
12600 C
12700 C
12800 C
12900
13000 C
13100 C
13200 C
13300 C
13400 C
-----

      DECLARE COMMON BLOCKS FOR ABOVE DATA

COMMON /MBHV/  NAMEFI, NAMEDS, NAMENO, NAMEYR, NAMEMO, NAMEMA, NAMEY,
&             DATETS, STFFCD, NBLKS, NFCR,
&             LMPMAN, LMPFTYP, LMPROR, LMPHND, LMPSID

COMMON /BLKHV/ BLKNO, STEFCD, NSBLKS, NBCR, LNKREF,
&             BEAMDS, ELBMAN, BLBTYP, BLBSID, VOLTGE, CURRNT

COMMON /SBLKHV/ SBCNO, STSFCD, NIDSR, NSBCR, DTYPCD, DSTOCD, DSRCCD

      DECLARE BLOCK AND SUB-BLOCK ADDRESS VARIABLES

INTEGER BSA(MNOBIF), SBSA(MNOBIF, MNOSIB)

BSA (MNOBIF)      - BLOCK STARTING ADDRESSES
SBSA (MNOBIF, MNOSIB) - SUB-BLOCK STARTING ADDRESSES

      DECLARE COMMON BLOCK FOR ABOVE DATA

COMMON /ADDR/  BSA, SBSA

      DECLARE VARIABLES USED IN THIS SUBROUTINE

INTEGER BLK, SBLK

BLK - BLOCK CURRENTLY BEING PROCESSED
SBLK - SUB-BLOCK CURRENTLY BEING PROCESSED

```

```

13500 C DECLARE VARIABLES FOR SUBROUTINE RECRD
13600 C
13700 C INTEGER UN,REC,RETCOD,RETREC
13800 C CHARACTER*128 RECDAT
13900 C
14000 C INITIALISE VARIABLES
14100 C
14200 C DATA UN / 7 /
14300 C
14400 C
14500 C
14600 C
14700 C
14800 C PROCESSING STARTS HERE
14900 C
15000 C
15100 C READ PDF IDENTIFICATION SECTION AND STOP EXECUTION IF
15200 C FILE IS NOT A PDF, VERSION V1.00
15300 C
15400 C REC = 1
15500 C CALL RECRD (UN,REC,RECDAT,RETCOD,RETREC)
15600 C IF (RETCOD.NE.0) CALL RDERR (RETCOD,RETREC)
15700 C
15800 C READ (RECDAT,10) PDFID,PDFPVC
15900 C 10 FORMAT (A17,A5)
16000 C
16100 C IF ((PDFID.NE.'PHOTOMETRICDATAFILE').AND.(PDFPVC.NE.'V1.00'))
16200 C &STOP 'FILE IS NOT A PHOTOMETRIC DATA FILE, V1.00'
16300 C
16400 C READ MAIN BODY RECORD 1
16500 C
16600 C REC = 2
16700 C CALL RECRD (UN,REC,RECDAT,RETCOD,RETREC)
16800 C IF (RETCOD.NE.0) CALL RDERR (RETCOD,RETREC)
16900 C

```

```

17000 READ (RECDAT,20) NAMEFI,NAMEFS,NAMEMO,NAMEYR,NAMEMO,NAMEMA,
&
17100 NAMEY,DATEFS,STFFCD,NBLKS,NFCR
17200 20 FORMAT (A3,A1,A4,A3,A3,A2,A8,A8,A16,I4,I4)
17300 C
17400 C READ MAIN BODY RECORD 2
17500 C
17600 REC = 3
17700 CALL PECD (UN,REC,RECDAT,RETCOD,RETREC)
17800 IF (RETCOD.NE.0) CALL RDERR (RETCOD,RETREC)
17900 C
18000 READ (RECDAT,30) LMPMAN,LMPYTP,LMPROR,LMPHND,LMPSID
18100 30 FORMAT (A16,A16,A1,A1,A16)
18200 C
18300 C DO TO 200 FOR EACH BLOCK
18400 C
18500 DO 200 BLK = 1,NBLKS
18600 C
18700 C CALCULATE BLOCK STARTING ADDRESS
18800 C
18900 IF (BLK.EQ.1) THEN
19000 BSA (BLK) = 4 + NFCR
19100 ELSE
19200 BSA (BLK) = SBSA ( (BLK-1), ( NSBLKS (BLK-1) ) ) +
&
19300 NSBCR ( (BLK-1), ( NSBLKS (BLK-1) ) ) +
&
19400 NTDSR ( (BLK-1), ( NSBLKS (BLK-1) ) ) + 1
19500 ENDIF
19600 C
19700 C READ BLOCK HEADER RECORD 1
19800 C
19900 REC = BSA(BLK)
20000 C
20100 CALL RECD (UN,REC,RECDAT,RETCOD,RETREC)
20200 IF (RETCOD.NE.0) CALL RDERR (RETCOD,RETREC)
20300 C

```

```

20400 READ (RECDAT,40) BLKCNO (BLK), STBFCD (BLK), NSBLKS (BLK),
20500 & NBCR (BLK), LNKREF (BLK)
20600 FORMAT (I4,A16,3I4)
20700 C
20800 IF ( BLKCNO(BLK).NE.BLK ) THEN
20900 PRINT *, ' FILE CONSTRUCTION ERROR'
21000 PRINT 45, BLK,BLKNO(BLK)
21100 & FORMAT (' BLKCNO(',I4,') = ',I4)
21200 STOP
21300 ENDIF
21400 C
21500 C READ BLOCK HEADER RECORD 2
21600 C
21700 REC = BSA(BLK) + 1
21800 C
21900 CALL RECRD (UN,REC,RECDAT,RETCOD,RETREC)
22000 IF (RETCOD.NE.0) CALL RDERR (RETCOD,RETREC)
22100 C
22200 READ (RECDAT,50) BEAMDS (BLK), BLBMAN (BLK), BLBTYP (BLK),
22300 & BLBSID (BLK), VOLTGE (BLK), CURRNT (BLK)
22400 FORMAT (A48,3A16,2F6.3)
22500 C
22600 C DO TO 100 FOR EACH SUB-BLOCK
22700 C
22800 DO 100 SBLK = 1,NSBLKS(BLK)
22900 C
23000 C CALCULATE SUB-BLOCK STARTING ADDRESS
23100 C
23200 IF (SBLK.EQ.1) THEN
23300 SB SA (BLK,SBLK) = BSA (BLK) + 2 + NBCR (BLK)
23400 ELSE
23500 SB SA (BLK,SBLK) = SB SA ( BLK, (SBLK-1) ) +
23600 & NSBCR ( BLK, (SBLK-1) ) + NTDSR ( BLK, (SBLK-1) ) + 1
23700 END IF
23800 C

```

```

23900 C      READ SUB-BLOCK HEADER RECORD
24000 C
24100      REC = SBSA (BLK,SBLK)
24200      CALL RECD (UN,REC,RECDAT,RETCOD,RETREC)
24300      IF (RETCOD.NE.0) CALL RDERR (RETCOD,RETREC)
24400 C
24500      READ (RECDAT,60) SBCNO (BLK,SBLK), STSFCD (BLK,SBLK),
      & NSBCR (BLK,SBLK), NTDSR (BLK,SBLK),
24600      & DTYPCD(BLK,SBLK), DSTOCD (BLK,SBLK),
24700      & DSRCCD(BLK,SBLK)
24800      FORMAT (I4,A16,2I4,3A16)
24900 C
25000 C
25100      IF ( SBCNO(BLK,SBLK).NE.SBLK ) THEN
25200          PRINT *, ' FILE CONSTRUCTION ERROR'
25300          PRINT 65, BLK,SBLK,SBCNO(BLK,SBLK)
25400          FORMAT (' SBLKCNO(',I4,',',I4,') =',I4)
25500          STOP
25600          ENDIF
25700 C
25800 C      NEXT SUB-BLOCK
25900 C
26000      100 CONTINUE
26100 C
26200 C      NEXT BLOCK
26300 C
26400      200 CONTINUE
26500 C
26600      RETURN
26700      END

```

H.2.4 Subroutine RECRD

00100 C
00200 C
00300 C
00400 C
00500 C
00600 C
00700 C
00800 C
00900 C
01000 C
01100 C
01200 C
01300 C
01400 C
01500 C
01600 C
01700 C
01800 C
01900 C
02000 C
02100 C
02200 C
02300 C
02400 C
02500 C
02600 C
02700 C
02800 C
02900 C
03000 C
03100 C
03200 C

PHOTOMETRIC DATA FILE PROCESSING SOFTWARE

SUBROUTINE RECRD (UN, REC, RECDAT, RETCOD, RETREC)

VERSION
V1.1

AUTHOR
S. J. CARTWRIGHT

DESCRIPTION
RECRD READS A SPECIFIED RECORD OF A SEQUENTIAL FILE
CONTAINING RECORDS OF LENGTH 128 BYTES. THE RECORD IS
SPECIFIED BY MEANS OF ITS RELATIVE RECORD NUMBER ; THE
SUBROUTINE ENABLES THE CALLING PROGRAM TO ACCESS THE
FILE AS THOUGH IT WERE A DIRECT ACCESS FILE.

INPUT PARAMETERS
UN (INTEGER) - I/O UNIT NUMBER
REC (INTEGER) - RELATIVE RECORD NUMBER OF RECORD TO BE READ

| | | |
|-------|---|---|
| 03300 | C | OUTPUT PARAMETERS |
| 03400 | C | |
| 03500 | C | RECDAT (CHARACTER*128) - RECORD DATA |
| 03600 | C | |
| 03700 | C | RETCOD (INTEGER) - 0 : RECORD NO. REC SUCCESSFULLY READ. |
| 03800 | C | 1 : EOF DETECTED IN READING RECORD |
| 03900 | C | NO. RETREC. |
| 04000 | C | 2 : ERROR DETECTED IN READING RECORD |
| 04100 | C | NO. RETREC. |
| 04200 | C | |
| 04300 | C | RETREC (INTEGER) - NO. OF RECORD WHERE EOF OR ERROR DETECTED. |
| 04400 | C | |
| 04500 | C | |
| 04600 | C | SUBROUTINES CALLED |
| 04700 | C | |
| 04800 | C | NONE |
| 04900 | C | |
| 05000 | C | |
| 05100 | C | USAGE |
| 05200 | C | |
| 05300 | C | THE CALLING PROGRAM MUST MAKE THE FOLLOWING DECLARATIONS |
| 05400 | C | BEFORE THE SUBROUTINE IS CALLED. |
| 05500 | C | |
| 05600 | C | INTEGER UN,REC,RETCOD,RETREC |
| 05700 | C | CHARACTER*128 RECDAT |
| 05800 | C | |
| 05900 | C | |
| 06000 | C | |
| 06100 | C | |
| 06200 | C | |

```

06300 SUBROUTINE RECRD (UN,REC,RECDAT,RETCOD,RETREC)
06400 C
06500 INTEGER UN,REC,RETCOD,RETREC,RECNUM
06600 CHARACTER*128 RECDAT
06700 C
06800 SAVE RECNUM
06900 DATA RECNUM / 1 /
07000 C
07100 C RECNUM IS THE RELATIVE RECORD NUMBER OF THE RECORD
07200 C THAT THE NEXT READ STATEMENT WILL ACCESS.
07300 C
07400 C
07500 C IF (RECNUM.NE.REC) THEN
07600 C
07700 C IF (RECNUM.GT.REC) THEN
07800 C REVIND (UN)
07900 C RECNUM = 1
08000 C END IF
08100 C
08200 C WHILE RECNUM < REC DO TO 200
08300 C IF (RECNUM.EQ.REC) GO TO 200
100
08400 C
08500 C READ (UNIT=UN,FMT='(A128)',IOSTAT=IOS) RECDAT
08600 C RECNUM = RECNUM + 1
08700 C
08800 C EXIT LOOP IF ERROR OR EOF DETECTED
08900 C
09000 C IF (IOS.NE.0) GO TO 300
09100 C
09200 C GO TO 100
09300 C 200 CONTINUE
09400 C
09500 C END IF

```

```

09600 C
09700 READ (UNIT=UN,FMT='(A128)',IOSTAT=IOS) RECDAT
09800 RECNUM = RECNUM + 1
09900 C
10000 300 IF (IOS.EQ.0) THEN
10100   RETCOD = 0
10200   RETREC = 0
10300 ELSE
10400   IF (IOS.LT.0) THEN
10500     RETCOD = 1
10600     RETREC = RECNUM - 1
10700   ELSE
10800     RETCOD = 2
10900     RETREC = RECNUM - 1
11000   END IF
11100 END IF
11200 C
11300 RETURN
11400 END

```

H.2.5 Subroutine RDERR

```

00100 C PHOTOMETRIC DATA FILE PROCESSING SOFTWARE
00200 C
00300 C
00400 C SUBROUTINE RDERR(RETCOD, RETREC)
00500 C
00600 C
00700 C VERSION
00800 C
00900 C V1.1
01000 C
01100 C
01200 C AUTHOR
01300 C
01400 C S. J. CARTWRIGHT
01500 C
01600 C
01700 C DESCRIPTION
01800 C
01900 C RDERR IS FOR USE IN CONJUNCTION WITH SUBROUTINE RECD WHEN
02000 C A RETCOD VALUE OF 1 OR 2 IS RETURNED. RDERR PRINTS A
02100 C MESSAGE GIVING THE DETAILS OF WHY THE SPECIFIED RECORD WAS
02200 C NOT SUCCESSFULLY READ AND TERMINATES EXECUTION OF THE PROGRAM.
02300 C (IF THE VALUE OF RETCOD PASSED TO RDERR IS NOT 1 OR 2, THEN
02400 C THE PROGRAM RETURNS CONTROL TO THE CALLING PROGRAM WITHOUT
02500 C PERFORMING ANY OPERATION.)
02600 C
02700 C INPUT PARAMETERS
02800 C
02900 C
03000 C RETCOD (INTEGER) - RETURN CODE ( FROM SUBROUTINE RECD )
03100 C
03200 C RETREC (INTEGER) - NO. OF RECORD WHERE EOF OR ERROR DETECTED.
03300 C ( FROM SUBROUTINE RECD )
03400 C
03500 C

```

| | |
|---------|---|
| 03600 C | OUTPUT PARAMETERS |
| 03700 C | |
| 03800 C | NONE |
| 03900 C | |
| 04000 C | |
| 04100 C | SUBROUTINES CALLED |
| 04200 C | |
| 04300 C | NONE |
| 04400 C | |
| 04500 C | USAGE |
| 04600 C | |
| 04700 C | |
| 04800 C | RDERR SHOULD BE CALLED DIRECTLY AFTER CALLING RECRD WHEN A |
| 04900 C | RETCOD VALUE OF 1 OR 2 IS RETURNED: - |
| 05000 C | |
| 05100 C | CALL RECRD(LIN, REC, RECDAT, RETCOD, RETREC) |
| 05200 C | IF (RETCOD.NE.0) CALL RDERR(RETCOD, RETREC) |
| 05300 C | |
| 05400 C | NO DECLARATIONS OTHER THAN THOSE REQUIRED FOR RECRD ARE NEEDED. |
| 05500 C | |
| 05600 C | |

```

05700 C
05800 C
05900 C
06000 C
06100 C
06200 C
06300 C
06400 C
06500 C
06600 C
06700 C
06800 C
06900 C
07000 C
07100 C
07200 C
07300 C
07400 C
07500 C
07600 C
07700 C
SUBROUTINE RDERR(RETCD,RETREC)
INTEGER RETCD,RETREC
IF (RETCD.EQ.1) THEN
PRINT *, 'END OF FILE DETECTED IN READING RECORD NO.',RETREC
STOP
ELSE IF (RETCD.EQ.2) THEN
PRINT *, 'ERROR DETECTED IN READING RECORD NO.',RETREC
STOP
ELSE
RETURN
END IF
END

```

H.2.6 Example of Printout Produced by PDFLC

PDF CONTENTS LISTING ROUTINE V1.1

FILE NAME - PDF.A.A123.Y85.M02.LU.FR24

LAMP DETAILS -
MANUFACTURER : LUCAS TYPE : 24FR
RULE OF ROAD : R HAND : R
SAMPLE : R/T

DATE OF TEST - 14/9/82

COMMENTS -
ROAD TEST SAMPLE WITH MODIFIED LENS

BLOCK 1 -

BEAM - DIPPED

BULB DETAILS - TYPE : H4
MANUFACTURER : PHILIPS
SAMPLE : 1

VOLTAGE - 12.000

SUB-BLOCK 1 -

DATA TYPE - ILLUM, 2 D ARRAY

DATA SOURCE - E&D AUTO PHOT

END OF LISTING

LIST OF REFERENCES

- 1 The Chairman's Review to Shareholders and Employees, 1984.
Lucas Industries, plc
1984

- 2 Vocational PhD's: Aston's IHD Scheme. A Review of
Methodology and Operating Experience
Compiled by Cochran, A J
University of Aston
1981

- 3 Stevens, W R
Principles of Lighting
Constable and Company
1951

- 4 Yerrell, J S
Vehicle Headlights
Lighting Research and Technology
Vol. 8, No. 2
1976
Pp 69-79

- 5 Headlamp Reflector Design
Lucas Electrical Limited, Lighting Division
1983

- 6 Olson, P L
Illumination Vs. Glare: The 'Catch-22' of Safe Headlighting
HSRI Research Review
January-February, 1978
Pp 1-16
- 7 Plastics Headlamps
Lucas Electrical Limited, Lighting Division
1977
- 8 Styled Headlamps for Aerodynamic Car Designs
Lucas Electrical Limited, Lighting Division
1983
- 9 Agreement Concerning the Adoption of Uniform Conditions of
Approval and Reciprocal Recognition of Approval for Motor
Vehicle Equipment and Parts - ECE Regulations 1, 8 and 20
United Nations
1958 Onwards
- 10 Henderson, S T and Marsden, A M (General Editors)
Lamps and Lighting (Second Edition)
Edward Arnold
1972
Pp 21-23
- 11 Lighting Equipment and Photometric Tests (1984 Edition)
Society of Automotive Engineers
1984

- 12 Henderson, S T and Marsden, A M (General Editors)
Lamps and Lighting (Second Edition)
Edward Arnold
1972
Pp 19, 76-80
- 13 Keitz, H A E
Light Calculations and Measurements
Macmillan
1971
Pp 60-62
- 14 Steers, J A
An Introduction to the Study of Map Projections
University of London Press
1962
- 15 Stimson, A
Photometry and Radiometry for Engineers
Wiley
1974
Pp 17-38
- 16 Stimson, A
Photometry and Radiometry for Engineers
Wiley
1974
Pp 16-17, 364-365

- 17 Keitz, H A E
Light Calculations and Measurements
Macmillan
1971
Pp 239-248
- 18 Stimson, A
Photometry and Radiometry for Engineers
Wiley
1974
Pp 41-45
- 19 Silicon Photodetector Design Manual
United Detector Technology Inc
P2
- 20 Silicon Photodetectors (Catalogue)
Centronic Limited
P4
- 21 Stimson, A
Photometry and Radiometry for Engineers
Wiley
1974
Pp 54-55

- 22 Stimson, A
 Photometry and Radiometry for Engineers
 Wiley
 1974
 P 45
- 23 Product Catalogue
 LMT Lichtmesstechnik GmbH Berlin
- 24 Detector/Filter Combinations (Data Sheet No. 9F006)
 United Detector Technology Inc
- 25 Silicon Photodetector Design Manual
 United Detector Technology Inc
 P6
- 26 Silicon Photodetector Design Manual
 United Detector Technology Inc
 P7
- 27 Condensed Catalogue of Optical Instruments and Photodetectors
 United Detector Technology Inc
- 28 SBC 80/10 Single Board Computer - Hardware Reference Manual
 Intel Corporation
 1976

- 29 Zaks, R
 The CP/M Handbook with MP/M
 Sybex
 1980
- 30 Kirk, M
 Lucas Photometer Software Overview
 ERA Technology Limited
 1982
- 31 Lucas Photometer Software Listings
 ERA Technology Limited
 1982
- 32 PL/M-80 Programming Manual
 Intel Corporation
 1976
- 33 Smith, W J
 Modern Optical Engineering
 McGraw-Hill
 1966
 Pp 153-155, 167-168
- 34 Keitz, H A E
 Light Calculations and Measurements
 Macmillan
 1971
 Pp 104-106, 152-158

- 35 Ballard, D H and Brown, C M
Computer Vision
Prentice-Hall
1982
Pp 22-24
- 36 Dunn, J F and Wakefield, G L
Exposure Manual (Third Edition)
Fountain Press
1974
Pp 211-212
- 37 Hansen, G L
Introduction to Solid-State Television Systems
Prentice-Hall
1969
Pp 97-102
- 38 Clayden, R T
TV Picture Generating Equipment
Electronic Data Library Volume 3: Video Techniques
Morgan-Grampian
1969
Pp 66-75

- 39 The Mariner 9 TV Experiment
 Images and Information Unit 12
 The Open University Press
 1978
 Pp 30-34
- 40 Lackman, P L
 Utilization of a Reseau for Reducing Electronic Scanning
 Non-Linearity in Surveyor Television Space Systems
 Journal of the Society of Motion Picture and Television
 Engineers.
 Vol. 77
 1968
 Pp 299-303
- 41 Smokler, M I
 Calibration of the Surveyor Television System
 Journal of the Society of Motion Picture and Television
 Engineers.
 Vol. 76
 1971
 Pp 394-417

- 42 Rindfleisch, T C et al
Digital Processing of the Mariner
6 and 7 pictures
Journal of Geophysical Research
Vol. 76
1971
Pp 394-417
- 43 Green, W B et al
Removal of Instrument Signature from Mariner 9 Television
Images of Mars
Applied Optics
Vol. 14
1975
Pp 105-114
- 44 Bannister, B R and Whitehead, D G
Fundamentals of Modern Digital Systems
Macmillan
1983
- 45 Atkinson, R M and Brook, R A
Selection and Application of Image Processing Systems
SIRA Limited
1984
Pp 2.1-2.19

- 46 Engineering Product Handbook
 Datel Systems, Inc
 1977-78
- 47 Castleman, K R
 Digital Image Processing
 Prentice-Hall
 1979
 Pp 139-249
- 48 Brown, E B
 Modern Optics
 Reinhold
 1965
- 49 Cox, A
 Photographic Optics
 Focal Press
 1974
- 50 Optical Self-Scanned Arrays - A Symposium
 Edited by Beynon, J D E
 Radio and Electronic Engineer
 Vol. 49, No. 10
 Pp 493-513

- 51 Atkinson, R M, Claridge, J F, Purll, D J and West, R N
Automatic Inspection
SIRA Limited
1985
Pp 17-32
- 52 CCD Image Primer
Thomson - CSF
1983
- 53 Burt, D J
Development of CCD Area Image Sensors for 625-Line Television
Applications
The Radio and Electronic Engineer
Vol. 50, No. 5
1980
Pp 205-212
- 54 Fry, P W
Silicon Photodiode Arrays
Journal of Physics E: Scientific Instruments
Vol. 8
1975
Pp 337-349

- 55 Murphy, H E
Performance Characteristics of a Producibile NTSC - Compatible
Charge-Coupled Device (CCD) Image Sensor
Society of Photo-Optical Instrumentation Engineers (SPIE)
Vol. 203
1979
Pp 80-87
- 56 Le Couteur, G M
Performance Tests on a Selection of 100 - Element
Charge-Coupled Devices
British Broadcasting Corporation, Research Department,
Engineering Division
1976
- 57 Longford, A H
Using Solid-State Self-Scanning Image Sensors
Electronic Engineering
February 1981
Pp 41-49
- 58 Ulatowski, J K
Solid-State Monolithic Photodiode Array - A System Component
Society of Photo-Optical Instrumentation Engineers (SPIE)
Vol. 182
1979
Pp 110-117

- 59 Atkinson, R M, Claridge, J F, Purl, D J and West, R N
Automatic Inspection
SIRA Limited
1985
Pp 4-16
- 60 Dunn, J F and Wakefield, G L
Exposure Manual (Third Edition)
Fountain Press
1974
Pp 6-7, 18-19
- 61 Hansen, G L
Introduction to Solid-State Television Systems
Prentice-Hall
1969
- 62 Bohlman, K J
Colour and Mono Television for City and Guilds and Tec Courses
Vol. 1 Television Reception: Principles and Circuits
Norman Price
1980
- 63 Charge Coupled Device Catalogue (1982-1983)
Fairchild
Pp 119-120, 120A-120D

- 64 CCD3000 Video Communications Camera Operating Manual
 Fairchild
 1983
- 65 Charge Coupled Device Catalogue (1982-1983)
 Fairchild
 Pp 67-75
- 66 Monolithic Video A/D Converter, Model TDC1007J
 (Data Sheet)
 TRW LSI Products
 1978
- 67 12 Bit Video Analogue to Digital Converter, Model CAV-1210
 (Data Sheet)
 Analog Devices
 1982
- 68 Erasmus, S J
 Reduction of Noise in TV Rate Electron Microscope Images by
 Digital Filtering
 Journal of Microscopy
 Vol. 127, Pt. 1
 1982
 Pp 29-37
- 69 Semper Image Processing Language (Brochure)
 Toltec Computer Limited

- 70 Smith, W J
Modern Optical Engineering
McGraw-Hill
1966
Pp 254-257
- 71 RLP Program Output for Reduced-Length Photometer
Configurations Discussed in Thesis
Lucas Electrical Limited, Lighting Division (Internal Document)
1985
- 72 Software Product Description: RT-11 2780/3780 Protocol
Emulator, Version 4.1
Digital Equipment Corporation
1983
- 73 Atkinson, R M and Brook, R A
Selection and Application of Image Processing Systems
SIRA Limited
1984
- 74 Video Photometry System - Image Processing Equipment
Requirements
Lucas Electrical Limited, Lighting Division (Internal Document)
1983
- 75 Computer Graphics Systems (Brochure)
Gresham Lion (PPL) Limited

- 76 Supervisor 214 - Computer Graphics and Image Processing System
- System Summary
Gresham Lion (PPL) Limited
- 77 Intellect 100 Image Processing System (Brochure)
Microconsultants Limited
1982
- 78 Intellect 100 Image Processing System User Guide
Microconsultants Limited
1982
- 79 Intellect 200 Image Processing System (Brochure)
Microconsultants Limited
1982
- 80 Gems System 33 (Brochure)
Gems of Cambridge Limited
1983
- 81 Gems Image Processing System - Hardware Reference Manual
Gems of Cambridge Limited
1983
- 82 GEMLIB2 Fortran Routines (Brochure)
Gems of Cambridge Limited
1984

- 83 Solid-State CID Surveillance and Security Cameras Series
TN2505/TN2506 (Brochure)
General Electric (New York)
1982
- 84 Solid-State CID Surveillance Camera Models TN2505A, TN2506A,
TN2507A User's Manual
General Electric (New York)
1983
- 85 MC9000 Series Cameras for Machine Vision Systems (Brochure)
EG&G Reticon
1984
- 86 MC9000 Series Cameras User's Manual
EG&G Reticon
- 87 RA256X256A Solid-State Image Sensor Array (Data Sheet)
EG&G Reticon
1983
- 88 IS200 Range of Solid-State Matrix Array Cameras (Brochure)
Industrial Monitoring Equipment Limited
- 89 Charge-Coupled Device Image Sensor TH7852 (Data Sheet)
Thomson-CSF, Division Tubes Electroniques
1983

- 90 IS400 High-Resolution Industrial Camera (Data Sheet)
Industrial Monitoring Equipment Limited
- 91 Micro/PDP-11 Handbook
Digital Equipment Corporation
1983
- 92 Silicon Photodetectors (Catalogue)
Centronic
P 19
- 93 OPA2111 Dual Low Noise Precision Difet Operational Amplifier
(Data Sheet)
Burr-Brown Corporation
1984
- 94 Ealing Optics Catalogue 1984/1985
Ealing Beck Limited
Pp 26-38
- 95 Motorised Tables (Brochures)
Laser Lines Limited
- 96 Unislides (Brochures)
Time and Precision (Sales) Limited
- 97 Unimatic Product Guide
Unimatic Engineers Limited

- 98 Standard Digital Interface for Programmable Instrumentation
Institution of Electrical and Electronic Engineers (IEEE)
Standard 488
1975
- 99 PDP-11 Software Handbook
Digital Equipment Corporation
- 100 PPS250S IEEE Programmable Power Supply (Data Sheet)
Prism Instruments Limited
- 101 Moralee, D
Paving the Way to All-Digital Broadcasting
Electronics and Power
Vol. 31, No. 6
June 1985
Pp 435-440
- 102 Keitz, H A E
Light Calculations and Measurements
Macmillan
1971
Pp 115-120
- 103 Keitz, H A E
Light Calculations and Measurements
Macmillan
1971
Pp 120-145

- 104 Keitz, H A E
Light Calculations and Measurements
Macmillan
1971
Pp 205-207, 324-325, 329-330
- 105 VS Fortran Application Programming: Language Reference
(Fourth Edition)
IBM Corporation
1983
- 106 VS Fortran Application Programming: Guide (Fourth Edition)
IBM Corporation
1983
- 107 Monro, D M
Fortran 77
Edward Arnold
1982
- 108 McGowan, C L and Kelly, J R
Top-Down Structured Programming Techniques
Petrocelli/Charter
1975

- 109 Kingslake, R
Lens Design Fundamentals
Academic Press
1978
Pp 24-29
- 110 Smith, W J
Modern Optical Engineering
McGraw-Hill
1966
Pp 247-253
- 111 Hebditch, D L
Data Communications - An Introductory Guide
Paul Elek (Scientific Books)
1975
- 112 OS/VS2 TSO Command Language Reference
Fifth Edition
IBM Corporation
1978

BIBLIOGRAPHY OF USEFUL READING

- 1 Stimson, A
 Photometry and Radiometry for Engineers
 Wiley
 1974

- 2 Keitz, H A E
 Light Calculations and Measurements
 Macmillan
 1971

- 3 Smith, W J
 Modern Optical Engineering
 McGraw Hill
 1966

- 4 Brown, E B
 Modern Optics
 Reinhold
 1965

- 5 Gregory, B A
 An Introduction to Electrical Instrumentation and Measurement
 Systems (Second Edition)
 Macmillan
 1981

- 6 Healey, M
Minicomputers and Microprocessors
Hodder and Stoughton
1976

- 7 Castleman, K R
Digital Image Processing
Prentice-Hall
1979

- 8 Green, W B
Digital Image Processing - A System's Approach
Van Nostrand
1983

- 9 Hansen, G L
Introduction to Solid-State Television Systems
Prentice-Hall
1969